Some spectroscopic, kinetic and equilibria studies of Cyano- and nitro- substituted anisoles and phenols and their reactions with nucleophiles

Castilho, Paula C.M.F.

Some Spectroscopic, Kinetic and Equilibria Studies of Cyano- and Nitro- Substituted Anisoles and Phenols and their Reactions with Nucleophiles

by

Paula C.M.F. Castilho

(Graduate Society)

A thesis submitted for the degree of Ph.D. in the University of Durham, 1990

Acknowledgements

I wish to thank my supervisors, Dr M.R. Crampton and Dr J. Yarwood, for their constant encouragement and help.

I acknowledge receipt of a research studentship from Junta Nacional de Investigacao Cientifica e Tecnologica, PORTUGAL.

Thanks are also due to Mr V. McNeilly for help with n.m.r. and mass spectrometry work and to Mr C. Greenhalgh for typing this thesis.

Declaration

The material in this thesis is the result of research carried out in the Department of Chemistry, University of Durham, between October 1987 and June 1990.

It has not been submitted for any other degree and is the author's own work, except where acknowledged by reference.

List of Publications

Some of the results described in this work have been published in the following papers:

Competition between Methoxide Attack at Ring-Carbon and at the Cyano-group of Cyanonitroanisoles, The Effect of Cations.

by Paula C.M.F. Castilho, Michael R. Crampton and Jack Yarwood

J. Chem. Research (1989), (S)370, (M)2801

Dealkylation of Ring-activated Alkyl Aryl Ethers in Dimethyl Sulphoxide

by Paula C.M.F. Castilho, Michael R. Crampton and Jack Yarwood

J. Chem. Research (1990), (S)394

Abstract

The reactions of ring-activated alkyl aryl ethers with nucleophiles have been examined. The main pathways involve attack by the nucleophiles at the alkyl carbon to give substituted phenoxide ions, or at ring carbon atoms to give σ–adducts.

The dealkylation reactions have been observed by both ^1H nuclear magnetic resonance spectroscopy and spectrophotometrically using dimethyl sulphoxide as solvent. The reactivity order for nucleophiles in this solvent is $SCN^- < I^- < Br^- < Cl^- < CN_3^-$ and is markedly different from that found for S_N2 reactions in protic solvents. These differences probably reflect changes in the relative solvation of the nucleophiles on charge of solvent. Dealkylation is also observed in dimethyl sulphoxide alone and is thought to yield S-alkylated DMSO.

In methanol reaction of 4-cyano-2,6-dinitroanisole and 2-cyano-4,6-dinitroanisole with methoxide ions results in competition between attack at ring carbon and at the cyano-group. Kinetic and equilibrium data are reported for reaction of 4-cyano-2,6-dinitroanisole where rapid formation of the 1,1-dimethoxy adduct is followed by slower equilibration with the imido-ester solvate. There is evidence for strong association with cations of the 1,1-dimethoxy adduct, and values of the association constants decrease in the order of cations, $Ba^{2+} > Ca^{2+} > K^+ > Na^+ > Li^+$. This explains a longstanding discrepancy in the literature between the values of equilibrium constants for attack of lithium methoxide and of sodium methoxide.

In concentrated solutions of sodium or potassium methoxide in methanol nitro-activated anisoles form adducts with 2:1 and 3:1 stoichiometry. Here methoxide addition occurs at two or three ring positions respectively. Such equilibria have been examined spectrophotometrically for 2,4,6-trinitroanisole, the isomeric cyanodinitroanisoles and the spiro-adduct formed by cyclisation of picryl glycol ether. For these equilibria the "basicity" of sodium methoxide solutions in methanol is appreciably greater than that of corresponding potassium methoxide solutions. This is in contrast with other measures of basicity and is attributed to the association of the multi-charged adducts with cations which is stronger with sodium ions than with potassium ions.

The infrared spectra of the parent and nitro-cyanoanisoles and their Meisenheimer complexes have been examined in the NO_2 group, benzene ring and CN group regions. In order to attempt to understand their chemical and spectral behaviour the corresponding phenols and their Na^+ and K^+ salts have also been studied both in solution in dimethyl sulphoxide and in the solid state. Band shifts, widths and intensities have been interpreted in terms of the nature and extent of intra-molecular electronic rearrangements caused by the intermolecular interactions (hydrogen-bonding and cation coordination). Interesting, although not fully understood, differences in behaviour between the 2 and 4-CN substituted dinitrophenols and anisoles have been noted.

CONTENTS

CHAPTER FOUR

CHAPTER FIVE

Chapter 1
Introduction

1. Introduction

Alkyl aryl ethers carrying electron-withdrawing ring substituents are very reactive substrates and may undergo a variety of reactions[1-8] Reactions with nucleophiles may involve S_N2 attack at aliphatic carbon and/or attack at aromatic ring positions.

Reaction by the S_N2 pathway results in cleavage of the bond to the alkyl group with the formation of a phenoxide ion. There is evidence for reaction with anionic (equation 1) and neutral (equation 2) nucleophiles[1,6-8] Reaction at the aromatic

$$ArOR + Nu^- \longrightarrow ArO^- + NuR \qquad (1\text{–}1)$$

$$ArOR + Nu \longrightarrow ArO^- + NuR^+ \qquad (1\text{–}2)$$

ring may result in the formation of stable σ-adducts or in substitution by the S_NAr mechanism[2-5] (equation 3). This process involves the formation of an intermediate carrying an sp^3 hybridised carbon atom.

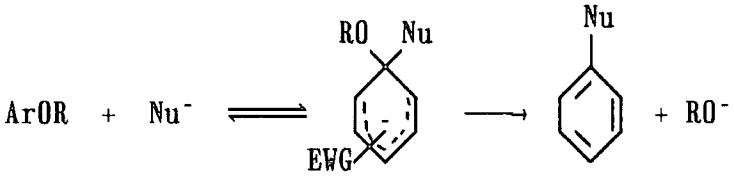

(1–3)

EWG : Electron withdrawing group

The presence of electron-withdrawing groups in the aromatic ring is necessary to stabilise the anionic intermediates in this pathway.

1.1. The Products of Reaction of the S_NAr Attack

1.1.1. Characterization of σ–adducts

The anionic σ-adducts of trinitroaromatic compounds have been known since the beginning of the century and structures (1) were then proposed[9,10] for the strong coloured species. Evidence for such type of structure came from Meisenheimer's investigations on the reactions of 2,4,6-trinitrophenetole with

methoxide and of 2,4,6-trinitroanisole with ethoxide, both leading to the same

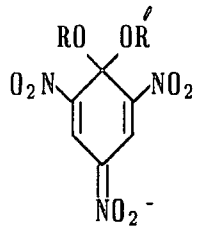

(1)

product of reaction. The red crystalline material found earlier by Lobry de Bruyn (1895)[12] for the interaction of 1,3,5-trinitrobenzene with methoxide is better described by a similar kind of structure (2) rather than his first suggestion of

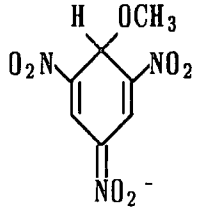

(2)

ionisation by loss of a ring proton![11] The research on S_NAr as a two step pathway of addition-elimination involving intermediates formally analagous to the Meisenheimer complexes lead to many investigations[3-5,13] on their structural characterisation which is now accepted to be best represented by a delocalised structure (3)

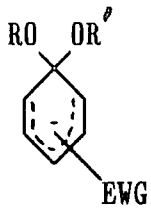

(3)

The formation of Meisenheimer complexes from the interactions of alkoxides with various aromatic substrates results in deep changes in the U.V./visible spectrum during the course of the reaction![14] While the substituted aryl ethers absorb in the UV region, the σ-adducts are strongly coloured species showing two maxima of absorption in the visible region of the electromagnetic spectrum, the wavelength

of these maxima varying with the number, nature and position of the substituents in the ring. The higher energy band, which appears around 410–420nm in the trinitro adducts moves to lower wavenumbers when there is replacement of nitro groups by substituents of lesser electron–withdrawing ability, irrespectively to the relative position of the ring. The lower energy band, $\lambda > 470$nm, usually shifts to lower energy as the electronegativity of the substituent *para* to the sp^3 carbon decreases[16,17,21,23] For the 1,1–dimethoxy–2–6–dinitro–4–X– adducts, the position of this maximum has been reported to be 540nm for X = CN,[18,20] 525nm for X = CO_2CH_3[19,24] and 640 for X =F[18,25]; in the 2–X–4,6–dinitro series, these three substituents give rise to adducts with a band near 475nm.[14,20,21,22,25]

Another very important tool for the understanding of the chemistry of σ-adducts is NMR spectroscopy which may provide very precise structural information. The first report on NMR spectra of σ-adducts was that of Crampton and Gold (1964)[15] on ^1H spectra of methoxy adducts of TNA and TNB. TNA in DMSO show NMR bands at δ4.1 and 9.1 due to methoxy and ring protons respectively while in the corresponding 1,1-dimethoxy adduct the methoxy band is shifted upfield to δ3.0, consistent with a change in hybridisation from sp^2 to sp^3 at the C1 position, and the band due to the ring protons is shifted upfield to δ8.6. These changes are typical of those accompanying the formation of 1,1-dialkoxy adducts from picryl ethers. Most measurements have been made in DMSO which has proved to be a particularly useful solvent for NMR work as it shows good solvation properties for σ-adducts without evidence for strong chemical interaction. For 1,1-dialkoxy adducts of alkyl ethers activated by nitro groups together with other electron-withdrawing substituents;[18,23] X, the ^1H NMR spectra show a single ring proton band when the substitution is 4-X-2,6-dinitro– and a correlation was found between the chemical shift and the Hammett σ_R value of the substituent X; for 2-X-4,6-dinitro– adducts, the ^1H NMR spectra show two spin-coupled bands with J 2.5-3 Hz due to the ring protons;[5,20,21] the shift of the proton situated between nitro groups being less sensitive to the nature of the substituent X than that of the proton between X and a nitro group.

In the reaction of 2,4,6-trinitroanisole (4) with methoxide ions, ^{1}H NMR measurements[17] showed that nucleophilic attack occurs initially , under kinetic control, at the 3-position to give (6) but the 1,1-dimethoxy adduct (5) is thermodynamically more stable and isomerisation takes place[5,21]

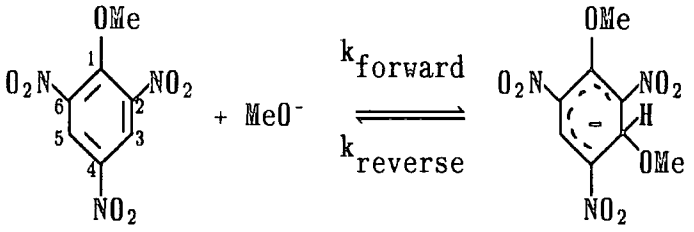

(4) TNA (6)

K_{eq} =7.7x10^{-3}lmol^{-1}
$k_{forward}$=2.71 lmol^{-1}s^{-1}
$k_{reverse}$=350 s^{-1}

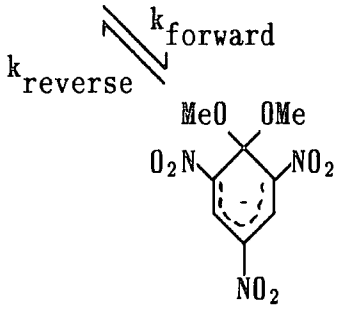

(5)

K_{eq} =17000 lmol^{-1}
$k_{forward}$=17.3 lmol^{-1}s^{-1}
$k_{reverse}$=10^{-3} s^{-1}

Kinetic measurements[13,21] have allowed the determination of the rate coefficients shown in the scheme.

The ^{1}H NMR spectrum of (6) shows spin-coupled bands, J=2 Hz, at δ6.15 and δ8.45 due to the ring protons and singlets at δ3.85 and δ3.20 due to the methoxy–groups at the 1– and 3– positions respectively![17,18] Also with 4-X-2,6-dinitro–anisoles it has been found that attack at the 3-position precedes isomerisation to give the 1,1-dimethoxy– adduct. With the non-symmetrical 2-X-4,6-dinitro-anisoles, both 1,3– and 1,5-dimethoxy– adducts have been observed[20,22] as transient species. Here, attack at an unsubstituted carbon is readily detected by NMR since the ring proton at that position suffers a large shift to high field,with spin-coupling J 1–2 Hz being observed between the two non-equivalent ring protons of the adducts and the alkoxy group at the 1-position shows a band close to that of the parent compound; the alkoxy group at the 3-position giving rise to a

band at a higher field. X–Ray diffraction analysis[25-29] on alkyl aryl ethers and the corresponding 1,1-dialkoxy– adducts (5) show that the cyclohexadienate ring of the σ-adducts is approximately planar and the 2– and 6– nitro groups are essentially coplanar with the ring while those nitro groups in corresponding ethers are rotated from the ring plane due to steric congestion[24] This steric interaction is not relieved with the formation of the kinetically favourable 1,3-dialkoxy– adduct but is eliminated in the 1,1-dialkoxy complexes where the plane containing the two oxygen atoms of the alkoxy groups is perpendicular to the ring plane. The similar repulsion of the geminal methoxy groups tends to balance on each side of the ring and contribute to its planarity[5]

The C(4)–N bond proved to be much shorter than the C(2)–N or C(6)–N bonds;[26,27] which means that the *p*-nitro group carries a greater amount of negative charge than the *ortho*-nitro groups.

^{13}C NMR spectroscopy confirms the structures of the σ-adducts and provides information on the effect of substituents on the charge distribution in the complexes[30] Comparisons of the chemical shifts in the parent nitro-aryl ethers and their 1,1-dimethoxy adducts indicated that the overall charge on the cyclohexadienate ring was greater by 0.3–0.4 e, mainly concentrated on the carbon atoms attached to NO_2 groups, the other positions showing slightly reduced charge density values[4,5,27,30] These results refute the HMO calculations of charge orders of Zollinger *et al.* (1967)[31] that attribute a decrease on π-charge density in the ring with the formation of the σ-adducts. More sophisticated calculations[32-34] indicate that there is a greater π-electron density in both the ring and substituents in the complexes. The composite molecules (CM) method[32] predicts that a considerable amount of the negative charge in the adduct lies on the carbon atoms of the ring. It also predicts a greater amount of charge on the *para*-nitro group of a 2,4,6-trinitro adduct than on its *ortho*-nitro groups. Some studies on the infra-red spectra of Meisenheimer complexes were published[35-39] during the 1950's and 60's. Among the several reviews on σ-complexes, that of Strauss (1970)[3] provides a good survey of the early literature on IR studies. Since

then, relatively little new work has been carried out[5,34,40] Adducts from trinitrobenzene and triactivated alkyl aryl ethers have been the most commonly studied species[34,36,39]

For trinitro 1,1-dialkoxy-adducts, the IR spectrum is dominated by the bands due to the symmetric and anti-symmetric stretching vibrations of the NO_2 groups and by the group of bands due to the ketal vibrations (R–O–C_1–O–R').

In an aromatic nitro-substituted compound, the symmetric stretching band of a NO_2 group occurs at *ca.* 1350 cm^{-1}.[37,39] In the negatively charged σ-adducts, these frequencies are lower[3,7] due to the decrease of the NO bond order.

There is some disagreement in the published literature as to the assignment of the observed bands in the σ-adducts spectra.

Dyall[37] noticed strong bands about 1513 cm^{-1}, 1493, 1297, 1238 and 1206 cm^{-1} for 1,1-dialkoxy-2,4,6-trinitrobenzene adducts and could not decide which of the first two bands was due to the γ_s (NO_2) mode and the other two are considered to be due to ketal vibrations together with some lower frequency bands.

In 1980, in one of the most recent publications on this subject, Ohsawa and Takeda[40] follow exactly the same assignment, attributing the *ca.* 1490 band to the γ_{as} of NO_2 and the band at higher wavenumber to the ring vibration.

On the other hand, Kaminskaya *et al*[34] observed pairs of overlapping bands at 1506 and 1480 cm^{-1} and at 1237 and 1207 cm^{-1} in the methoxy adduct of 1,3,5-trinitrobenzene, both in the solid state and in DMSO solution, which they assigned to the γ_{as} and γ_s modes of NO_2 respectively. Working on related adducts, such as 1,1-dimethoxy-2,4-dinitro– and 1,1-dimethoxy-2,4,6-trinitrocyclohexadienate, these authors found pairs of bands close to these frequencies. Their interpretation of this splitting of γ_{as} and γ_s bands is formulated in terms of the non-equivalence of the NO_2 groups in the anion; quantum chemical calculations, type composite molecule (CM), indicate greater π-charge on the nitro group in the *para*-position to the sp^3 carbon: this would be the NO_2 group responsible for the lower frequency γ_{as} and γ_s bands. The other NO_2 groups, both in *ortho*-positions are equivalent and their γ_{as} and γ_s bands would lie to higher frequencies.

The other important group of bands is the one related to the C–O–C vibrations[37,40] It has been reported that the picryl ethers normally show two bands of medium intensity about 1270 and 1040 cm^{-1} due to the antisymmetric and symmetric stretching modes of this group; the spectra of the complexes formed upon the reaction of these picryl ethers with metal alkoxides show 4–5 strong bands in this region, sometimes poorly separated.

These bands have been taken as characteristic of a Meisenheimer complex and as proof of its fully covalent structure[37]

In the complex, the ketal structure appears like

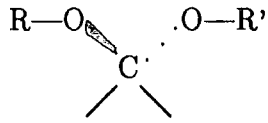

in a plane perpendicular to the one defined by the ring, so several coupled stretching vibrations are to be expected.

The ring stretching vibrations result in several bands, the most easy to identify being the one occurring about 1600 cm^{-1}. This band has been reported for a large number of alkoxy triactivated benzenes and their adducts but no interpretation has been attempted due to the fact that it does not show a relevant shift in frequency on going from parent compound to complex; that is, from aromatic ring to cyclohexadienate.

There has been little research on the C–H or the CH_3 vibrations in σ-complexes. Nevertheless, according to Dyall[37] the out-of-phase and in-phase in-plane C–H deformation bands appear at *ca.* 1190 and 1085 cm^{-1} in picryl ethers and at 1163-1152 cm^{-1} and 1063-1053 cm^{-1} in σ-complexes. The out-of-plane C–H deformation modes give rise to bands near 910 and 750 cm^{-1} in both parent aromatic compound and complex.

For 4-cyano-2,6-dinitrocyclohexadienate, the IR spectra have been reported[35] only as a list of wavenumbers between 1600 and 500 cm^{-1} and no assignment is made. The presence of 5 bands between 1225 and 1040 cm^{-1} is often considered sufficient evidence for the Meisenheimer complex formation.

Because of the solubility of σ-adducts of triactivated benzenes and picryl ethers in the non-polar solvents (normally used in IR work) is very small, almost all recorded spectra of these compounds have been taken on KBr disk mixtures or Nujol mulls. Kaminskaya *et al.*[34] present some results in DMSO solution, reporting only on the NO_2 stretching frequencies : the split of the two γ_{as} (NO_2) bands is smaller in solution than in the solid state for all complexes; the split between the γ_s (NO_2) bands increases in solution for some of the σ-complexes but decreases in others.

Theoretical and crystallographic studies[25,33,41] predict that the behaviour of *ortho*– and *para*-NO_2 groups in solution should be more similar as the difference between C(4)–N and C(2)–N bond lengths is lower than in the solid state.

1.1.2. Stability of Meisenheimer Complexes

The thermodynamic stability of anionic σ-adducts is one of their most studied properties[3-5,13] and is dependent on a large number of factors, ranging from the nature of the aromatic substrate and of the nucleophile to experimental conditions such as type of solvent, counterion interaction and temperature effects.

The influence of the structure of the alkyl aryl ether on the stability of the corresponding 1,1-dialkoxy adduct is related to the type, number and position of the substituents in the aromatic ring[13] For example, addition of methoxide to 2,4,6-trinitroanisole, TNA, gives (5), a more stable complex than the resultant of the identical addition to 1,3,5-trinitrobenzene, TNB:

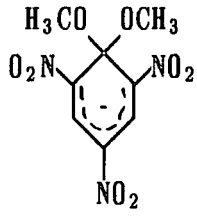

K_{eq} (5) = 17000 $lmol^{-1}$ [21]

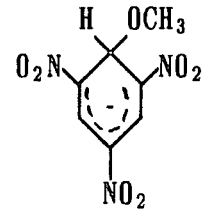

K_{eq} (7) = 15.4 $lmol^{-1}$ [16]

The addition of methoxide to 2,4-dinitroanisole or 2,4-dinitrobenzene, which may be regarded as the result of removing one nitro group respectively from TNA or TNB, lead to the rather unstable complexes[5,13] (8) and (9):

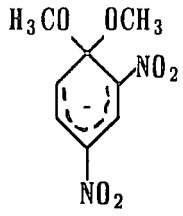

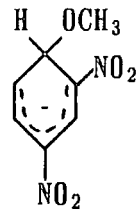

K_{eq} (8) = 4.6 x 10^{-5} $lmol^{-1}$ [42] K_{eq} (9) = 5 x 10^{-7} $lmol^{-1}$ [15]

This remarkable drop in the values of equilibrium constant indicates the stabilising effect of an *ortho*-nitro group[13] Replacement of one nitro group by a substituent with different electron-withdrawing power causes large changes in the stability of the complex[13,21] It has been shown that the higher the electron-withdrawing ability of the substituents on the aromatic parent compound, the more stable the 1,1-dimethoxy adduct becomes. For example, replacement of the 4–NO_2 group of TNA by SO_2CF_3 gives rise to an even more stable complex (10).

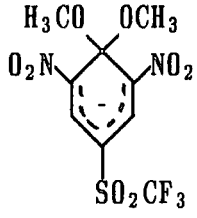

$K_{eq}(10)$ = 1.2 x 10^{6} $lmol^{-1}$ [13]

The stability order for 1,1-dimethoxy-4-X-2,6-dinitro– adducts is

$SO_2CF_3 > NO_2 > CN, SO_2\ CH_3 > CHO > COOCH_3 > CF_3 > Cl > F, H$[13]

paralleling the electron-withdrawing ability of X.

Particularly relevant for the stability of the complex is the type of substituent in *para*-position to the carbon atom under nucleophilic attack. The equilibrium constant, K_{eq} for the 1,1-dimethoxy-2,4,6-trinitro adduct (5) is 17000 $lmol^{-1}$ and for the 1,1-dimethoxy-2-cyano-4,6-dinitro adduct (11) is 2600 $lmol^{-1}$ and for the 1,1-dimethoxy-4-cyano-2,6-dinitro complex (12) K_{eq} is 280 $lmol^{-1}$ [21].

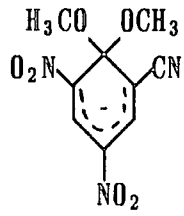

(11)

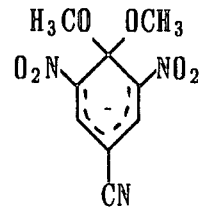

(12)

The decrease in stability is much larger when the 4–NO_2 group is replaced by a CN group than when replacement occurs with an *ortho*-group[13,21]

Steric factors in both substrate and corresponding σ-adducts also have influence on the stability of the anionic species. The greater stability of the 1,1-dimethoxy adduct of TNA (5) in relation to the 1,3-dimethoxy complex (6) has been attributed[43] to the release of steric strain from the molecule and to the stabilising influence of the two methoxyl groups at the sp^3 hybridised carbon[4,24] In fact, the *ortho* 1-methoxyl and the 2– and 6–nitro groups suffer steric compression which causes the NO_2 groups to rotate out of the ring plane decreasing their conjugation; in the adduct (5) the methoxy groups are situated in a plane perpendicular to the ring[4] and the nitro groups are coplanar and highly conjugated with the ring.

More recently[44-47] spiro Meisenheimer complexes have been formed using bi-functional nucleophiles such as ethanediol or catechol. The electronic spectra of

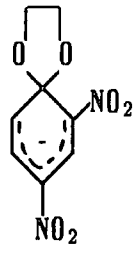

(13)

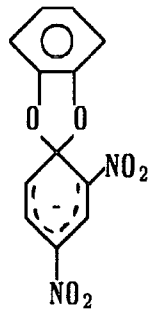

(14)

the spiro adducts are, in general, similar to those of the corresponding 1,1-dialkoxy compounds although it has been found[48] that the catechol group causes a shift of the bands to shorter wavelengths due to its greater electron-withdrawing ability.

The formation of such compounds involves intramolecular nucleophilic attack and proton transfer, the order of which depends on the system under study. For the examples above, the rapid proton transfer precedes internal cyclisation which becomes the rate determining step.[45-47]

It has been shown[46] that these spiro complexes are much more stable than their 1,1-dialkoxy analogues, presumably because of the rigidity of the cyclic substituent perpendicular to the benzenic ring, although they decompose much faster. This increased lability of the spiro adducts relative to the corresponding 1,1-dialkoxy complexes is explicable in terms of stereo-electronic factors, i.e., the stabilisation of the transition state for the spiro formation and decomposition through p–π overlap between one of the lone pairs of the oxygen atom of the nucleophile and the aromatic π system; this stabilisation is absent in the 1,1 complex (Fig.1)

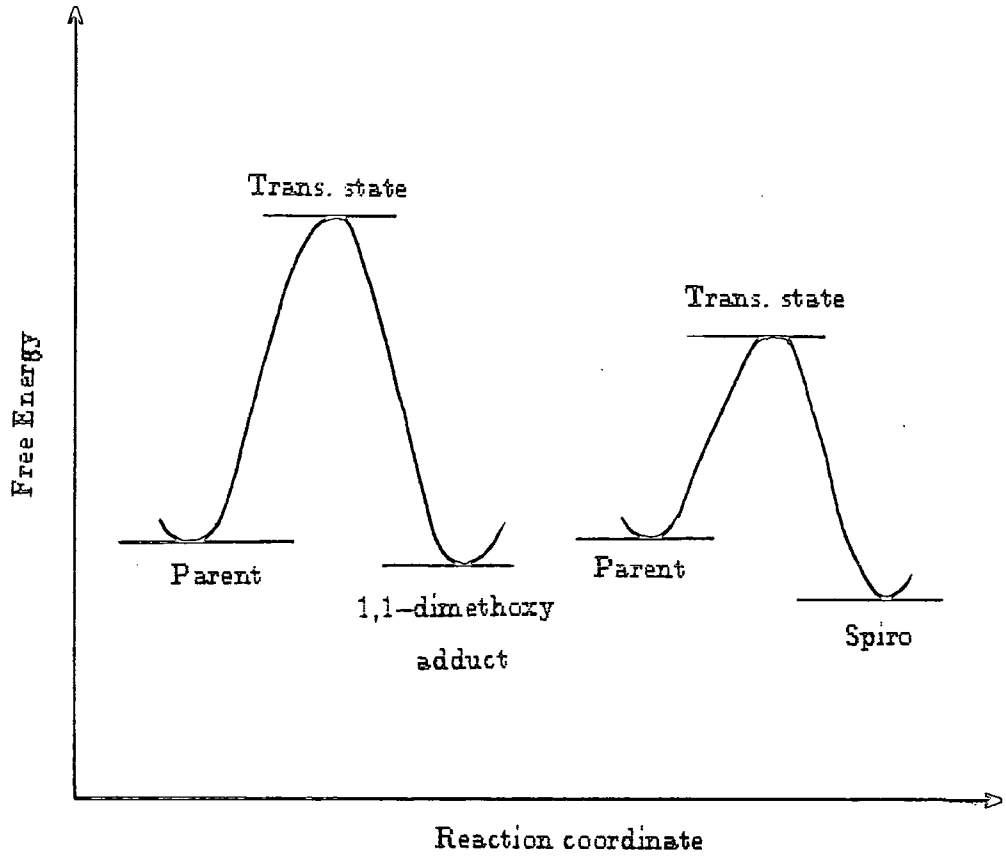

Figure 1–1 Free energy profile for S_NAr reaction

Other bifunctional nucleophiles that have been very recently reported[49-53] to cause the formation of spiro Meisenheimer complexes are micelles of cetyl(2,3-dihydroxypropyl) dimethylammonium bromide (15)

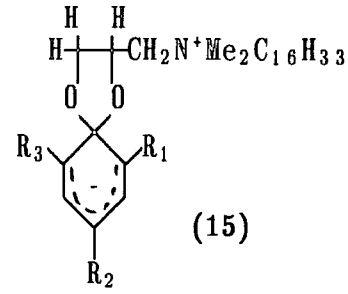

(15)

R_1, R_2 and R_3 being NO_2, H or CO_2^-

These spiro adducts may get further stabilisation from intramolecular electrostatic interaction involving the negatively charged or dipolar *ortho*-substituents and the positive nitrogen atom of the side chain;[53] as in (16). Intramolecular cyclisation is also favoured for amine addition to an alkoxy bearing carbon;[53] as shown in (17)

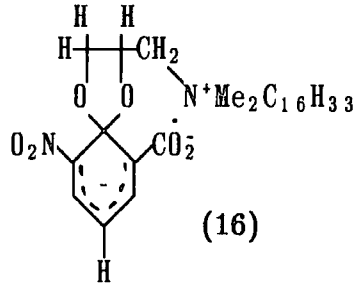

(16)

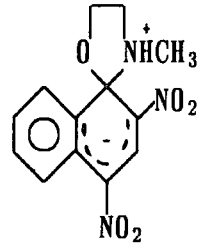

(17)

1.1.3. Effect of solvents on σ–adduct stability

The stability of a σ-complex in solution is, to some extent, dependent on its interaction with the solvent;[5,13] i.e., its degree of solvation, and also on the solvation of the nucleophile.[4]

The solvents more often used in Meisenheimer complex studies may be divided into two groups: protic solvents, like water or alcohols, and dipolar aprotic solvents, like DMSO, acetonitrile or DMF. These two groups behave differently with respect to ion solvation: small polar ions like OH^- or OR^- are better solvated by protic solvents while large polarisable species are well solvated in dipolar aprotic solvents but not so well by the protic ones. Consequently, σ-adduct formation is often favoured in DMSO, compared with methanol. For example, the equilibrium constant for the formation of the 1,1–dimethoxy adduct from the reaction of TNA with methoxide ions which has the value of 1.7 X $10^4 lmol^{-1}$ at 25°C, in pure methanol,[21] increases to 9.26 X $10^4 lmol^{-1}$ in MeOH:DMSO 90:10 nd to 4.65 X $10^5 lmol^{-1}$ in a mixture of MeOH:DMSO 70:30 at the same temperature.[26]

Visible and ^1H NMR spectroscopic data show that the change of solvent does not affect the nature of the interaction between the nucleophile and the aromatic parent but only its efficiency. However, in some cases, it has been shown that the solvent may have a more active role in the overall reaction rather than simple solvation.[59,60] For example, in methanolic solutions, the 1,3-dimethoxy adduct formed from TNA (6) is much more labile[4] than in DMSO because methanol catalyses its isomerisation to the 1,1-dimethoxy adduct (5).

By competitively reacting with the aromatic parent compound the solvent may have a de-stabilising effect on the Meisenheimer complex. Both methanol and DMSO have been found[4,59] to attack the alkoxy group of aryl ethers, such as TNA, leading to the formation of phenoxides. Competitive interactions were also found in the present work during the formation of the 1,1-dimethoxy-4-CN-2,6-dinitro adduct from the corresponding methoxy ether in methanol. The equilibrium constant for this reaction in DMSO-MeOH 50:50 was determined to be

70500 $lmol^{-1}$ [13]; for the reaction in pure methanol several very different values of K_c have been quoted ranging from 2.5 $lmol^{-1}$ for interaction with lithium methoxide measured by NMR[35], to 168 $lmol^{-1}$ [13] or even 280 $lmol^{-1}$ [21] obtained by U.V./visible spectroscopy using sodium methoxide as the nucleophile. The base catalysed reaction of 4-cyano-2,6-dinitroanisole with methanol leading to the formation of an imido-ester compound, competing with σ-adduct formation may be the origin of this discrepancy and is discussed in Chapter 3

Several authors[21,55-57] studied interactions of methoxide ions with triactivated benzenes and anisoles in solvent mixtures. The equilibrium constant in one solvent is related to that in the other solvent by their activity coefficients:[43]

$$K_{(MeOH)} = K_{(DMSO)} \frac{{}^{MeOH}\gamma^{DMSO}_{p.MeO^-}}{{}^{MeOH}\gamma^{DMSO}_{OMe^-} \; {}^{MeOH}\gamma^{DMSO}_{p}} \qquad (1\text{–}4)$$

The parent, p, and the complex $p.MeO^-$ are both large polarisable species and would be expected to be stabilised on transfer from methanol to DMSO. Thus, the increased activity of the methoxide ion in DMSO must be an important factor accounting for the increase in the stability of the adduct in DMSO relative to methanol.

Generally, the ability of DMSO to enhance the thermodynamic stability of complexes formed from similarly activated substrates but different nucleophiles should depend primarily on the nature of these nucleophiles. Experimental observations, mainly derived from calorimetric studies[13] confirm this expectation.

For all systems reported, the effect of DMSO, and of other dipolar aprotic solvents, on the stabilisation of 1,1-dialkoxy complexes is the result of an increase in the rate of formation, k_1, together with a decrease in the rate of decomposition, k_{-1}, for the equilibrium

$$\text{Parent} + MeO^- \underset{k_{-1}}{\overset{k_1}{\rightleftharpoons}} \text{1,1 complex} \qquad (1\text{–}5)$$

The effect upon k_1 is likely to be due to the poor solvation of the methoxide ions by DMSO and also to the enhanced dissociation of the metal methoxide since

$$MOCH_3 \rightleftharpoons M^+ + OCH_3^- \qquad (1\text{–}6)$$

DMSO is able to form strong complexes with the cation $(CH_3)_2\overset{\delta^+}{S}{=}\overset{\delta^-}{O}\ldots M^+$. So, it can be said that DMSO promotes the presence of "free" methoxide ions in solution.

The observed lowering of the rate of decomposition is likely to be caused by the efficiency of solvation of the 1,1 complex.

1.1.4. Salt effects

An important observation relating to salt effects is the finding that ion pairing affects the equilibrium formation of 1,1-dialkoxy complexes in alcohols.[61-72] Intensive studies of this effect have been made in methanol where the rate constants for the forward (k_1) and the reverse (k_{-1}) reaction, and therefore the stoichiometric equilibrium constant K_C, depend to some extent on the concentration of the base or the electrolyte and on the nature of the cation. It has been shown that addition of electrolyte does not greatly affect the activity of the substrate, which means it affects either the state of the attacking species ROM or the σ-complex. As K_C for formation of the methoxide adduct of TNB does not change with sodium methoxide concentration,[67,69] it seems likely that the observed phenomenon is due to stabilization of the anionic σ-complex by association with the cation, as suggested by Crampton.[19,61] Conclusive evidence favouring the effect of association was obtained[65] in the presence of 18-crown-6-ether where the values of k_1, k_{-1} and K_C are practically independent of sodium methoxide concentration over a wide range. In accordance with these facts, Crampton and Khan[19,61] have proposed the following ion association scheme for the interaction of a triactivated aromatic compound, P, with a metal alkoxide, MOR, in methanolic solution of low ionic strength.

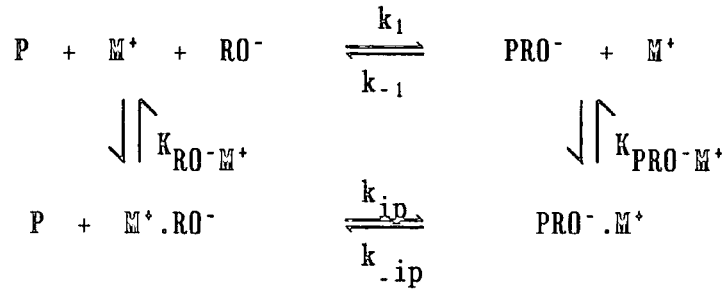

M^+, RO^- and $PRO^-:M^+$ represent the associated species. The thermodynamic equilibrium constant K_1 is defined as

$$K_1 = {}^{k_1}/_{k_{-1}} \qquad (1\text{-}7)$$

The observed equilibrium constant can be related to K_1 and the ion-pair association constants[57] as shown in equation (1-8)

$$K_c = K_1(1 + K_{PRO^-:M^+}[M^+]) / (1 + K_{RO^-:M^+}[M^+]) \qquad (1\text{-}8)$$

In very dilute solutions, the base is almost all in the dissociated form. It is then, evident that if the cation coordinates better with the σ-complex than with the alcoholate ion, $K_{PRO^-:M^+} > K_{RO^-:M^+}$, K_c will increase with M^+ concentration and vice versa.

In the formation of 1,1-dimethoxy adducts, in contrast to what happens for TNB complexes, the experimental values of K_c strongly depend on the base concentration and on the nature of the counterion[19,61,65-67,72]

The increase of K_c caused by the $n\text{–}Bu_4N^+$ ion is small as the cation is too bulky to actually associate with the complex but, being large and diffusely charged, interacts with the polarisable σ-adduct, contributing to its stabilisation through this kind of interaction; this effect is virtually independent of the nature of the substrate.

The value of K_c remains constant when LiOMe is used as the interacting base.

The lithium ions, being strongly associated with the methoxide ion, do not associate strongly with the σ-complex. The dissociated lithium ions are certainly very well solvated by methanol and so their ability to form ion-pairs would be reduced.[4,5,57] Sodium and potassium methoxides cause pronounced increases in K_C with base concentration. Figure 2 shows the general effect of these counterions with the increase in base concentration.

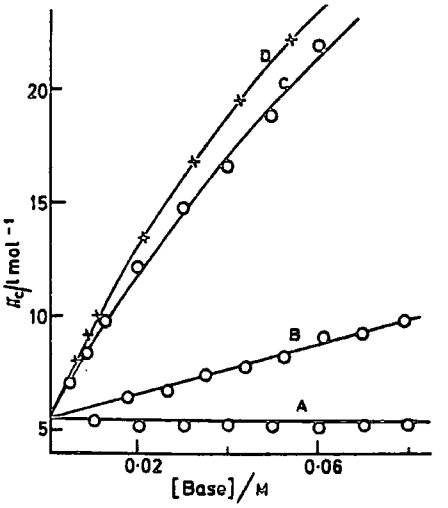

FIGURE 2. Variation of K_C with base concentration for Meisenheimer complex formation from 4-methoxycarbonyl-2,6-dinitroanisole with the following methoxides: A, lithium; B, tetra-n-butylammonium; C, sodium; and D, potassium

The addition of electrolytes, such as sodium or potassium perchlorate, to the reacting mixture causes intense increases in K_C, on account of the common-ion effect, dependent on the concentration of the salt. Bivalent cations give rise to even more drastic effects.[62] On the other hand, the addition of crown ethers, which reduce the cation association with all negative species, both complex and methoxide, results in very small changes in K_C. The structure of the parent compound is an important factor in ion-pair formation; this has been related[5] with a particular interaction between the cation and the oxygen atoms of the alkoxy groups attached to the sp^3 carbon and the substituents in *ortho*-position to this carbon;[5,69,74] as shown in (18).

The favourable disposition of the lone pairs of electrons of the oxygen atoms is absent in the TNB complex as well as in the spiro-complexes where no association is observed.[70,73,75] Replacement of *ortho*-NO_2 groups by CN also results in smaller ion-association;[5,21] due to the reduction of the number of lone electron pairs to interact with the positive species.

(18)

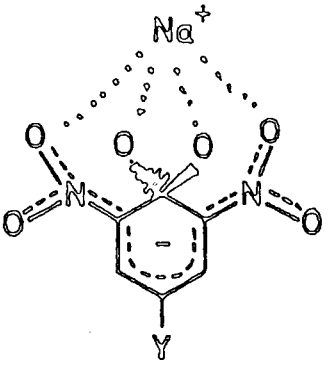

1.2. Multiple Addition

At high base concentrations, when powerful electron-withdrawing groups are attached to the ring, the σ-complexes are susceptible to further nucleophilic attack[13] and the formation of 1:2 complexes may occur:

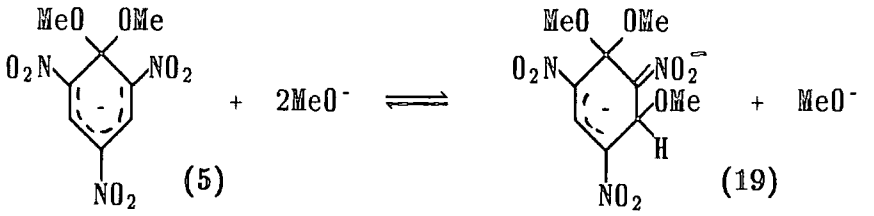

(5) (19)

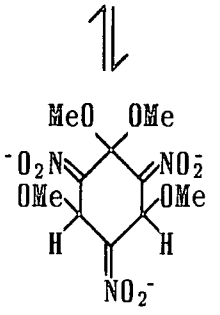

(20)

The presence of more than one negative charge in these species reduces the delocalisation found in the 1:1 complex. Accordingly, 1:2 and 1:3 complexes are better solvated and have greater stability in protic than in dipolar aprotic solvents.

The formation of a 1:2 complex is much slower than that of the corresponding 1:1 complex and is strongly dependent on the ionic strength.[4,5,13]

These systems are good indicators for the study of excess basicity of alkali metal methoxides in methanol and respective acidity functions.[76] The necessity for the introduction of these acidity functions arises from the fact that the acidity or basicity variations of a non-ideal solution with concentration are more dramatic than the corresponding variations of pH when the ionic strength is greater than *ca.* 0.1. Each base defines its own acidity function in each solvent or mixture of solvents, containing its own set of acidity coefficients.[78] For solutions of bases in methanol, two types of acidity functions are defined:[76,77]

The H_M acidity function is related to an equilibrium of proton transfer

$$SH + MeO^- \rightleftharpoons S^- + MeOH \qquad (1\text{-}9)$$

$$H_M = pK_{SH} + \log([S^-]/[SH]) \qquad (1\text{-}10)$$

K_{SH} is the ionisation constant of the substrate SH in methanol.

H_M scales for methanolic solutions of lithium, sodium and potassium methoxides have been calculated[76] using substituted anilines and diphenylamines as indicators. Tables of these scales are published showing that, for the same value of base concentration, the H_M values increase in the order

$$LiOMe < NaOMe < KOMe$$

reflecting the degree of association of the cation with the methoxide ion, which grows in the opposite order

$$KOMe < NaOMe < LiOMe$$

On the calculation of pK_{SH}, the autoprotolysis of methanol must be considered[76,77] The value for the autoprotolysis constant pK_{MeOH} is 16.92 $mol^{-2}l^{-2}$ at 25°C and 16.71 in $molal^{-2}$ units at the same temperature.[79]

The other acidity function, J_M, is related to an equilibrium of base addition:

$$R + MeO^- \overset{K}{\rightleftharpoons} R.MeO^- \qquad (1\text{-}11)$$

$$J_M = p(KK_{MeOH}) + \log_{10}\frac{[ROMe^-]}{[R]} \qquad (1\text{-}12)$$

where K is the equilibrium constant for the reaction and K_{MeOH} is the autoprotolysis constant of methanol. The most common indicators for the measurement of this function are α-cyanostilbenes and polynitroanisoles[5,77] Generally, the J_M values are larger than the H_M values for the same base concentration. The differences are due in part to differences in solvation during reaction and are dependent on the nature of the substrate.

$$R(a\ MeOH) + MeO^-(b\ MeOH) \rightleftharpoons RMeO^-(c\ MeOH) + (a+b-c)MeOH \qquad (1\text{-}13)$$

Some molecules of solvent are released during the reaction. If R is a polynitro-aromatic compound, the negative charge is largely delocalised in the σ-adduct $RMeO^-$ formed in the reaction. When R is a substituted benzaldehyde the product

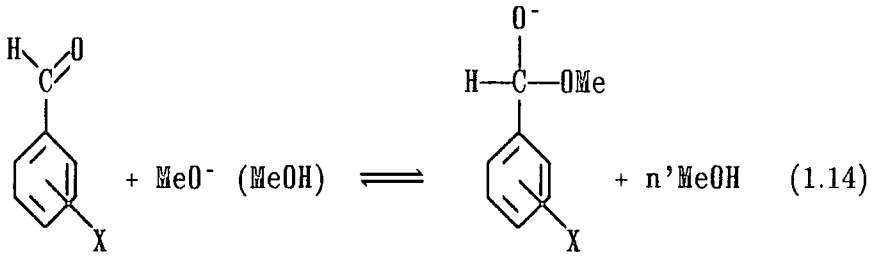

(1.14)

of the reaction is not a Meisenheimer complex but a species with a localised negative charge on an oxygen atom; thus, it will be much better solvated by methanol than the delocalised charge of the former indicator. This means that the term (a+b–c) will be smaller in the later case and a less steep dependence of J_M on base concentration is expected.

J_M scales calculated using methoxide interaction with indicators such as substituted benzaldehydes show lower values and less increase with base concentration than those based on indicators with delocalised charges. For the same reason, a similar effect might be expected when the reaction involves the formation of a 1:2 complex.

$$\text{1:1 complex} + MeO^- \rightleftharpoons \text{1:2 complex} \qquad (1\text{-}15)$$

J_M scales for methanolic sodium methoxide have been calculated[55,77] using this equilibrium as well as for

$$\text{1:2 complex} + MeO^- \rightleftharpoons \text{1:3 complex} \qquad (1\text{-}16)$$

H_M values decrease in the order KOMe > NaOMe > LiOMe, attributed to increasing association of cations with methoxide ions, the effect being negligible in very dilute solutions. However if cations can also associate with σ-adducts, then this can have dramatic results on the effective basicity of the medium.

In dilute (less than 0.1M) solutions of alkali metal methoxides the H_M function is independent of the cation due to the large dissociation of base[76] J_M however, being defined by the equilibrium $P + MeO^- \rightleftharpoons PMeO^-$, depends on the base

concentration even in dilute solutions, whenever the stabilisation of the complex by ion-pairing has to be considered. In more concentrated solutions, both types of cation association (with methoxide ions and with complex) must be taken into account[5,57] In the present work, the effects have been examined for the variation between NaOMe and KOMe solutions in 1:2 adduct forming reactions.

1.3. The products of reaction of the S_N2 attack

Nucleophilic attack, via an S_N2 mechanism, on alkyl aryl ethers results in the formation of the respective phenoxides. The presence of substituents in the phenyl ring leads to interesting modifications of the electronic redistribution during the dealkylation process. Even more interesting is the electronic distribution on the corresponding substituted phenols, namely in the presence of groups capable of hydrogen-bonding to the hydroxyl group.

Several theoretical studies[82-86] on these substituent effects have been published mainly for disubstituted benzenes, and correlation with infrared and NMR results have been made[87-92]

1.3.1. Infrared spectra of complex molecules

The applications of infrared spectroscopy to structural problems of complex molecules are based essentially on the appearance of specific bands in the spectra of these molecules so that empirical or semi-empirical correlations of characteristic frequencies and changes in IR features with molecular structural details can be established. The frequency and intensity of bands are determined primarily by the electronic structure of a particular group and by the nature of the bonding between the atoms. The influence of the molecular structure is shown in the variability of frequency or intensity within a more or less limited range, leading to the concept of "group frequencies"[93] Theoretical analysis of this concept reveals that, under controlled conditions, the features of a specific band can be taken as quantitative measures of bond character. Variations of frequency and/or intensity, as well as in the band shape, can arise from a variety of sources that include changes in

molecular symmetry and changes of inter- or intramolecular environment. These variations can be used to follow electronic influences upon bond properties provided that the vibrational interactions of the group with the molecular framework are small compared to electronic interactions.

In principle, the frequency of a group vibration may be used to characterize the bond or bonds between the atoms only if the "group" can be regarded as an isolated (localised) vibrator, i.e. the observed frequency depends only upon the masses of the atoms (μ_M) involved and the force constant between them K, without coupling to other vibrations as in a simple harmonic oscillator,

$\bar{\nu}(cm^{-1}) = \frac{1}{2\pi c}\sqrt{\frac{K}{\mu_M}}$. This seldom occurs with complex molecules but it is a situation sometimes approached with contribution from other vibrations to a particular mode amounting to a very small percentage.

Some vibrations are "localised" in a group of atoms within a large molecule and give rise to a frequency which is characteristic of that particular group. These vibrations are not necessarily localized in bonds or angles of the group, i.e. one or more bond lengths may change simultaneously with some angle bending but without influencing the other molecular framework vibrations. This will be possible if the coupling coefficients between the symmetry coordinates of the group and the rest of the molecule are small.

The stretching vibrations of (X–H) bonds are generally highly localised because their coupling with other stretching vibrations is negligible due to the large difference in the masses of the atoms involved.

The coupling coefficients are usually not equal between all symmetry coordinates of the group and therefore not all vibrations of a particular group will be equally localised. An example of this difference, which will be referred to throughout the present work, is the nitro group stretching vibrations in nitrobenzenes.

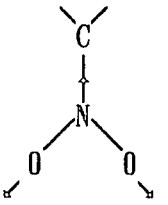

$\nu_s(NO_2)$

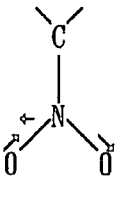

$\nu_{as}(NO_2)$

There is a high degree of coupling between the stretching vibration of (C–N) bond and the symmetric stretching vibration of the NO_2 group since the motion of the N atom in the (C–N) stretch can be resolved into components along the direction of the symmetric NO_2 group vibration:

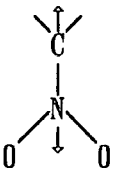

The antisymmetric stretching vibration $\nu_{as}(NO_2)$ involves bending of the C–N bond relatively to the ring rather than (C–N) stretching. As bending force constants are much smaller than bond-stretching force constants no significant coupling between those vibration is expected. Indeed, the $\nu_{as}(NO_2)$ is primarily determined by the N–O bond order and consequently the N–O stretching force constant. Thus, $\nu_{as}(NO_2)$ is more constant in both frequency and intensity than $\nu_s(NO_2)$[94] and can be more generally used for the classification of substituent effects in nitrobenzenes[95,96]

Variations in group frequencies are generally caused by changes in the force constant which are caused by the group environment and may originate from intra- or intermolecular effects. The latter effects are related to solvent interactions, hydrogen-bonding between molecules or electrostatic interactions (ion-ion or ion-molecule). Internal effects are those transmitted mainly through chemical bonds within a molecule or ion.

Every distinct absorption band in the infrared is characterised not only by the frequency at which maximum absorption occurs but also by the absorption

integrated intensity which is related in a fundamental way to the electronic structure of the molecule or part of the molecule?[97] The integrated intensity of an infrared band, A, corresponding to a fundamental vibrational transition, is expressed as

$$A = \frac{N_A \pi}{3c^2} \left[\frac{\partial \mu}{\partial \phi}\right]^2 \qquad (1\text{–}17)$$

where N_A is the Avogadro number, c is the velocity of light, μ is the dipole moment and ϕ is the normal coordinate of the vibration. A is commonly expressed in units of $10^4 mol^{-1} dm^3 cm^{-2}$.

When a bond is stretched by an amount dr, a moment $(\partial\mu/\partial r)$ is produced in the direction of the bond; the principal contribution to $\partial\mu/\partial r$ comes from variation in the overlap moment and in partial ionic character. A particularly large $\partial\mu/\partial r$ arises when one or both of the atoms involved forms part of a π–electron system. The charge distribution in such molecules is quite sensitive to bond distances and large values of $\partial\mu/\partial r$ may result from certain stretching vibrations. Bond moment derivatives determined from different vibration in the same molecules are frequently very different in magnitude.

The measurement of intensity for molecules in solution or as a pure liquid is simpler than gas–phase measurements because the rotational structure of the bands disappears and is replaced by a very simple contour for almost all molecules in the liquid phase. In the majority of cases a single band arises for a particular vibrational transition and, if no appreciable overlap with adjacent band occurs, its shape approaches the form of a Lorentz curve where ν_m is the frequency of the

$$\ln \frac{I_0}{I} = \frac{a}{(\nu - \nu_m)^2 + b^2} \qquad (1\text{–}18)$$

maximum absorption and a and b are constants. The integrated intensity corresponds to the area under the curve. The half-intensity width $\Delta\nu_{\frac{1}{2}}$, generally

referred to as "halfwidth" is defined as the frequency interval separating the points on the curve at which $\ln(I_0/I)$ has a value of one half the maximum.

1.3.2. Substituent Electronic Effects

The influence of internal group environment upon a stretching or bending force constant is parallel to the influence on chemical equilibria or reaction kinetics. Thus, in the study of substituent electronic effects there is an analogy between the "reactive centre" analysed in organic chemistry and the group whose characteristic frequencies are under scrutiny. Four primary kinds of substituent effects may be defined.[86] The inductive effect originates primarily from differences in electronegativity and consists of a polarization of the σ-electronic system. The resonance effect involves delocalisation of the π-electronic system including substituents and the molecular framework. Inductive and mesomeric, or resonance, effects are both transmitted through bonds of the involved groups and the molecular framework; either of them may be positive or negative depending on the direction of displacement of the electronic negative charge in the probe group. Substituents may exhibit one type of effect or both simultaneously; in the latter case the inductive and resonance effect may work in the same or in opposite directions.

Field effects, interpreted as across space intramolecular interactions, and polarizability effects originate from charge-charge, charge-dipole† or dipole-dipole† interactions between different sites of the molecule or ion and are generally transmitted through space rather than through bonds; these effects do not involve transfer of charge to or from a substituent.[84]

There is some controversy about the importance of a π–inductive effect, that is, whether the polar nature of a substituent can polarize a π–system without charge transfer.[98] The effect of a polar substituent on a π–system can arise either by

---

†permanent dipole for field effects, induced dipole in polarizability effects

induction of charge differences on the underlying π framework ($\pi\sigma$) or it may polarise the π–system directly (π_F). For a polar substituent attached directly to an unsaturated system, there is the possibility of large variations in charge transfer between the π–system and suitable orbitals of the substituent, through resonance effect. The interaction of substituent orbitals of appropriate symmetry with the π–orbitals of the ring can lead to charge transfer either to or from the substituent. Theoretical calculations[82] and the physical properties of molecules like aniline are in agreement with a charge transfer as represented below.

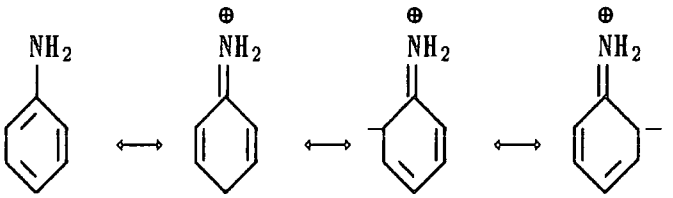

(21) (22) (23) (24)

For molecules like nitrobenzene the charge transfer would be expected to be in the opposite direction. Recent calculations[102] and experimental results[91,99-101] question the importance of this approach for electron acceptor groups since the two effects (inductive and resonance) are of the same direction and the inductive effect is usually much stronger. The redistribution of π–electron populations in the ring is found to be far greater than the overall transfer of electrons. The actual mechanism of this additional redistribution within molecular orbital theory has been described[83,92] as a mixing of π and π^* orbitals in the unsaturated system brought about through interaction with the substituent. Theoretical calculations[82,83,85] for highly polar substituents indicate that the total π–inductive effect is significant. The *ab initio* calculated changes in the π–system for nitrobenzene,[100] both in the planar and in the orthogonal (perpendicular) form where resonance is eliminated, are shown on the following page.

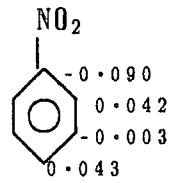

Planar
(25)

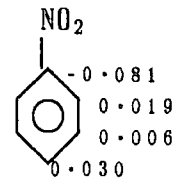

Orthogonal
(26)

Clearly the π–inductive effect is more important here than the π transfer (0.031 electron[82]) that can only occur in the planar form.

In compounds such as disubstituted benzene it is possible to have resonance interactions between the substituents, particularly when one is a strongly π-electron-donating group and the other strongly π-accepting group. This additional interaction has been referred to as through-conjugation and can be visualized in terms of canonical structures as shown below for *para*-nitroaniline.

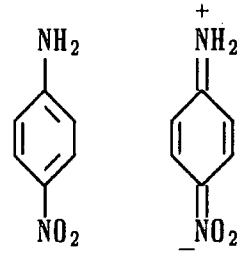

(27) (28)

There is little experimental evidence that such effects cause significant changes in the structure of neutral molecules.[86]

The π–electron transfer from the planar amino group increases only from 0.120 e in aniline to 0.139 e in paranitroaniline while the π–electron transfer into the NO_2 group increases from 0.031 e in nitrobenzene to 0.044 e for the nitroaniline.[100]

Comparison of ^{17}O NMR shifts for different substituents should give good indication of the charge transfer they induce towards the oxygen atoms of the nitro group since NMR shifts are expected to closely parallel the variations of electronic

density. Several studies of these shifts[90,91,99] have been published and are in total disagreement with one another. Lipkowitz[99] claimed that the electron density of the oxygen is invariant to substitution in the *meta* and para positions and, thus, the NO_2 group withdraws a constant amount of electron density from the ring regardless of what substituent is attached to those positions. Fraser *et al*[90] covered a wider range of substituents with a better resolution of spectra and reported chemical shifts consistent with a through conjugation effect, while Craik*et al*[91] obtained contradictory information from their ^{15}N and ^{17}O NMR studies.

An important contribution from a quinoid structure like (28) should lead to significant changes in C–C bond length.

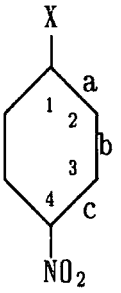

X: e–donor group

(29)

X-ray studies in N,N-diethyl-*p*-nitroaniline (X = NEt_2) show lengthening of a and c and shortening of b relative to benzene as a result of π-electron effects (contribution of quinoid structures like (28); c is also affected by the electron–withdrawing NO_2 (shortened by σ-effect) whereas a is increased by σ-effect due to interaction with the electron-donor NMe_2. Calculated bond lengths for *p*-nitroanilines and *p*-nitrophenols have been published[83,88] but no agreement has been reached as some authors[83] report very little change in a, b or c unless a very strongly π-electron-donor group, such as O^-, is paired with the π-acceptor NO_2. The use of a different method of calculation (CNDO/2 instead of STO-3G) leads to results indicating that in p-NO_2-phenol, a and c lengths are increased and the C-OH bond and b are shortened.

Recent studies on the geometry of methyl derivatives of N,N-dimethyl–*p*-nitroaniline[100] are in line with earlier findings that the classical picture of through-resonance is not justified and that the assumed conjugation of the nitro group through the benzene ring is merely of the donating substituent with the benzene π-system, while the accepting groups acts directly by its inductive effect. The introduction of methyl groups ortho to either the π-acceptor NO_2 or the donor group $NAlk_2$ causes a significant twist of these groups out of the ring plane.

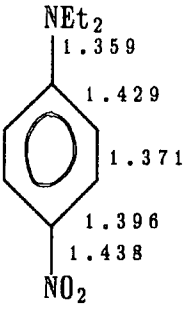

(30)

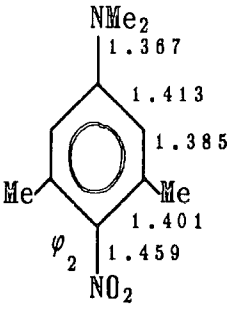

$\varphi_2 = 50.6^\circ$

(31)

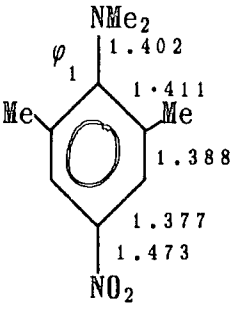

$\varphi_1 = 60.4^\circ$

(32)

The disturbance in bond length caused by the twist of the donor group NMe_2 is greater than that caused by the twist of NO_2, implying that the conjugative effect from the $NAlk_2$ group to the ring is of high importance while the electron withdrawing property of NO_2 is less important as far as the π-electron charge transfer to this group is concerned. Structures like (33 – 35) are accepted by several authors[99-101] to be more important to the overall hybrid than the quinoid form (28).

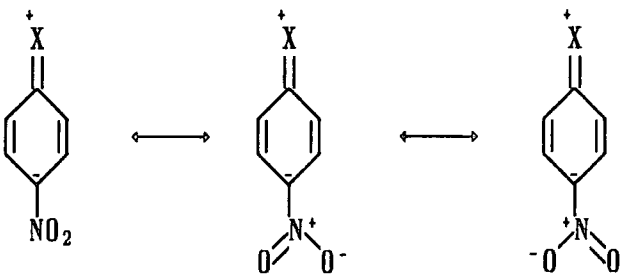

(33) (34) (35)

The existence of a significant through conjugation effect in π-donor *para*-substituted nitrobenzenes is generally used to explain the dipole moment differences between these compounds and nitrobenzene as well as between derivatives with a planar and orthogonal nitro group. Also the IR intensities[103] of some of the ring vibrations of *para*-disubstituted benzenes whose dipole transition moments are higher than the sum of the dipole derivatives for the corresponding monosubstituted benzenes, have been accounted for in terms of charge transfer from the π-donor to the π-accepting group through the ring. However, structures like (34) and (35) also have quite a large dipole moment and could be used in the same way to account for experimental data. The polarization of the six-membered ring provides an important contribution to the total dipole moments and could be a logical explanation for the increased intensities of the ring stretching modes in the IR spectrum.

Another result that has been used as an indicator of the importance of the through resonance effect is the shortening of the bond linking the ring to the nitro group on going from nitrobenzene to nitroaniline. However, this decrease in length could be accounted for by the ionic character of this bond in (34) or (35)![104]
also the increase of electron density around the oxygen atoms of the NO_2 group revealed by ^{17}O NMR chemical shifts[90,91] could be explained by the polarization of the π-system of the nitro group by the presence of a negative charge on the adjacent carbon on the ring, so that there appears a partial positive charge on the nitrogen and negative charges on the terminal oxygens.

This approach cannot however account for sterically induced decrease of dipole moment found in nitrophenols[83] and other substituted nitrobenzenes[85]. The dipole moment of the molecule is always smaller when the NO_2 group is twisted out of the ring plane. This suggests that there is some interaction between the π-system of the ring and the π-system of the nitro group that disappears when the two are orthogonal.

It seems that theoretical and experimental results from the past decade have led to a new picture of 1,4-disubstituted benzenes with a π-donor and a nitro

group. While an interaction between the two substituents does exist, it does not go through a charge transfer from one substituent to the other but rather through a charge transfer to the ring, inducing a polarization of the π-system of the nitro group. This picture differs from the classical resonance effect in that the ($C-N_{nitro}$) bond does not acquire double bond character.[89,99]

It should be stressed that the contribution of the through resonance effect represented by a quinoid structure like (28) is increased for neutral molecules in polar solvents where polarization by the solvent favours structures with exposed charges, or for those cases when the π-donor is negatively charged.[85]

For example, the substituent O^- is known to be a powerful π-donor and a poor σ-donor and so, the deprotonation of phenol to yield phenoxide has the effect of raising the energy of all the orbitals associated with the oxygen atom and both HOMO and LUMO orbitals of the ring π-system; the high interaction energies of phenoxide with electron-accepting substituents (over 80 kJ/mol whereas values for neutral phenols are usually under 20 kJ/mol)[83] may be understood as resulting from perturbations to this π-system since the important interaction here is donation of π-charge by the phenoxide HOMO into the substituents π^* orbital and since this HOMO is higher than that of benzene the interaction is favourable.

Mulliken charges and overlap population calculations (some results from ref[83] are shown in Table 1.1) show that the O^- donation into the ring as well as the double bond character of the ($C-O^-$) bond is increased by the presence of an NO_2 group. However, although this group gains π-electron density (0.15 e), the double bond character of the (C–N) bond is not very high. Even the orthogonal NO_2 group which is known to be a σ-acceptor (better still than planar NO_2) but not a π-acceptor interacts favourably with the O^- group, resulting in better π-donation by the charged substituent compared to phenoxide itself although the total ($\sigma + \pi$) charge density withdrawn by the NO_2 is greater in the planar conformation. This σ-accepting – π-donation effect has been justified by the lowering of all the π and π^* orbitals by the NO_2 group through a deshielding mechanism which can be thought of in terms of enhanced nuclear-electronic attraction for the remaining

electrons following electron withdrawal. The phenomenon in orthogonal *p*-nitrophenoxide has been described by the following resonance structures[83]

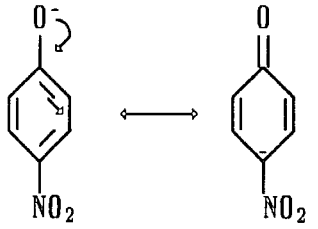

(36) (37)

Table 1–1 : **Mulliken charges and overlap populations for *p*–YC_6H_4X [83]**

Y	X	$q_\pi(Y)$	$q_\pi(X)$	π(Ph–Y)	π(Ph–X)
OH	H	–0.102	–	0.052	–
OH	NO_2	–0.115	0.039	0.061	0.035
OH	NO_2[a]	–0.111	0.0	0.059	0.007
O^-	H	–0.506	–	0.221	–
O^-	NO_2	–0.589	0.150	0.238	0.069
O^-	NO_2	–0.548	0.015	0.232	0.010

[a] orthogonal NO_2

Kaminskaya *et al* (1975)[34] interpret the decrease in frequency and increase on intensity of the infrared $\nu_s(NO_2)$ band of σ–complexes like those mentioned in section 1.2 as a result of high conjugation between the nitro groups and the ring. This interpretation is, to some extent, supported by quantum mechanical calculations[27,33] showing that the formation of σ–adducts leads to an increase in the double bond character of the (C–N) bond, from 0.21 e (i.e. effective bond order 1.21) in trinitrobenzene to 0.45 e in its 1,1-H,H-complex, and to a decrease in the bond order of the (N-O) bonds. The same calculations indicate that the valence

bond forms in which the charge is located on the ring carbons is of minor importance and that the resonance with the *p*-nitro group is slightly higher than with the *o*-nitro groups. Although the calculated π charges and bond orders for the three nitro substituents are very similar, the (C-C) bond parallel to the symmetry axis has more double bond character than in the parent compound.

The fraction of negative charge on each of the nitro groups is different for di- and trinitro compounds, so that the greater π-charge of the dinitro-complexes, which have the same amount of electron density distributed within a smaller delocalized system, leads to a greater shift of the $\nu_s(NO_2)$ band in these complexes. Decrease of double bond character of the N-O bond shifts the band to lower frequency while the increase on its polarity leads to higher intensity.[34]

Infrared studies on substituent effects in benzonitriles show that other electron withdrawing groups cause the ν(CN) frequency to increase and the intensity of the band to decrease independent of their relative position in the ring.[105,106] The shift to high frequency is more accentuated if the substitution is *meta*- to the nitrile group. Electron-donor substituents in *meta*-position to the nitrile group causes little or no disturbance in the ν(CN) band but the band is shifted to lower frequency and its intensity enhanced when this type of substitution occurs in *ortho* or *para*-position. The good correlation[105,106] found between the ν(CN) frequency (as well as its intensity) and the substituent parameters has been considered to be evidence that as the CN bond stretches and contracts during the vibration it undergoes considerable mesomeric interaction with the ring and variable "through conjugation" with a *para*-substituent. The change in conjugation and hence in the dipole moment is thought to be proportional to the tendency of the substituent to donate electrons through the ring to the electron demanding cyanide group. However the arguments used in the discussion of the conjugation of the NO_2 group can also be applied here, i.e. it is possible that a structure with accumulated charge in the ring carbon attached to the CN group is more important than the quinoid form and the CN group may withdraw electron density by inductive effect. With a triple bond between the two atoms of the group, that electron density would go

into the antibonding orbitals. Thus the overall effect is a decrease in the bond order of the CN group.

1.3.3. Solvent effects

In the liquid and solution phase, the shape of the vibrational bands can normally be approximated by a Lorentz-type curve. Rotational fine structure is usually absent and the bands have widths caused by the frequent collisions and by specific short-lived molecular interactions. In principle the molecules in a liquid have no preferred orientation but have a range of environments and a considerable freedom of movement.[93,107]

When IR absorption spectra are measure in solvents of different polarity, it is found that the frequency, intensity and shape of IR bands are usually modified by these solvents.[108,109] These changes result from intermolecular solute-solvent interaction forces which tend to alter the energy difference between ground and excited states of the absorbing species. Thus solvent effects on IR absorption spectra can be used to provide information about solute-solvent interactions.[109] Such intermolecular interactions modify the infrared spectra in a number of ways. The wavenumber of the normal vibrational modes may be shifted to higher or lower values, intensities can be altered and the half-widths of bands may be changed.[110,111] In solution, the maxima for stretching vibrational are displaced to lower frequencies, compared to the gas phase, whereas the maxima of bending vibrations are shifted to higher wavenumbers. In polar media, specific molecular interactions are particularly important and the already difficult correlation between frequency shifts and medium bulk parameters such as refractive index or dielectric constant is rendered virtually impossible.[107]

The IR stretching modes of X=O bonds (X = C, N, P, S) and X—H bonds (X = C, N, O, S) are among the most solvent-sensitive vibrations.[112,114]

The wavenumber displacement of a solute vibration band is a complex function of both solute and solvent properties. Thus weak nonspecific electrostatic interactions (dipole-dipole, dipole-induced dipole etc.), as well as stronger specific

association such as hydrogen bonding, must be taken into consideration[115]

In aprotic solvents, the observed shifts for X=O stretching vibrations may be explained by the degree of dipolarity as determined by the relative contribution of the two mesomeric forms. In protic solvents, H-S, hydrogen bonding superimposes this non-specific solvent effect according to (1-19).

$$\left[X{=}\underline{\overline{O}} \longleftrightarrow \overset{+}{X} - \underline{\overline{O}}^{-} \right] + H{-}S \rightleftharpoons X{-}\overset{\delta^+}{O}\cdots\overset{\delta^-}{H}{-}S \qquad (1\text{-}19)$$

For the X—H groups, the free end of the dipole available for specific association is of positive sign. Consequently, the greatest solvent shifts tend to occur in proton-accepting rather than proton-donor solvents[113,116] The frequency shifts of X—H bonds are primarily due to specific group interactions. The positive end of the solute (X—H) dipole seeks out a negatively charged polar group of the solvent with which to associate. This may be a lone pair orbital of a nitrogen or oxygen atom or a π-electron system. The smooth transition in passing from polar solvents, where the interaction is well recognised as hydrogen bonding;[117] to non-polar solvents in which the interaction is envisaged as a weak electrostatic attraction directed towards the negative end of the bond dipole, such as $Cl^{\delta-}—C^{\delta+}$ in carbon tetrachloride, indicates that the type of interaction is fundamentally the same throughout, differing only in magnitude.

In general, infrared absorption intensities are due to specific interactions with the solvent such as intermolecular hydrogen bonding[121,122] Usually an increase of the integrated band intensity A is obtained in passing from vapour to solution in a non-polar solvent.

Although a fair parallelism is often found between solvent effects on intensity A and on relative frequency shifts;[120] it does not always happen as the intensities of absorption bands arising from localised vibrations are determined by the electronic properties of the bond and are influenced by the group environment to the extent to which the latter induces changes in these properties[121] Although both the frequencies and intensities depend ultimately on the electronic structure

of the bond, there is not necessarily a relationship between them, the former being determined by the second derivative of energy with respect to the coordinate (Q) and the latter by the dipole moment, $\delta\mu$ / δQ. A particular change in the group environment may cause the frequency and the intensity of the corresponding band to vary in opposite directions. For example, the frequency of the (O—H) stretching vibration of the hydroxyl group in phenols is lowered by electron-withdrawing substituents and by hydrogen-bonding whereas both these factors are known to cause a rise in the integrated intensity of the vibrational band.

1.3.4. Hydrogen–bonding effects on Infrared spectra

The main vibrational modes of a hydrogen-bonded system A—H···B may be approximated as[1 2 3] :

(1)	$\overleftarrow{A}—\overrightarrow{H}\cdots B$	stretching ν
(2)	A↓—H↑···B	in–plane bending δ
(3)	$A^{+}—H^{-}\cdots B^{+}$	out–of–plane bending γ
(4)	$\overleftarrow{A}—H\cdots\overrightarrow{B}$	stretching σ

For symmetric systems A—H···A , (1) is an antisymmetric stretching and (4) a symmetric stretching. The most information yielding band is that due to (1) and its characteristic changes on hydrogen-bonding are the low wavenumber shift, the increase of the IR intensity and the broadening and/or appearance of submaxima. Hydrogen-bonding in polyatomic systems affects also other vibrational modes by alteration of force constants, as shown by the shifts to lower frequencies of the bands of proton-accepting groups. These shifts are accompanied also by broadening and by intensity changes, but these modes have been studied to a much lesser extent than the ν_{A-H} band.

The band shift of mode (1), defined as $\Delta\bar{\nu} = \nu_{A-H\cdot\cdot B} - \nu_{A-H}$ may be taken as an indicator of the extent of hydrogen-bonding and it is usually assumed that this shift depends only on changes in the bond A–H caused by the influence of the

proton-acceptor B. However, considering the low frequency shift as a weakening of the A–H bond is an over-simplification since the observed ν_{A-H} wavenumber depends on the dynamics of the whole hydrogen-bonded complex. A correct treatment would require the knowledge of the multidimensional potential function governing the motion of all nuclei or, at least, both stretching vibrations of the A—H···B nuclei. Hydrogen-bonded association leading to "rings" or "chains" and the influence of medium in liquid system are also factors that should be taken under consideration. The influence of the medium on $\Delta\tilde{\nu}$ presents quite a complex problem which is closely connected to the structure of liquids. It has been studied[124] on ternary systems consisting of a proton donor, a base (which may form various types of complexes with the donor) and a non-polar solvent. The bonded ν_{AH} frequency varies in general with the composition of the medium and sometimes distinct peaks were observed indicating different types of complexes with different $\Delta\tilde{\nu}$. Non-polar solvents exhibit small influence on the hydrogen-bonded complexes. However, specific interactions leading to short-lived collision complexes are also found even in non-polar solvents[125,126]

The intensity enhancement of the ν_{AH} band is very important for the study of hydrogen-bonding. It does not depend only on the polarity of the A—H bond but on the charge re-distribution in the whole hydrogen-bonded complex. The intensity of the (O—H) stretching band is determined by the changes which occur in the O—H bond moment and by changes in the hybridization of the oxygen orbitals that will affect lone-pair and overlap moments[93] Because these contributing factors do not operate necessarily in the same direction, the sign of $\partial\mu / \partial Q$ will be strongly dependent on the nature of the group attached to the OH. The ground electronic state may be described by the two extreme structures

R—O—H R—O$^-$ H$^+$

(38) (39)

Any small change in the contribution of the ionic form represented by structure (2) will result in a rather large change in dipole moment because the dipole represented by this form is large. In phenols, in which there is an interaction of

the lone pairs of the hydroxyl oxygen with the π-electron system of the ring, the charge-separated structure is stabilized by resonance and the O—H intensities of phenols are, as expected, considerably greater than those of aliphatic alcohols.

Hydrogen bonding of O—H groups to relatively strong proton acceptors results in the appearance of a distinctly separate OH band with an intensity much greater than than of the free OH.[95,123] As hydrogen bonding causes an increase of the OH bond distance the ionic character should also be increased but this effect which results in a larger contribution from the $O^- H^+$ structure would certainly affect the intensity of the bending modes of OH which is not observed. Thus, the very large increase in intensity on hydrogen-bond formation cannot be ascribed to electrostatic effects but it is better explained by delocalisation of the electron density in the proton-acceptor, Y, and can be seen as a transfer of electrons from the proton-acceptor to the proton-donor system without formally modifying the charge on the hydrogen atom.[88] This idea may be represented by the structures

$$R—O—H \cdots Y—R' \qquad R—O^- \cdots H—Y^+—R'$$

Under the usual conditions of recording the vibrational spectra, band broadening is another indicator of hydrogen-bonding and it appears to be connected with the strength of the hydrogen-bond. The band width, usually measured at half the band height is generally designated $\Delta\nu_{\frac{1}{2}}$. The broadening of the ν_{AH} band is very often accompanied by the appearance of submaxima which leads to a variety of band shapes. Several mechanisms contribute to the band broadening and shape and they participate with different weight depending on the strength of the hydrogen-bond. In disorder phases (gas, liquid, solution) an important contribution comes from the possibility of self-associating molecules which may form different sorts of hydrogen-bonded aggregates. The hydrogen-bonding in various types of aggregation differs in strength and thus causes different band shifts. Since the relative intensities of component bands are dependent on concentration and medium, the band shape usually varies with dilution. Other factors related to structural disorder in the

liquid phase influence band broadening since the hydrogen-bond oscillator is sensitive to its immediate surrounding "bath" which causes fluctuations in the A···B distance and in the internal force field, through polarization effects. The presence of submaxima in the ν_{AH} band structure was studied[127] for pyridine complexes with several phenols as well as for several other hudrogen-bonded systems[128,129] and reported to be due to combination band and overtones enhanced by Fermi resonance.

Intramolecular hydrogen-bonds

Internal hydrogen-bonds have been found in several systems and they have great influence on stability, acidity and other aspects of chemical behaviour.

The characteristics of such hydrogen-bonds depend strongly on the number of atoms constituting the rings formed by the interaction and the nature and size of the the atom to which the hydrogen-bond is formed. In systems such as *ortho*-substituted phenols[99,130,132] benzaldehydes[133] and anilines[134] it was found that five and six-membered rings lead to the stronger hydrogen-bonds, while in aliphatic diamides with carbonyl groups as acceptors the nine-membered ring gives the strongest hydrogen-bond![135] *Ortho*-nitrophenols in which a six-membered ring is formed show a strong hydrogen-bond only broken by proton-accepting solvents![132] However, it seems that the induced moment in the pseudoaromatic ring closed by the internal hydrogen-bond compensates largely for energetically unfavourable factors such as the non-linearity of the intramolecular hydrogen-bond The OH group is orientated at an angle of *ca.* 130° to the lone pair of the oxygen atom of the nitro group.[136]

Intramolecular hydrogen-bonds give rise to large shifts of the ν_{AH} band and in contrast with comparable intermolecular hydrogen-bonds, the integrated intensity is small. This is probably due to the electronic configuration of the chelate ring since the charge-transfer contribution to the usual intensity of the intermolecular hydrogen-bond is in the conjugate-chelate rings, compensated by electronic

rearrangement[88] and thus the dipole moment change with the proton vibration is small.

Early far infrared spectroscopic studies[137] in *ortho*-halogen-phenols showed that the intramolecular hydrogen-bond strength, in the vapour phase, decreases in the order F = Cl > Br > I apparently related to the order of electronegativities of the halogens and diminished in the case of the fluoride substituent by the small size of the F atom which prevents the OH group to get close enough for optimum bonding.

Spectral changes for weak intramolecular hydrogen-bonds, such as the Halogen···H—O in *ortho*-substituted phenols, with increasing polarity of the environment are very distinct and systematic. In contrast to complexes with intermolecular hydrogen-bonds, the transition from a non-polar solvent to a slightly polar one leads not to an increase but to a decrease of the ν(OH) band position accompanied by a large increase in bandwidth and a small increase in integrated intensity. This was also found, although to a lesser extent, for stronger internal hydrogen-bonds such as the one in *ortho*-nitrophenol. These observations have been explained[130-132,138-140] in terms of electrostatic interactions between the vibrating OH dipole and the random local field set up by solvent molecules.

Compounds with strong intramolecular hydrogen-bonds, such as substituted *ortho*-nitrophenols, have been found to form weak complexes with solvents such as 1,4-dioxan and by dipole-dipole interactions without significant evidence for breaking of the internal H-bond![141] The same sort of compounds interact with amines[142] with results that are dependent on the nature of the base: while aza-aromatic amines do not alter the contours of the ν_{OH} of the original phenol, i.e. leaving the intramolecular hydrogen-bond unchanged, the more basic triethylamine is able to cause the opening of the internal hydrogen-bond and in some cases even the dissociation of the phenol, depending on its pK_a, with formation of new (N^+—H···O^-) species by proton transfer.

For *ortho*-nitrophenols in polar solvents, such as CH_3CN or MeOH with pronounced proton-acceptor or proton-donor properties a high-frequency shift of

the ν(OH) band is observed[131] accompanied by significant alteration of the band shape and increase of the integrated intensity. This suggests the formation of complexes with solvent molecules in which the weakening and possibly the breaking of the intramolecular hydrogen-bond takes place.

In asserting that "*ortho*-substituted phenols with strong intramolecular hydrogen-bonds are only marginally dependent on the polarity of the medium" Bureiko *et al* (1990)[143] interpret the small upfield chemical shifts of the OH proton signal in ^{1}H NMR spectra of *ortho*-nitrophenol in presence of small amounts of DMSO and other strong proton acceptors in terms of formation of bifurcated hydrogen-bonds.

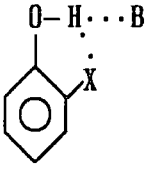

B : proton acceptor

(40)

The same explanation is given for the high-frequency shift of the gravity centre of the broad ν(OH) band of 2,6-dicarbomethoxy-4-methyl phenol on addition of a small quantity of DMSO

1.3.5. Effect of Hydrogen–bond on the proton–acceptor group

In the general case of a multiple bond X–Y where there is one or more unshared electron pairs on the more electronegative atom, donation of the unshared electron pair, either by formation of a complex or by hydrogen-bonding, lowers the ν(Y–X) frequency[145] This effect has been found for the ν(C=O) band in several compounds containing the carbonyl function;[93,143,146,147] for the very sensitive ν(P=O) band[143,145-147] and for the symmetric stretching vibration of nitro groups[95,147-149] For this last acceptor group, the antisymmetric vibration, $\nu_{as}(NO_2)$ is quite insensitive to hydrogen-bonding and $\nu_s(NO_2)$ is much more sensitive to intramolecular than intermolecular hydrogen-bonding. The lowering of the band frequency was also noticed for the ν(S=O) band of DMSO on interaction

with 2,6-disubstituted phenols[143] the shift being accompanied by a slight broadening.

Hydrogen-bonding to the nitrile group constitutes an exception in that the (C≡N) stretching frequency increases due to this process. This has been described as an interaction involving the formation of a σ molecular orbital between the occupied non-bonding orbital of the nitrogen atom and the hydrogen orbital which reduces the polarity of the C≡N bond and the ability of the nitrogen atom to withdraw electron density from the bonding π-orbitals of the triple bond[153] In early studies, it was suggested, from NMR results, that the association between nitriles and phenols takes place by means of the π-electrons of the triple CN bond and the OH proton is located perpendicularly to the triple bond of the nitrile group[154,155] For aromatic nitriles, such as benzonitrile, it has been observed that their interaction with phenol causes a shift to higher frequency and a broadening of the ν(CN) band by a factor of about two but the frequency and bandwidth of the ν(CN) band benzonitrile in aliphatic alcohols is nearly the same as in inert solvents.[140] It seems that the π-electron system of the phenyl group, either the one attached to the OH or the one bonded to the nitrile, have an important role here. In the benzonitrile, a molecular orbital is formed from the HOMO of the phenyl ring and the LUMO (π^*) of the nitrile group.[83] There is "transfer" of electron density from the ring to the nitrile group to an extent which depends on the relative energy of the orbitals. When a hydrogen-bond is formed involving the nonbonding orbital of the nitrogen atom, the energy of both the bonding and antibonding π orbitals of the nitrile group is lowered as a result of this interaction, decreasing the energy difference and increasing the interaction between the nitrile orbital and the ring orbital. In other words, the possibility of a variable interaction with the ring may compensate the effect of the hydrogen-bond to methanol or ethanol by keeping approximately unchanged the electronic structure of nitrile group.[140] However, the result of this interaction may not be enough to balance the stronger[157,158] hydrogen-bond formed with phenols.

References

1 Burwell, R.L., *Chem. Rev.* (1954), 54, 615

2 Miller, J., "*Nucleophilic Aromatic Substitution*", Elsevier, Amsterdam, 1968

3 Strauss, M.J., *Chem Rev.* (1970), 70, 667

4 Artamkina, G.A.; Egrorov, M.P.; Beletskaya, I.P., *Chem Rev.* (1982), 82, 427

5 Buncel, E.; Crampton, M.R.; Strauss, M.I., Terrier, F., "*Electron Deficient Aromatic and Heteroaromatic – Base Interactions. The Chemistry of Anionic Sigma Complexes*", Elsevier, Amsterdam, Oxford, N.Y., Tokyo, 1984

6 Tiecco, M., *Synthesis*, (1988), 749

7 Testaferri, l.; Tiecco, M.; Tingoli, M; Chianelli, D.; Montanucci, M., *Synthesis*, (1983), 751

8 Page, I.D.; Pritt, J.R.; Whiting, M.C., *J. Chem. Soc. Perkin Trans. II*, (1972), 906

9 Jackson, C.J.; Gazzolo, F.H., *Amer. Chem. J.* (1900) 23, 376

10 Meisenheimer, *J. Ann.*, (1902), 205

11 Meyer, V., *Ber.* (1894) 27, 3153

12 Lobry de Bruyn, M.C.; van Leent, F.H., *Recl. Trav. Pays–Bas*, (1895) 14, 150

13 Terrier, F., *Chem. Rev.*, (1982) 82, 77

14 Pollitt, R.J.; Saunders, B.C., *J. Chem. Soc.*,(1964) 1132

15 Crampton, M.R.; Gold, V.; *J. Chem. Soc.*,(1964) 4293

16 Gold, V.; Rochester, C.H., *J. Chem. Soc.*, (1964) 1687

17 Servis, K.L., *J. Am. Chem. Soc.*, (1967) 89(6), 1508

18 Simmonin, M.P.; Lecourt, M.J.; Terrier, F.; Dearing, C.A., *Can. J. Chem.*, (1972) 50, 3558

19 Crampton, M.R.; Khan, H.A., *J. Chem. Soc. Perkin Trans. II*, (1972), 1173

20 Millott, F.; Terrier, F., *Bull. Soc. Chim. France*, (1969) 2692

21 Fendler, J.H.; Fendler, E.J.; Griffin, C.E., *J. Org. Chem.*, (1969) 34, 689

22 Terrier, F.; Halle, J.–C.; Simmonin, M.P., *Org. Magn. Res.*, (1971) 3, 361

23 Fendler, E.J.; Fendler, J.H.; Griffin, C.E.; Larsen, J.W., *J. Org. Chem.*, (1970) 35, 289

24 Cooney, A.; Crampton, M.R., *J. Chem. Soc. Perkin Trans. II*, (1984), 1793

25 Terrier, F.; Millot, F.; Leteillier, P. *Bull. Soc. Chim. France*, (1970), 1743

26 Fendler, J.H.; Larsen, J.W. *J. Org. Chem.*, (1976) 37, 2608

27 Destro, R.; Gramacioli, C.M.; Simonetta, M., *Acta Cryst. B24*, (1968) 1369

28 Veda, H.; Sakabe, N.; Tanaka, J.; Furusaki, A., *Bull. Chem. Soc. Japan*, (1968) 41, 2866

29 Nudelman, N.S.; MacCormack, P., *J. Chem. Soc. Perkin Trans. II*, (1987), 227

30 Cody, V.; Hazel, J.; Lehmann, P.A., *Acta Cryst.*, (1978) 3349

31 Grimacioli, C.M.; Destro, R.; Simonetta, M., *Chem. Commun.*, (1967), 331; *Acta Cryst.*B24, (1968), 129

32 Olah, G.A.; Mayr, H., *J. Org. Chem.*, (1976) 41, 3348

33 Caveng, P.; Fischer, P.B.; Heilbronner, E.; Miller, A.L.; Zollinger, H., *Helv. Chim. Acta*, (1967) 50, 848

34 Hasoya, H.; Hasoya, S.; Nagakura, S., *Theorect. Chim. Acta*, (1978) 12, 117

35 Wennerstrom, H.; Wennerstrom, O., *Acta Chem. Scan.* (1972) 26, 2283

36 Kamiskaya, E.G.; Gitis, S.S.; Kaminskii, A.Ya., *Dokl. Akad. Nauk SSSR*, (1975) 221, 617

37 Dickeson, J.E.; Dyall, L.K.; Pickles, V.A., *Austr. J. Chem.*, (1968) 21, 1287

38 Brown, J.F., *J. Am. Chem. Soc.*, (1955) 77, 6341

39 Dyall, L.K., *J. Chem. Soc.*, (1960) 5160

40 Kross, R.D.; Fassel, V.A., *J. Am. Chem. Soc.*, (1956) 78, 4225

41 Bellamy; Lake; Place, *Spectrochim. Acta*, (1963), 19, 443

42 Ohsawa, S.; Takeda, M., *Ibaraki Daigaku Kogakubu Kenkyo Shuhu*, (1980) 28, 101

43 Gropen, O.; Skancke, P.N., *Acta Chem. Scand.*, (1969) 23, 2685

44 Bernasconi, C.F., *J. Am. Chem. Soc.*, (1970) 92, 4682

45 Crampton, M.R., *Adv. Phys. Org. Chem.*, (1969) 7, 221

46 Foster, R.; Fyfe, C.A.; Morris, J.W., *Rec. Trav. Chim.*, (1965) 84, 516

47 Crampton, M.R., *J. Chem. Soc. Perkin Trans. II*, (1973) 2157

48 Fendler, J.F.; Fendler, E.J.; Merritt, M.V., *J. Org. Chem.*, (1971) 36, 2172

49 Bernasconi, H.F.; Cross, H.S., *J. Org. Chem.*, (1974) 39, 1054

50 Drozd, V.N.; Knyazev, V.N.; Klimov, A.A., *J. Org. Chem. USSR*, (1974) 10, 828

51 Bunton, C.A.; Cuenca, A., *J. Org. Chem.*, (1987) 52, 901

52 Bunton, C.A.; Moffatt, J.R., *J. Phys. Chem.*, (1988) 92, 2896

53 Cipiciani, A.; Fracassini, M.C.; Germani, R.; Savelli, G.; Bunton, C.A., *J. Chem. Soc. Perkin Trans. II*, (1987) 547

54 Broxton, T.J.; Christie, J.F.; Chung, R.P.–T., *J. Phys. Org. Chem.*, (1989) 2, 519

55 Broxton, T.J.; Chung, R.P.–T., *J. Org. Chem.*, (1990) 55, 3886

56 Bernasconi, C.F.; Gehriger, C.L.; Rossi, R.H., *J. Am. Chem. Soc.*, (1976) 98, 8451

57 Terrier, F.; Millott, F.; Morel, J., *J. Org. Chem.*, (1976) 41, 3892

58 Crampton, M.R., *J. Chem. Soc. B*, (1968) 1208

59 Crampton, M.R.; Ghariani, M.A.; Khan, H.A., *J. Chem. Soc. Perkin Trans. II*, (1972) 1178

60 Terrier, F.; Millot, F.; Schall, R., *J. Chem. Soc. Perkin Trans. II*, (1972) 1192

61 Miller, J.; Moran, P.J.G., *J. Chem. Res.*, (1980)M, 501

62 Terrier, F.; Millot, F.; Norris, W.P., *J. Am. Chem. Soc.*, (1976) 98, 5883

63 Crampton, M.R.; Khan, H.A., *J. Chem. Soc. Perkin Trans. II*, (1972), 2286

64 Crampton, M.R.; Khan, H.A., *J. Chem. Soc. Perkin Trans. II*, (1973), 1103

65 Szwarc, M., ed. "*Ions and Ion Pairs in Organic Reactions*", Wiley, N.Y., *vol.1*, 1972, *vol.2*, 1974

66 Barthel, J.; Wachter, R.; Knerr, M., *Electrochim. Acta*, (1971) 825

67 Crampton, M.R., *J. Chem. Soc. Perkin Trans. II*, (1975), 825

68 Crampton, M.R., *J. Chem. Soc. Perkin Trans. II*, (1977), 1442

69 Crampton, M.R.; Gibson, B.; Gilmore, F.W., *J. Chem. Soc. Perkin Trans. II*, (1979) 44, 3921

70 Sekiguchi, S.; Hirose, T.; Tsutsumi, K.; Aizawa, T.; Shizuka, H., *J. Org. Chem.*, (1979) 44, 3921

71 Alaruri, A.D.A.; Crampton, M.R., *J. Chem. Res.* (1980)S, 140; M, 2157

72 Sekiguchi, S.; Aizawa, T.; Aoki, M., *J. Org. Chem.*, (1981) 46, 3657

73 Bernasconi, C.F.; Gandler, J.R., *J. Org. Chem.*, (1977) 42, 3387

74 Bernasconi, C.F.; Howard, K.A., *J. Am. Chem. Soc.*, (1982) 104, 7248

75 Crampton, M.R., *J. Chem. Soc. Perkin Trans. II*, (1973), 2157

76 Bernasconi, C.F.; Muller, C.M., *J. Am. Chem. Soc.*, (1978) 100, 5530

77 Sekiguchi, S.; Aizawa, T.; Tomoto, N., *J. Org. Chem.*, (1981) 46, 3657

78 Rochester, C.H., *J. Chem. Soc.*, (1965), 2404

79 Rochester, C.H., *Acidity Functions*", Academic Press, London, 1970

80 Bagno, A.; Scorrano, G., *J. Chem. Soc. Perkin Trans. II*, (1990), 1017

81 More O'Ferrall, R.A.; Ridd, J.H. *J. Chem. Soc.* (1963), 5030, *ibid*, 5035

82 Hehre, W.J.; Radom, L.; Pople, J.A. *J. Am. Chem. Soc.*, (1972), 94, 149

83 Pross,A.; Radom, L. *Prog. Phys. Org. Chem.* (1981), 13, 1

84 Topsom, R.D. *Prog. Phys. Org. Chem.* (1976), 12, 1

85 Topsom, R.D. *Prog. Phys. Org. Chem.* (1987), 16, 85; *ibid.*, 125

86 Taft, R.W.; Topsom, R.D. *Prog. Phys. Org. Chem.* (1987), 16, 1

87 Topsom, R.D. *Prog. Phys. Org. Chem.* (1987) 16, 193

88 Seguin, J.P.; G–Vilport, F; Uzan, R.; Doucet, J.P. *J. Chem. Soc. Perkin Trans. II* (1986), 773

89 Exner, O.; Folli, V.; Marcaccidi, S.; Vivarelli, P. *J. Chem. Soc. Perkin Trans. II* (1983), 757

90 Fraser, R.R.; Strothers, J.B.; Ragauskas, A.J. *J. Am. Chem. Soc.*, (1982), 104, 6475

91 Craik, D.J.;Levy, G.C.; Brownlee, R.T.C. *J. Org. Chem.* (1983), 48, 160

92 Libit, L.; Hoffmann, R. *J. Am. Chem. Soc.*, (1974), 96, 1370

93 Hadži, D. in "*Infrared Spectroscopy and Molecular Structure*", ed. M. Davies, Elsevier, London, 1963

94 Popov *et al, Optics and Spect.* (1963), 15, 174

95 Bellamy, L.J. "*The Infrared Spectra of Complex Molecules*", Chapman and Hall, London, 1980

96 Kross, R.D.; Fassel, V.A. *J. Am. Chem. Soc.*, (1956), 78, 4225

97 Brown, T.L., *Chem. Rev.*, (1958), 58, 581

98 Katritzky, A.R.; Topsom, R.D. *Angew. Chem.* (1970), 9, (2), 87

99 Lipkowitz, L.B. *J. Am. Chem. Soc.*, (1982), 104, 2647

100 Krygowski, T.M. *Prog. Phys. Org. Chem.* (1990), 1, 239

101 Krygowski, T.M.; Anulewicz, R.; Kruszewski, J. *Acta Cryst.* (1983), B39, 732

102 Vorpagel, E.R.; Streitweiser, A.; Alexandratos, S.D. *J. Am. Chem. Soc.*, (1981), 103, 3777

103 Brownlee, R.T.C.; Cameron, D.G.; Topsom, R.D.; Katritzky, A.R.; Pozharsky, A.F. *J. Chem. Soc. Perkin Trans. II* (1974), 247

104 Hiberty, P.C.; Ohasessian, G. *J. Am. Chem. Soc.*, (1984), 106, 6963

105 Deady, L.; Katritzky, A.R.; Shanks, R.A.; Topsom, R.D. *Spectrochim. Acta* (1973), 29A, 115

106 Binev, I.; Kuzmanova, R.; Kaneti, K.; Yukhnovski, I. *Izv. Khim.* (1981), 14(7), 470

107 Reichardt, C. "*Solvent Effects in Organic Chemistry*" Weinheim, N.Y., 1978

108 Rao, C.N.R.; Singh, S.; Senthilnathan, V.P. *Chem. Soc. Rev.* (1976), 5, 277

109 Jauquet, M.; Laszlo, P. in "*Solutions and Solubilities*" vol.III(1) Wiley Interscience, N.Y., 1975

110 Joesten, M.D.; Schaad, L.J. in "*Hydrogen Bonding*", ed. M. Dekker, N.Y., 1974

111 Agami, C. *Bull. Soc. Chim. Fr.* (1969), 2183

112 Thompson, H.W.; Jewell, D.J. *Spectrochim. Acta* (1958), 13, 254

113 Burden, A.G.; Collier, G.; Shorter, J. *J. Chem. Soc. Perkin Trans. II* (1976), 1627

114 Oi, N.; Coetzee, J.F. *J. Am. Chem. Soc.*, (1969), 91, 2473

115 Horák, M.; Pliva, J. *Spectrochim. Acta* (1965), 21, 911

116 Hallam, H.E. *J. Mol. Struct.* (1969), 3, 43

117 Hallam, H.E. in "*Infrared Spectroscopy and Molecular Structure*" ed. M. Davies, Elsevier, London, 1963

118 Buckingham, A.D. *Proc. Roy. Soc. London*, Ser. A (1957), 248, 169

119 Kakimoto, M.; Fujiyama, T.; *Bull. Chem. Soc. Japan* (1975), 48, 2258

120 Fruwert, J.; Geiseler, G.; Luppa, D. *Z. Chem.* (1968), 8, 238

121 Brown, T.L. *Spectrochim. Acta* (1957), 10, 149

122 Bellamy, L.J.; Hallam, H.E. *Trans. Faraday Soc.* (1959), 54, 220

123 Hadži, D.; Bratos, S. in "*The Hydrogen Bond*" vol.II ed. P. Schuster, G. Zundel, C. Sandorfy, North-Holland Publ. Corp., Amsterdam, N.Y., Oxford, 1976

124 Allerhand, A.; Schkyer, P.R., *J. Am. Chem. Soc.*, (1963), 85, 371

125 Horák, M.; Moravec, J,; Pliva, J. *Spectrochim. Acta* (1965), 21, 919

126 Osawa, E.; Yoshida, Z.I. *Spectrochim. Acta* (1976), 23A, 2029

127 Hall, A.; Wood, J.L. *Spectrochim. Acta* (1967), 23A, 1257

128 Iogansen, A.V. *Opt. Spectry.* (1968), suppl.3, 113

129 Dementyeva, L.A.; Iogensen, A.V. *Opt. Spectry.* (1970), 29, 868

130 Broda, M.A.; Hawranek, J.P. *Spectrochim. Acta* (1987), 43A, 617

131 Hawranek, J.P.; Broda, M.A. *Chem. Phys. Lett.* (1983), 98, 373

132 Schreiber, V.M. *J. Mol. Struct.* (1989), 197, 73

133 Brzezinsky, B.; Paszyl, S.; Zundel, G. *Chem. Phys. Lett.* (1990), 167(1), 7

134 Denisov, G.S.; Kuzina, L.A.; Miller, A.O.; Smolyanskii, A.L.; Furin, G.G. *Zh. Prikl. Spektr.* (1989), 51(2), 278

135 Gellman, S.H.; Addams, B.R. *Tetrahedron Lett.* (1989), 30, 3381

136 Leavell, S.; Curl, R.F. *J. Mol. Spectrosc.* (1973), 45, 428

137 Carlson, G.L.; Fateley, W.G.; Manocha, A.S.; Bentley, F.F. *J. Phys. Chem.* (1972), 76, 1553

138 Janoschek, R.; Weidemann, E.G.; Zundel, G. *J. Chem. Soc. Faraday* II (1973), 69, 505

139 Nösch, N.; Ratner, M.A. *J. Chem. Phys.* (1974), 61, 3344

140 Yuchnovsky, I.N.; Binev, I.G., "*Infrared Spectra of Cyano and Isocyano Groups*", The Chemistry of Functional Groups, Suppl. C., Ed. S. Patas and Z. Rappoport, Wiley, N.Y., 1982

141 Magee, M.D.; Walker, S. in "*Molecular Relaxation Processes*" ed. the Chemical Society and Academic Press, London, N.Y., 1966

142 Lutskii, A.E.; Klepanda, T.I.; Sheina, G.G.; Batrakova, L.P. *Zh. Prikl. Spectr.* (1976), 25(4), 735

143 Bureiko, S.F., Golubev, N.S. Mattinen, J.; Pihlaja, K. *J. Mol. Liq.* (1990), 45, 139

144 Katritzky, A.R.; Topsom, R.D., *Chem. Rev.*, (1977), 77(5), 639

145 Rose, J. "*Molecular Complexes*", Pergamon Press, Oxford, 1967

146 Rasmusson, R.S.; Brattain, R.R. *J. Am. Chem. Soc.*, (1949), 71, 1073

147 Bellamy, L.J.; Pace *Spectrochim. Acta* (1963), 19, 1831

148 Aksnes, G.; Gramstad, T., *Acta Chim. Scand.* (1960), 14, 1485

149 Aksnes, G. *Acta Chim. Scand.* (1960), 14, 1475

150 Baitinger, ; Schleyer, ; Murty, ; Robinson *Tetrahedron* (1964), 20, 1635

151 Danilova, ; Smakova *Bull. Tech. Inst. Tomsk.* (1962), 91

152 Granzhan, V.A.; Semenenko, S.V.; Zaitsev, P.H.; *Zh. Prikl. Spektr.* (1970), 12(5), 922

153 Yarwood, J. "*Spectroscopy and Structure of Molecular Complexes*", Plenum Press, London, N.Y., 1973

154 Baraton, M.I.; *J. Mol. Struct.* (1971), 10, 231

155 Gramstadt, T.; Simmonsen, O.R. *Spectrochim. Acta* (1976), 32, 723

156 Gramstadt, T.; Tjessem, K. *J. Mol. Struct.* (1977), 41, 231

157 Abramczyk, H.; Reimshüssel, W. *Chem. Phys.* (1985), 100, 243

Chapter 2
Dealkylation of Aryl Alkyl Ethers

2. Dealkylation of Aryl Alkyl Ethers

2.1 Introduction

The cleavage of aryl alkyl ethers (1) is a reaction with wide use in synthesis as a simple method for the production of phenols and to obtain other ethers in transalkylation reactions[1] Several methods of dealkylation have been

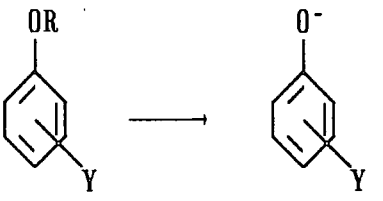

(1) (2) (2–1)

investigated[1,2,3] in each case the reaction leads to the formation of the phenolates which are readily protonated by acidification. Similar procedures were performed with thioethers and selenoethers with the formation of thiophenolates and selenophenolates, respectively.

Cleavage may be induced by acids such as hydrogen halides

$$ArOR + HX \rightleftharpoons RX + ArOH \qquad X : \text{halogen} \qquad (2\text{–}2)$$

In the gas phase or in the concentrated HX conditions required for the reaction to take place, the neutral phenols, ArOH, are produced directly[3,4] Cleavage in acid solution requires equilibrium protonation of the ether oxygen atom prior to nucleophilic displacement of phenol from the alkyl carbon by the halide ion. Such protonation serves to polarize the alkyl carbon-oxygen bond making the carbon more susceptible to nucleophilic attack and converts phenoxide into a neutral phenol leaving group.

In acidic media, dealkylation is usually a slow reaction[4] that occurs only at high temperatures, the conditions depending strongly on both the nature of the alkyl group (phenetoles reacting more easily than anisoles) and on the nature and

number of substituents on the aromatic ring: while 2-bromo-4-nitrophenetole reacts with sulphuric acid, 80% at 100°C, to give the corresponding phenol with a fairly high yield, anisole under the same conditions is disulphonated but not demethylated[3].

There have been several studies on the reactions of alkyl aryl ethers and similar compounds, such as thio– and selenoethers, with nucleophiles and different reacting sites have been characterized. These compounds are able to undergo a large variety of reactions via different mechanisms each dependent on several factors, from the nature of the nucleophile and the structure of the aromatic substrate to the type of solvent in which the reaction takes place and its degree of interaction with all the reacting species. Dealkylation reactions in neutral or slightly basic conditions have been used to establish the nucleophilicity order of molecules and ions in different solvents[5,6,7,8] In these conditions, the ether generally undergoes nucleophilic aliphatic substitution via an S_N2 mechanism.

$$Y + RX \longrightarrow [YRX] \longrightarrow YR + X \qquad (2\text{–}3)$$

the nucleophile Y being a neutral molecule or a negative ion, providing it is not a very strong base, in which case other reactions may occur, such as elimination or or attack at a ring carbon. The neutral species most widely used are nitrogen nucleophiles such as amines[7,40] pyridine, imidazole, and thiourea[6]; sulphoxides have been reported to be demethylating agents for arenesulphonates and alkyl halides[31] Sulphur nucleophiles such as methanethiolate ions are very good dealkylating reagents for synthetic purposes[12] Ethanethiolate ions in DMF demethylate substituted anisoles with high yields being achieved in about three hours at 100°C, although the reactions are quite slow at room temperature[13] Lithium iodide in boiling pyridine or collidine is quite able to cleave the ArO–Me bond in several compounds[4,14] including *ortho*-anisic acid but not *para*-anisic acid, suggesting that an intramolecular hydrogen bond, as shown in (3), can stabilise the incipient phenoxide ion thus favouring the nucleophilic attack by the halide ion[15]

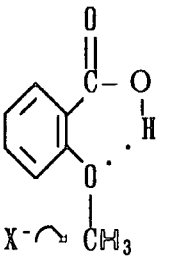

(3)

Similar intramolecular interactions have been investigated in the demethylation of several salicylates[16,17] In pyridine, only iodide salts are able to attack the alkyl group effectively but in boiling DMF chlorides were found to dealkylate aryl ethers with reasonable yields[4] Sodium cyanide in DMSO is a good demethylating agent for most aryl alkyl ethers, the conversion being completed in 5 – 48 hours at high temperatures of 160 – 180°C. However, cyanide ions in DMSO do not demethylate nitroaromatic ethers due to the occurence of the von Richter reaction[4,18,19]

The high reactivity of the alkyl aryl ethers is a consequence of the relative positive charge carried by the oxygen atom due to effects of through conjugation with the ring[20,21] Resonance structures such as (4) and (5) become particularly

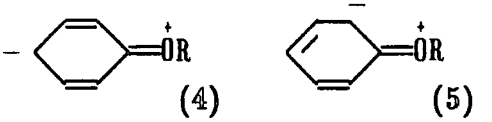

(4) (5)

important when there are electron-withdrawing groups in *ortho*– or *para*– position to the alkoxy group[3,20] The removal of electron density from the oxygen atom favours the nucleophilic attack at the alkyl group; in other words, electron-accepting substituents increase the leaving group ability of aryloxide ions[22]

The high sensitivity of the reaction to a wide range of experimental factors is easily understandable if it is taken in account that the charge distribution effects which facilitate the S_N2 reaction may also favour a reaction by the S_NAr mechanism[1,2] with possible formation of σ-adducts. The same mechanism is probable when the attacking species is a strong base such as an alkoxy anion, which usually attacks the ring carbon leading to the formation of another aryl

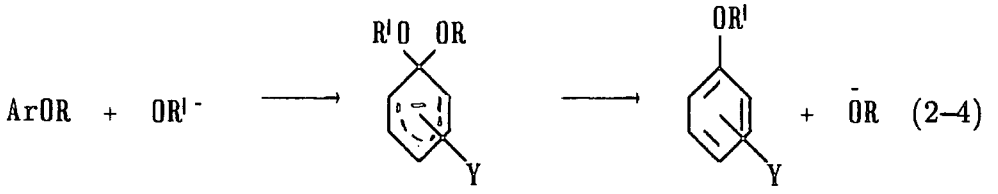

alkyl ether when R ≠ R' . However, reactions of strong bases with an ether carrying a branched alkyl group may give selective elimination.

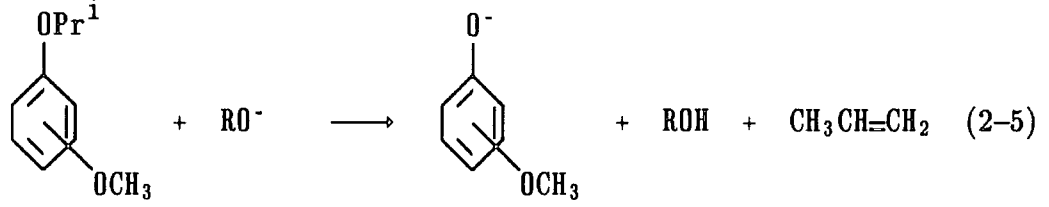

The attack at the hydrogen atom of the isopropyl group is much faster than the attack at the carbon atom of a methyl group[23]

2.2 Demethylation of 2,4,6-trinitroanisole (TNA)

TNA reacts with amines by both S_NAr and S_N2 mechanisms, depending mainly on the type of amine and solvent. In methanol, picramides may be formed via σ-adduct intermediates[24]; in aprotic solvents like acetone, chloroform or toluene[7] TNA is promptly attacked by a tertiary amine, such as triethylamine, and demethylation occurs via S_N2 reaction, leading to the formation of picrate[10] as shown in (6). In mixtures containing diethylamine,

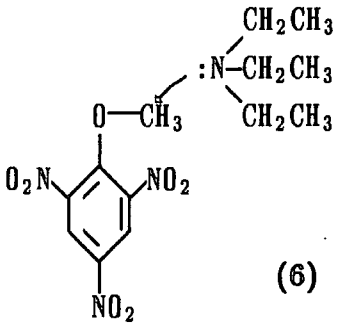

(6)

TNA reacts preferentially with it, possibly because the transition state for demethylation can be stabilized by hydrogen bonding[7,25] as shown in (7).

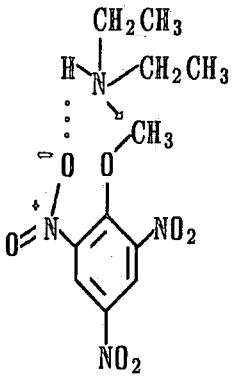

(7)

TNA was found to have methylating properties towards several iodides in DMSO[26,27] Other halides also undergo efficient methylation by TNA; the time required for the reactions to occur, monitored by ^{1}H NMR is stated[26] to be from a few minutes up to a week, depending on the nature of the reagent, solvent and presence of 18-crown-6-ether. Reacting with DMSO itself, TNA is converted to picric acid to an extent of 50% within a week. A similar reaction happens between 2,4,6-tricyanoanisole and iodide or thiocyanate ions in DMSO, though in these cases the reaction is very slow. Also in methanol, the conversion of TNA into picrate, or picric acid, has been found to occur although it is a very slow reaction,

$$\begin{array}{ccccccccc} \mathrm{ArOMe} & + & \mathrm{MeOH} & \rightleftharpoons & \mathrm{ArO^-} & + & \mathrm{H^+} & + & \mathrm{Me_2O} \\ & & & & \downarrow\uparrow & & & & \\ & & & & \mathrm{ArOH} & & & & \end{array} \qquad (2\text{–}6)$$

$k = 5.4 \times 10^{-7}$ lmol^{-1}s^{-1} at 59°C.[9] Chloride ions in methanol do not compete in the conversion but iodide competes with methanol for the demethylation of TNA.

$$\mathrm{TNA} + \mathrm{I^-_{(MeOH)}} \longrightarrow \mathrm{Picrate} + \mathrm{MeI} \qquad (2\text{–}7)$$

The same reaction occurs in acetonitrile and is considerably faster than in methanol.

It is well established that the rates of S_N reactions in solution are strongly dependent on solvation factors.[28,29] Most of the reported dealkylation reactions are faster in dipolar aprotic than in protic solvents and reactions that do not occur in protic media may become possible in a dipolar aprotic one.

Because in the course of a nucleophilic substitution reaction a new bond is formed between the substrate and a free electron pair of the nucleophile, a reagent should be the more nucleophilic the more readily the electron pair can be engaged in a chemical bond.[30] Thus, the nucleophilicity of a negative ion might be proportional to its basicity.

In the course of the activation process, the solvent shell of the nucleophile must be removed while a new solvation shell is formed around the activated complex. So, the activation energy will be higher the more strongly the molecules of the solvent are bound to the nucleophile: the less solvated a nucleophile is, the more reactive it will be. Small anions with a large charge density, which are strong hydrogen bond acceptors are more stongly solvated by protic solvents.[28,32,33] For the common dipolar aprotic solvents, the dipole moment is larger than in aprotic solvents and the negative end of the dipole is more fully exposed. Thus, cations are very well solvated, probably better than in protic media.[6,32] With the positive end of the dipole well shielded and lacking the ability to form hydrogen bonds with anions, aprotic solvents interact poorly with small anions although they solvate large anions to an extent comparable with protic solvents due to mutual polarizability interactions.[30]

Especially for halide ions, the relative reactivity is completely reversed in both classes of solvent: the "traditional" order of halide nucleophilicities $I^- > Br^- > Cl^- > F^-$ applies only when the nucleophile is deactivated through solvation by protic solvent, whereas the natural order $Cl^- > Br^- > I^-$ is observed in dipolar aprotic solvents.[34] For example, the reaction

$$CH_3{-}OTs + X^- \longrightarrow CH_3{-}X + TsO^- \qquad (2\text{–}8)$$

has been studied in both classes of solvents showing the sequence of decreasing reactivity of $CH_3O^- > I^- > SCN^- > \simeq CN^- > Br^-$ in methanol, at 25°C [31] and $HO^- \simeq CH_3O^- > F^- > N_3^- > Cl^- > Br^- > I^- > SCN^-$ in DMSO, 25°C[35,36] The sequence for the reaction between methyl bromide and anions in the gas phase is $HO^- > CH_3O^- \simeq F^- > CH_3S^- >> CN^- > Cl^- > Br^-$ [37,38,39,40] and is opposite to the one found for the same reaction in methanol[41] Nucleophilic reactivities of anions obtained in the gas phase are approximately the same order as in dipolar aprotic solvents[37,39]; this suggests that specific solvation of anions is responsible for the reversed order obtained in protic solvents relative to the dipolar aprotic ones.

In the present work, the dealkylation reactions of some ring-activated aromatic ethers have been investigated using ^1H NMR, Infrared and U.V./visible spectroscopic methods. The kinetics of these reactions were studied using U.V./visible and ^1H NMR techniques. Most work relates to DMSO as solvent although measurements were also made in acetonitrile and in water. The only previous kinetic study[9] relates to reactions of 2,4,6-trinitroanisole in methanol and was limited to the observation that demethylation was accelerated by iodide ions while chloride ions were ineffective.

The reactions under investigation in this work may be presented by the scheme:

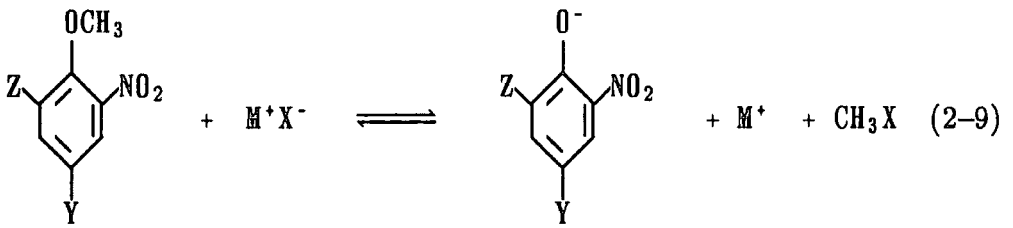

(8) (9)

a) $Z = Y = NO_2$
b) $Z = NO_2$, $Y = CN$ X = halide
c) $Z = CN$, $Y = NO_2$

The infrared spectra of both 4-cyano-2,6-dinitroanisole (8b) and 2-cyano-4,6-dinitroanisole (8c), either in the solid state or dissolved in methanol, dichloromethane or benzene, show a single band at 2240 ± 2 cm^{-1}, corresponding to the stretching vibration of the C≡N bond. However, when the solvent is DMSO or DMF and potassium bromide windows are used in the liquid holder cell, two bands appear in this region of the spectrum, one at 2240 cm^{-1} and another at 2215 cm^{-1}, the intensity of the latter increasing with time. This effect, shown in Figure 2–1, is prevented by the use of calcium fluoride windows. The potassium salts of (9b) and (9c) prepared independently show one single band at 2215 cm^{-1} due to CN vibration.

The ^1H NMR spectrum of (8b) in DMSO.d_6 shows two singlets at δ 8.94 (ring protons) and δ 4.04 (methoxy group protons) relative to internal TMS. With the addition of solid dry potassium bromide two other singlets appear at δ 8.10 and δ 2.72, their intensities increasing with time at expense of the lines of the pure substituted anisole. Similar effects were noticed for addition of potassium iodide (δ 8.12 and δ 2.19) and potassium chloride (δ 8.08 and δ 3.07). Potassium fluoride does not dissolve in DMSO. The potassium salt of (9b) prepared independently shows a singlet at δ 8.12, confirming that the phenoxide ion is formed from the methyl ether. The assignment of the new line between 2–3 ppm to the methyl halide was confirmed by the spectra in [$^2H_6$]–DMSO of commercially available methyl iodide, δ 2.18 (lit. δ 2.16[42]), methyl bromide, δ 2.69 (lit. δ 2.65[42]). For methyl chloride, the chemical shift is reported to be δ 3.10[42]

Conversion of (8) and similar ethers to the corresponding phenoxides was also found in pure DMSO. For (8b), a singlet at δ 8.17 grows in intensity, at expense of the line at δ 8.94 of the parent compound, together with a singlet at δ 4.00. The ^1H NMR spectrum recorded one week after dissolving (8b) in DMSO.d_6 revealed relative intensities of 8b : 9b of 8 : 3 (Figure 2–2b). The reaction of (8c) with DMSO causes a decrease of the intensity of its lines at δ 9.06 (multiplet) and δ 4.26

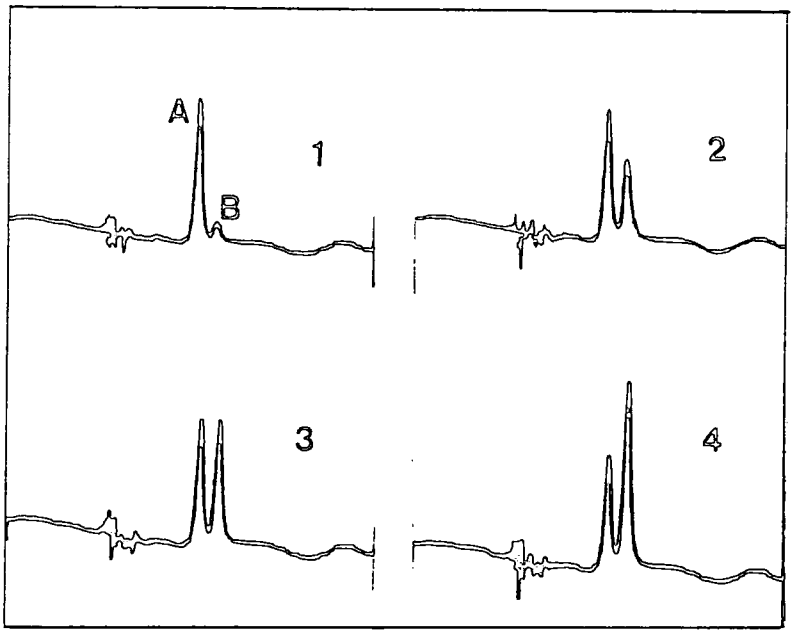

FIGURE 2-1

Infrared spectra of 4-cyano-2,6-dinitroanisole in DMSO, in the υ(CN) region, between 2300-2150 cm^{-1}.

Spectra 1,2,3 and 4 were recorded with 10 minute intervals.

Band A, 2240 cm^{-1}, corresponds to the anisole.

Band B, 2215 cm^{-1}, is assigned to the phenolate ion.

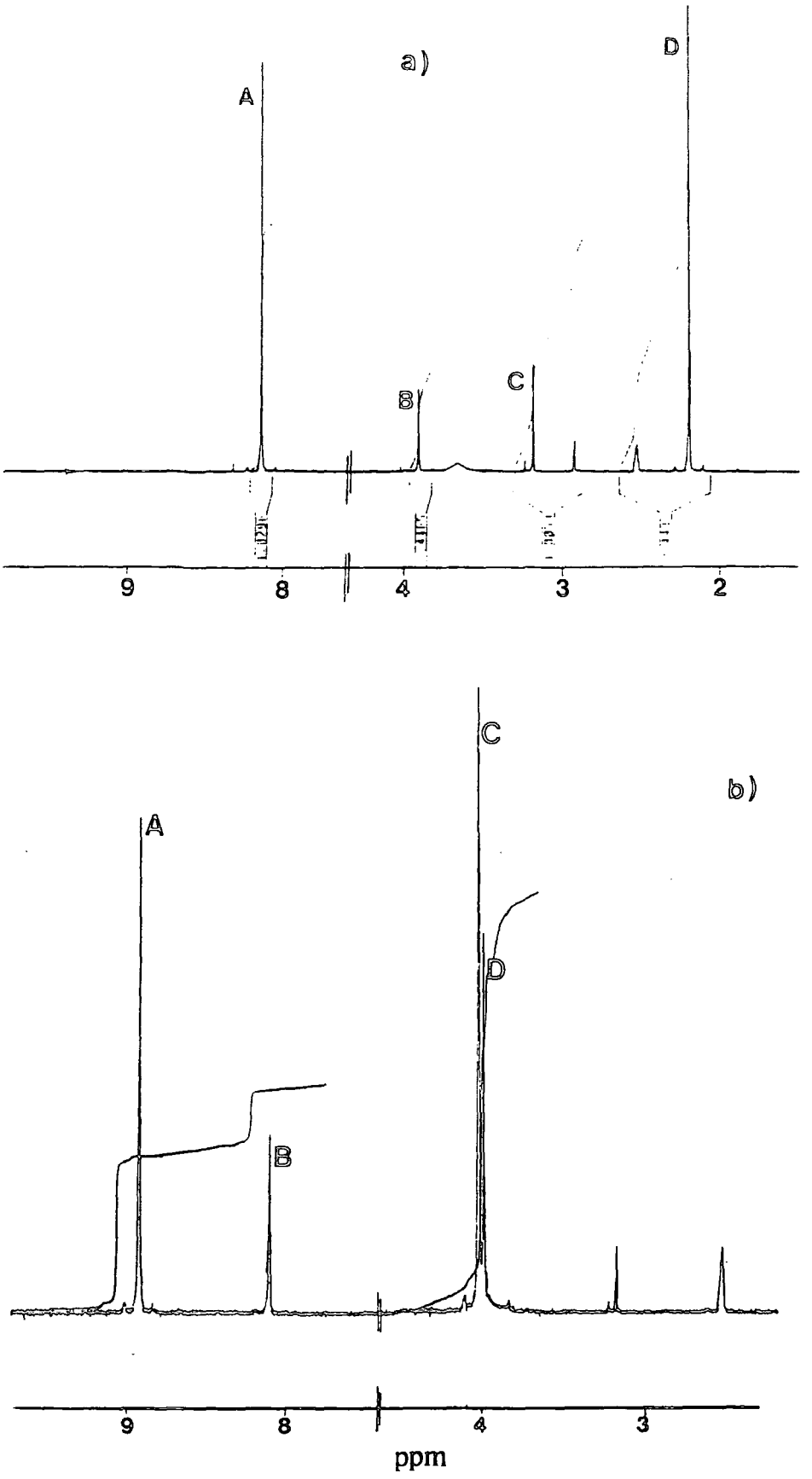

Figure 2–2 ^{1}H NMR spectra of 4CDNA in DMSO.d_6

a) Reaction with KI

A: 2–CN–4,6–dinitrophenoxide $\delta(H_3,H_5)$: 8.12

B: $[DMSO\cdot CH_3]^+$ C:MeOH D: $\delta(CH_3I)$: 2.19

b) with DMSO, one week at room temperature

A,C: 4CNDNA B: 2–CN–4,6–dinitrophenoxide D:$[DMSO\cdot CH_3]^+$

(singlet) and the appearance of two new doublets centred at δ 8.62 and δ 8.35, J = 3.5 Hz, attributed to (9c), and a singlet at δ 3.99. After one week at room temperature the proportion ether : phenoxide was 5 : 4 (Figure 2–3).

2,4,6-Trinitroanisole (8a) is converted to picrate by DMSO, the increasing lines appearing at δ 8.60, due to (9a), and δ 4.00; a ratio of two parts (8a) to nine parts (9a) was found after a week. In all cases, a small amount of methanol, δ 3.17, is formed. The ^{1}H NMR results are summarised in Table 2–1.

The dealkylation of some other 1-X-2,4,6 triactivated benzenes in DMSO was also studied and it was found that 2,4,6-trinitrophenetole (10) is dealkylated by halide ions in DMSO to give picrate.

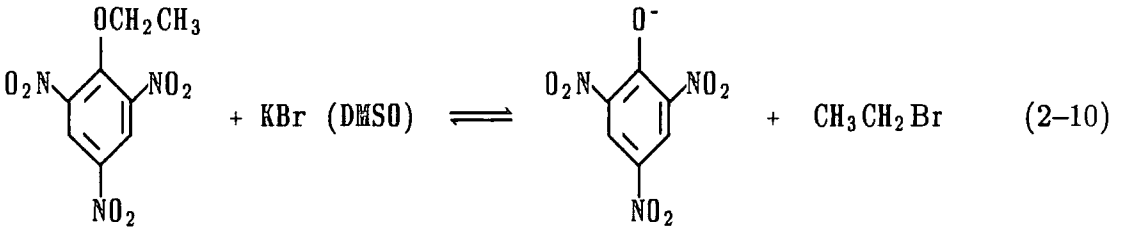

(2–10)

(10)

The ^{1}H NMR spectrum of (10) (Fig. 2–4a) shows peaks at δ 9.10 (ring protons), δ 4.27 (CH_2 protons,q, J=7 Hz) and δ 1.33 (CH_3 protons,t, J=7 Hz). After a week, (10) is found to be completely converted to picrate (δ 8.59); bands are also observed for ethyl bromide, δ 3.54 (CH_2,q, J=7 Hz) and δ 1.61 (CH_3,t, J=7 Hz)

The dealkylation of (10) by [$^2H_6$]–DMSO is a slower reaction that leads to the formation of picrate and a species here designated by (DMSO.Et)$^+$ which shows lines at δ 4.32,q, and δ 1.30,t, J = 7 Hz ; a small amount of ethanol, δ 3.45 (CH_2,q, J = 7 Hz) and δ 1.07 (CH_3,*t*, J = 7 Hz) is also formed due to the reaction with traces of water found in the solvent (Figure 2–4b)

Similar processes were found for the conversion of 1-isopropoxy-2,4,6-trinitro-benzene (11)

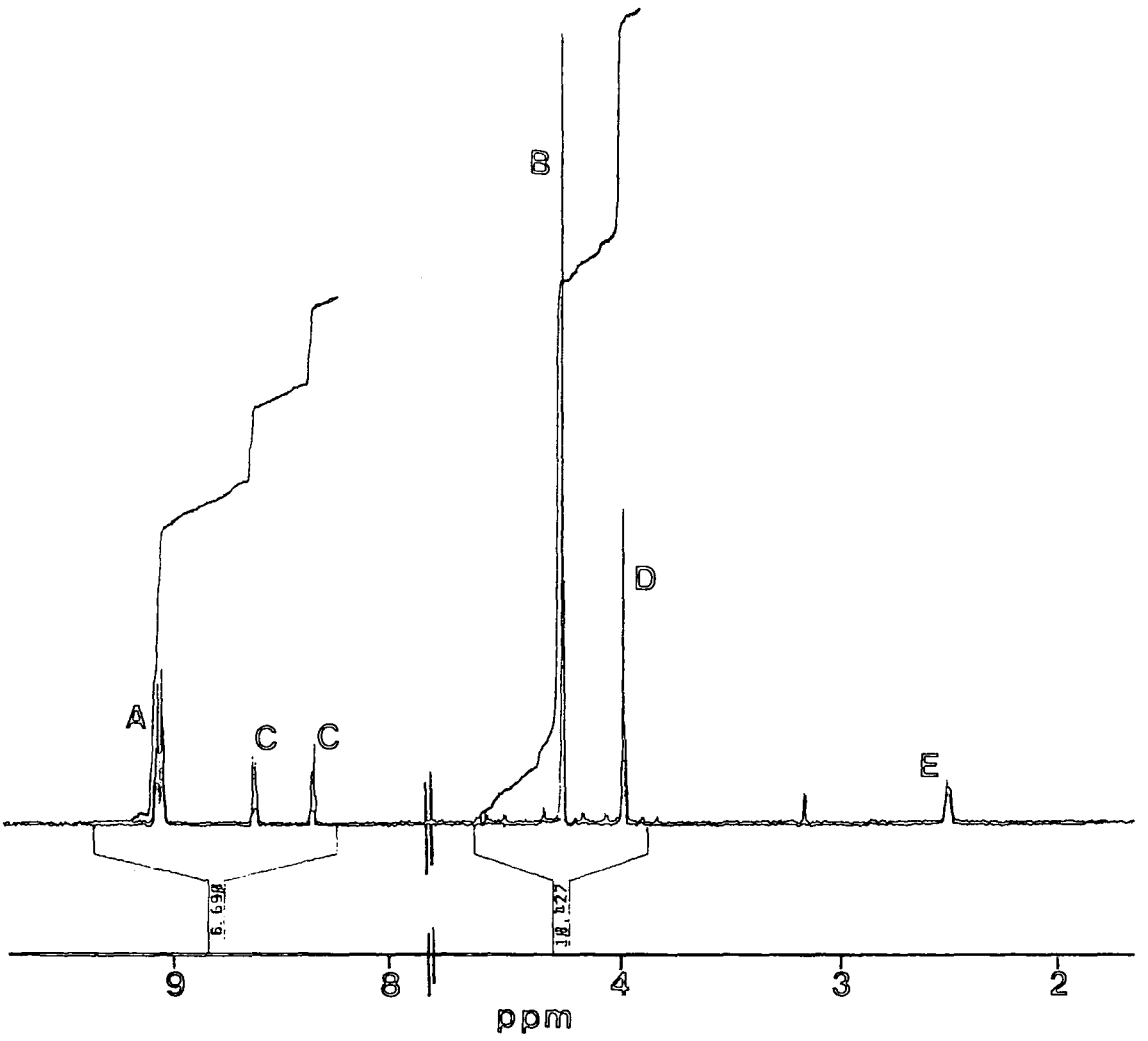

Figure 2–3 ^{1}H NMR spectrum of 2CNDNA in DMSO.d_6, one week at room temperature.

A,B are the lines of the parent compound

C : ring protons of 2–CN–4,6–dinitrophenoxide

D : $[DMSO \cdot CH_3]^+$

E : DMSO

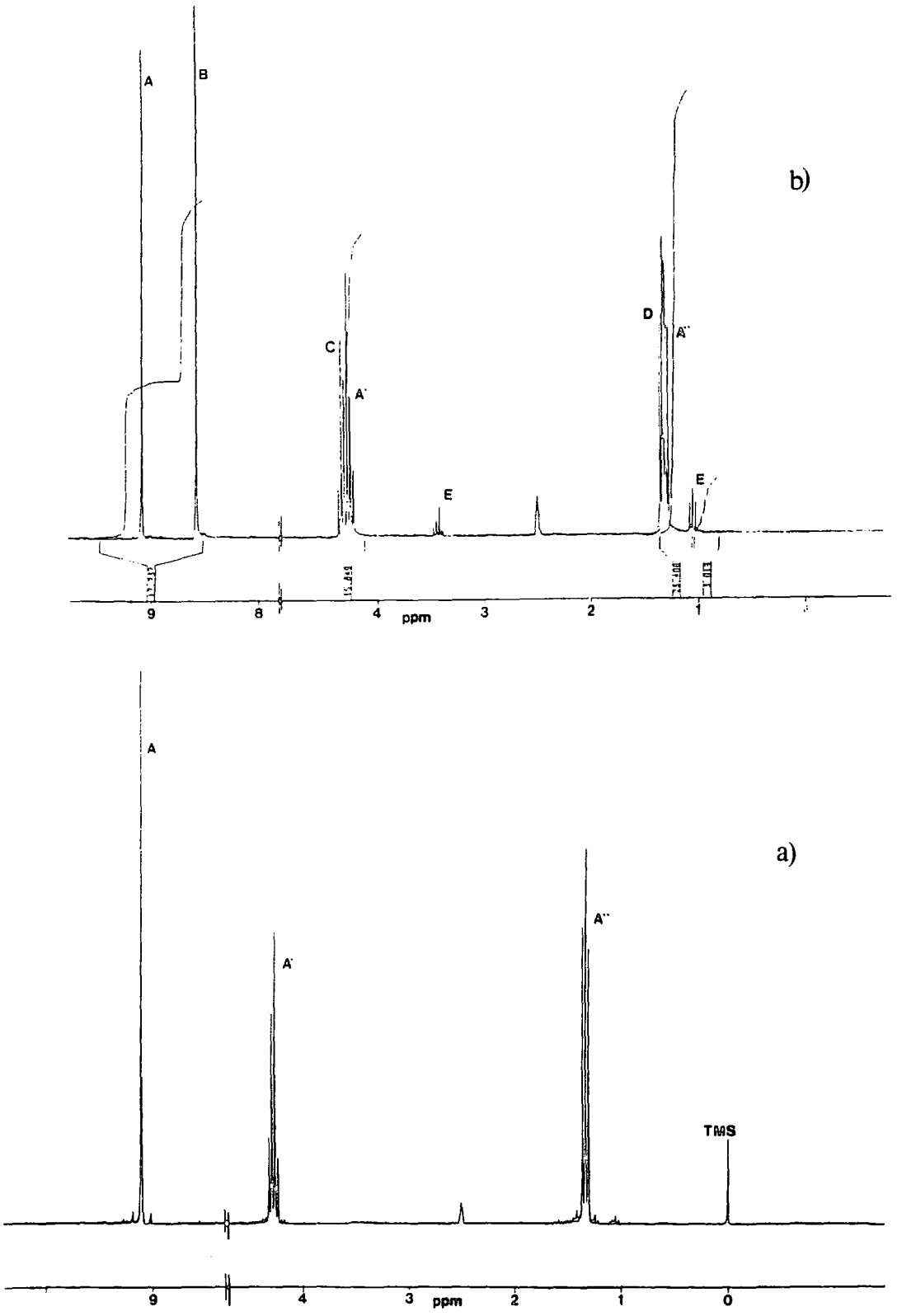

Figure 2–4 a) 2,4,6–trinitrophenetole (TNP) in DMSO·d_6

A: δ(ring): 9.10 ; A': $\delta(CH_2)$: 4.27 ; A'': $\delta(CH_3)$: 1.33

b) TNP in DMSO·d_6, one week at room temperature.

A,A',A'' are the lines of unreacted TNP

B: trinitrophenoxide δ(ring) : 8.59

C,D: Ethyl bromide

Ethanol : E

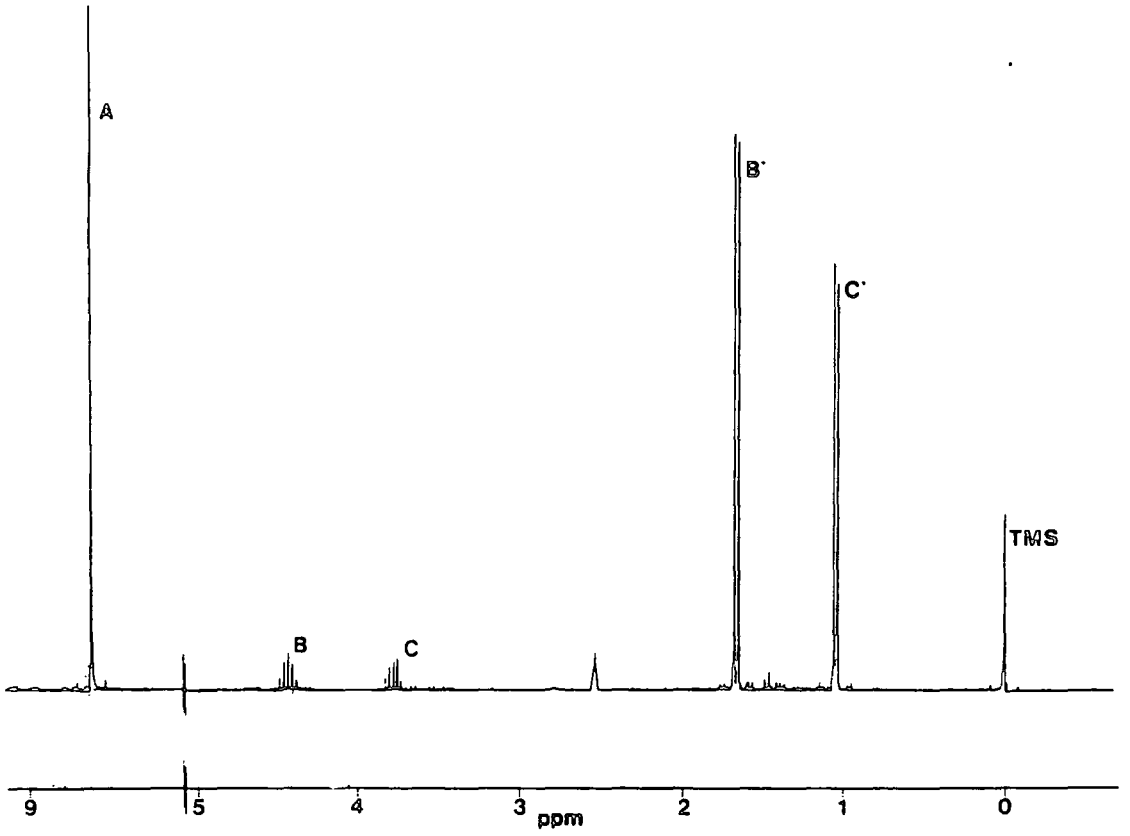

Figure 2–5 ^{1}H NMR spectrum of 1–isopropoxy–2,4,6–trinitrobenzene with KBr in DMSO·d_6

A: Picrate

B,B': Isopropyl bromide

C,C': Isopropanol

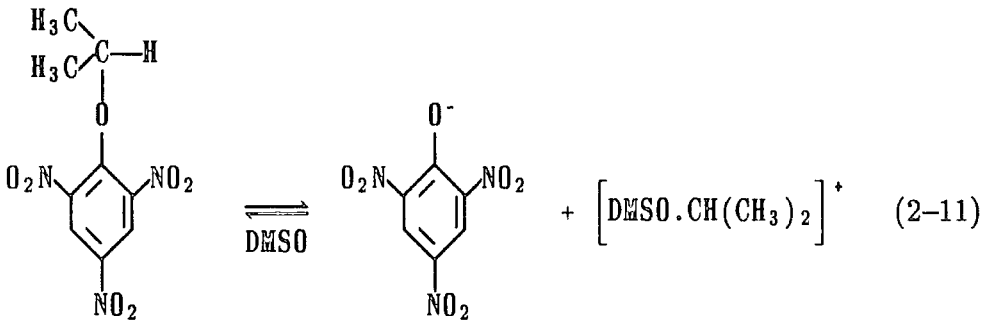

(11) (12)

The attack of (11) by bromide results in picrate and isopropyl bromide (δ 4.43,*h*, and δ 1.65,*d*) and the reaction with DMSO leads to the appearance of new lines in the NMR spectrum at δ 4.28 and δ 1.35, assigned to species (12) and formation of isopropanol (δ 3.76,*h*, and δ 1.02,*d*, J = 6.25 Hz) (Figure 2–5).

Table 2–1 ^{1}H NMR data for ethers (8) and phenolate ions (9) in DMSO

		(8)		(9)	
Y	Z	δ(ring)	δ(Me)	δ(ring)	(DMSO.Me)$^+$
CN	NO_2	8.94	4.04	8.17	4.00
NO_2	CN	9.06(*m*)	4.26	8.62(*d*) 8.35(*d*)	3.99
NO_2	NO_2	9.09	4.08	8.60	4.00

2.3 U.V./Visible results

None of the ethers (8a), (8b) or (8c) absorb light in the visible region. 4-cyano-2,6-dinitrophenol and the corresponding phenoxide (9b) absorb at 280 nm (ϵ = 2.4 x 10^4 $dm^3mol^{-1}cm^{-1}$ for the phenol and ϵ = 2.9 x 10^4 $dm^3mol^{-1}cm^{-1}$, for the phenoxide) and at 440nm (ϵ = 9380 $dm^3mol^{-1}cm^{-1}$ and ϵ = 1.15 x 10^{-4} $dm^3mol^{-1}cm^{-1}$, respectively). Both (9a) and (9c) have a maximum of absorbance at 380 nm.

The rates of formation of the products of reaction (9) were determined by the measurement of the increased absorbance at their λ_{max} in the visible region for several hours (up to 30 hours) in solutions of the respective ethers (8) in DMSO containing known amounts of potassium halides. Infinity values were measured at completion of the reactions. Good first order kinetics were observed.

The rate constants for the formation of (9b) were calculated for the reaction of (8b) with potassium iodide, bromide and chloride in DMSO, at several halide concentrations. The results are shown in Table 2–2. Figure 2–6 shows the linear increase of the observed rates with salt concentration. The positive intercept represents the rate constant for the spontaneous reaction that occurs with the solvent. The second order rate coefficients are given by the slope of the plots. The presence of water in the reactive mixture, 1% (v/v), was found to result in a small decrease of the rate constant.

Table 2–2

$[I^-]$/M	k_{obs} (s^{-1})	$[Br^-]$/M	k_{obs} (s^{-1})	$[Cl^-]$/M	k_{obs} (s^{-1})
0.053	$1.06x10^{-4}$	0.040	$1.16x10^{-4}$		
0.021	$4.40x10^{-5}$	0.021	$6.30x10^{-5}$	0.015	$7.52x10^{-5}$
0.010	$2.79x10^{-5}$	0.010	$3.53x10^{-5}$	0.010	$5.66x10^{-5}$

[8] = 5 x 10^{-5}M

Kinetic data were obtained for the dealkylation of ethers (8) and (10) by several anions in DMSO and are summarised in Table 2–3. No reaction occurs when the substrate is 2,4-dinitroanisole.

Table 2–3 First order rate constants for demethylation of (8) and (10) in DMSO

	$10^5 k_{obs}$ /s^{-1}			
salt[a]	(8a)	(8b)	(8c)	(10)
—	1.20	0.745	0.850	0.266
KSCN	1.91	0.925	1.39	0.425
KI	8.01	2.79	2.78	0.528
KBr	11.10	3.53	3.65	0.576
KCl	16.60	5.66	5.44	0.802
NaN_3	26.70	7.02	6.71	2.78

a [salt] = 0.01M
[8] = 5 x 10^{-5}M

The formation of the phenolate ions from (8a), (8b) and (8c) was also examined in water. First order rate coefficients in the presence of 0.01M salts are in Table 2–4. The results show that salts other than sodium azide and sodium fluoride have no effect on the rate coefficients for decomposition. In the cases of (8a) and (8b), azide and, to a lesser extent, fluoride had an accelerating effect. The most likely mechanism for reaction of (8) with the solvent is S_NAr attack at the 1-position of the aromatic ring with the expulsion of methoxide.

It is difficult to explain the greater reactivity of azide and fluoride on the basis of S_N2 attack at the alkyl group, as the order of nucleophilicity in water has been reported to be $I^- > N_3^- > F^-$.[28] A possible explanation is that azide and fluoride may themselves attack the aromatic ring to give intermediates which are then rapidly hydrolysed.

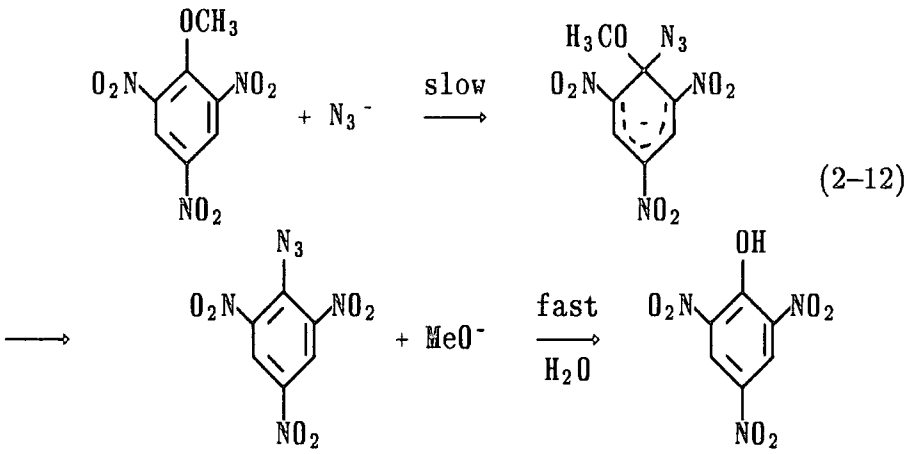

(2–12)

This would then be an example of nucleophilic cataylsis. There is evidence in the literature for the formation of σ-adducts by attack of fluoride[43] and of azide[44] at the aromatic ring but no examples of attack by chloride, bromide or iodide have been reported.

Table 2–4 First order rate coefficients for demethylation of (8) in water

	10^6k /s^{-1}		
salt[a]	(8a)[c]	(8b)[d]	(8c)[c]
—	5	0.4	—
KI	5	0.2	2
KSCN	5	b	3
KBr	5	b	3
KCl	5	b	3
KF	14	b	4
NaN_3	60	0.3	17

a) [salt] = 0.01M b) no reaction occurs c) Absorbance measured at λ_{max}= 354nm d) Absorbance measured at λ_{max}= 410nm

2.4 Discussion

The products of reaction in DMSO are consistent with nucleophilic attack by the anions by an S_N2 mechanism. Second order rate coefficients are collected in

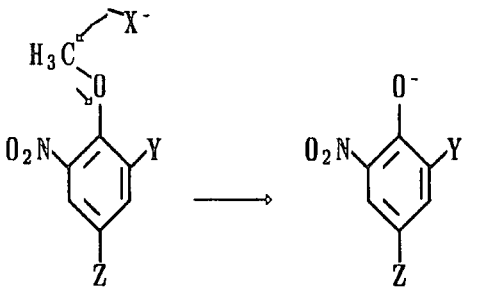

(8) (9) (2–13)

Table 5. The reactivities of 2-cyano- and 4-cyano-dinitroanisoles are reduced by a factor of *ca.* 3.5 compared to 2,4,6-trinitroanisole, corresponding to a reduction in the electron withdrawing ability of the leaving group. The reduction by a factor of *ca.* 30 in the reactivity towards halide ions of the ethyl ether (10) compared to the methyl ether (8a) is consistent with the steric interactions expected in an S_N2 reaction[45]

Table 2–5 **Rate coefficients for reactions in DMSO at 25°C**

	10^3k /dm^{3}mol^{-1}s^{-1}				
salt	(8a)	(8b)	(8c)	(10)	relative a reactivity
KI	6.8	2.0	1.9	0.26	1
KBr	9.9	2.8	2.8	0.31	1.5
KCl	15.4	4.9	4.6	0.54	2.4
KSCN	0.7	0.2	0.5	0.16	0.1
NaN_3	25.5	6.3	5.9	2.5	3.2

a) Relative reactivities, compared to iodide, of the nucleophiles for reaction with anisoles (8).

In DMSO, the order of nucleophilicity is $SCN^- < I^- < Br^- < Cl^- < N_3^-$ for all dealkylation reactions examined and it is markedly different from that found in S_N2 reactions in protic solvents, where iodide is the most reactive.[9,28] These differences probably largely reflect the changes in relative solvation of the nucleophiles in going from water (good at solvating small anions by hydrogen bonding interactions) to DMSO (good at solvating large polarisable anions). The decreased reactivity observed for the bromide ion DMSO in the presence of water is in good agreement with the assumption that the reaction is due to the attack of "free" desolvated and dissociated halide ions present in the DMSO solution, as this solvent strongly complexes the cation :

$$KX^- (DMSO) \longrightarrow (DMSO.K)^+ + X^- \qquad (2\text{–}14)$$

In the presence of water, the anion will be partially solvated and, hence, less effective at the reactive site of the substrate. In water, only N_3^- and F^- compete with the solvent, as stated earlier. This competition may involve nucleophilic catalysis by attack at the ring rather than S_N2 reaction.

The possibility of nucleophilic attack by DMSO at the aromatic ring must also be considered. Biffin and Paul[46] have shown that, at 100°C, attack by DMSO at the chloro- substituted ring position of di- and trinitrochlorobenzenes occurs and leads to the formation of the corresponding phenols together with chloromethyl sulphide. The analogous pathway for the reaction of aryl alkyl ethers is shown below. The initial step would involve attack by DMSO at the 1-position of the ring to yield an intermediate which expels methoxide to give the cationic species (14).

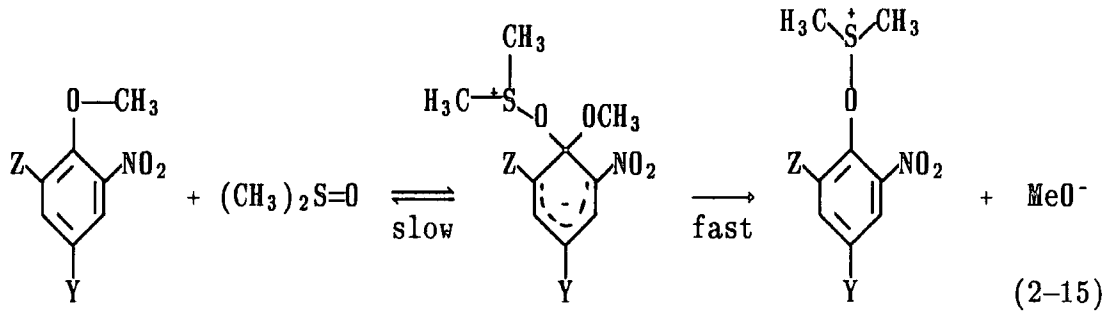

(2–15)

(8) (13) (14)

There are two different possibilities for the subsequent formation of the picrate species; by the attack of methoxide ions at one of the methyl groups adjacent to the S atom.

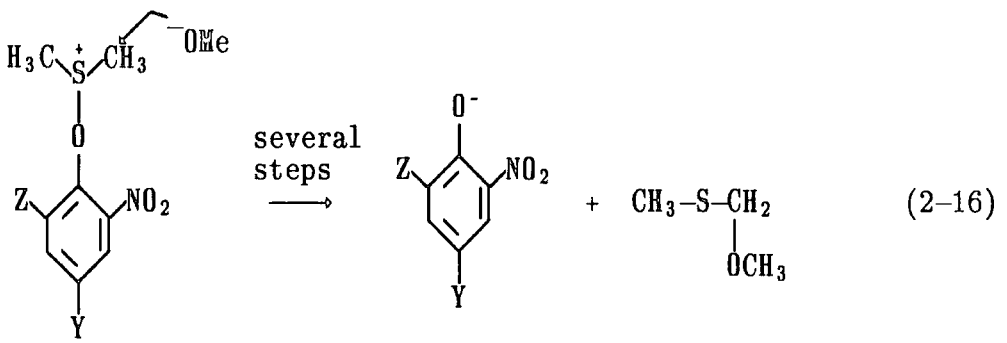

(14) (9) (2–16)

or, in an intramolecular process, by decomposition of (13)

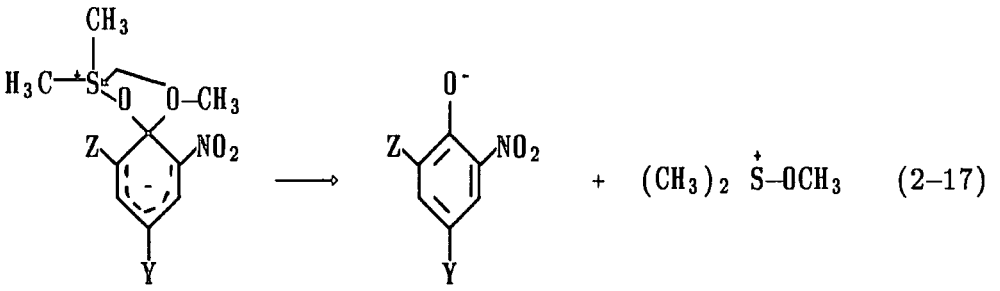

(13) (9) (2–17)

Both of these pathways lead to O-methyl species being formed from DMSO and are thought to be unlikely on the grounds of the ^{1}H NMR evidence which favours the formation of the S-methyl derivative, $(CH_3)_3^+SO$. The observed chemical shift (see Table 2–1) is precisely as expected for this species, the corresponding trimethylsulphoxonium chloride and iodide showing methyl bands at δ 4.03 and 3.89 respectively. Although both S-methylated and O-methylated cations are known to be formed[11] from DMSO, the latter cations have been found to be unstable and to rapidly rearrange to their more stable isomers. The species

observed on the present work was indefinitely stable in time and showed no tendency to isomerise as would have been expected for the O-methyl derivative.

A more likely mechanism is direct attack at the alkyl group by DMSO in a S_N2 reaction analogous to that of anionic nucleophiles. Reaction via sulphur would lead directly to the S-methylated DMSO adduct while reaction via the oxygen

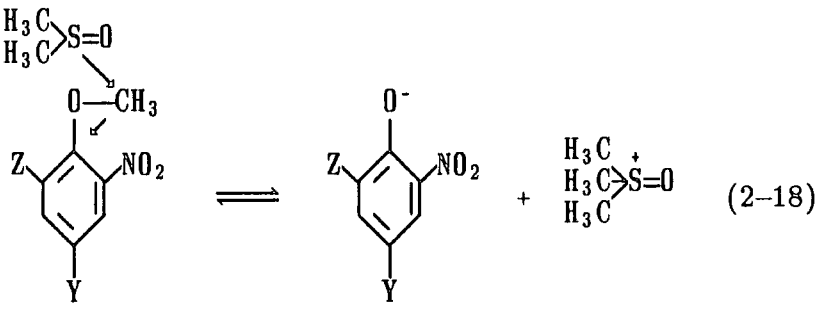

(8) (2–18)

atom of DMSO would lead initially to O-methylated DMSO, which could subsequently rearrange to the thermodynamically more stable S-methylated derivative. The formation of an O-methyl adduct as a short-lived intermediate cannot be entirely dismissed.

One way of conclusively distinguishing between attack by DMSO at the aromatic ring (S_NAr reaction) and at the alkyl side chain (S_N2 reaction) would be to prepare (8) labelled with ^{18}O in the ether function and to determine the location of this isotope in the products. S_NAr reaction would result in loss of the heavy isotope from the aromatic species, whereas in the S_N2 reaction it would be retained. Unfortunately an attempt to prepare 2,4,6-trinitroanisole marked with ^{18}O by reacting picryl chloride with $H_2{}^{18}O$ and consequent methylation with diazomethane was unsuccessful.

In the presence of traces of water small amounts of methanol, from the methyl ethers, or ethanol, from the ethyl ethers are formed. Water is able to react with the ethers as shown in (2–19).

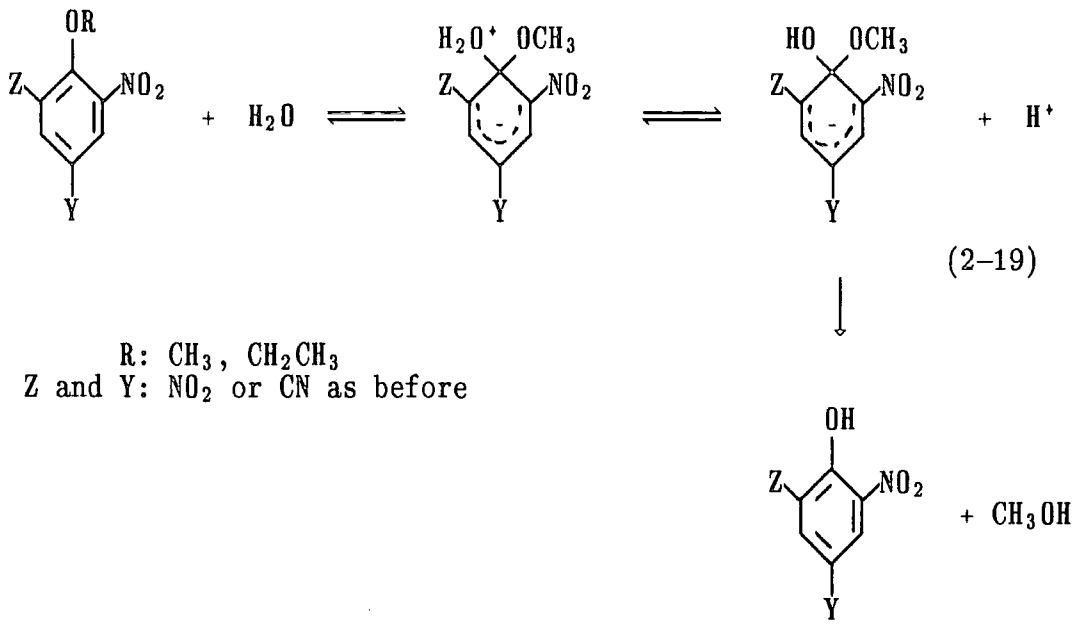

(2–19)

R: CH_3, CH_2CH_3
Z and Y: NO_2 or CN as before

It is also possible that the methylated cation of DMSO might react with water:–

$$\left[(CH_3)_2SO.CH_3\right]^+ + H_2O \longrightarrow \left[(CH_3)_2SO.H\right]^+ + CH_3OH \quad (2\text{–}20)$$

However, there are two reasons to discount this pathway. First, the overall rate of reaction increased in the presence of water (Figure 2–7), second, the ^1H NMR bands due to the methylated DMSO cation and due to methanol increased concurrently and there was no tendency for the latter line to increase at the expense of the former.

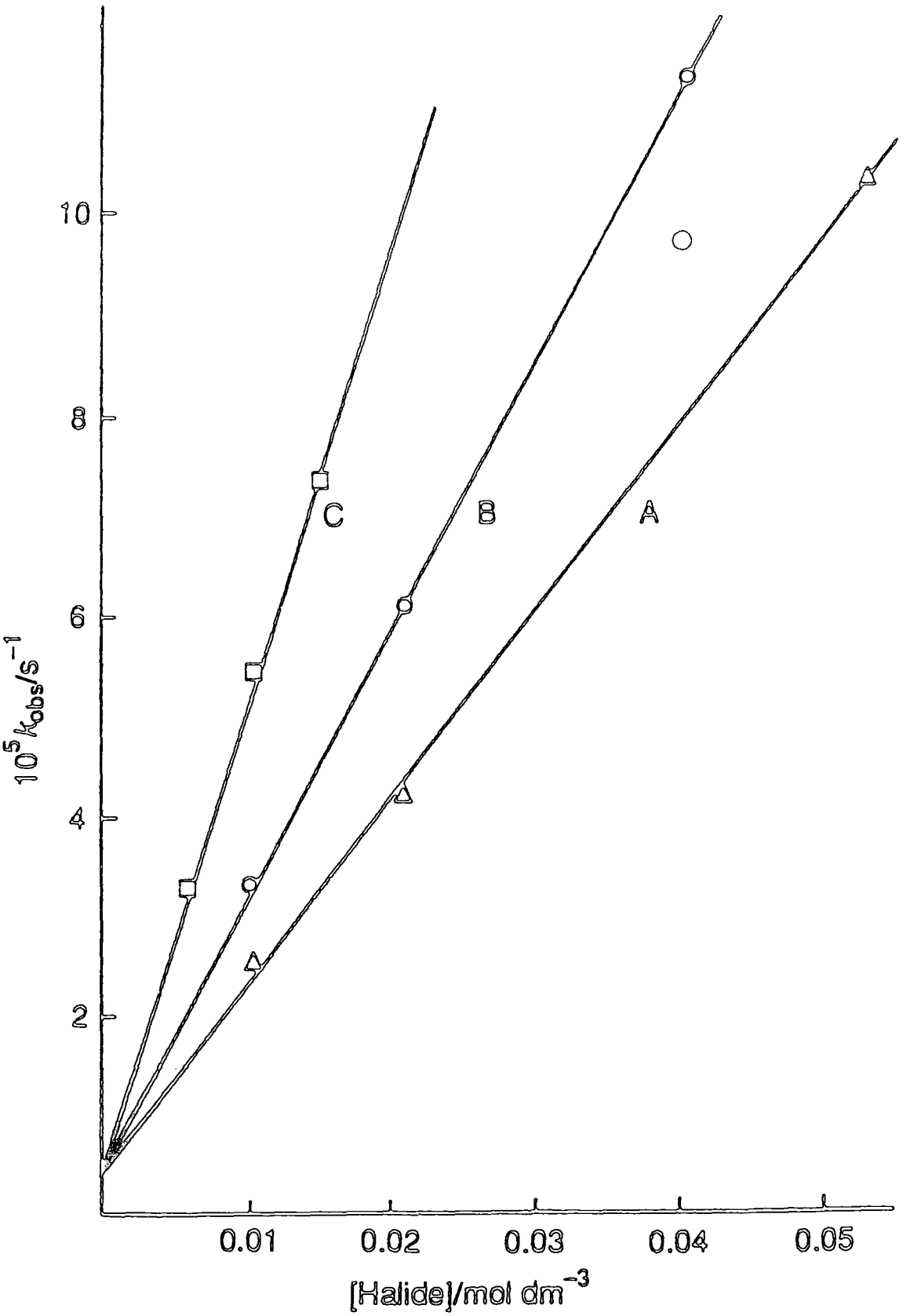

Figure 2–6 First order rate coefficients for the reaction in DMSO of 4CNDNA with A, KI ; B, KBr ; C, KCl. The filled circle (○) corresponds to reaction with KBr, 0.04 mol dm^{-3}, in 99:1 (v/v) DMSO:water

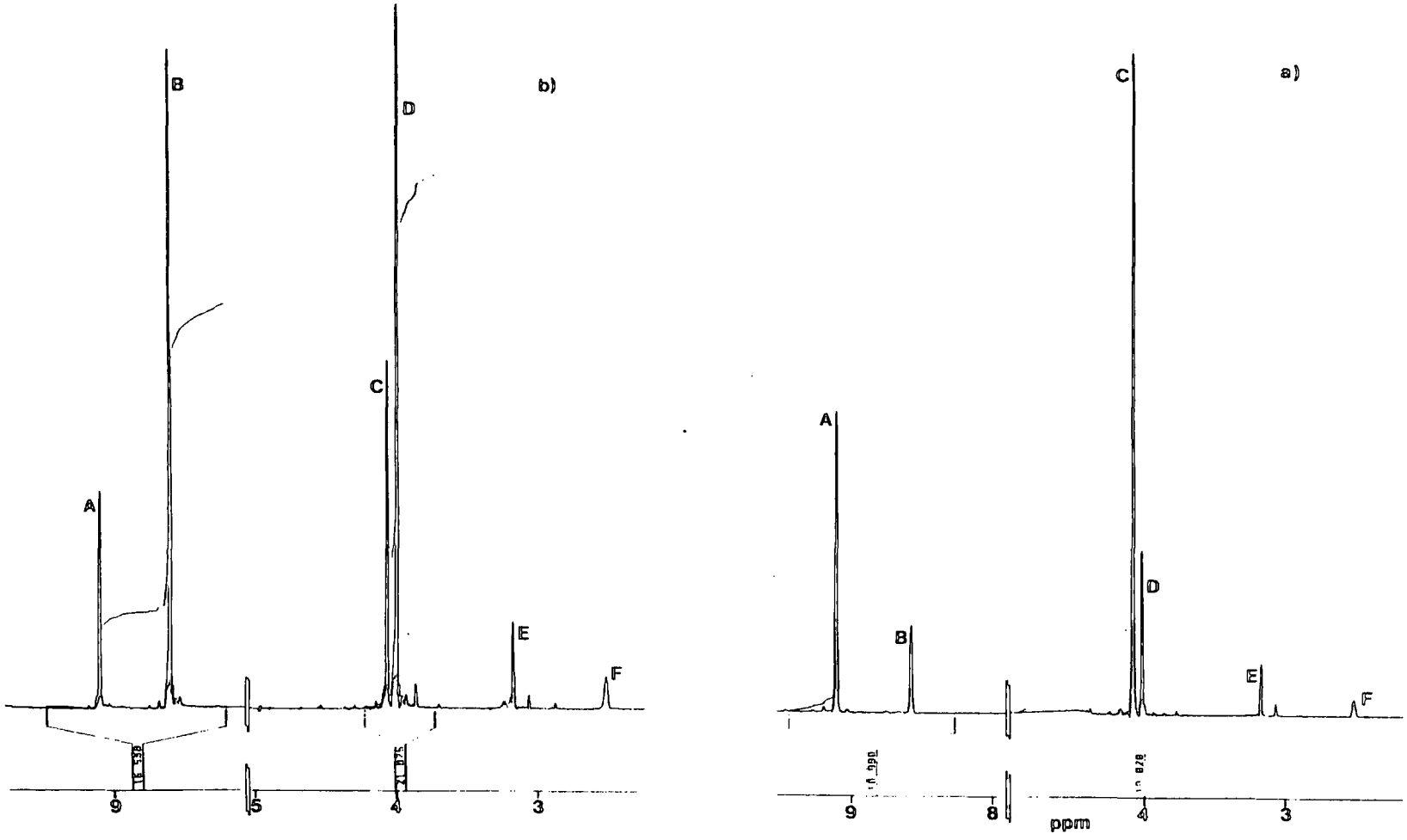

Figure 2–7 Reaction of TNA with DMSO a) in the absence of water, b) in the presence of trace of water.
A,C: lines of TNA B: picrate D: $[DMSO \cdot CH_3]^+$ E: MeOH
F: DMSO

References

1 Tiecco, M., *Synthesis* (1988), 749

2 Testaferri, L.; Tiecco, M.; Tingoli, M.; Chianelli, D.; Montanucci, M., *Synthesis* (1983), 751

3 Burwell, R.L., *Chem. Rev.* (1954), 54, 615

4 Bernards, A.M.; Ghiani, M.R.; Piras, P.P.; Rivoldini, A., *Synthesis* (1989), 287

5 Bowden, K.; Prasana, S., *J. Chem. Soc. Perkin Trans. II*, (1987), 185

6 Zima, V.; Pytela, O.; Kavalek, J.; Vecera, M., *Collect. Czech. Chem. Commun.* (1989) 54, 2715

7 Strauss, M.; Torres, R., *J. Org. Chem.*, (1989), 54, 756

8 Bhatt, M.V.; Kulkarni, S.U., *Synthesis* (1983), 249

9 Miller, J.; Moran, P.J.S., *J. Chem. Res.* (1980), M, 501

10 Clapp, L.B. *et al*, *J. Org. Chem.*, (1968), 33, 4262

11 Smith, S.G.; Winstein, S., *Tetrahedron* (1958), 3, 317

12 Testaferri, L. *et al*, *Tetrahedron* (1983), 39,193

13 Feutrill, G.I.; Mirrington, R.N., *Tetrahedron Lett.* (1970), 1327

14 Harrison, L.T., *Chem. Commun.* (1969), 616

15 Buchanan, D.H.; Takemura, N.; Sy, N.O.J., *J. Org. Chem.*, (1968), 51, 4291

16 Khan, M.N., *J. Org. Chem.*, (1983), 48, 2046

17 Bender, M.L.; Kezdy, F.J.; Zerner, B., *J. Am. Chem. Soc.*, (1963), 85, 3017

18 Ingold, C.K., "*Structure and Mechanism in Organic Chemistry*", 2nd ed. Bell, G. and Sons Ltd., London, 1969

19 McCarthy, J.R.; Moore, J.L.; Cregge, R.J., *Tetrahedron Lett.* (1978), 5183

20 Katritzky, A.R.; Topsom, R.D., *Angew. Chem.* (1970), 9(2), 87

21 Katritzky, A.R.; Topsom, R.D., *Chem. Rev.* (1977), 77(5), 639

22 Page, I.D.; Pritt, J.R.; Whiting, M.C., *J. Chem. Soc. Perkin Trans. II*, (1972), 906

23 Tiecco, M.; Tingoli, M.; Testaferri, L.; Chianelli, D.; Maiolo, F., *Synthesis* (1982), 478

24 Servis, K.L., *J. Am. Chem. Soc.*, (1967), 89(6), 1508

25 Bernasconi, C., *J. Chem. Phys.*, (1971), 75, 3636

26 Artamkina, G.A. *et al*, *Zh. Org. Khim.* (1981), 17(1), 29

27 Byvalkevich, O.G.; Leshina, T.N.; Shein, S.M., *Izv. Sib. Otd. Akad. Nauk SSSR, Ser. Khim. Nauk*, (1973), 114

28 Parker, A.J., *Chem. Rev.*, (1969) 69(1), 1

29 Bunnett, *Ann. Rev. Phys. Chem.*, (1963), 14, 271

30 Reichardt, C., "*Solvent Effects in Organic Chemistry*", Verlag Chemie, Weinhem, N.Y., 1978

31 Pearson, R.G.; Songstad, J., *J. Org. Chem.*, (1967), 32, 2899

32 Alexander, R.; Ko, E.C.F.; Parker, A.J.; Broxton, T.J., *J. Am. Chem. Soc.*, (1968), 90(19), 5049

33 Miller, J., *J. Am. Chem. Soc.*, (1961), 371

34 Ritchie, C.D. in: "*Solute–Solvent Interactions*", Ed. J.F. Coetzee and C.D. Ritchie, Marcel Dekker Inc., N.Y., London, 1969

35 Liotta, C.L. *et al*, *Tetrahedron Lett.*, (1975), 4205

36 Fuchs, R.; Mahendran, K., *J. Org. Chem.*, (1971), 36, 730

37 Braunman, J.I.; Olmstead, W.N.; Lieder, C.A., *J. Am. Chem. Soc.*, (1974), 96, 4030

38 Bohme, D.K.; Mackay, G.I.; Payzant, J.D., *J. Am. Chem. Soc.*, (1974), 96, 4027

39 Tanaka, K.; Mackay, G.I.; Payzant, J.D.; Bohme, D.K., *Can. J. Chem.*, (1976), 54, 1643

40 Olmstead, W.N.; Braunman, J.I., *J. Am. Chem. Soc.*, (1977), 99, 4219

41 Pearson, R.G.; Sobel, H.; Songstad, J., *J. Am. Chem. Soc.*,(1968), 90, 319

42 Kemp, "*Organic Spectroscopy*"

43 Terrier, F.; Ah–Kow, G.; Pover, M–J.; Simonnin, M.P., *Tetrahedron Lett.* (1976), 227

44 Caveng, P.; Zollinger, H., *Helv. Chim. Acta.*, (1967), 50, 861

45 Streitweiser, A., "*Solvolytic Displacement Reactions*", McGraw Hill, N.Y., 1962

46 Biffin, M.E.C.; Paul, D.B., *Aust. J. Chem.*, (1974), 27, 777

Chapter 3
Competition between Methoxide attack at Ring-Carbon and at the cyano group of cyanonotroanisole

3.1 Introduction

There have been several reports[1] of σ-adduct formation by nucleophitic attack on cyano–substituted aromatic compounds. The reaction of 3,5-dinitrobenzonitrile[2,3] has been shown to yield isomeric adducts by hydroxide attack at the 2– and 4– positions in water-DMSO mixtures, the former more than ten times more stable than the latter. Results in the literature for reactions of cyanodinitroanisoles with methoxides reveal that the 1,1-dimethoxy adducts are produced as the thermodynamically stable species. However, the equilibrium constants for their formation are lower than those for their picryl analogues. Because the stability of Meisenheimer complexes depends on the extent of the delocalisation of the negative charge in the anion, the relative stabilities of the 1,1–dialkoxy adducts are expected to parallel the total electron–withdrawing ability of the substituents on the aromatic ring. This is confirmed by studies on dicyanonitro complexes showing that these are even less stable than the cyanodinitro adducts. For each set of isomers, greater stability is achieved with nucleophilic attack at a carbon atom *para*– to a nitro group rather than *para*– to a cyano group.

The formation of 1,3 adducts as transient species further shows the stabilising effects of a nitro group *para*– to the position of attack. Thus, for aromatic systems where there are two possibilities of attack at an unsubstituted carbon atom, such as 2,4–dicyano–6–nitroanisole, the only transitory adduct detected is the one with the entering methoxide group *para*– to the nitro substituent, i.e., there is formation of (1) rather than (2).

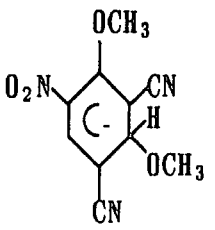

(1)

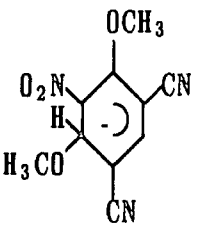

(2)

Accordingly, the isomer 2,6-dicyano-4-nitroanisole has been reported[4] to react with methoxide to yield only the 1,1 dimethoxy adduct (3).

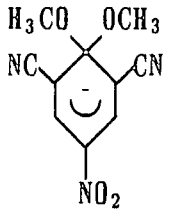

(3)

Studies on the formation of the 1,1–dimethoxy adduct of 4-cyano-2,6-dinitroanisole show an intriguing discrepancy for the values quoted for the equilibrium constant which vary from 2.5 $mol^{-1}dm^3$, obtained[5] by NMR using lithium methoxide, to 168 or 280 $mol^{-1}dm^3$, obtained by u.v./visible spectrophotometry[6,7] using sodium methoxide.

In this work, the reactions of 4–cyano–2,6–dinitroanisole with sodium, potassium and lithium methoxides are examined and the effects of added barium and calcium ions are studied. For comparison some data for 2-cyano-2,6-dinitroanisole are reported. The results show the presence of two effects not noted by previous workers. These are: i) competition between nucleophilic attack at ring carbon to give 1,1-dimethoxy adducts and attack at the cyano group to give imidoester, and ii) strong association of the dimethoxy adducts with cations.

3.2 Results

In methanol 4-cyano-2,6-dinitroanisole (4) absorbs in the u.v. region at 218nm (ϵ 2.1 x 10^4 $dm^3mol^{-1}cm^{-1}$). In the presence of dilute sodium methoxide two reversible processes are observed. The faster results in increased absorbance in the visible region to give a species with λ_{max} 350nm (ϵ 0.95 x 10^4) and 528nm (1.9 x 10^4 $dm^3mol^{-1}cm^{-1}$). In the slower process partial fading of the colour occurs although there is no change in spectral shape. It was noticed that at a given

methoxide concentration the presence of increased concentrations of sodium ions (added in the form of sodium tetraphenylboron) resulted in increased colour at completion of both the faster and slower processes and in a decreased rate of the slower fading reaction. The results can be quantitatively described by Scheme 3–1 which shows the competition between methoxide attack at the 1–position to give the σ–adduct (3), which is stabilised by association with cations in (5), and at the cyano group leading to the solvate (7). This analysis is confirmed by n.m.r. results (Figure 3–1). The ^{1}H NMR. spectrum of (5) in [$^2H_6$]-DMSO showed bands at δ 8.04 (s, 2H) and 3.03 (s, 6H) which were more shielded than those of the parent, (4), at δ 8.71 (s, 1H) and 3.86 (s, 3H). The spectrum of the parent equilibrated with excess sodium methoxide in [$^2H_4$]-methanol showed bands due to the ring protons of (5) at δ 8.17 and (7) at δ 8.62.

There is precedent in less activated systems for the methanolysis of ring–cyano substituents in basic media,[8,9,10] and Miller *et al*[11] attributed the abnormal activation parameters observed for the methoxy–dechlorination of some cyano-chlorobenzenes to imido–ester formation.

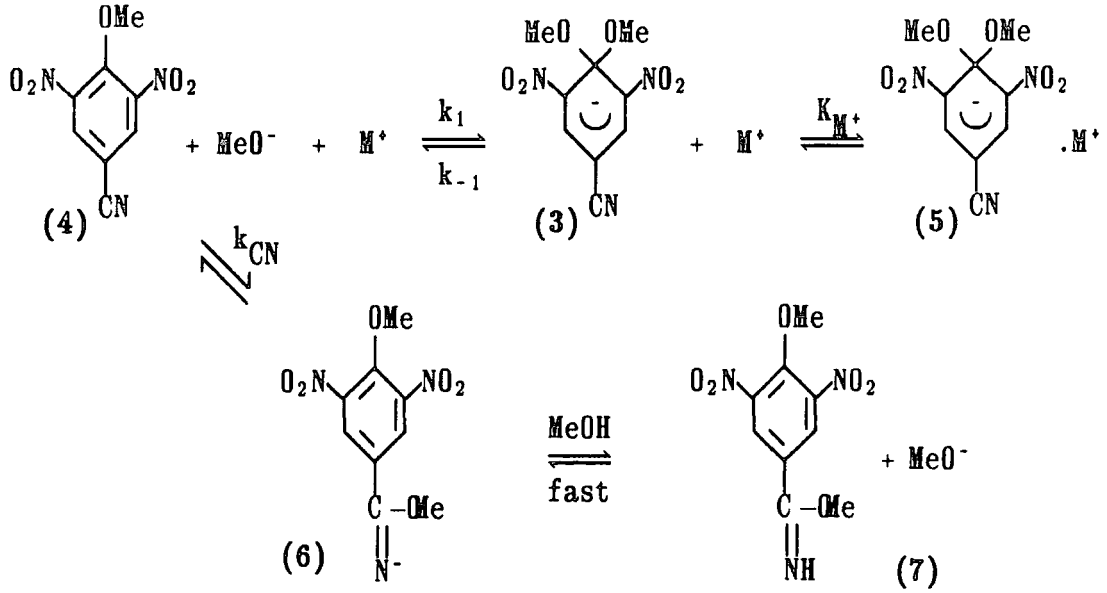

Scheme 3–1

Interaction of 4–cyano–2,6–dinitroanisole with metal methoxide in methanol.

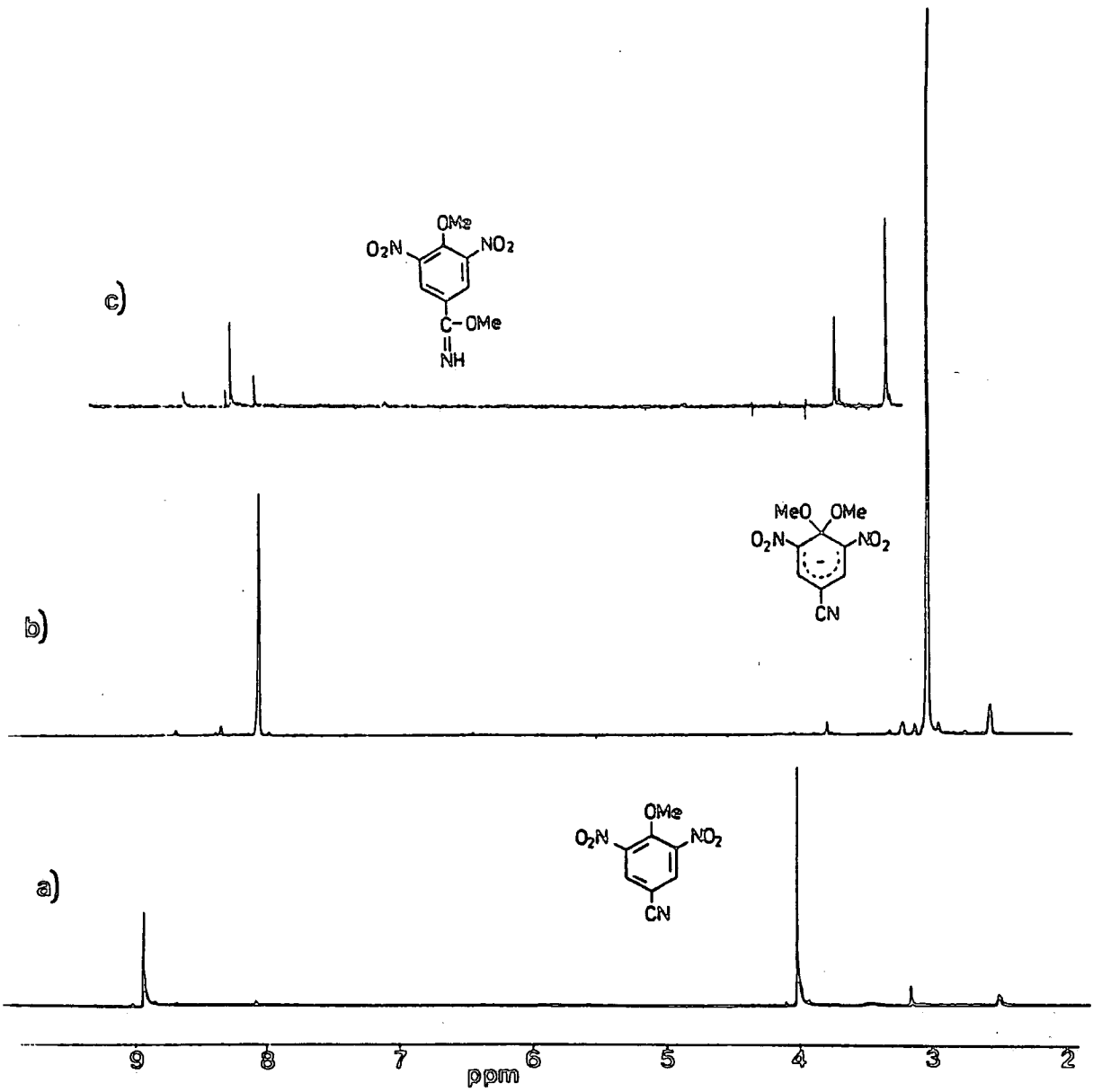

Figure 3–1 ^{1}H NMR spectra of 4CNDNA, its 1,1-dimethoxy adduct and the imido ester obtained after two weeks of reaction.

Dickeson *et al* (1967) previously noticed the fading of colour of mixtures of 4-CN-2,6-dinitroanisole in methanol containing sodium methoxide solutions and considered it impossible to calculate equilibrium constants from U.V./visible spectra. Because they were able to isolate the 1,1-dimethoxy adduct as a crystalline material, by removing the solvent soon after mixing equimolar amounts of substituted anisole and methoxide, and record its ^{1}H NMR and IR spectra these authors ruled out the possibility of methoxide attack at the nitrile group.

In the present work, the 1,1–dimethoxy adduct was effectively isolated using the same experimental procedure but removal of solvent two weeks after addition of methoxide to the methanolic solution of 4-CN-2,6-dinitroanisole yield a substance with very different properties from the 1,1-dimethoxy adduct, consistent with an imido-ester (5) (Figures 3–1 to 3–4) the mass spectrometry patterns are quite conclusive as for both the anisole and the product recovered after two weeks reaction with methanolic sodium methoxide it is possible to detect a peak corresponding to the molecular ion, although the latter species appears to be auto-protonated. An attempt to explain the fragmentation patterns of both species is presented in Schemes 3–2 and 3–3.

Kinetic and equilibrium measurements were made at 528 nm with base concentrations in large excess over substrate concentration and two first–order processes, well separated in time, were observed. The dependence on base concentration of the faster, colour–forming process is given by equation (3–1) and that of the slower, fading reaction by equation (3–2). In deriving equation (3–2) it is assumed that methoxide attack at the cyano–group is rate–limiting in the second stage of the reaction and that the contribution of the reverse process is negligible.

$$k_{fast} = k_f[MeO^-] + k_r \qquad (3\text{–}1)$$

$$k_{slow} = \frac{k_{CN}[MeO^-]}{1 + K_1[MeO^-][1 + K_{M^+}[M^+]]} \qquad (3\text{–}2)$$

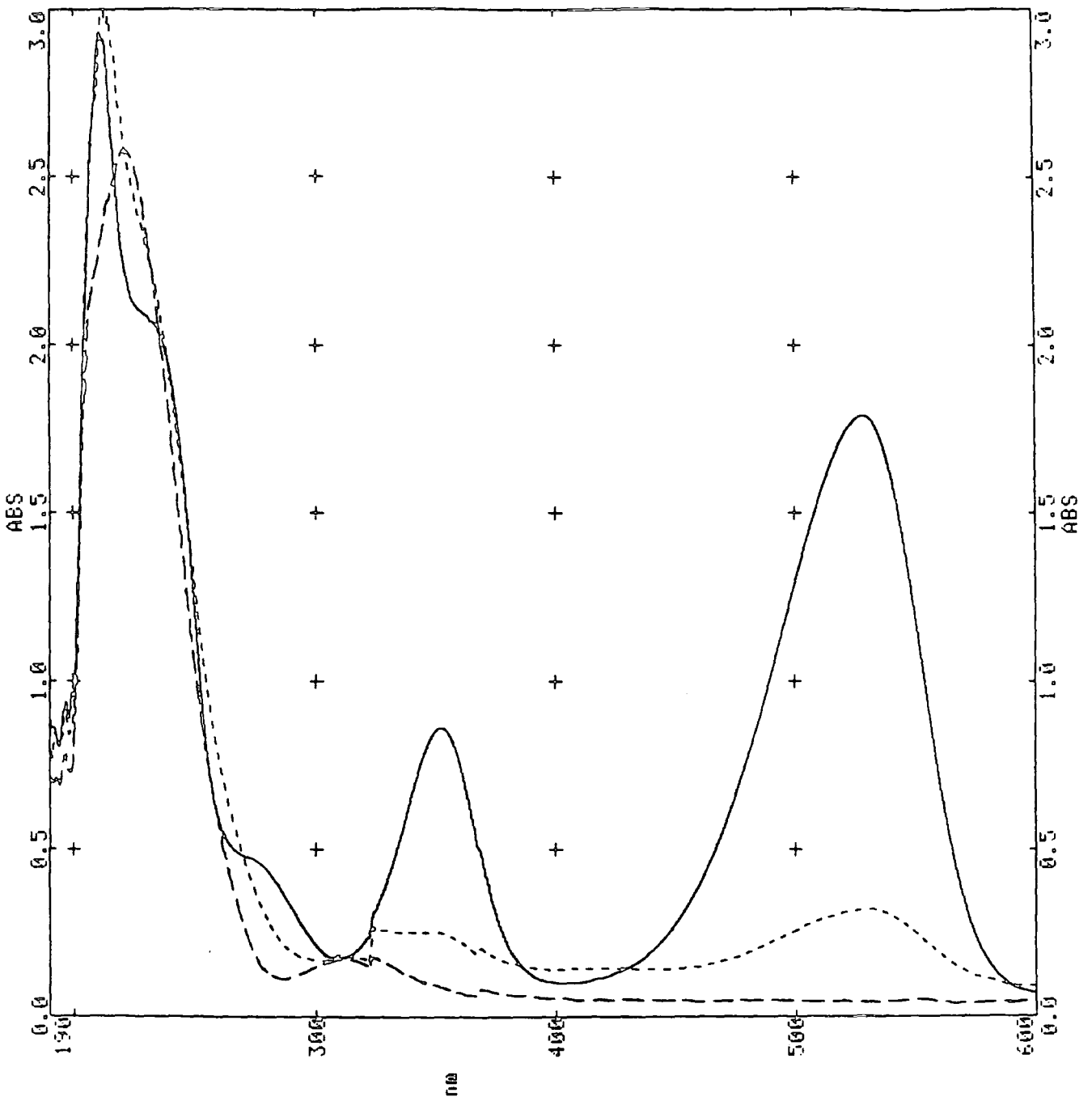

FIGURE 3-2 U.V./vis spectra of

--- Parent (4)

___ Adduct (3), formed by the addition of NaOMe to (4), after completion of fast colour forming reaction.

..... After slower fading reaction.

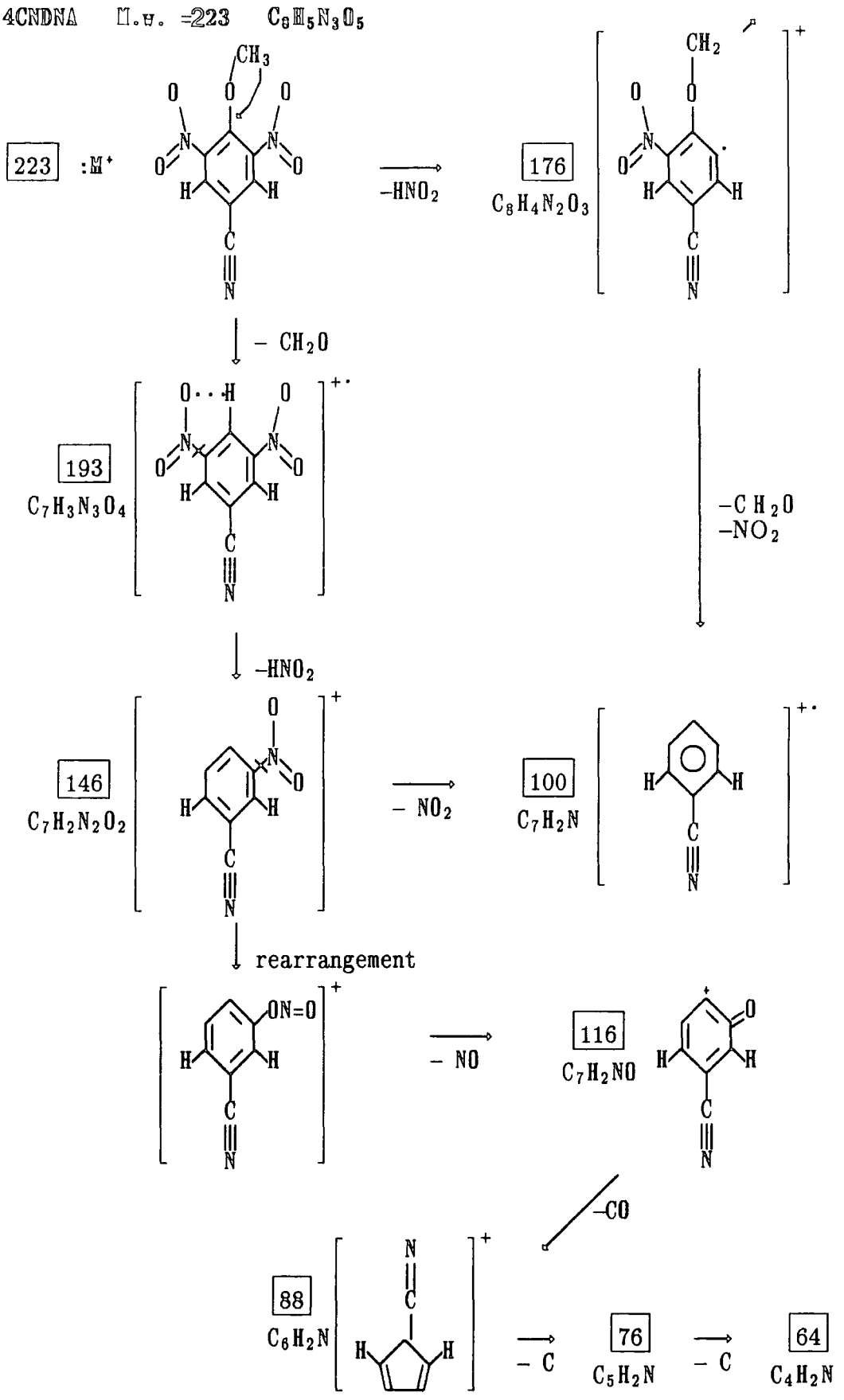

Scheme 3–2

Interpetation of fragmentation pattern for 4-CN-2,6-dinitroanisole

BpA=0 I=10v Ha=564 TIC=311832000 Acnt Sys:ACE HAR 965300A
PAULA PT= 0° Cal:PFK261 MASS 52

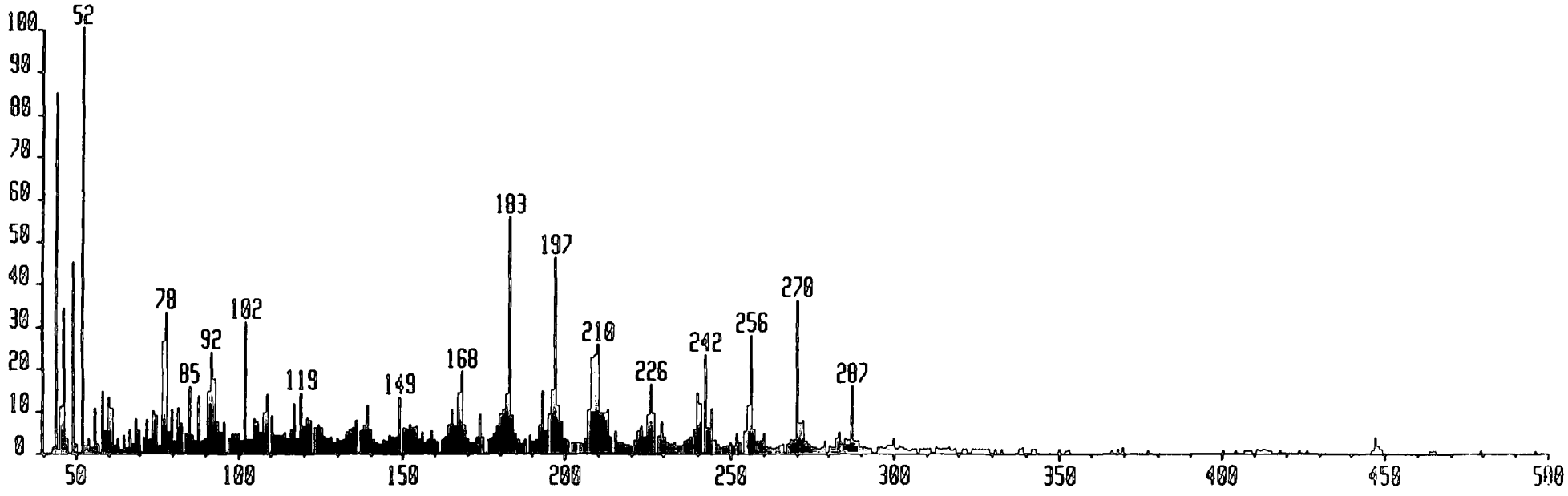

PC3IH053◇ x1 Bgd=32 31-MAR-89 12:2◇0:03:48 70E EI◇
BpA=0 I=1.2v Ha=446 TIC=58943000 Acnt: Sys:ACE HAR: 7621000
PAULA PT= 0° Cal:PFK261 MASS: 226

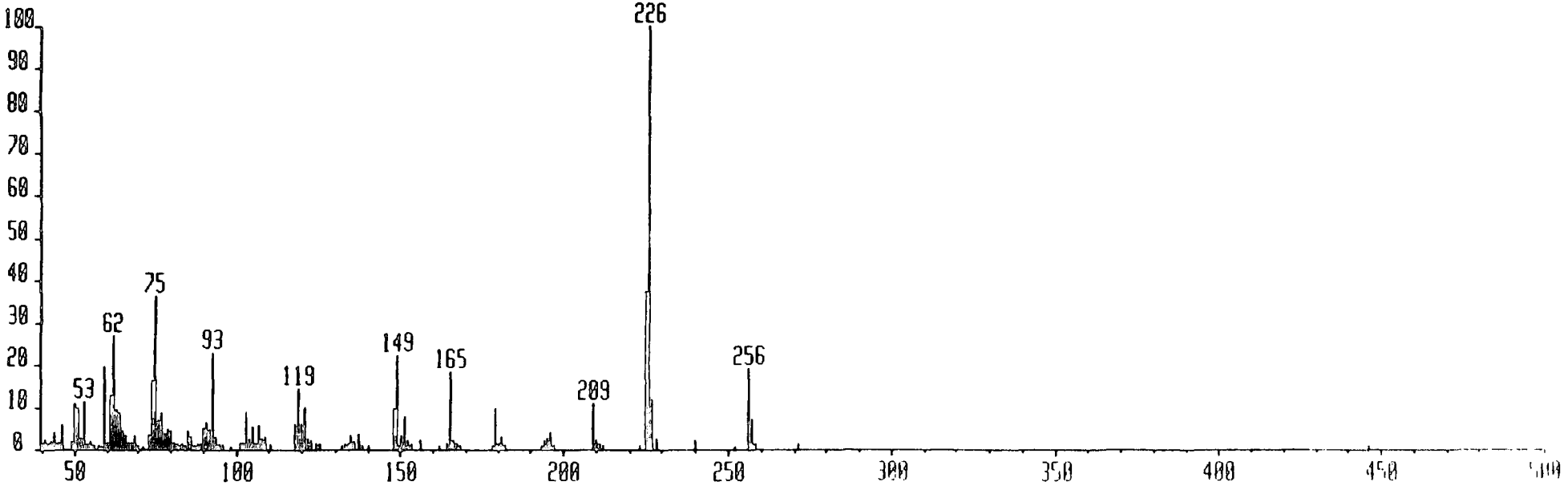

BpA=30 I=2.5v Ma=448 TIC=86569000 Acnt: Sys:ACE MAR: 7620000
P.CASTILHO PT= 0° Cal:PFKAJ MASS: 193

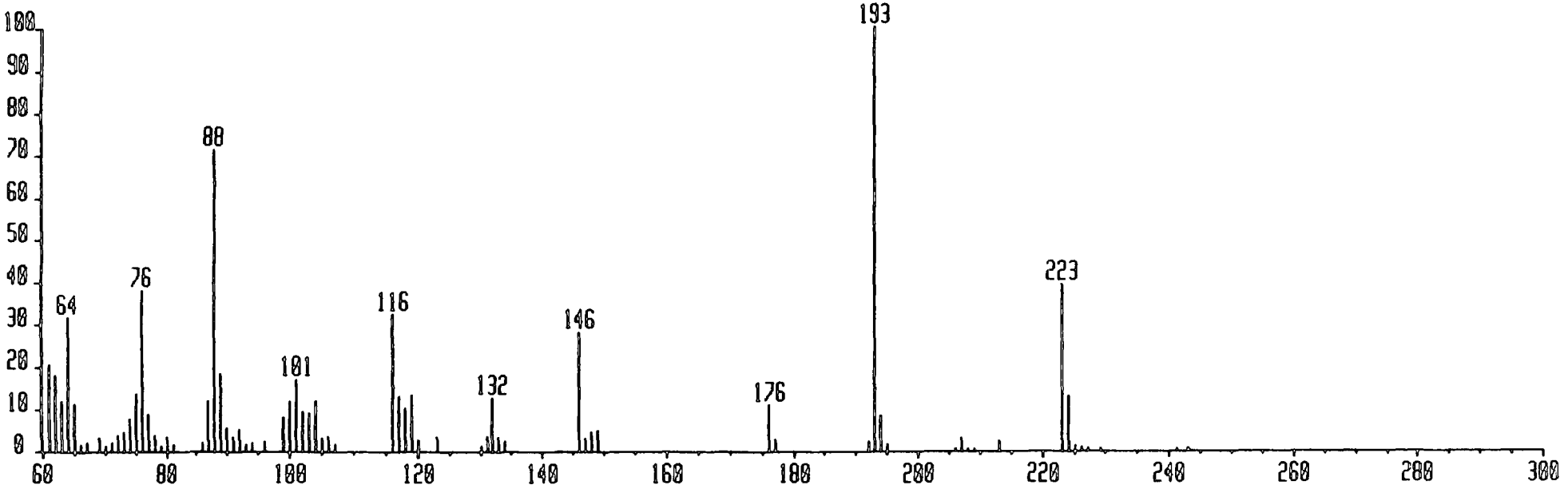

PCCNDNA048◇ x1 Bgd=8 26-MAY-88 05:1◇:03:40 70E Cl◆
BpA=41 I=10v Ma=528 TIC=628907000 Acnt: Sys:ACE MAR: 65534000
P.CASTILHO PT= 0° Cal:PFKAJ MASS: 224

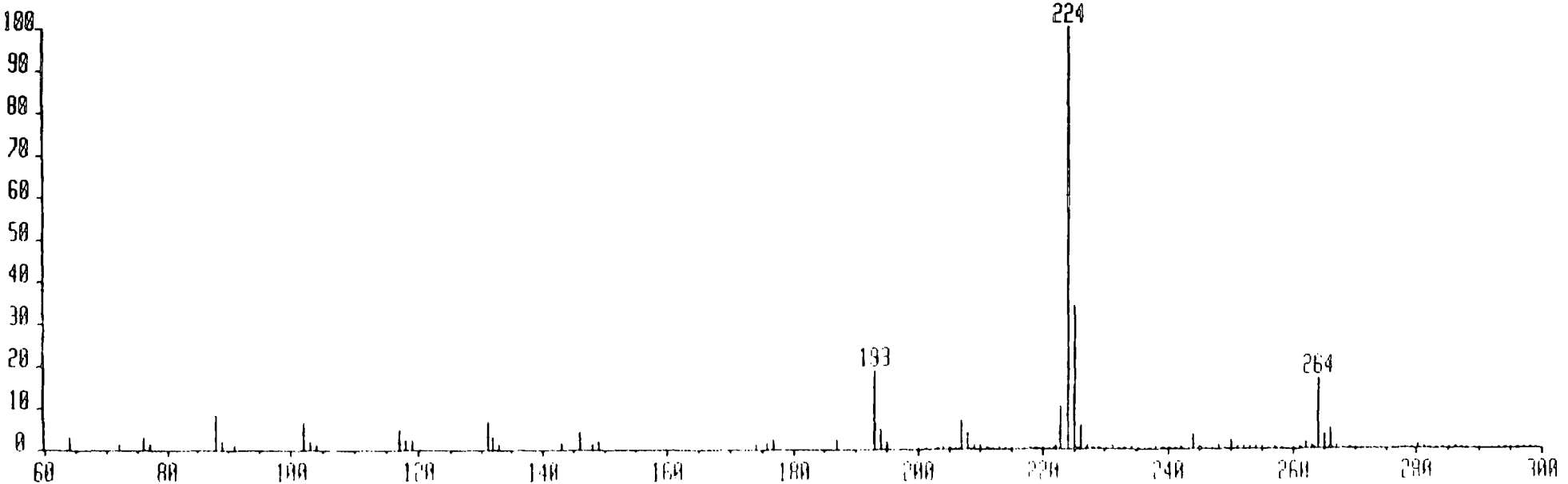

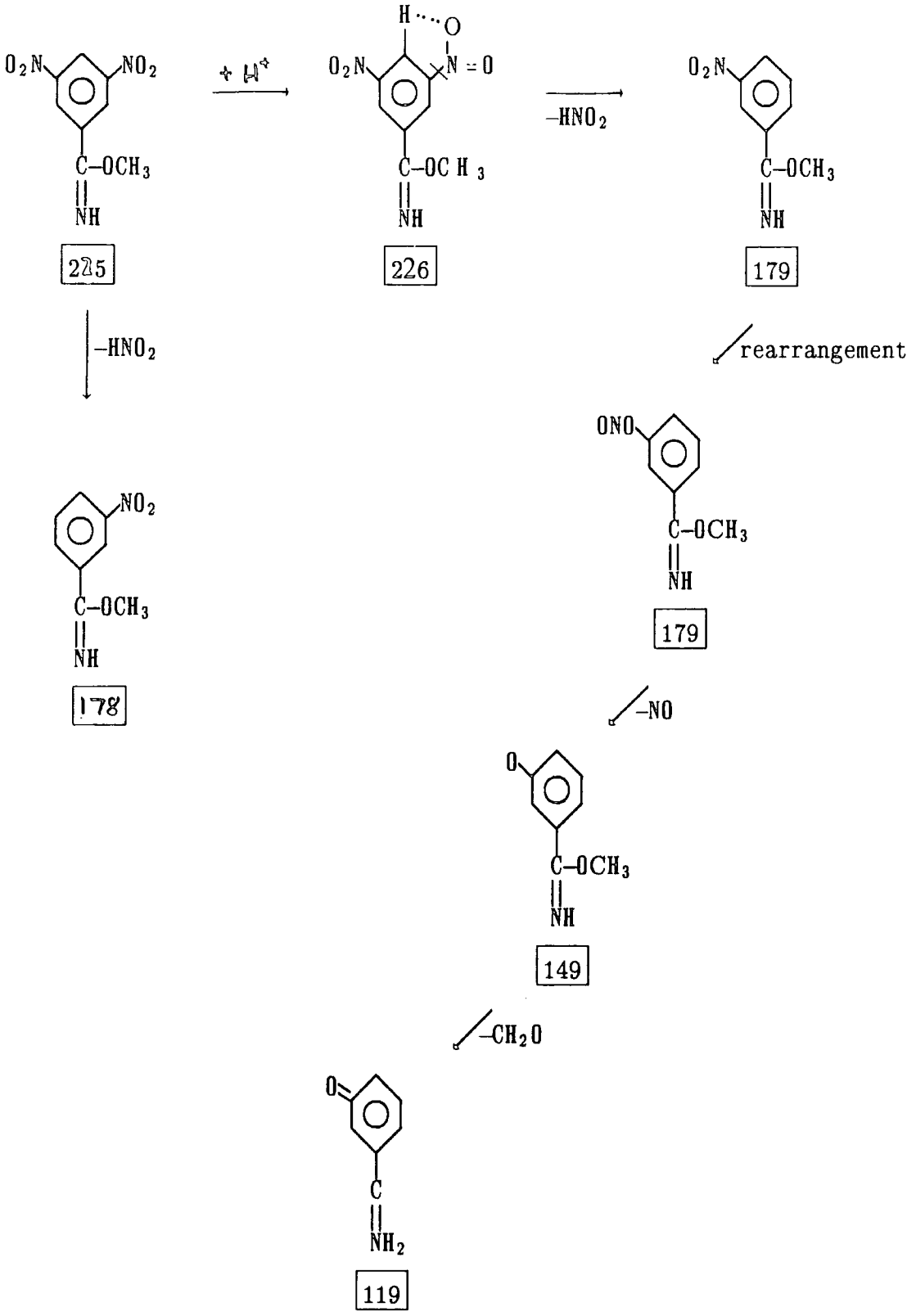

Scheme 3–3

Interpretation of the fragmentation pattern shown in Figure 3–4

The equilibrium constant K_C is defined, equation (3–3), in terms of the concentrations at the end of the fast process and is related to K_1 and K_{M^+} by equation (3–6). The results show that association with cations causes little change in spectral shape or position of absorption maxima and the assumption is made that (3) and (5) have identical extinction coefficients.

$$K_C = \frac{[3] + [5]}{[\underset{\sim}{4}][MeO^-]} \qquad (3\text{–}3)$$

$$K_1 = \frac{[3]}{[4][MeO^-]} \qquad (3\text{–}4)$$

$$K_{M^+} = \frac{[5]}{[3][M^+]} \qquad (3\text{–}5)$$

$$K_C = K_1(1 + K_{M^+}[M^+]) \qquad (3\text{–}6)$$

The equilibrium constant K_C' is defined, equation (3–7), in terms of the concentrations at the completion of the slower process. K_S and K_{S^-} are, respectively, the equilibrium constants for formation of the solvate, (7), and its anion, (6), from the parent. The general equation relating these quantities is equation (3–10) and this reduces to equation (3–11) when, as in the present studies, the equilibrium concentrations of (6) are negligible.

$$K_C' = \frac{[3] + [5]}{([4]+[6]+[7])[MeO^-]} \qquad (3\text{–}7)$$

$$K_S = \frac{[7]}{[4]} \qquad (3\text{–}8)$$

$$K_{S^-} = \frac{[6]}{[4][MeO^-]} \qquad (3\text{–}9)$$

$$K_C' = \frac{K_1(1 + K_{M^+}[M^+])}{1 + K_S + K_{S^-}[MeO^-]} \qquad (3\text{–}10)$$

$$K_C' = \frac{K_1(1 + K_{M^+}[M^+])}{1 + K_S} \qquad (3\text{–}11)$$

These two reactions, forming (fast) and fading (slow), were followed, in a range of base concentration from 2.4×10^{-3}M to 0.1M, by u.v./visible spectroscopy at 528 nm. The fast forming reaction was also followed by stopped–flow technique at the same wavelength.

For the fading reaction, the decrease of absorbance with time was recorded for approximately 30 minutes; 24 hours after mixing the absorbance at 528nm was measured to give the value of A'_{528} at completion of fading reaction. A plot of $\ln(OD - A'_{528})$ *vs* time (sec) has slope = $-k_{fading}$ and permits the extrapolation to the beginning of the reaction (time = 0) of the absorbance, A_{528}. This extrapolated value, A_{528} is used in the calculation of the rate constant of the forming reaction:

$$\ln(A_{528} - OD) = k_{fast}\, t + \text{constant}$$

the same procedures were performed in solutions where the cation (Na^+) concentration was made constant by the addition of an appropriate amount of $NaBPh_4$ in methanolic solution.

For base concentrations greater than 0.1M, the rate constant of formation, k_{fast}, was difficult to measure even by stopped-flow; for these concentrations (0.1M – 2.8M), only the slow fading reaction was studied.

The graph in Figure 3–5 is an example of the determination of k_{slow} from the experimental absorbance values:

[NaOMe] = 0.0096 M

A'_{528}0.014 slope = $-1.03 \times 10^{-3} = -k_{slow}$

intercept = $-1.1315 \Rightarrow A_{528}(t=0) - A'_{528} = 0.322$

$A_{528}(time=0) = 0.336$

for

[NaOMe] = 0.0096 and [Na^+] = 0.1 M by $NaBPh_4$

A'_{528} = 0.052 slope = $-5.28 \times 10^{-4} = -k_{slow}$

intercept = 0.8946 $\Rightarrow A_{528}(t=0) - A'_{528} = 0.408$

$A_{528}(t=0) = 0.460$

where A'_{528} is the value of optical density at 528nm after completion of the fading process.

Data for reaction with sodium methoxide are in Tables 3–1 and 3–2. Values of K_C, which increase with increasing sodium methoxide concentration but are constant at constant sodium ion concentration, yield K_1 106 dm^3mol^{-1} and K_{Na^+} 23 dm^3mol^{-1} (Figure 3–6). The increases in value of k_f with increasing sodium methoxide concentration, and the decreases in values of k_r are attributed to stablisation by sodium ions of the σ–adduct and of the transition state leading to it. On extrapolating to zero base concentration, values of k_1 2.4 $dm^3mol^{-1}s^{-1}$ and k_{-1} 0.023 s^{-1} were obtained. Combination of these values gives K_1 $(=k_1/k_{-1})$ 104 dm^3mol^{-1} which is in excellent agreement with the value obtained independently. A linear plot, shown in Figure 3–7, of k_{slow} versus base concentration at [Na^+] = 0.1 mol dm^3 gives values of k_f 3.8 $dm^3mol^{-1}s^{-1}$ and k_r 0.010 s^{-1}. Values of K_C' accord with equation (3–11) with K_S 50. The values of K_C' are independent of base concentration at constant [M^+] (Figure 3–8) showing that, in this case, equation (3–10) reduces to equation (3–11) indicating that the solvate is very largely present in its neutral form, (7). The rates of the fading reaction allow the calculation using equation (3–2) of a value for k_{CN} of 0.24 $dm^3mol^{-1}s^{-1}$ It should be noted that under the present experimental conditions with dilute methoxide solutions, little association between sodium ions and methoxide ions is expected[12,13]

Figure 3-5

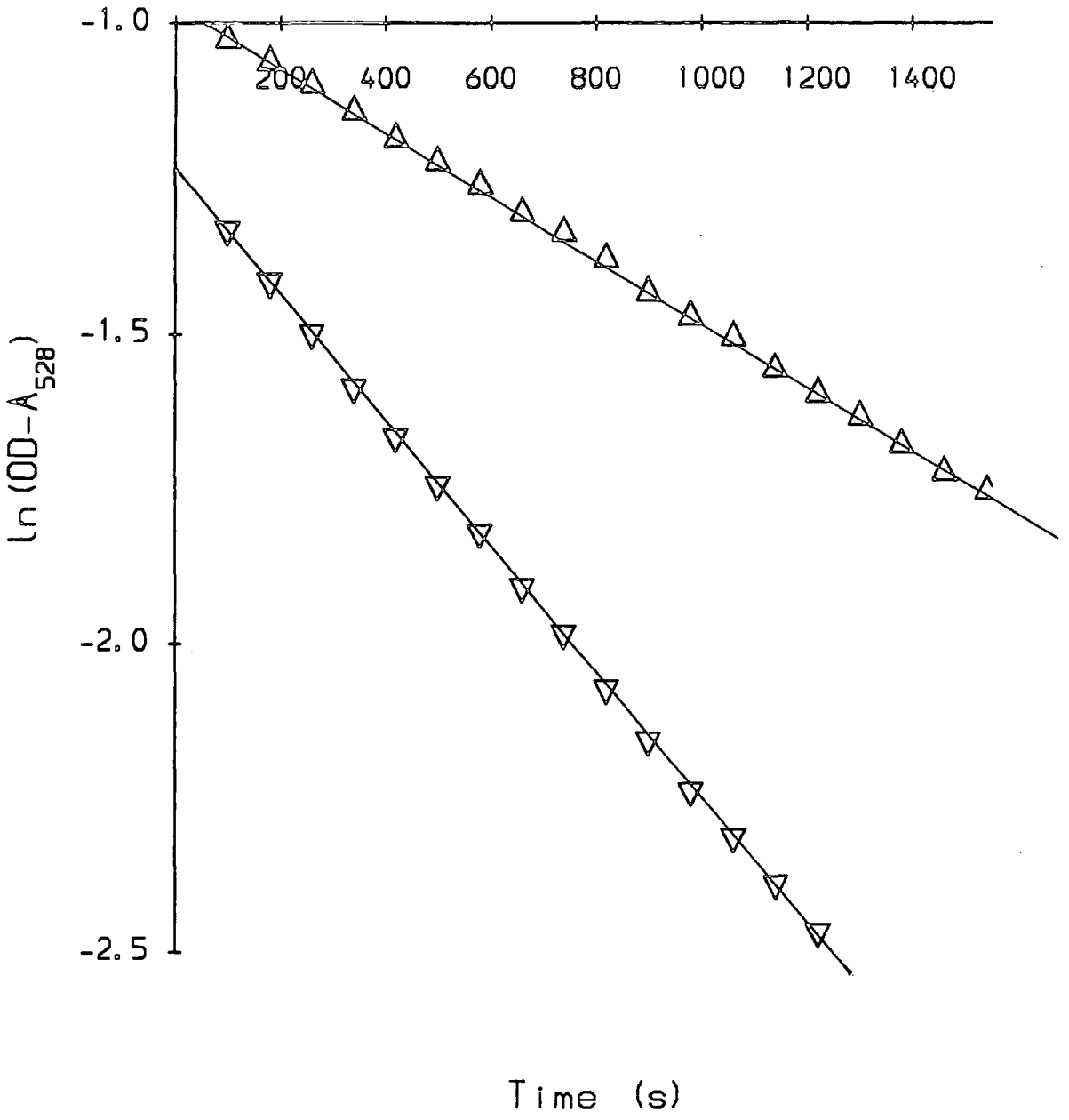

Figure 3–5 Determination of k_{slow} from OD_{528} at [NaOMe] = 0.0096M

1) $[Na^+]$ = [NaOMe] 2) $[Na^+]$ = 0.1M by $NaBPh_4$

The values obtained from these calculations are all consistent with

$K_1 = 106\ dm^3mol^{-1}$

$K_{Na^+} = 23\ dm^3mol^{-1}$

$k_{CN} = 0.24 \pm 0.03\ dm^3mol^{-1}s^{-1}$

$k_f = 2.3\ dm^3mol^{-1}s^{-1}$
$k_r = 0.022\ s^{-1}$
} at $[Na^+]=0$

$k_f = 3.8\ dm^3mol^{-1}s^{-1}$
$k_r = 0.010\ s^{-1}$
} at $[Na^+]=0.1$ M

TABLE 3–1 [Fast Process]

Kinetic and equilibrium data at 25°C for reaction of (4)[a] with sodium methoxide in methanol

[NaOMe]/ mol dm^{-3}	[$NaBPh_4$]/ mol dm^{-3}	Abs[b] (528nm)	K_c/[c] mol dm^{-3}	K_c(calc)[d]	k_{fast}/ s^{-1}	k_f §	k_r / s^{-1}
0.0024	–	0.12	109	112	0.028	2.4	0.022
0.0048	–	0.21	118	118	0.031	2.3	0.020
0.0072	–	0.27	121	124	0.033	2.1	0.018
0.0096	–	0.33	138	130	0.043	2.6	0.018
0.020	–	0.44	157	155	0.070	2.7	0.017
0.030	–	–	–	–	0.110	3.1	0.017
0.040	–	0.515	198	203	0.160	3.5	0.018
0.070	–	0.55	–	–	0.260	3.5	0.011
0.096	–	0.56	–	–	0.390	3.8	0.011
0.0024	0.098	0.29	417	350	0.014	–	–
0.0048	0.095	0.34	300	350	0.019	–	–
0.0072	0.093	0.41	340	350	0.032	–	–
0.096	0.090	0.46	400	350	0.042	–	–
0.020	0.080	0.50	310	350	0.080	–	–
0.030	0.070	–	–	–	0.130	–	–
0.040	0.060	0.52	–	–	0.170	–	–
0.060	0.040	–	–	–	0.220	–	–
0.070	0.030	0.55	–	–	–	–	–
0.080	0.020	–	–	–	0.310	–	–

§ $dm^3 mol^{-1} s^{-1}$

a Concentration is 3×10^{-5} mol dm^{-3}

b At completion of the fast colour forming process

c Calculated as Abs (528)/(0.58 – Abs (528)) [NaOMe]

d Calculated from equation (6) with K_1 106 $dm^3 mol^{-1}$ and K_{Na^+} 23 $dm^3 mol^{-1}$

TABLE 3-2 [Slow Process]

Kinetic and equilibrium data at 25°C for reaction of (4)[a] with sodium methoxide in methanol

[NaOMe]/ mol dm^{-3}	[NaBPh$_4$]/ mol dm^{-3}	Abs[b] (528nm)	K_c'/[c] mol dm^{-3}	K_c'(calc)[d]	$10^4 k_{slow}$ /s^{-1}	kCH §
0.0024	–	0.003	2.2	2.2	5.0	0.26
0.0048	–	0.007	2.5	2.3	6.7	0.22
0.0072	–	0.011	2.7	2.4	10.1	0.27
0.0096	–	0.014	2.6	2.5	10.3	0.24
0.020	–	0.035	3.2	3.0	12.0	0.25
0.030	–	–	–	–	–	–
0.040	–	0.089	4.5	4.0	10.2	0.23
0.070	–	0.160	5.4	5.5	9.2	0.27
0.096	–	0.234	7.0	6.8	8.6	0.30
0.0024	0.098	–	–	–	3.1	0.24
0.0048	0.095	0.020	7.4	6.8	4.0	0.22
0.0072	0.093	0.035	8.8	6.8	4.5	0.22
0.0096	0.090	0.050	9.8	6.8	5.3	0.24
0.020	0.080	0.067	6.5	6.8	5.8	0.23
0.030	0.070	–	–	–	–	–
0.040	0.060	0.119	6.5	6.8	6.2	0.23
0.060	0.040	–	–	–	–	–
0.070	0.030	0.187	6.8	6.8	7.1	0.26
0.080	0.020	–	–	–		–

§ = dm^{3}mol^{-1}s^{-1}

a Concentration is 3 x 10^{-5} mol dm^{-3}.

b At completion of the fading reaction

c Calculated as Abs (528)/(0.58 – Abs (528))[NaOMe]

d Calculated from equation (11) with K_1 106 dm^{3}mol^{-1} and K_{M^+} 23 dm^{3}mol^{-1} and K_S 50

e Calculated from equation (2) with K_1 106 dm^{3}mol^{-1} and K_{M^+} 23 dm^{3}mol^{-1} and K_S 50

Values obtained with lithium methoxide, in Table 3–3, indicate negligible association of the adduct (3) with lithium ions. The values obtained for K_c 103 dm^3mol^{-1} and for K_c' 2.0 dm^3mol^{-1} are independent of base concentration and are similar to those obtained by extrapolation to zero base concentration of the sodium methoxide data. Methoxide attack at the cyano group does not involve any cation assistance and the value obtained for k_{CN} 0.26 $dm^3mol^{-1}s^{-1}$ is identical, within experimental error, to that obtained with sodium methoxide.

Data corresponding to that given in Table 3–1 were obtained for reaction with potassium methoxide in methanol. They showed strong interaction of the σ-adduct (3) with potassium ions and yielded values for K_1 105 dm^3mol^{-1}, K_{K^+} 40 dm^3mol^{-1}, K_S 50 and k_{CN} 0.26 dm^3mol^{-1}. An alternative approach was used to examine the effects of K^+, Ba^{2+} and Ca^{2+}. Rate and equilibrium constants were measured for solutions containing dilute tetrabutylammonium methoxide with added potassium, barium and calcium salts. Previous work[12] has shown that tetrabutylammonium ions have only very weak interactions with σ–adducts. The data in Tables 3–4 and 3–5 show good fit with the known values of K_1, K_S and k_{CN} and with values of K_{K^+} 40 ± 10 dm^3mol^{-1}, $K_{Ba^{2+}}$ 1000 ± 200 dm^3mol^{-1}, and $K_{Ca^{2+}}$ 200 ± 100 dm^3mol^{-1}.

In agreement with previous work[7,16] we found that the reaction of 2–cyano-4,6-dinitroanisole (8) with alkali metal methoxides resulted in the rapid production of (9) with λ_{max} 374, 382 and 466 nm (ϵ $1.8x10^4$ $dm^3mol^{-1}cm^{-1}$). Rate and equilibrium data for this process obtained using lithium methoxide are in Table 3–6. The results indicate that, as with the 4-cyano isomer, there is negligible association with lithium ions. Values of K_c are independent of lithium concentration leading to a value of K_1 of 100 mol dm^{-3}. A linear plot of k_{slow} vs base concentration gives k_1 11 $dm^3mol^{-1}s^1$ but has a very small intercept so that the value of k_{-1} is best determined from k_1/K_1 as 0.010 s^{-1}. The values obtained for K_1 and k_1 are lower than those previously reported[7] from measurements using sodium methoxide. This can be attributed to the effects of association of (9) with sodium ions. However, because adduct formation is extensive, >90% at 0.01 mol

dm^{-3} in very dilute base solutions quantitative determination of cation association constants was impractical

Table 3–3

Kinetic and equilibrium data at 25°C for reaction of (4)[a] with lithium methoxide in methanol

[LiOMe]/ mol dm^{-3}	k_{fast}[b] /s^{-1}	Abs[c] (528nm)	K_c/[d] $mol^{-1}dm^3$	Abs[e] (528nm)	K_c'/[f] $mol^{-1}dm^3$	$10^4 k_{slow}$ /s^{-1}	k_{CH}[g] §
0.0036	0.035	0.11	96	0.003	2.0	6.6	0.25
0.0048	–	0.14	101	0.004	2.0	8.2	0.26
0.0060	–	0.16	99	0.006	2.3	9.4	0.25
0.0072	0.046	0.19	110	0.008	2.6	12.0	0.28
0.0084	–	0.20	104	0.011	2.7	12.5	0.28
0.0096	0.054	0.22	114	–		13.0	–
0.040	0.12	–	–	–		–	–
0.070	0.21	–	–	–		–	
0.100	0.28	0.39	–	0.120	1.9	–	
0.600	–	0.42	–	0.230	1.9	–	
0.800	–	0.42	–	0.270	2.1	–	
1.00	–	0.43	–	0.290	2.1	–	

§ = $dm^3 mol^{-1} s^{-1}$

a Concentration is 2.3×10^{-5} mol dm^{-3}.

b Measured by stopped–flow spectrophotemetry at 528. A linear plot gives k_1 2.6 $dm^3 mol^{-1} s^{-1}$ and k_{-1} 0.025 s^{-1}.

c Measured with Lambda 3 instrument at completion of rapid colour forming reaction.

d Calculated as Abs (528)/(0.43 – Abs (528)) [LiOMe].

e Measured at completion of slower fading reactions.

f Calculated as Abs' (528)/(0.43 – Abs (528)) [LiOMe].

g Calculated from equation (2) with K_1 103 $dm^3 mol^{-1}$ and K_{M^+} zero.

Figure 3-6

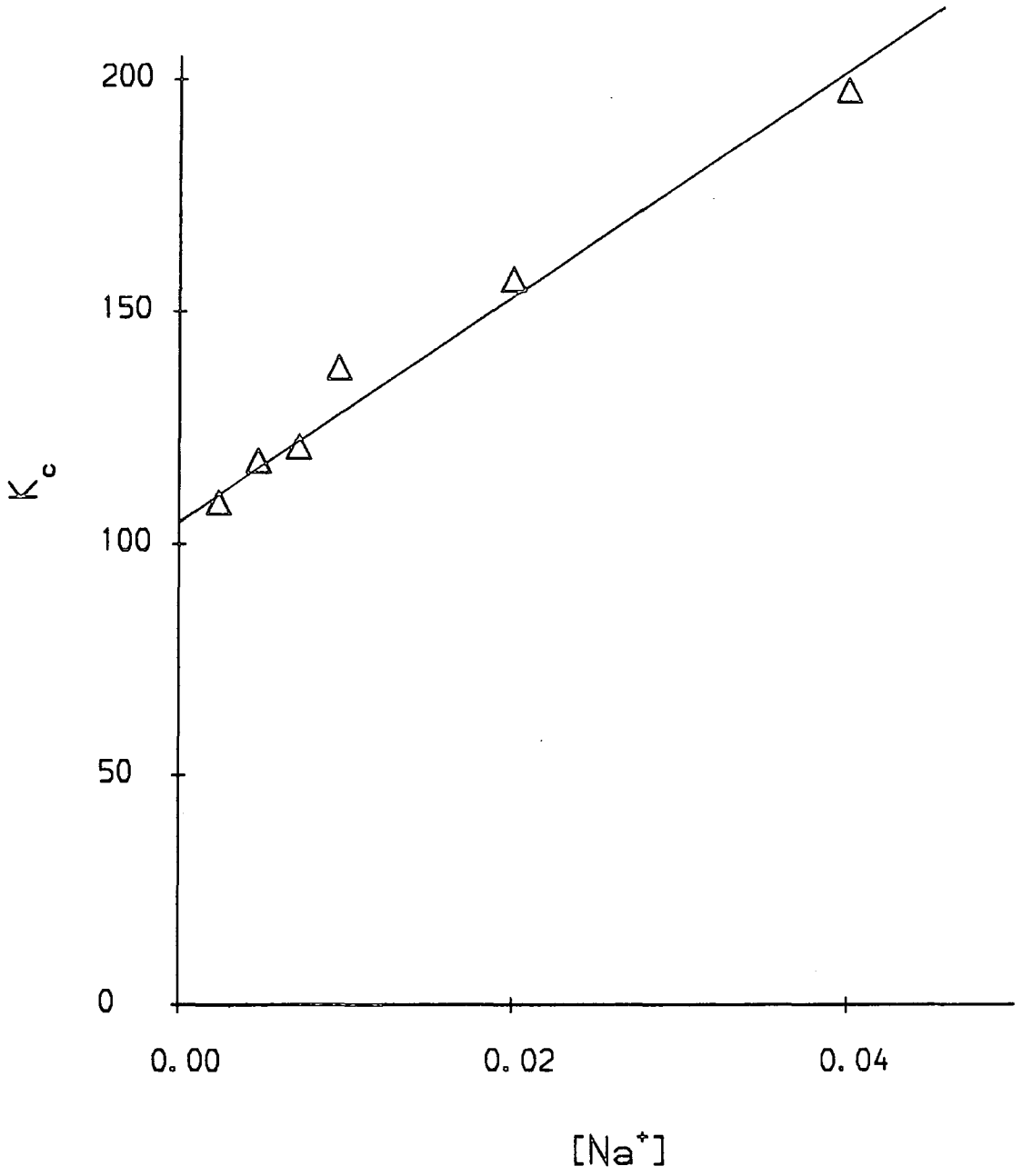

Figure 3-7

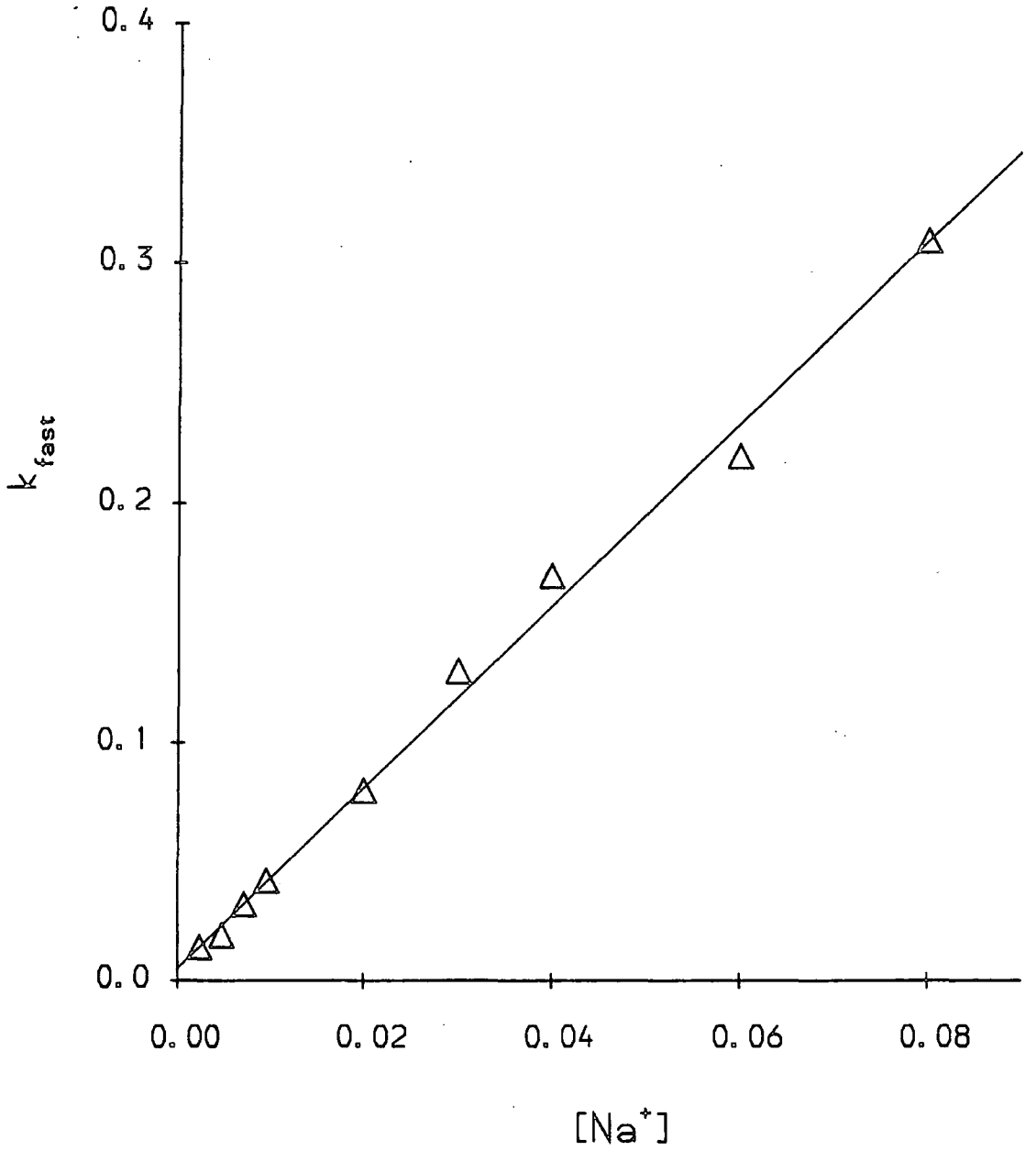

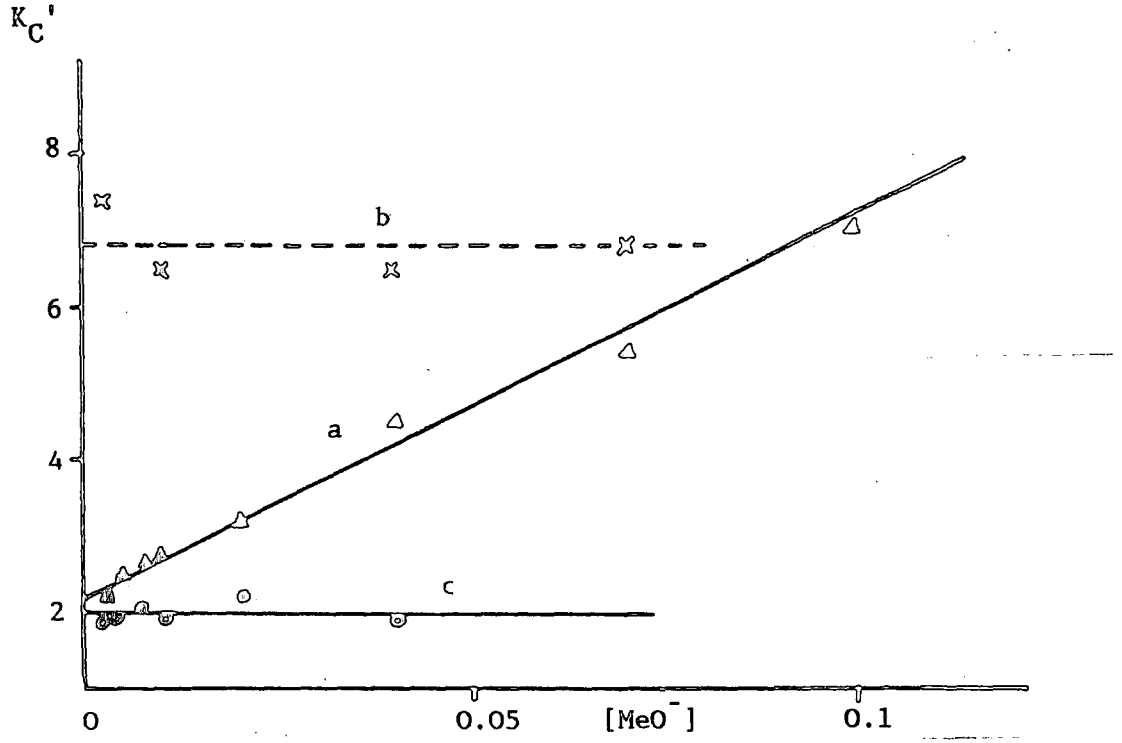

Figure 3—8 Variation of equilibrium constant after formation of the solvate

(a) with sodium methoxide;
(b) constant sodium concentration; 0.1M;
(c) with lithium methoxide.

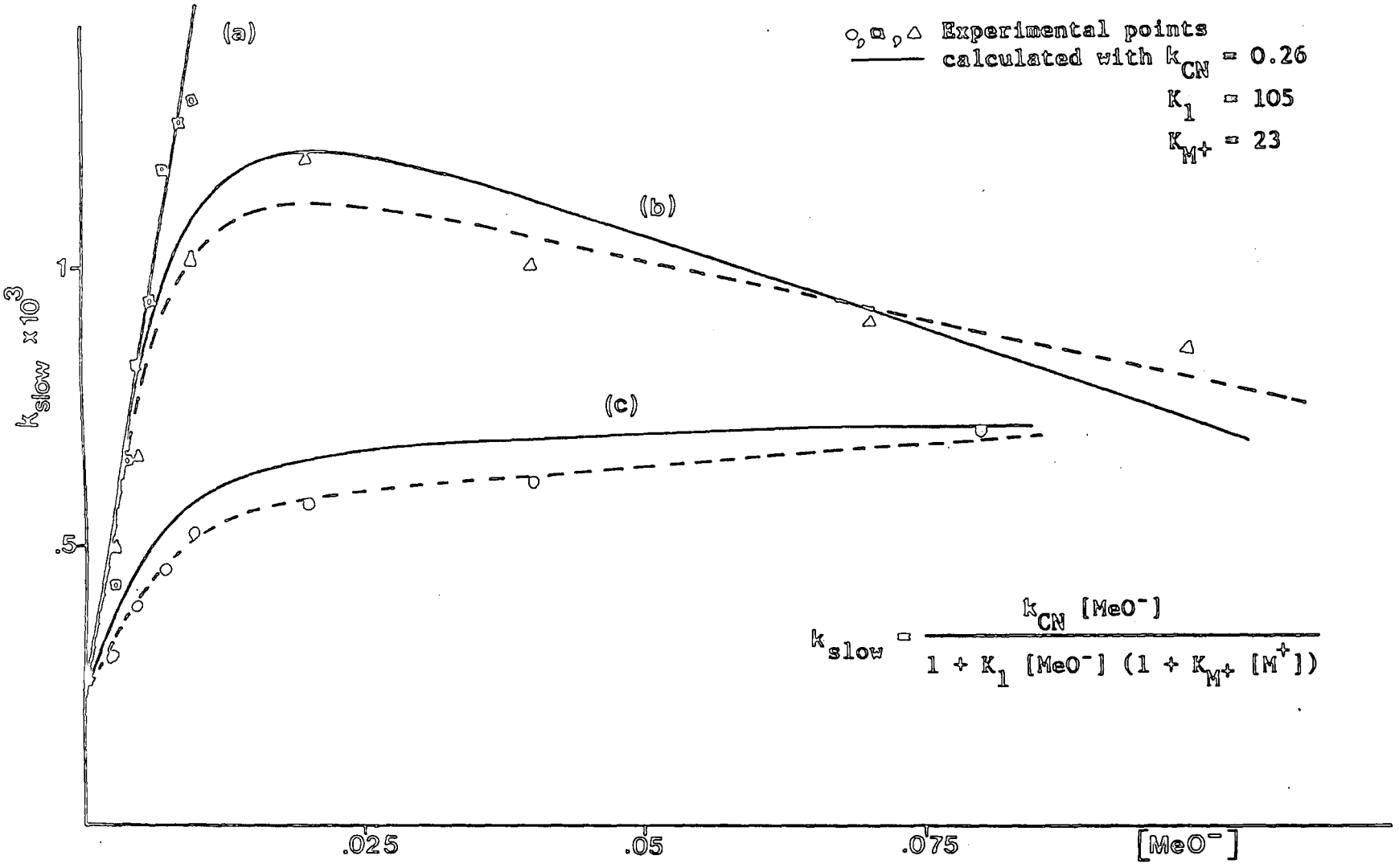

FIGURE 3-9. Variation of k_{slow} with base concentration

(a) lithium methoxide; (b) sodium methoxide;
(c) sodium ion concentration constant, 0.1M

Table 3–4 [Rapid Process]

Effects of K^+, Ba^{2+} and Ca^{2+} on reaction of (4)[a] with methoxide ions in methanol at 25°C

$[Bu_4NOMe]$ mol dm^3	Added salt/ mol dm^3	Abs[b] (528 nm)	K_c/[c] mol dm^{-3}	K_c[d] (calc)
0.005	–	0.186	102	102
	KI			
0.005	0.03	0.313	260	230
0.005	0.07	0.358	370	390
0.005	0.10	0.40	530	510
	$BaCl_2$			
0.005	0.001	0.25	170	200
0.005	0.002	0.34	320	300
0.005	0.004	0.40	530	510
0.005	0.007	0.44	800	820
0.005	0.010	0.46	1020	1100
	$CaCl_2$			
0.005	0.001	0.22	130	120
0.005	0.002	0.24	140	140
0.005	0.004	0.26	180	180
0.005	0.007	0.29	240	240
0.005	0.010	0.30	200	300

a Concentration is 2.9×10^{-5} mol dm^{-3}.

b At completion of rapid colour forming reaction.

c Calculated as Abs (528)/(0.55 – Abs (528)) $[Bu_4NOMe]$.

d Calculated from equation (6) with K_1 102 $dm^3 mol^{-1}$ and K_{K^+}, 40 $dm^3 mol^{-1}$, $K_{Ba^{2+}}$ 1000 $dm^3 mol^{-1}$ or $K_{Ca^{2+}}$ 200 $dm^3 mol^{-1}$.

Table 3–5 [Slow Process]

Effects of K^+, Ba^{2+} and Ca^{2+} on reaction of (4)[a] with methoxide ions in methanol at 25°C

$[Bu_4NOMe]$ mol dm^3	Added salt /mol dm^3	Abs[b] (528nm)	K'_c[c] /mol dm^{-3}	K_c[d] (calc)	$10^4 k_{slow}$/ s^{-1}	k_{CN}[e] §
0.005	–	–	–	–	9.3	0.28
	KI					
0.005	0.03	–	–	–	6.1	0.26
0.005	0.07	0.016	6	7.6	4.9	0.29
0.005	0.10	0.028	11	10	–	–
	$BaCl_2$					
0 005	0.001	–	–	–	6.4	0.26
0.005	0.002	0.026	10	6	4.6	0.23
0.005	0.004	0.038	15	10	3.2	0.23
0.005	0.007	0.043	17	16	2.5	0.25
0.005	0.010	0.052	21	22	2.2	0.29
	$CaCl_2$					
0.005	0.001	–	–	–	7.9	0.25
0.005	0.002	–	–	–	6.5	0.22
0.005	0.004	0.011	4.0	3.6	5.1	0.20
0.005	0.007	0.013	4.8	4.8	–	–
0.005	0.010	0.018	6.8	6.0	4.8	0.24

§ = $dm^3 mol^{-1} s^{-1}$

a Concentration is 2.9×10^{-5} mol dm^{-3}.

b At completion of slower fading reaction.

c Calculated as Abs' (528)/(0.55 – Abs' (528)) $[Bu_4NOMe]$.

d Calculated from equation (11) with K_1 102 $dm^3 mol^{-1}$ K_s50 and with K_{K^+} 40 $dm^3 mol^{-1}$, $K_{Ba^{2+}}$ 1000 $dm^3 mol^{-1}$ or $K_{Ca^{2+}}$ 200 $dm^3 mol^{-1}$.

e Calculated from equation (2) using k_{slow} values and the parameters quoted above.

Table 3–6 Kinetic and equilibrium data for reaction of 2–cyano-4,6–dinitroanisole[a] with lithium methoxide in methanol at 25°C

[LiOMe] / mol dm^{-3}	k_{fast}[b] / s^{-1}	Abs[c] (466 nm)	K_c[d] / mol dm^{-3}	Abs'[e] (466 nm)	K_c'[f] / mol dm^{-3}
0.004	0.05	0.491	1200	0.408	500
0.007	0.09	0.512	900	0.455	500
0.010	0.14	0.547	1300	0.483	500
0.015	0.17	0.556	1100	0.489	300
0.020	0.22	0.565	1100	0.504	300
0.050	0.57	0.582	–	0.534	–

a Concentration is 3.3×10^{-5} mol dm^{-3}.

b Measured by stopped–flow spectrophotometry at 466 nm. A linear plot of k_{fast} versus [LiOMe] gives k_1 11.6 $dm^3 mol^{-1} s^{-1}$.

c At completion of rapid colour forming reaction.

d Calculated as Abs (466)/(0.59 – Abs (466)) [LiOMe].

e At completion of slower fading reaction.

f Calculated as Abs' (466)/(0.59 – Abs' (466)) [LiOMe].

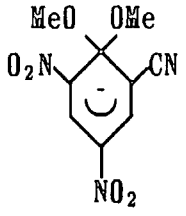

(9)

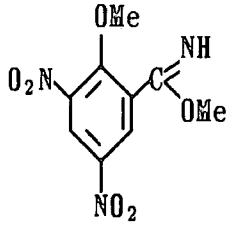

(10)

Also observed was a slow reversible fading reaction not previously reported, which can be attributed to methanolysis of the cyano–group to give (10). The decreases in absorbance, which were much less pronounced than those found with (4), were used to obtain a value of K_c' of 400 ± 100 mol dm^{-3}. The use of equation (3–11) gives a value for K of 3 ± 1. In 0.01M lithium methoxide solution the rate constant for the fading reaction had a value of $1.5 \times 10^{-4} s^{-1}$ and substitution in equation (3–2) allows the calculation of a value for k_{CN} of 0.18 $dm^3 mol^{-1} s^{-1}$.

3.1 DISCUSSION

Kinetic and equilibrium data are compared in Table 3–7. The ten–fold higher value of K_1 for reaction of (8) than for the corresponding reaction of (4) indicated the importance of a strongly electron withdrawing group *para* to the position of attack. This effect has been noted previously.[1] The overall increase in K_1 reflects an increased value of k_1 and decreased value for k_{-1}. These results show the previously unrecognised importance in these systems of methoxide attack at the cyano–group to yield solvates. The value of K_S is considerably higher for (4) than for (8) probably reflecting the different steric environments of the cyano–groups. Addition of solvent to the cyano–group at the carbon atom will result in a considerable increase in size. This will have no serious effect in (4) where the cyano–group has no *ortho* substituents, however in (8) will result in severe steric interaction with the methoxy–group resulting in rotation from the ring plane with consequent loss of conjugation.

Table 3–7 **Comparison of Data for (4) and (8)**

	(4)	(8)
K_1/dm^3mol^{-1}	105	1100
$k_1/dm^3mol^{-1}s^{-1}$	2.4	11
k_{-1}/s^{-1}	0.023	0.010
K_S	50	3
$k_{CN}/dm^3mol^{-1}s^{-1}$	0.26	0.18

These results show the source of the discrepancy in literature values for the equilibrium constant for adduct formation. The lower value corresponds to K_C' after equilibration of parent with σ-adduct and solvate, while the higher values correspond to K_C involving equilibrium between parent and σ-adduct only. Due to stabilisation of the adduct (3) by association with cations values of K_C increase with increasing sodium ion concentration. The value for K_1 of 105 ± 3 dm^3mol^{-1}

is lower than previous values[6,7] assigned to this quantity since these were obtained in solutions of varying sodium ion concentration.

It has been demonstrated[12,14,17] that association of 1,1-dimethoxy adducts with cations involves the oxygen atoms of the methoxy groups and of the *ortho*-ring substituents as shown in (11). The present results show that association

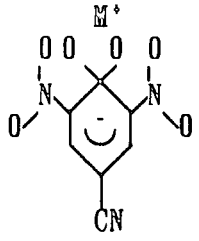

(11)

decreases in the order $Ba^{2+} > Ca^{2+} > K^{+} > Na^{+} > Li^{+}$. Divalent cations complex more strongly than monovalent cations and there is some correlation with size[15] of the unsolvated cations, Ba^{2+} 1.34Å, Ca^{2+} 0.99Å, K^{+} 1.33Å, Na^{+} 0.97Å, Li^{+} 0.68Å. This correlation suggests that the larger size of the barium and potassium ions allows most effective interaction with the oxygen atoms at the reaction centre.

REFERENCES

1 For a survey of adduct formation see: Buncel,E.; Crampton, M.R.; Strauss M.J.; Terrier,F., "*Electron deficient aromatic– and heteroaromatic-base interactions*", Elsevier, Amsterdam, 1984

2 Millot,F.; Terrier, F., *Bull. Soc. Chim. France*, 1974, 1823

3 Fendler, E.J.; Fendler, J.H. ; Arthur, N.L.; Griffin, C.E., *J. Org. Chem.*, 1972, 37, 812

4 Fendler, E.J.; Fendler, J.H.; Griffin, C.E.; Larsen, J.W., *J. Org. Chem.*, 1970, 35(2), 287

5 Dickeson, J.E.; Dyall L.K.; Pickles, V.A., *Aust. J. Chem.*, 1968, 21, 1267

6 Terrier, F.; Millot, F; Morel, J., *J. Org. Chem.*, 1976, 24, 3892

7 Fendler, J.H.; Fendler, E.J.; Griffin, C.E., *J. Org. Chem.*, 1969, 34, 689

8 Schaefer,F.C; Peters, G.A., *J. Org. Chem.*, 1961, 26, 412

9 Doddi, G.; Illuminati, G.; Stegel, F., *Tetrahedron Letters*, 1973, 34, 3221

10 Abe, T., *Bull. Chim. Soc. Japan*, 1983, 56, 1206

11 Miller, J., *J. Amer. Chem. Soc.*, 1954, 76, 448; Heppolette R.L.; Williams, V.A.; *ibid*, 1956, 78, 1975; Bayliss, N.S.; Heppolette, R.L.; Little L.H.; Miller, J., *ibid*, 1956, 78, 1978

12 Crampton M.R.; Khan, H.A., *J. Chem. Soc., Perkin Trans. II*, (1972), 1173; *ibid*, (1973), 1103; Crampton, M.R. *J. Chem. Soc., Perkin Trans. II*, (1977), 1442

13 Terrier, F., *Ann. Chim. France*, 1969, 4, 153

14 Sekiguchi, S.; Aizawa, T.; Aoki, M., *J. Org. Chem.*, 1981, 46, 3657; Sekiguchi, S.; Aizawa,T.; Tomoto, N. *J. Org. Chem.*, 1984, 49, 93

15 Handbook of Chemistry and Physics, Weast, R.C., Ed., CRC Press, 1977, F213

16 Caveng, P.; Fischer, P.B.; Heilbronner, E.; Miller, A.L.; Zollinger, H., *Helv. Chim. Acta.*, 1967, 50, 848

17 Gold, V.; Toullec, J., *J. Chem. Soc., Perkin Trans. II*, 1979, 596

Chapter 4
The Formation of 1:2 and 1:3 Adducts; Effects of cation complexing

4.1 Introduction

In chapter 3 it was seen that 1:1 adducts from 4-cyano-2,6-dinitroanisole and from 2-cyano-4,6-dinitroanisole may associate strongly with sodium and potassium ions. Also the association constants for the adducts with these cations have rather similar values. The first, and minor, part of the present chapter involves the determination of the association constants with Na^+ and with K^+ of the 1:1 adduct of 2,4,6-trinitroanisole (equation 4.1). The major part of the chapter involves the

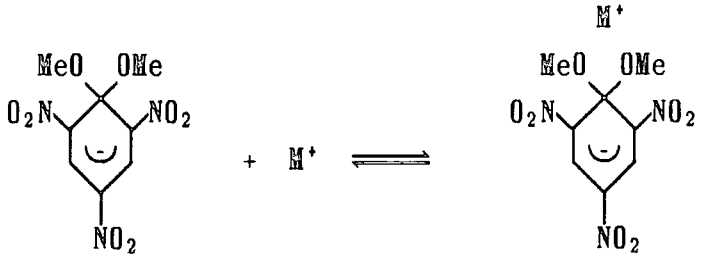

(4.1)

formation of 1:2 (2) and 1:3 (3) adducts by methoxide addition at two and three ring positions respectively. In most cases, the formation of these higher adducts

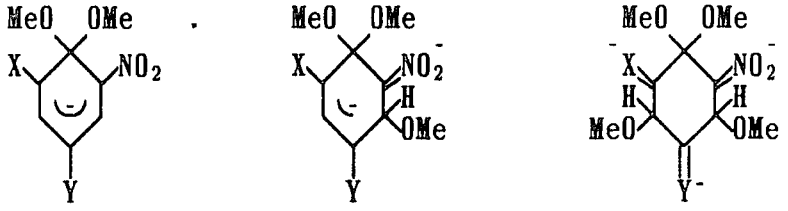

(1) (2) (3)

occurs only at high base concentration with [NaOMe] > 1M. However, it is known[1] that the 1:2 adduct of N,N-dimethylpicramide is formed at relatively low base concentrations. The equilibria involved here are shown in (4.2). It was possible to carry out a kinetic study of the equilibria

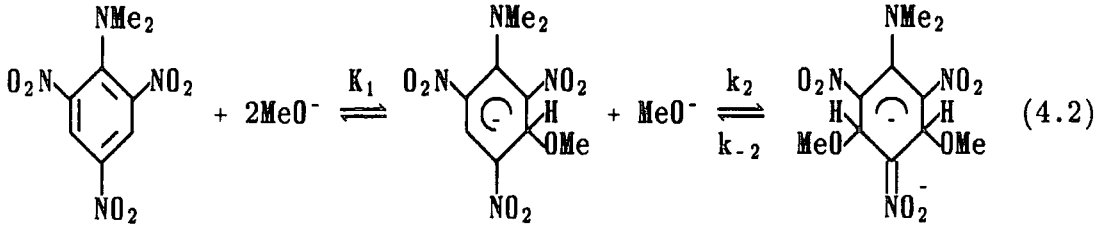

(4.2)

leading to the formation of the 1:2 adduct.

To achieve 1:2 adduct formation from 4-cyano-2,6-dinitroanisole and from 2-cyano-4,6-dinitroanisole it is necessary to work with concentrated base solutions. Similarly with 2,4,6-trinitroanisole and the spiro-adduct (4) formation of 1:2 and 1:3 adducts occurs only at high base concentrations.

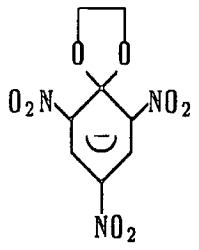

(4)

These equilibria have been used to examine the basicities of concentrated methoxide solutions. A particular point of interest was the relative basicity of sodium methoxide versus potassium methoxide. Previous attempts have been made to quantify the basicity of these media using acidity functions.[2-6] When ionisation involves proton loss (equation 4.3) the H_M function, defined in equation 4.4, is appropriate. With aromatic amines as indicators values of H_M fall, at a

$$SH + MeO^- \rightleftharpoons S^- + MeOH \qquad (4.3)$$

$$H_M = pK_{SH} + \log_{10} \frac{[S^-]}{[SH]} \qquad (4.4)$$

given base concentration, in the order KOMe > NaOMe > LiOMe. This order has been attributed to ion-association in the metal alkoxides which results in a reduction in their activities, the effect being greatest for lithium methoxide and smallest for potassium methoxide[5,7] Values of H_M may also be affected by differences in the relative solvation of reactants and products, i.e. the value of n in equation 4.3. Thus scales obtained using the ionisation of indole derivatives[6], where the anions are expected to be well solvated leading to low values of n, increases less steeply with base concentration than those obtained with aromatic

amines. Nevertheless the basicity order KOMe > NaOMe > LiOMe is preserved.

Recently[8] the "excess basicity" approach has been applied to solutions of metal methoxides in methanol. Again two important factors were thought to be ion-association of the methoxides, so that the basicity decreases in the order KOMe > NaOMe > LiOMe, and differences in solvation, reflected in variations in the value of a parameter m^* which relates activity coefficient ratios.

For parent molecules, P, which react by covalent addition of methoxide ions to give σ-adducts (equation 4.5), the basicity may be represented by the J_M function (equation 4.6)[2-5,9]

$$P + MeO^- \rightleftharpoons P.OMe^- \qquad (4.5)$$

$$J_M = pK + pK_{MeOH} + \log_{10} \frac{[P.OMe^-]}{[P]} \qquad (4.6)$$

As already noted, a third factor, in addition to those stated for proton loss equilibria, is important here. This factor is ion-association of the 1:1 dimethoxy adducts (2) with cations. Since the ion-pair association constants vary with the nature of the substrate no single J_M function can adequately describe the behaviour of all compounds. In this work the possible influence of association with cations of the 1:2 adducts (2) and 1:3 adducts (3) is examined.

4.2 Association of the 1,1-dimethoxy adduct of 2,4,6-trinitroanisole (TNA) with cations.

Evidence for the association given in (4.1) has been presented in previous work[10] The aim of the present work was to calculate association constants with Na^+ and with K^+.

$$K = \frac{[\text{TNA. MeO}^-.M^+]}{[\text{TNA . MeO}^-][M^+]} \qquad (4.7)$$

It is known that interaction with metal cations causes changes in the position of absorption maxima in the UV/visible spectrum. The equilibrium constant for the reaction of methoxide with TNA has a value of *ca.* $2x10^4$ dm^3mol^{-1} so that conversion to the adduct is virtually complete at 0.01M methoxide. Using tetramethylammonium methoxide where the cation does not strongly associate[10], absorption maxima at 415nm and 478nm were observed for the 1:1 adduct. The results in Table 4–1 show that increasing the concentration of sodium ions using either sodium perchlorate or sodium tetraphenylboron caused a small increase in the separation of these peaks. The limiting values at high Na^+ concentration were 410nm and 485nm.

Values of the association constant, K, were calculated using equation 4.8.

$$K[M^+] = \frac{\Delta\lambda - (\Delta\lambda)_0}{(\Delta\lambda)_\infty - \Delta\lambda} \qquad (4.8)$$

where $(\Delta\lambda)_0 = 478 - 415 = 63$nm, in the absence of Na^+ ions

and $(\Delta\lambda)_\infty = 485 - 410 = 75$nm, with excess Na^+ ions

Table 4–1 Effect of sodium ions on visible maxima of the 1:1 adduct of TNA in methanol

$[NaClO_4]$ M	λ_1 (nm)	λ_2 (nm)	$\Delta\lambda$	K $dm^3 mol^{-1}$
0.0054	413.4	481.0	67.6	115
0.0011	412.0	481.8	69.8	119
0.051	411.2	484.1	72.9	93
$[NaBPh_4]$ M				
0.002	414.0	479.4	65.4	120
0.005	412.5	480.0	67.5	118
0.01	412.0	480.8	68.8	93
0.02	411.2	482.1	70.9	96
0.05	410.4	483.4	73.0	100

Reacting system consisting of TNA, 2.5×10^{-5}M + Me_4NOMe, 0.01M

Values obtained in the process with increasing concentration of potassium methoxide are in Table 4–2. It is expected[11] that potassium methoxide should be largely dissociated in dilute solution so that the K^+ concentrations are taken as those of the potassium methoxide.

Table 4–2 **Effect of potassium ions on visible maxima of 1:1 adduct of TNA in methanol. Reacting system consisting of TNA, 3.0×10^{-5}M + KOMe, varying concentration.**

[KOMe] M	λ_1 (nm)	λ_2 (nm)	$\Delta\lambda$	K $dm^3 mol^{-1}$
0.0005	414.1	477.6	63.5	80
0.001	414.4	480.0	65.6	(250)
0.002	413.6	479.3	65.7	131
0.005	413.1	481.2	68.1	129
0.01	412.8	482.7	69.9	113
0.02	412.3	484.8	72.5	136
0.05	412.0	485.6	73.6	88
0.1	411.8	486.5	74.7	90

K calculated with $(\Delta\lambda)_0 = 63$nm, $(\Delta\lambda)_\infty = 487 - 411 = 76$nm

Although no great precision is claimed for these results, they suggest that the adduct (1) associates with K^+ and Na^+ with nearly equal strength.

The visible spectrum of the sodium salt of the 1:1 adduct of TNA was also recorded in a series of solvents (Table 4–3). Here the sodium ion concentration will be equal to that of the anion, $3x10^{-5}M$, so that ion-association is unlikely to be important.

Table 4–3 Visible maxima for 1:1 adduct of TNA in various solvents

Solvent	λ_1 (nm)	λ_2 (nm)	$\Delta\lambda$	Abs1/Abs2
CH_3CN	419.1	489.1	70.0	1.515
DMSO	423.1	496.0	72.9	1.516
MeOH	414.4	477.7	63.3	1.555
$CHCl_3$	408.6	511.2	102.6	1.178
Dioxan	403.2	510.4	107.2	1.073

Abs1/Abs2 corresponds to the ratio between the optical densities of the maxima at λ_1 and λ_2.

The results show that the spectrum is quite dependent on the type of solvent. The protic solvent, methanol, leads to the smallest separation of the two peaks and to the highest ratio of intensities. The aprotic, low-polar solvents chloroform and dioxan give rise to spectra that have two overlapping bands near 500nm. Addition of sodium tetraphenylboron to the solution of adduct (1) causes changes in the position of the maxima in the opposite direction of the shifts in methanol; in the presence of sodium ions the bands appear closer together with λ_1 = 405.7nm and λ_2 = 488.0nm and the ratio Abs1/Abs2 increases to 1.333.

Some measurements were also made in acetonitrile (Table 4–4) and these suggest that, in this solvent, association with Na^+ is stronger than in methanol.

Table 4–4 Effect of sodium ions on the visible spectrum of 1:1 adduct of TNA in acetonitrile

$[NaBPh_4]$ □	λ_1 (n□)	λ_2 (n□)	$\Delta\lambda$	K^* d□^{3}□ol^{-1}
0	419.1	489.1	70	
0.001	417.0	490.4	73.4	379
0.002	415.5	491.4	75.9	379
0.01	411.2	492.8	81.6	370
0.02	410.4	493.6	83.2	(255)

* K calculated assuming $(\Delta\lambda)_0 = 69$, $(\Delta\lambda)_\infty = 85$

Reacting system consisting of

TNA.MeO^-Na^+, $8x10^{-5}$M + $NaBPh_4$, varying concentration.

4.3 Reactions of TNA with Methoxides in solutions of high basicity

As stated previously, the interaction of 2,4,6-trinitroanisole, TNA, with potassium methoxide in methanolic solution gives rise to the formation of 1:1, 1:2 and 1:3 adducts, the concentration of each species in the solution being dependent on the concentration of the attacking base. The formation of these species may be followed by U.V./visible spectroscopy as they show absorption maxima at different wavelengths. These equilibria have been investigated in potassium methoxide solutions and the results are compared with data obtained by Rochester[9] in sodium methoxide solutions.

While the absorbance of TNA is negligible in the visible region, its only maximum of absorption appearing at 215nm, $\epsilon = 1.6 \times 10^4$ $dm^3 mol^{-1} cm^{-1}$, the addition of potassium methoxide causes the formation of 1:1 dimethoxy complex (1) exhibiting two new absorption bands at 410nm and 484nm; the intensity of these bands rises rapidly with increasing concentration of methoxide and remains constant up to a concentration of 1.6M, approximately, the ratio between intensities OD_{410}/OD_{484} being constant at *ca.* 1.5. For higher values of base concentration the 1:2 complex (2) is formed and because it shows only one maximum of absorbance at 484nm, the intensities ratio OD_{410}/OD_{484} decreases when the methoxide concentration increases.

Up to a base concentration of *ca.* 3.5M, the spectra of the two species in the interacting mixture show an isosbestic point, IP, at 436nm; equation (4-9) shows how the absorbance at the isosbestic point (OD_{IP}) is related to the stoichiometric concentration of the substrate and the extinction coefficient of the adduct. The optical density at this wavelength may be used to calculate the concentration of the 1:3 complex (3) which does not absorb in this region of the spectrum. (equation 4-10).

$$OD_{IP} = \epsilon([1:1] + [1:2]) = \epsilon \times TNA_{St} \qquad (4.9)$$

The subscript St denotes a stoichiometric concentration. When some 1:3 complex is formed, the OD at 436nm becomes lower.

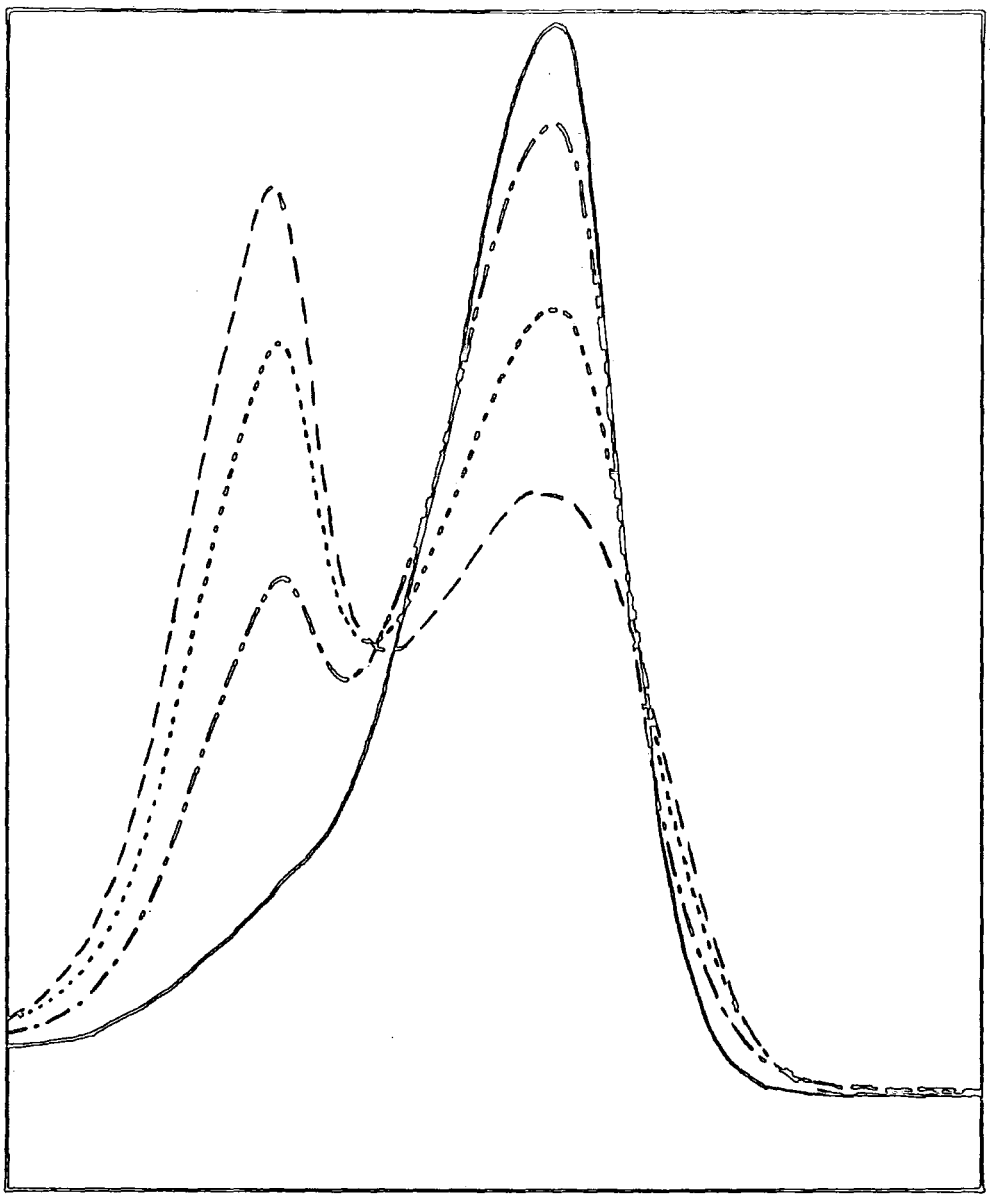

Figure 4–1 Visible spectra of TNA / MeO^- mixtures at different base concentrations

1. [KOMe] = 1.635 M
2. [KOMe] = 3.038 M
3. [KOMe] = 3.737 M
4. [KOMe] = 4.141 M

$$[1:3] = TNA_{St}\,(1 - OD_{436} / OD_{IP}) \qquad (4.10)$$

Hence the sum of the concentrations of 1:1 and 1:2 adducts could be found. The individual values of the two concentrations were determined from the OD at 410 using the known extraction coefficient at the wavelength (equation 4-11).

$$OD(410) = 2.47x10^4[1:1] + 7.9x10^3[1:2] \qquad (4\text{-}11)$$

These concentrations are listed in Table 4.5. The values have been used to calculate the experimental equilibrium constants, according to equation 4.12 and 4.13.

$$K_{exp}(1:2) = \frac{[1:2]}{[1:1][Base]_{Total}} \qquad (4.12)$$

$$K_{exp}(1:3) = \frac{[1:3]}{[1:2][Base]_{Total}} \qquad (4.13)$$

$[Base]_{Total}$ was calculated from the concentration of a stock solution, diluted with pure methanol, and includes free methoxide ions as well as ion-associated base, which is appreciable in the working range of concentration[10]

Table 4–5 Interaction of TNA with concentrated potassium methoxide

[KOMe] /M	OD_{410}	OD_{484}	OD_{436}	[1:1]x10^5 [a]	[1:2]x10^5 [b]	[1:3]x10^5 [c]
1.168	0.750	0.502	0.379	3.038		
1.635	0.750	0.514	0.390	3.038		
1.869	0.747	0.522	0.390	3.020	0.018	
2.336	0.730	0.555	0.385	2.92	0.12	
2.570	0.708	0.576	0.383	2.79	0.25	
2.686	0.691	0.585	0.380	2.66	0.38	
3.038	0.625	0.652	0.375	2.29	0.74	
3.387	0.525	0.738	0.375	1.70	1.34	
3.535	0.427	0.802	0.352	1.23	1.58	0.22
3.737	0.360	0.840	0.340	0.86	1.85	0.32
3.939	0.270	0.865	0.307	0.45	2.01	0.58
4.141	0.207	0.931	0.288	0.15	2.15	0.74

$$[TNA]_{St} = 3.038x10^{-5} M$$

a. Assuming that $OD_{410} = 0.750$ corresponds to the complete conversion of TNA to the 1:1 complex

$$\epsilon(1:1) = \frac{0.750}{3.038x10^{-5}} = 2.47x10^4 \text{ lmol}^{-1}\text{cm}^{-1}$$

b. Using a value at 410nm for $\epsilon(1:2) = 7.9x10^3 \text{ lmol}^{-1}\text{cm}^{-1}$ [9]

c. OD at the isosbestic point $OD_{IP} = 0.0380$

$$[1:3] = 3.038x10^{-5}\left[1 - \frac{OD_{436}}{0.380}\right]$$

Table 4–6

[KOMe] /M	① log [1:2]/[1:1]	$K_{1,2}$	② $\log K_{1,2}$	③ log [1:3]/[1:2]	$K_{2,3}$	④ $\log K_{2,3}$
1.168						
1.635						
1.869	–2.225	3.19×10^{-3}	–2.496			
2.336	–1.386	0.017	–1.770			
2.570	–1.048	0.035	–1.458			
2.686	–0.845	0.053	–1.274			
3.038	–0.491	0.106	–0.973			
3.387	–0.103	0.223	–0.633			
3.535	0.109	0.363	–0.440	–0.856	0.039	–1.405
3.737	0.333	0.576	–0.240	–0.762	0.046	–1.335
3.939	0.650	1.134	0.055	–0.540	0.073	–1.135
4.141	1.156	3.461	0.539	–0.463	0.083	–1.080

The results shown in Table 4–6 were used in figures 4.2 – 4.5. These graphs include plots of the relevant functions *vs* sodium methoxide concentration, calculated using results published by Rochester (1965)[9] for the interaction of TNA with NaOMe, for comparison purposes.

Figure 4–3 shows that the plot of $\log K_{1,2}$ *vs* [NaOMe] is linear for both NaOMe and KOMe and the lines are approximately parallel.

For NaOMe: slope = 1.155 For KOMe slope = 1.081

intercept = –3.276 intercept = –4.250

Figure 4-2

Interaction of TNA with concentrated methoxides
(a) M = Na^+. Calculations made upon results reported b
Rochester (1965)[9]. (b) M=K^+

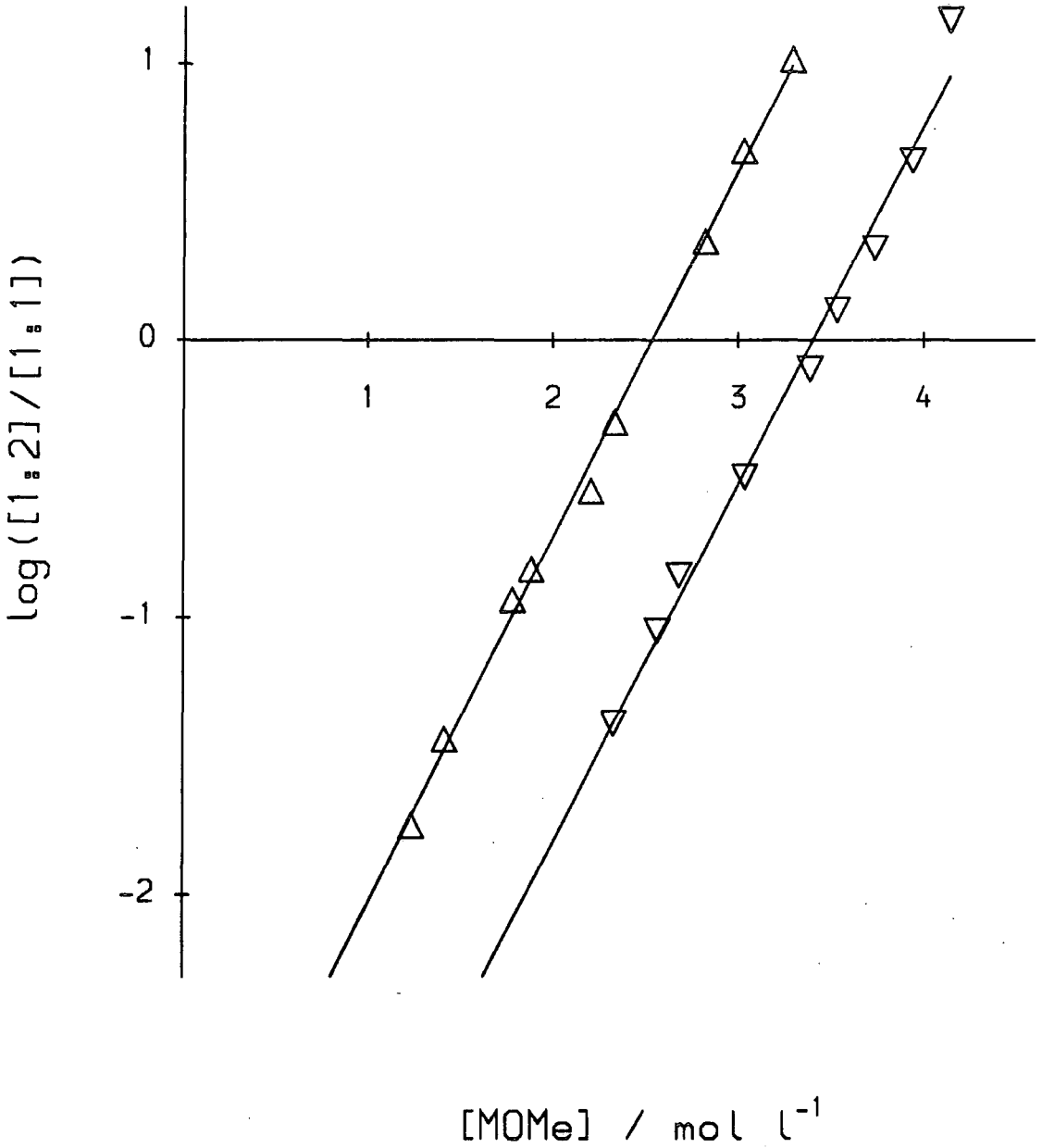

Figure 4-3

(a) M = Na^+. Calculations made upon results reported by Rochester (1965)[9]. (b) M=K^+

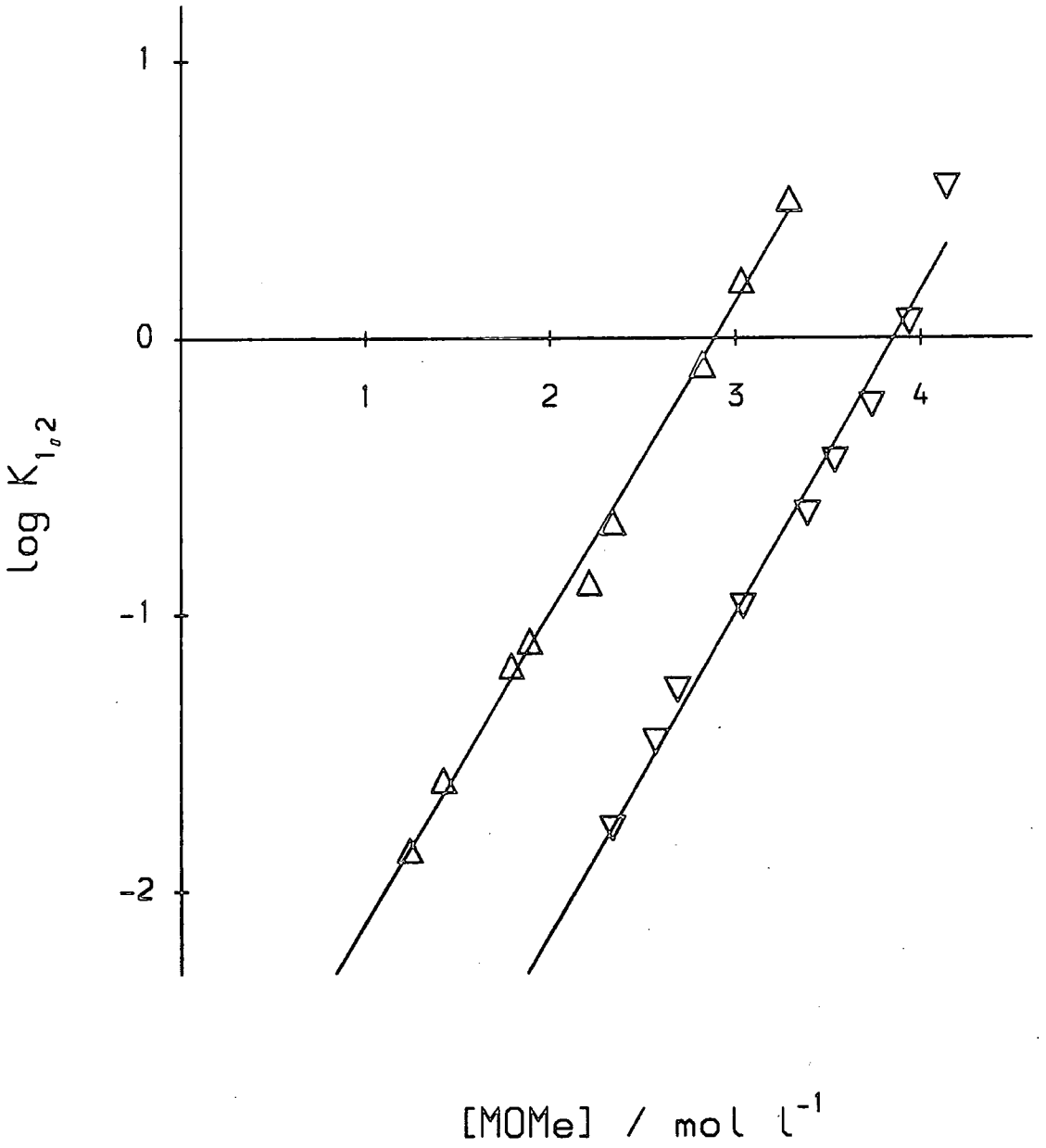

Figure 4-4

Formation of 1,3 adduct from the interaction of TNA wit
concentrated methoxides

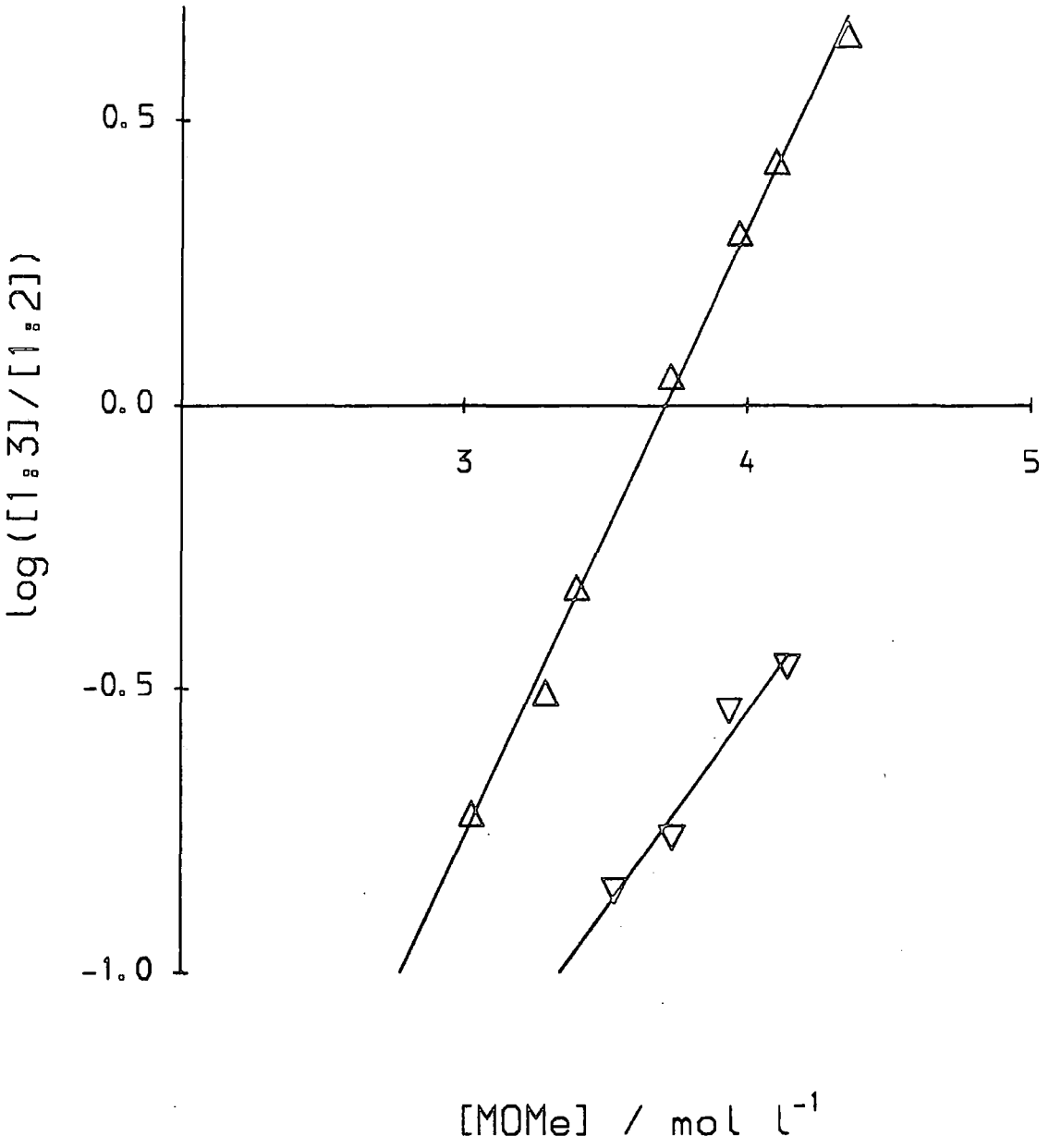

▽ potassium methoxide

△ sodium methoxide

Figure 4-5

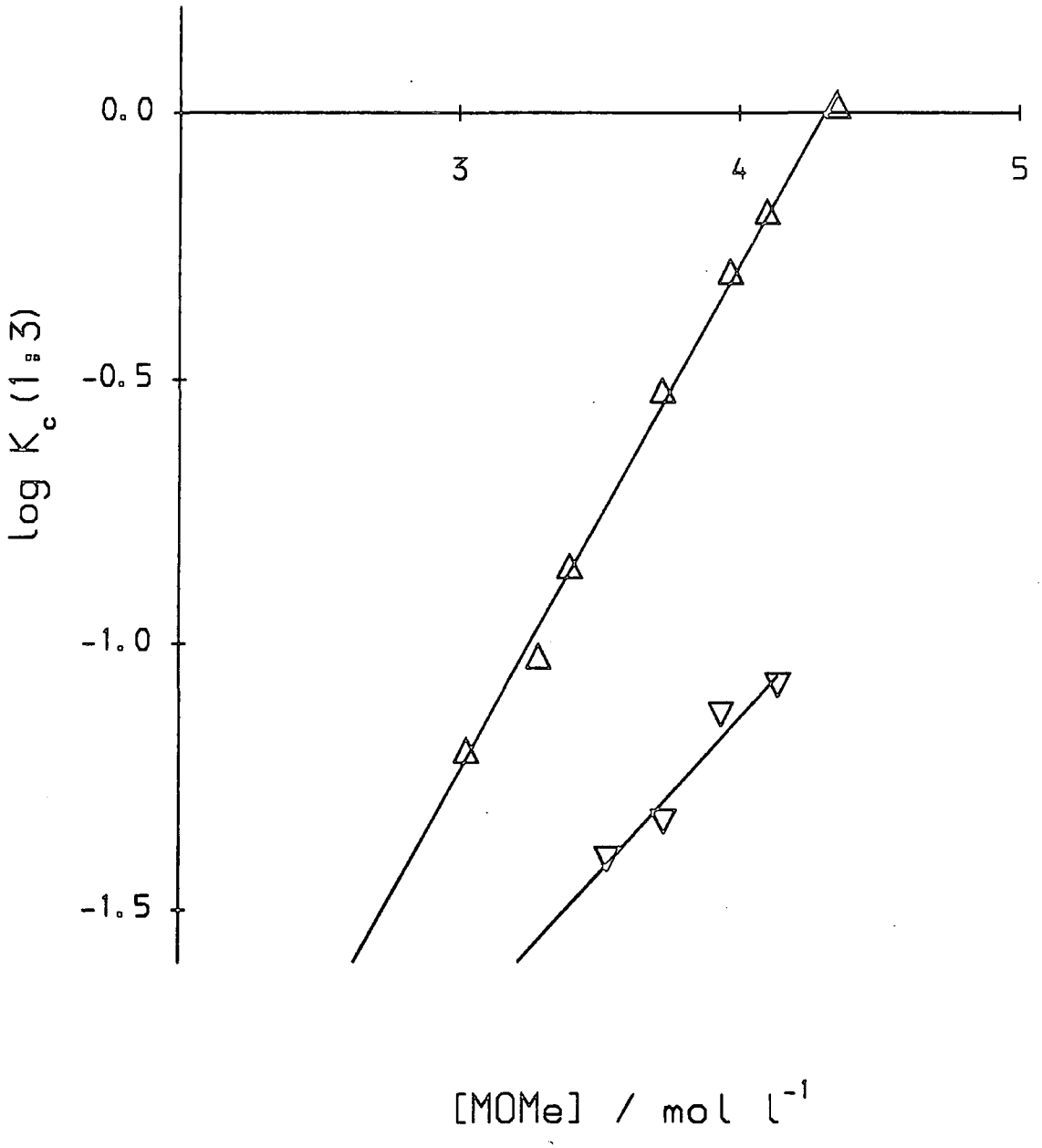

▽ potassium methoxide

△ sodium methoxide

According to More O'Ferrall and Ridd's method (1963)[12], the intercept gives the value of $\log_{10} K_C$

$$\text{NaOMe: } K_{1,2} = 5.3\text{x}10^{-4} \quad \text{KOMe: } K_{1,2} = 5.3\text{x}10^{-5}$$

assuming $pK_{MeOH} = 16.92$, then

$$p_{1,2}(KK_{MeOH}) = 20.20 \text{ for NaOMe}$$

$$p_{1,2}(KK_{MeOH}) = 21.17 \text{ for KOMe}$$

$$J^{2-}_{2M}(Na) = 20.20 + \log([1:2]/[1:1]) \text{ for NaOMe} \qquad (4.14)$$

$$J^{2-}_{2M}(K) = 21.17 + \log([1:2]/[1:1]) \text{ for KOMe} \qquad (4.15)$$

Table 4–7

[MeO⁻]	$J^{2-}_{2M}(Na)^*$	$J^{2-}_{2M}(K)$
2.336	20.62	19.78
2.570	20.96	20.12
2.686	21.12	20.32
3.038	21.63	20.68
3.387	22.13	21.07
3.535	22.35	21.28
3.737	22.63	21.50
3.939	22.92	21.82

* the values of log([1:2]/[1:1]) at these concentrations were determined from Figure 4–2.

The H_M scales[37] for alkali–metal methoxides give lower values for NaOMe than for KOMe, as reported before. The results on Table 4–7 indicate that for the same value of concentration NaOMe gives rise to greater values of J_M than KOMe.

It can be shown that the J_M scales for the (3)/(2) equilibrium lead to similar results (Figures 4–4 and 4–5).

Table 4–8

[MOMe]	J_{3M}^{3-}(Na)*	J_{3M}^{3-}(K)
3.535	21.02	19.53
3.737	21.25	19.63
3.939	21.47	19.85
4.141	21.70	19.93

4.4 Reactions of 4-cyano-2,6-dinitroanisole, 4CNDNA, with concentrated methoxide

Because the formation of methoxy–adducts is not the only reaction occurring when 4CNDNA interacts with methoxides, the absorption in the visible region is time dependent and so, the information was not taken from full spectra in this region but from the absorbance at a fixed wavelength (528nm), extrapolated to t = 0. At this wavelength, the 1:1 adduct has one of its two maxima of absorption, the other one being at 350nm.

For base concentrations higher than *ca.* 1M, the absorbance at 528nm decreases due to the formation of 1:2 and eventually 1:3 complexes and the concentrations of the adducts can be determined and used to calculate the acidity functions for sodium and potassium methoxides in methanol. The 1:2 adduct absorbs at 350nm while the 1:3 adduct does not absorb in the visible region. Measurements were made at 528nm at base concentrations where negligible conversion to 1:3 adduct was observed. The results for interaction of 4CNDNA are summarised on Tables 4–9 to 4–13.

Table 4–9

[NaOMe]	$Abs_{528}(t=0)$	[1:1]x10^5	[1:2]x10^5
1.0	0.678	3.60	—
2.0	0.574	3.05	0.55
2.4	0.355	1.88	1.72
2.6	0.222	1.45	2.15
2.8	0.208	1.10	2.50
3.0	0.102	0.74	2.86
3.2	0.088	0.44	3.16

$[4CNDNA]_{st} = 3.6x10^5 M$

$\epsilon(528) = 18833\ 1mol^{-1}cm^{-1}$

$[1:1] = A_{528} / 18833$

$[1:2] = [4CNDNA]_{st} - [1:1]$

Table 4–10

[NaOMe]	$\left(\frac{[1:2]}{[1:1]}\right)$	$K_{1,2}$	log $K_{1,2}$
2.0	–0.744	0.090	–1.045
2.4	–0.039	0.380	–0.419
2.6	0.171	0.789	–0.244
2.8	0.357	0.817	–0.091
3.0	0.587	1.889	0.110
3.2	0.856	2.244	0.351

log $K_{1,2}$ vs [NaOMe] is represented in Figure 4–6 and has slope 1.130, intercept –3.231 to which corresponds a value of K_c 5.87 x 10^{-4} at infinite dilution and $p(KK_{MeOH})$=20.15

Table 4–11

[KOMe]	Abs_{528}(t=0)	[1:1]x10^5	[1:2]x10^5
1.0	0.575	3.055	–
1.2	0.570	3.055	–
1.5	0.556	3.954	0.101
1.8	0.545	3.896	0.159
2.0	0.538	3.858	0.197
2.5	0.500	2.651	0.404
3.0	0.389	2.067	0.988
3.5	0.212	1.126	1.929
4.0	0.087	0.462	2.593

$[4CNDNA]_{st} = 3.055x10^{-5}M$

Table 4–12

[KOMe]	$\left(\frac{[1:2]}{[1:1]}\right)$/	$K_{1,2}$	log $K_{1,2}$
1.5	–1.466	0.023	–1.642
1.8	–1.260	0.031	–1.516
2.0	–1.162	0.034	–1.463
2.5	–0.817	0.061	–1.215
3.0	–0.321	0.159	–0.798
3.5	0.234	0.489	–0.310
4.0	0.749	1.403	0.147

log $K_{1,2}$ vs [KOMe] is represented in Figure 4–6 and has slope 0.9148, intercept –3.517 to which gives $K_{1,2} = 3.04x10^{-4}$ at infinite dilution and $p(KK_{MeOH}) = 20.44$

The results in Tables 4–10 and 4–12 and in figure 4–6 allow the calculation of the J^{2-}_{2M} acidity functions for sodium and potassium methoxide in interaction with 4CNDNA, presented in Table 4–13.

Table 4–13

[MOMe]	J^{2-}_{2M}(Na)	J^{2-}_{2M}(K)
2.5	20.14	19.62
2.6	20.32	19.72
2.8	20.15	19.93
3.0	20.74	20.12
3.2	21.01	20.35
3.5	–	20.67
4.0	–	21.19

Figure 4-6

Interaction of 4-CN-2,6-dinitroanisole with concentrated methoxides

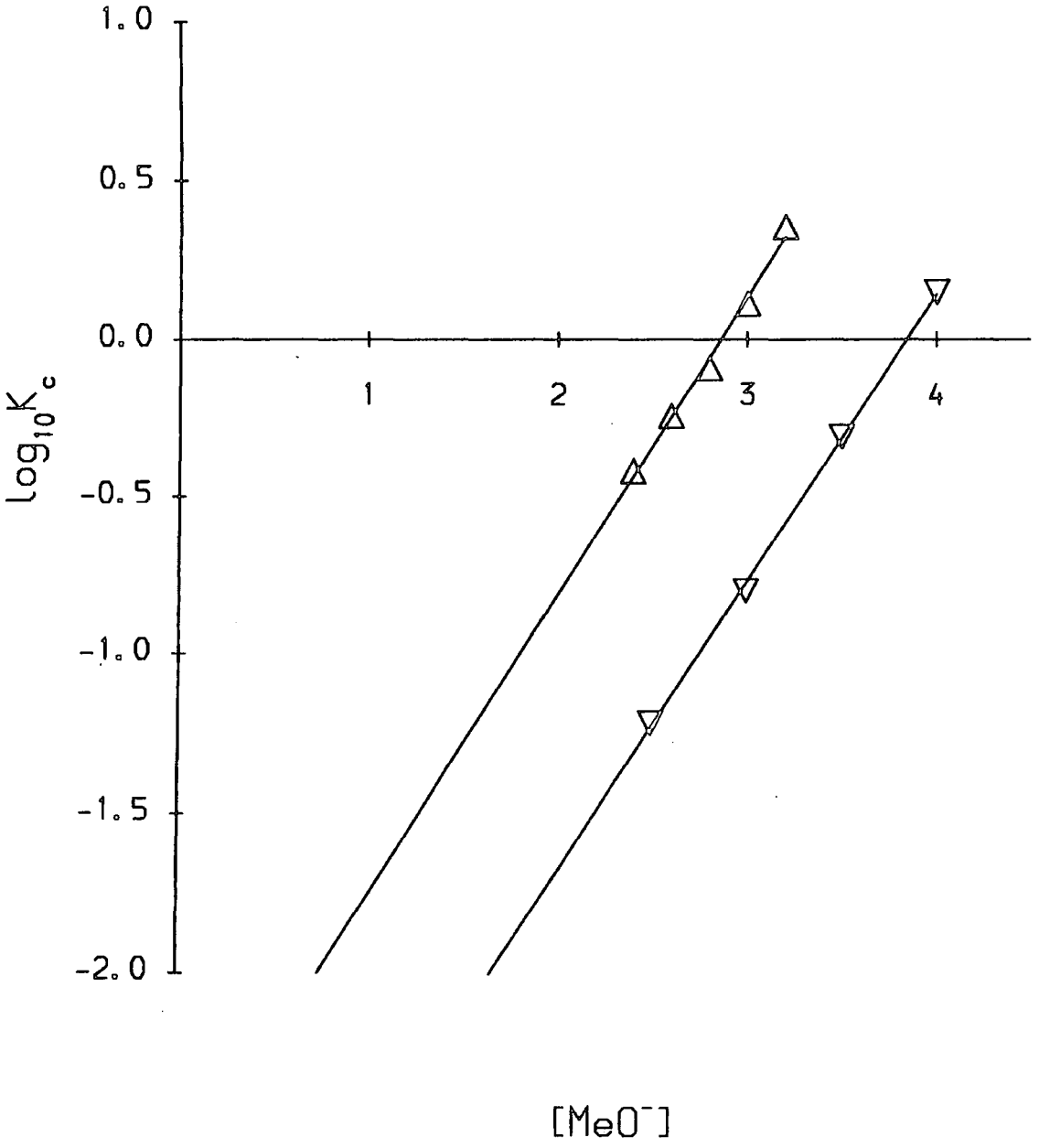

▽ potassium methoxide

△ sodium methoxide

4.5 Interaction of 2-cyano-4,6-dinitroanisole, 2CNDNA, with concentrated sodium methoxide

The 1:1 adduct formed in the reaction of 2CNDNA with sodium methoxide shows two bands of absorption at 368nm and 466nm; the bands of the equivalent complex with potassium methoxide appear slightly shifted at 375nm and 470nm respectively. In the spectra of the mixtures 2CNDNA and NaOMe there is an isosbestic point at 410nm, OD = 0.142, in the whole range of concentrations of 2.0M – 4.2M.

Table 4–14

[NaOMe]	A_{368}	A_{466}	[1:1]x10^5	[1:2]x10^5
2.0	0.450	0.450	2.5	–
2.3	0.445	0.428	2.38	0.12
2.6	0.463	0.388	2.16	0.34
3.0	0.470	0.296	1.64	0.86
3.3	0.483	0.184	1.02	1.48
3.5	0.503	0.105	0.58	1.92
3.7	0.507	0.071	0.39	2.11
4.0	0.512	0.028	0.16	2.34
4.1	0.517	0.018	0.10	2.40

$\epsilon_1(368) = \epsilon_1(466) = 18000$

$[1:1] = A_{466}/\epsilon_1(466)$

$[1:2] = [2CNDNA]_{st} - [1:1]$

$[2CNDNA]_{st} = 2.50x10^{-5}M$

Table 4–15

[NaOMe]	log([1:2]/[1:1])	$K_{1,2}$	log $K_{1,2}$
2.3	–1.297	0.022	–1.659
2.6	–0.802	0.061	–1.217
3.0	–0.280	0.175	–0.757
3.3	0.161	0.440	–0.357
3.5	0.520	0.946	–0.024
3.7	0.733	1.352	0.131
4.0	1.165	3.482	0.542
4.1	1.380	5.851	0.767

log $K_{1,2}$ *vs* [NaOMe] has slope = 1.2870

intercept = –4.5959

$K_c(0) = 2.53 \times 10^{-5}$

r = 0.99891

Table 4–16

[KOMe]	A_{375}	A_{470}	[1:1]x10^5	[1:2]x10^5
2.0	0.494	0.500	2.89	–
2.4	0.495	0.500	2.89	–
2.8	0.500	0.490	2.83	0.06
3.0	0.520	0.487	2.82	0.07
3.2	0.525	0.453	2.62	0.26
3.4	0.530	0.416	2.40	0.48
3.6	0.535	0.353	2.04	0.82
4.0	0.553	0.215	1.24	1.53

$[2CNDNA]_{st} = 2.89 \times 10^{-5}$ M

$[1:1] = A_{470} / \epsilon_1(470)$

$[1:2] = [2CNDNA]_{st} - [1:1]$

Table 4–17

[KOMe]	log([1:2]/[1:1])	$K_{1,2}$	log $K_{1,2}$
3.0	–1.605	0.008	–2.082
3.2	–1.003	0.031	–1.508
3.4	–0.699	0.059	–1.230
3.6	–0.396	0.112	–0.952
4.0	0.091	0.308	–0.511

log $K_{1,2}$ *vs* [KOMe] has slope = 1.130

intercept = –5.070

$K_C(0)$ = 8.51×10^{-5}

r = 0.9962

Table 4–18

[NaOMe]	J^{2-}_{2M}(Na)	J^{2-}_{2M}(K)
2.6	20.71	19.90
3.0	21.23	20.39
3.2	21.56	20.99
3.4	21.85	21.29
3.6	22.14	21.60
3.7	22.24	21.70
4.0	22.67	22.08
4.1	22.89	22.34

Figure 4-7

Interaction of 2-CN-4,6-dinitroanisole with concentrated methoxides

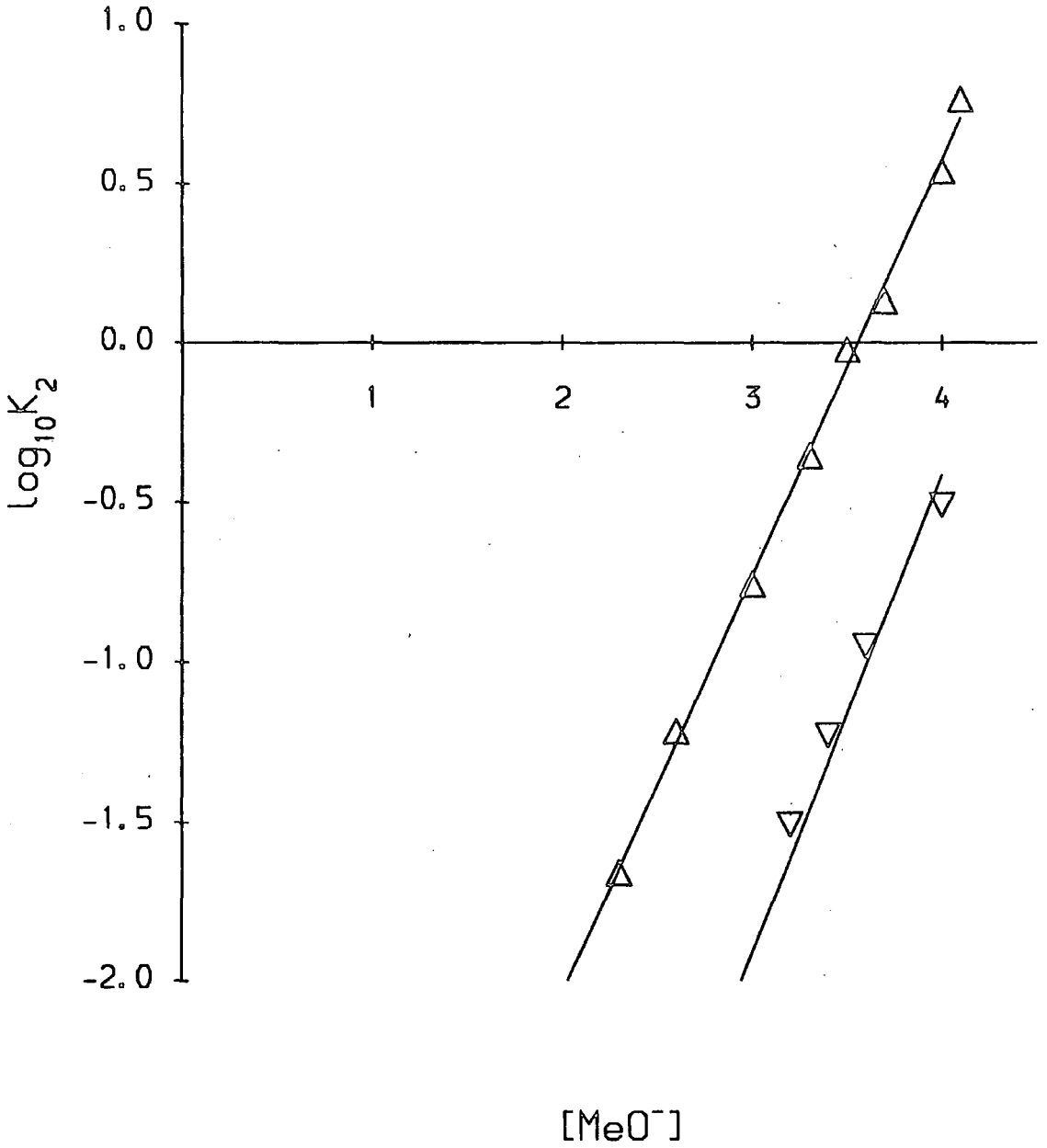

▽ potassium methoxide

△ sodium methoxide

4.6 Interaction of 1-[2 Hydroxyethoxy]-2,4,6-trinitrobenzene with methoxides

In very dilute base solutions[13] cyclisation of 1-[2 hydroxyethoxy]-2,4,6- trinitrobenzene (5) occurs to give the spiro-adduct (4) with maxima at 415 and

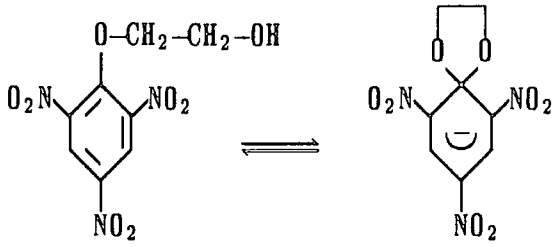

(5) (4)

474nm. In concentrated base solutions methoxide attack occur at the 3-position to give a di-anion with λ_{max} at 480nm, and at the 3- and 5- positions to give a tri-anion which is transparent in the visible region.

In solutions containing only mono- and di-anionic species an isosbestic point is observed at 445nm. Measurements of absorption at this wavelength and at 415nm allowed the relative concentrations of the three adducts present to be determined in a manner similar to that already described for TNA.

Table 4–21 Interaction of 1–[2–Hydroxyethoxy]–2,4,6–trinitrobenzene (5) with concentrated sodium methoxide

[NaOMe]	A_{415}	$A_{445}^{(IP)}$	A_{473}	[1:1]x10^5	[1:2]x10^5	[1:3]x10^5
1.0	0.786	0.525	0.540	3.14	–	–
1.5	0.805	0.540	0.556	3.22	–	–
2.2	0.786	0.542	0.562	3.14	0.08	–
2.4	0.772	0.542	0.573	3.09	0.13	–
2.6	0.737	0.543	0.591	2.95	0.27	–
2.8	0.680	0.525	0.639	2.72	0.40	0.10
3.0	0.610	0.510	0.623	2.44	0.59	0.19
3.2	0.522	0.483	0.609	2.09	0.78	0.35
3.4	0.374	0.444	0.585	1.50	1.14	0.58
3.6	0.287	0.396	0.545	1.15	1.23	0.87
3.8	0.240	0.312	0.460	0.56	1.71	1.37
4.0	0.060	0.207	0.315	0.24	0.99	1.99
4.2	0.015	0.100	0.150	0.06	0.53	2.63
4.4	0.000	0.075	0.096	–	0.45	2.77

$\epsilon_1(415) = 25000\ 1mol^{-1}cm^{-1}$

$[5]_{st} = 3.22x10^{-5}M$

$[1:1] = A_{415} / \epsilon_1(415)$

$[1:2] = [5]_{st} - ([1:1] + [1:3])$

$[1:3] = [5]_{st}(1 - A_{445} / 0.542)$

Table 4–22

[NaOMe]	$\log\left(\frac{[1:2]}{[1:1]}\right)$	$K_{1,2}$	log $K_{1,2}$
2.2	–1.594	0.012	–1.936
2.4	–1.376	0.017	–1.756
2.6	–1.038	0.035	–1.453
2.8	–0.833	0.053	–1.280
3.0	–0.616	0.081	–1.092
3.2	–0.428	0.132	–0.881
3.4	–0.119	0.224	–0.651
3.6	0.018	0.290	–0.538
3.8	0.485	0.804	–0.095
4.0	0.615	1.031	0.013
4.2	0.946	2.103	0.323

Table 4–23

[NaOMe]	$\log\left(\frac{[1:3]}{[1:1]}\right)$	$K_{1,3}$	log $K_{1,3}$
2.8	–0.602	0.089	–1.049
3.0	–0.492	0.107	–0.969
3.2	–0.437	0.114	–0.942
3.4	–0.293	0.150	–0.825
3.6	–0.140	0.201	–0.696
3.8	–0.096	0.211	–0.676
4.0	0.303	0.502	–0.299
4.2	0.696	1.181	0.072
4.4	0.789	1.399	0.146

Table 4–24

Interaction of (5) with concentrated Potassium Methoxide

[KOMe]	A_{415}	$A_{445}^{(1P)}$	A_{473}	[1:1]x10^5	[1:2]x10^5	[1:3]x10^5
2.0	0.830	0.545	0.588	3.33	–	–
2.3	0.820	0.545	0.592	3.29	0.04	–
2.5	0.792	0.545	0.608	3.18	0.15	–
2.8	0.724	0.545	0.679	2.90	0.43	–
3.0	0.704	0.545	0.695	2.82	0.51	–
3.3	0.571	0.529	0.761	2.29	0.94	0.10
3.8	0.246	0.425	0.770	0.99	1.61	0.73
4.0	0.131	0.390	0.725	0.53	1.85	0.95
4.3	0.100	0.384	0.674	0.40	1.95	0.98
4.5	0.020	0.290	0.300	0.08	1.69	1.56
4 8	0.000	0.233	0.420	–	1.42	1.91

[5]=3.33 x 10^{-5}M

From the results in Table 4–22 and plotted in Figure 4–9 as log $K_{1,2}$ *vs* [NaOMe], the intercept of this plot is –4 331, which implies K_C 4.66×10^{-5} at infinite dilution of sodium methoxide and $p(KK_{MeOH}) = 21.25$

Identical plots of the results for the interaction with potassium methoxide (Table 4–25 and Figure 4–9) show that the intercept f log $K_{1,2}$ *vs* [KOMe] is –4.485, thus $K_C = 3.27 \times 10^{-5}$ at infinite dilution and $p(KK_{MeOH}) = 21.40$

These calculated values of $p(KK_{MeOH})$ and the results shown on Figure 4–8 were used to calculate the J_M acidity functions for potassium and sodium methoxide (Table 4–27).

Table 4–25

[KOMe]	$\log\left(\frac{[2:1]}{[1:1]}\right)$	$K_{1,2}$	log $K_{1,2}$
2.5	–1.326	0.019	–1.724
2.8	–0.829	0.053	–1.276
3.0	–0.743	0.060	–1.220
3.3	–0.387	0.124	–0.950
3.8	0.211	0.428	–0.369
4.0	0.543	0.873	–0.059
4.3	0.688	1.133	0.055
4.5	1.325	4.694	0.671

Table 4–26

[KOMe]	$\log\left(\frac{[1:3]}{[1:2]}\right)$	$K_{1,3}$	log $K_{1,3}$
3.3	–0.973	0.032	–1.492
3.8	–0.344	0.119	–0.923
4.0	–0.289	0.128	–0.892
4.5	–0.035	0.205	–0.688
4.8	0.129	0.280	–0.552

Figure 4-8

Interaction of 1-[2-hydroxyethyl]-2,4,6-trinitrobenzene with concentrated methoxides

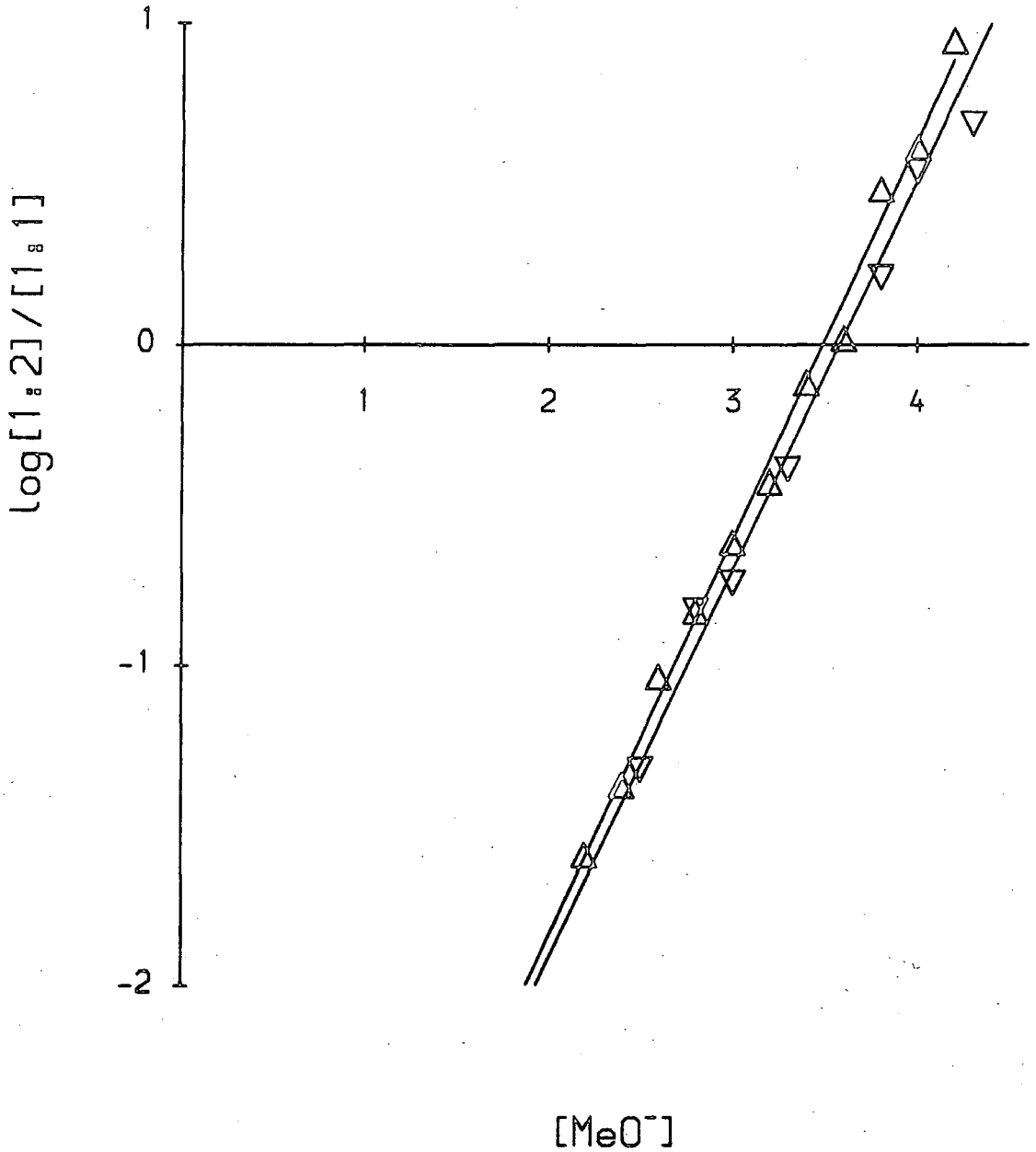

▽ potassium methoxide

△ sodium methoxide

Figure 4.9

Interaction of 1-[2-hydroxyethyl]-2,4,6-trinitrobenzene with concentrated methoxides

Formation of 1:2 adduct

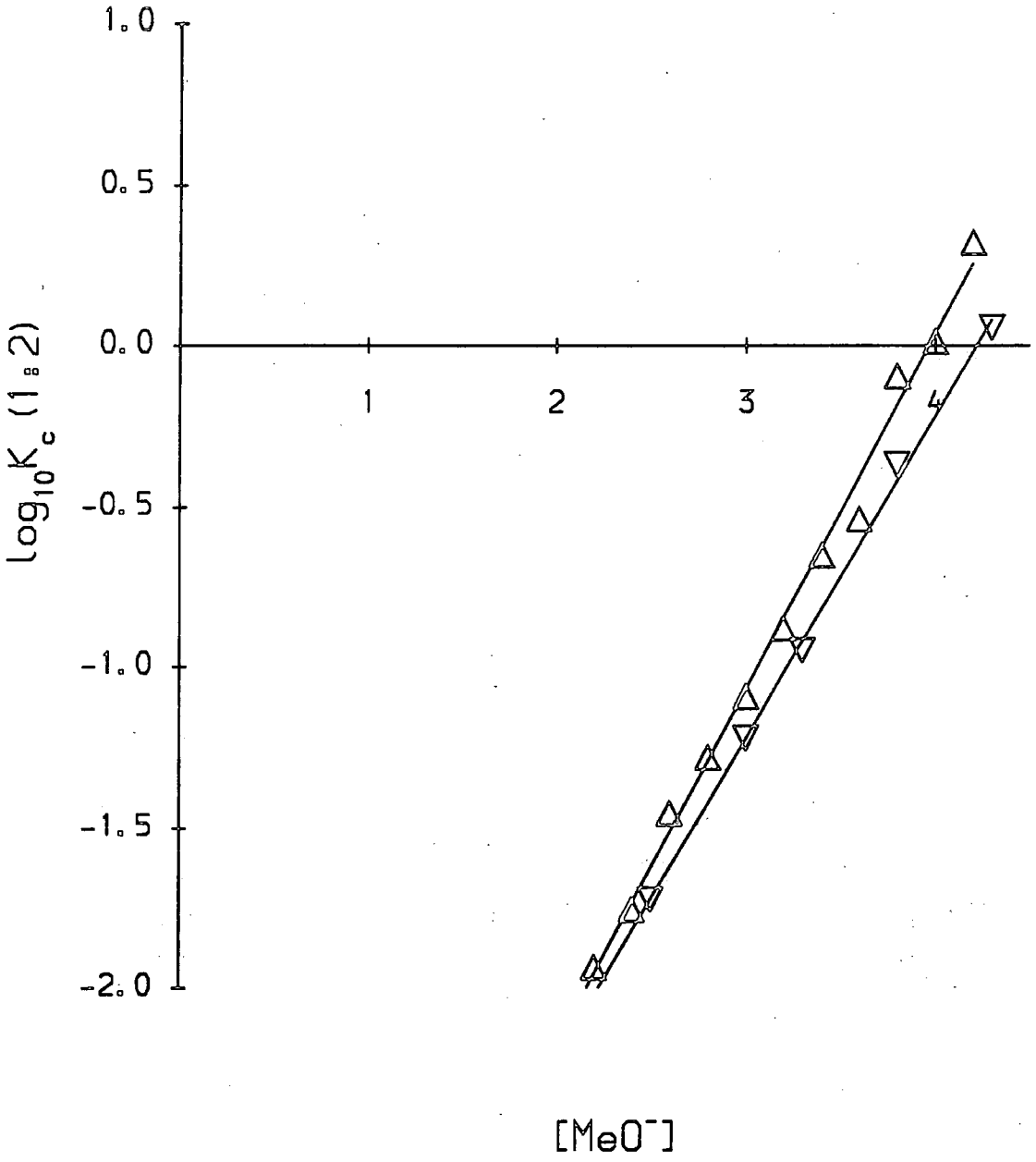

▽ potassium methoxide

△ sodium methoxide

Figure 4.10

Formation of 1,3 adduct from the interaction of 1-[2-hydroxyethyl]-2,4,6-trinitrobenzene with concentrated methoxides

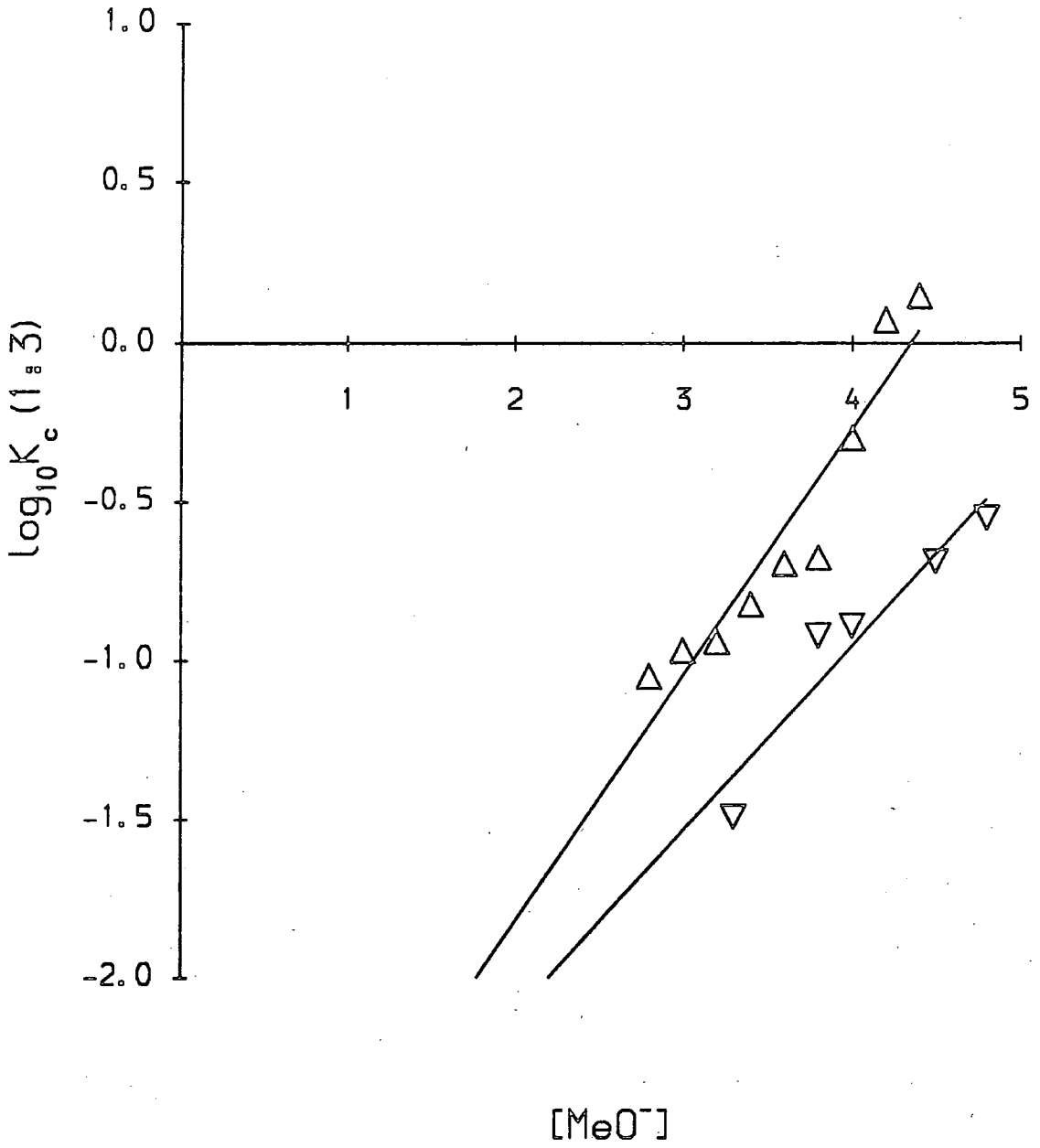

▽ potassium methoxide

△ sodium methoxide

Table 4–27

[MOMe]	J^{2-}_{2M}(Na)	J^{2-}_{2M}(K)
2.2	19.92	19.80
2.4	20.13	20.03
2.6	20.47	20.25
2.8	20.63	20.48
3.0	20.89	20.71
3.2	21.08	20.94
3.4	21.39	21.16
3.6	21.53	21.39
3.8	21.99	21.62
4.0	22.22	21.84
4.2	22.66	22.07

From Figure 4–10 and Table 4–23, it is possible to establish scales of the J_M acidity function for the formation of the 1:3 methoxy adduct for the interaction of the picryl compound with sodium methoxide; the results for the reaction with potassium methoxide are too disperse to allow the same type of calculation.

The intercept of log $K_{1,3}$ *vs* [NaOMe] is –3.4486 from which K_c at infinite dilution is determined to be $3.56x1^{-4}$ and $p(KK_{MeOH}) = 20.37$. The corresponding J^{3-}_{3M} function scale is on Table 4–28.

Table 4–28

[NaOMe]	J^{3-}_{3M}(Na)
2.8	19.77
3.0	19.88
3.2	19.93
3.4	20.88
3.6	20.23
3.8	20.27
4.0	20.67
4.2	21.07
4.4	21.16

4.7 Discussion

The equilibria studied may, formally, be used to define the acidity functions given in equations (4-16) and (4-17). Here J^{2-}_{2M} indicates addition at two ring-

$$J^{2-}_{2M} = pK_{1,2} + pK_{MeOH} + \log_{10}\frac{[2]}{[1]} \qquad (4\text{-}16)$$

$$J^{3-}_{3M} = pK_{2,3} + pK_{MeOH} + \log_{10}\frac{[3]}{[2]} \qquad (4\text{-}17)$$

positions to give a di-anionic adduct and J^{3-}_{3M} the corresponding addition at three ring-positions. $K_{1,2}$ and $K_{2,3}$ are, respectively, the thermodynamic equilibrium constants, referred to methanol as standard state, for conversion of (1) to (2), and of (2) to (3). In order to anchor the scales it is necessary to be able to either measure one or more equilibrium constant in dilute (ideal) solutions or to extrapolate data obtained from more concentrated solutions. The problem is that values of the indicator ratios [2]/[1] and [3]/[2] can only be made in concentrated base solutions and there is no accurate way to extrapolate to zero base concentration. For example, since $K_{1,2}$ must have a unique value independent of the cation, the essentially parallel lines A and B in Figure 4-2 must be extrapolated to hit the Y axis at zero base concentration with the same intercept! The problem of extrpolation has been noted previously[14,15] in studies of the formation of 1:1 adduct from neutral parent molecules and has been shown[10,14] to result from complexing of the 1:1 adducts with cations.

Nevertheless, since $K_{1,2}$ and $K_{2,3}$ are thermodynamic quantities they will have values which are independent of the cation, so that it is possible, using equations (4-16) and (4-17), to compare the J^{2-}_{2M} and J^{3-}_{3M} basicities for sodium methoxide and potassium methoxide. This requires only a knowledge of the experimentally observable indicator ratios. Values of ΔJ^{2-}_{2M}, defined in equation (4-18), and corresponding values of ΔJ^{3-}_{3M} calculated at different base concentrations are given in Table 4-29. Interestingly, the values for all indicators

$$\Delta J^{2-}_{2M} = J^{2-}_{2M}(\text{NaOMe}) - J^{2-}_{2M}(\text{KOMe}) \qquad (4\text{-}18)$$

are positive showing that for these equilibria sodium methoxide solutions are more "basic" than the corresponding potassium methoxide solutions. Also, at a given base concentration, the value of ΔJ^{2-}_{2M} depends on the indicator used showing that no uniqe J^{2-}_{2M} scales exist which are independent of the indicator. The values of $\Delta H_{M,}$ also given in Table 4-29, show that for the aromatic amines used as indicators, potassium methoxide solutions are more "basic" than corresponding sodium methoxide solutions. This latter observation has been attributed to the stronger ion-pairing of methoxide with sodium ions than with potassium ions;[5,7] and this factor will not vary with the nature of the indicator.

Two possible explanations for the basicity inversion observed here with the J^{2}_{2M} indicators are:- (i) differences between the solvating abilities of sodium and potassium methoxide solutions, or (ii) specific interactions with cations of anionic forms of the indicators. It has been widely recognised that the different solvational requirements of different indicator types may lead to important differences in acidity function behaviour;[2-6,16] this aspect was emphasised in a recent report.[8] However, the basicity inversion between the H_M and J^{2-}_{2M} scales requires a difference in solvating power between sodium methoxide and potassium methoxide solutions of the same concentration. To develop this argument, proton loss from the aromatic amines used to define the H_M function will produce delocalised anions in which solvation by methanol is likely to be less important than in the adducts (2) and (3) used to define J^{2-}_{2M} and J^{3-}_{3M} functions. The latter two adducts carry localised negative charges which may be strongly solvated by methanol by hydrogen-bonding interactions. Thus the attribution of the observed basicity inversion to solvation differences requires that methanolic sodium methoxide is a better solvating medium than methanolic potassium methoxide. Bagno *et al*[8] have argued oppositely that methanol in sodium methoxide solutions should be less available for solvation because the solvent is more involved in solvating the smaller cation. The case may be overstated since the stronger ion-pairing of

sodium methoxide than of potassium methoxide will reduce the concentration of free sodium ions. In fact, the measured activities of methanol in solutions of sodium and potassium methoxide are almost identical up to 4$\underline{\underline{M}}$ concentration. Thus it is unlikely that solvation is the major factor responsible for the positive values of ΔJ^{2-}_{2M}. The strong interactions of the 1:1 adducts (1), with cations are well-documented[10,14,17,18] so that it seems reasonable that the higher adducts (2) and (3) will also interact. The second explanation that the higher adducts show strong specific interaction with cations and that their stronger interaction with sodium than with potassium ions results in the enhanced J^{2-}_{2M} values for sodium methoxide solutions is preferred.

4.7.1 Relative strengths of association with Na^+ and with K^+

Included is the association of adducts with cations using the Scheme 4- . Here K_A is the association constant of the 1:1 adduct with cations, and K_B and K_C

$$\begin{array}{ccc} P.OMe^- + 2M^+ + MeO^- & \overset{K_{1,2}}{\rightleftharpoons} & P.(OMe)_2{}^{2-} + 2M^+ \\ \Big\| K_A & & \Big\| K_B \\ P.OMe^-, M^+ & & P(OMe)_2{}^{2-}, M^+ + M^+ \\ & & \Big\| K_C \\ & & P(OMe)_2{}^{2-}, 2M^+ \end{array}$$

Scheme 4–

measure the interaction of the 1:2 adduct with one and two cations respectively. The values of thermodynamic equilibrium constants, $K_{1,2}$, are not determinable, but an apparent equilibrium constant, K_{app}, may be defined in terms of the indicator ratios and the basicity of the medium. What is required here is a measure of the basicity which includes all deviations from ideality apart from the specific association of adducts with cations. There is no completely satisfactory way to do this. However, there is good evidence[5,8,10] that the aromatic amine

indicators used to define the H_M scale do not strongly associate with cations. Hence the use of h_m, defined in equation (4-19), in the determination of K_{app} as shown in equation (4-20).

$$\log_{10} h_m = H_M - pK_{MeOH} \qquad (4\text{-}19)$$

$$K_{app} = \frac{[2]}{[1] \times h_M} \qquad (4\text{-}20)$$

Since h_M values include basicity effects resulting from association of metal cations with methoxide ions, this association has not been shown in the Scheme. K_{app} may now be related in equation (4-21) to individual equilibrium constants.

$$K_{app} = \frac{K_{1,2}(1 + K_B[M^+])(1 + k_C[M^+])}{1 + K_A[M^+]} \qquad (4\text{-}21)$$

$$K_{app} = \frac{K_{1,2}.K_B(1 + k_C[M^+])}{K_A} \qquad (4\text{-}21)$$

If, as expected,[10] the values of the association constants K_A and K_B are greater than ten then equation (4-21) simplifies to equation (4-22). Combination of these equations with equation (4-16) leads to equation (4-23).

$$\log_{10} \frac{K_B}{K_A}(1 + K_C[H^+]) = J^{2-}_{2M} - H_M \qquad (4\text{-}23)$$

Absolute values of J^{2-}_{2M} are not known but using equation (4-18) values of ΔJ^{2-}_{2M}, reflecting the difference in basicities of sodium methoxide and potassium methoxide solutions, have been calculated and are given in Table 4-29. Ratios of association constants for Na^+ adn K^+ can therefore be compared, equation (4-24). Further, it is known[10,18] that 1:1 adducts associate with approximately equal strengths with sodium and potassium ions, so that the values of $K_A^{Na^+}$ and $K_A^{K^+}$ will be similar. Hence equation (4-24) can be simplfied to give

$$\log_{10} \frac{\left[\frac{K_B^{Na^+}}{K_A^{Na^+}}(1 + K_c^{Na^+}[Na^+])\right]}{\left[\frac{K_B^{K^+}}{K_A^{K^+}}(1 + K_c^{K^+}[K^+]\right]} = \Delta J^{2-}_{2M} - \Delta H_M \qquad (4\text{–}24)$$

$$\log_{10} \frac{K_B^{Na^+}(1 + K_c^{Na^+}[Na^+])}{K_B^{K^+}(1 + K_c^{K^+}[K^+])} = \Delta J^{2-}_{2M} - \Delta H_M \qquad (4\text{–}25)$$

equation (4–25). Values of the right-hand side of equation (4-25) are given in Table 4-30. Because of the assumptions made they should be regarded as giving orders of magnitude rather than precise values. However, they do reflect the very much stronger association of 1:2 adducts with sodium ions than with potassium ions. The increases in value with increasing base concentration (metal ion concentration) may reflect the higher values of K_c for sodium than for potassium ions. In a similar fashion the positive values of $(\Delta J^{3-}_{3M} - \Delta H_M)$ show the stronger association of 1:3 adducts (3) with sodium ions than with potassium ions.

It has been shown previously[10,17,18] that association of the 1:1 adducts (1) with cations involves the oxygen atoms of the methoxy groups and of the *ortho*–ring substituents as shown in (6), the presence of the dioxolan ring in

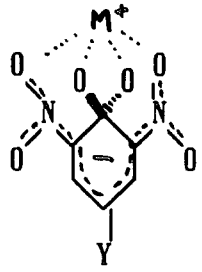

(6)

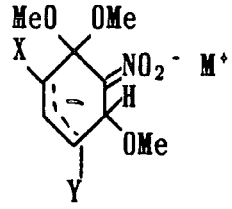

(7)

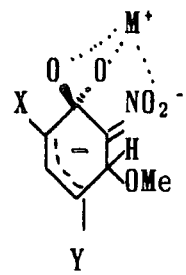

(8)

(4) precluding such association.[19] In the 1:2 adduct (2) and its spiro-analogue, and in the 1:3 adducts, (3), negative charge is localised on nitro-groups. The larger association constants of these adducts with sodium than with potassium ions may

be rationalised by the stronger association of the smaller cation with the localised negative charge as shown in (7). Nevertheless, the data in Table 4-30 show a distinction between the relative complexing abilities of 1:2 adducts formed from anisoles and from the spiro-adduct (4). It may be that the gem-dimethoxy function still has an active part to play in cation complexing so that interactions such as that shown in (8) are particularly favourable for sodium ions.

Table 4-29 **Relative 'Basicities' of Sodium Methoxide and Potassium Methoxide Solutions, given as ΔJ^{2}_{2M} (NaOMe – KOMe)[a]**

Indicator	Base Concentration					
	2.0M	2.5M	3.0M	3.5M	4.0M	4.5M
2,4,6–Trinitroanisole	1.08	1.13	1.17	1.23 (0.70)	(0.80)	
4–Cyano–2,6–dinitroanisole	0.86	0.93	1.00			
2–Cyano–4,6–dinitroanisole			1.02	1.06	1.08	
Spiro–adduct, (4)		0.14	0.18	0.22	0.26 (0.58)	(0.80)
Aromatic Amines,[b] ΔH_M	–0.49	–0.62	–0.69	–0.78	–0.87	–0.98

[a] Values in parenthesies are ΔJ^{3}_{3M} (NaOMe – KOMe)

[b] H_M values from reference 2

Table 4–30 Estimate of the Relative Strengths of Association of (2) and of (3) with Sodium and Potassium Ions

Indicator	$\Delta J^{2-}_{2M} - H_M$ Base Concentration					
	2.0M	2.5M	3.0M	3.5M	4.0M	4.5M
2,4,6–Trinitroanisole	1.57	1.75	1.86	2.01		
4–Cyano–2,6–dinitroanisole	1.35	1.55	1.69			
2–Cyano–4,6–dinitroanisole			1.71	1.84	1.95	
Spiro–adduct, (4)		0.76	0.87	1.00	1.13	
	ΔJ^{3-}_{3M}					
2,4,6–Trinitroanisole				1.48	1.67	
Spiro–adduct, (4)					1.45	1.78

4.8 Interaction of N,N–dimethylpicamide with Methoxides

The reaction of N,N–dimethylpicramide (9) in methanolic sodium methoxide solutions has been studied by Gold and Rochester.[1] They found evidence for rapid reactions producing addition complexes followed by a slower reaction involving displacement of the dimethylamino group by methoxide to give 2,4 6–trinitroanisole. Absorbance measurements for the initial adduct–forming reactions were compatible with the formation of a 1:1 adduct with an equilibrium constant of $7 dm^3 mol^{-1}$ and a higher adduct which was thought to have 1:2 stoichiometry. ^1H NMR measurement[20] confirmed the structures of the adducts as (10) and (11).

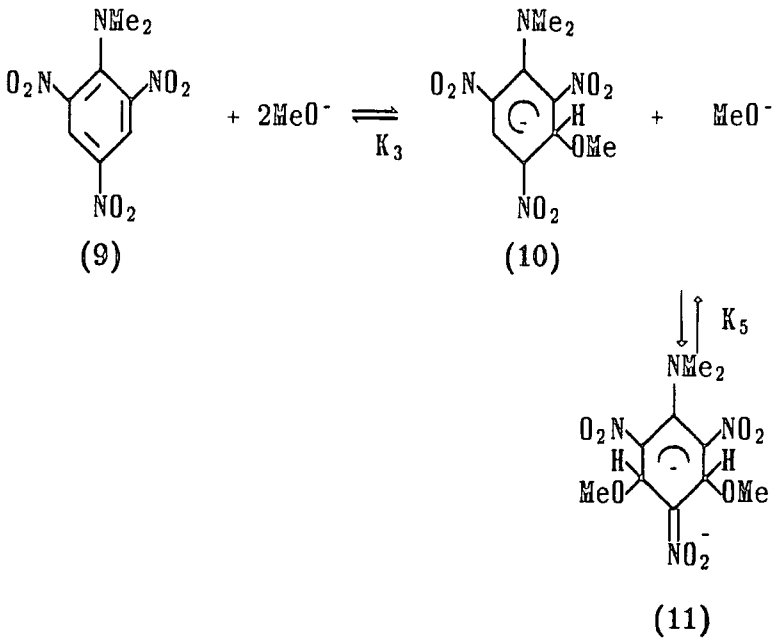

(9) (10) (11)

Some kinetic measurements using stopped flow spectrophotometry have been reported previously[21] for the reaction of (9) with sodium methoxide in methanol and it was thought of interest to compare these with results for corresponding reactions with potassium methoxide in methanol.

Measurements in the visible region were made in 50/50 (v/v) methanol/dimethylsulphoxide where the formation of the 1:1 and 1:2 adducts occur at distinct ranges of methoxide concentration. The 1:1 adduct (10) showed absorption at 470nm (ϵ 15800dm^{3}mol^{-1}cm^{-1}) and at higher methoxide concentration this was replaced by absorbance at 410nm due to the adduct (11). Stopped flow measurements were made in methanol at 470nm where the formation of (10) was seen as a rapid colour forming process. Equilibration with (11) was seen as slower fading process. Rate measurements and absorbances at 470nm at completion of the faster reaction are in Table 4–31.

Measurements were made in methoxide solutions up to 0.4M where the basicity will depend on an acidity function rather than the methoxide concentration. Since one of the main interests is in the effects of cation association, the basicity is represented by h_m values obtained using aniline derivatives where cation association is thought to be unimportant. The results for 1:1 adduct formation

indicate that there is probably no strong interaction with potassium ions. Thus a plot (Figure 4–11) of k_{fast} versus h_M is linear. Strong complexation of (10) with cations is likely to have resulted in a non–linear plot. The data conform to equation 4.26 with k_3 180dm^{3}mol^{-1}s^{-1} and k_{-3} 34s^{-1}, leading to a value for k_3

$$k_{fast} = k_3 h_m + k_{-3} \qquad (4.26)$$

($=k_3/k_{-3}$) of 5.3dm^{3}mol^{-1}. This value is close to those obtained from absorbance data at completion of the rapid reaction.

If it is assumed that ion association is also unimportant in the formation of the 1:2 adduct then equilibration of adducts (10) and (11) can be represented by

$$k_{slow} = k_{-5} + \frac{k_5 K_3 h_m^2}{1 + K_3 h} \qquad (4\text{-}27)$$

Values in Table 4–31 calculated with k_5 1.6dm^{3}mol^{-1}s^{-1}, k_{-5} 0.32s^{-1} and K_3 5.3dm^{3}mol^{-1} give reasonable agreement with observed values for k_{slow}. These values lead to a result of K_5 (k_5/k_{-5}) of 5dm^{3}mol^{-1}.

Table 4–31 Interaction of N,N–dimethylpicramide with potassium methoxide in methanol

[KOMe]	a h_{-}	b k_{fast}/s^{-1}	c Abs_{470}	d K_3/ $dm^3 mol^{-1}$	e k_{slow}/s^{-1}	f k_{calc}
0.02	0.022	38.6	–	–	–	–
0.04	0.040	43.4	0.0143	7.3	–	–
0.07	0.075	47.6	0.0174	5.1	0.355	0.355
0.1	0.117	51.3	0.0197	3.9	0.388	0.39
0.2	0.240	75.4	0.0327	4.5	0.520	0.56
0.3	0.400	109.1	0.0404	4.5	0.755	0.76
0.4	0.600	148.8	0.061	–	1.53	1.05

a $\log_{10} h_m = H_m - pK_{MeOH}$

H_M values calculated from aniline derivatives[5]

b Colour forming process, measured at 470nm

c 2mm cells, $[9] = 2\times10^{-5}$M. $Abs_{470} = 0.063$ for complete conversion

d calculated as $K_3 = \dfrac{Abs_{470}}{(0.063 - Abs_{470})h_m}$

e Measured either as forming process at 410nm or as fading process at 430nm

f calculated k_{slow} using $K_3 = 5.4 dm^3 mol^{-1}$, $k_{-5} = 0.32 s^{-1}$, $k_5 = 1.6 dm^3 mol^{-1} s^{-1}$ and equation (4.27).

It is interesting to compare these values with those for the same type of reactions with sodium methoxide[21] in methanol, where K_3 was found to be $4.0 dm^3 mol^{-1}$ and K_5 $8.3 dm^3 mol^{-1}$. The results for K_3 for the two methoxides are similar within the experimental error indicating little interaction of (10) with cations. The failure to observe cation–complexing with the 1:1 adduct is in agreement with previous results for 1:1 adducts from 1,3,5–trinitrobenzene and from dioxolane–spiro adducts.[19] Thus it is seen that the presence of the 1,1–dialkoxy functionality is required for strong cation complexing of 1:1 adduct. Nevertheless, the value obtained for K_5 for sodium methoxide solutions is significantly larger than that obtained with potassium methoxide and this may

indicate some interaction with sodium ions of the 1:2 adduct. It should be noted that the base concentration and hence the cation concentration used here were very much lower than those used previously to form 1:2 and 1:3 adducts. More extensive cation association might be expected at higher base concentrations.

REFERENCES

1 Gold, V,; Rochester, C.H., *J. Chem. Soc.* (1964), 1697

2 Rochester, C.H., "*Acidity Functions*", Academic Press, London, 1970

3 Rochester, C.H., *Quart. Rev.* (London) (1966), 20, 511

4 Bowden, K., *Chem. Rev.* (1966), 66, 619

5 Terrier, F., *Ann. Chim.* (Paris) (1969), 4, 153

6 Terrier, F.; Millot, F.; Schaal, R., *Bull. Soc. Chim. Fr.* (1969), 3002

7 Jones, J.R., *Chem. Commun.* (1968), 513

8 Bagno, A.; Scorrano,G.; Terrier, F., *J. Chem. Soc. Perkins Trans.2* (1990), 1017

9 Rochester, C.H., *J. Chem. Soc.* (1965), 2404

10 (a) Crampton, M.R.; Khan, H.A., *J. Chem. Soc. Perkin Trans. II* (1972), 1173,
(b) Crampton, M.R.; Khan, H.A., *ibid*, 2286,
(c) Crampton, M.R.; Khan, H.A., *ibid*, (1973), 1103,
(d) Crampton, M.R., *ibid*, (1975), 825

12 More O'Ferrall, R.A.; Ridd, J.H., *J. Chem. Soc.* (1963), 5030

13 Buncel, E.; Crampton, M.R.; Strauss, M.J.; Terrier, F., "*Electron Deficient Aromatic– and Heteroaromatic–Base Interactions*", Elsevier, Amsterdam, 1984

14 Gold, V.; Toullec, J., *J. Chem. Soc. Perkin Trans. II* (1979), 596

15 Bernasconi, C.F., *J. Am. Chem. Soc.* (1968), 90, 4982

16 Crampton, M.R., *J. Chem. Soc. Perkin Trans. II* (1975), 185

17 Sekiguchi, S.; Aizawa, T.; Aoki, M., *J. Org. Chem.* (1981), 46, 3657

18 Castilho, P.C.M.F.; Crampton, M.R.; Yarwood, J., *J. Chem. Res.* (1989) (S), 370, (M), 2801

19 Crampton, M.R., *J. Chem. Soc. Perkin Trans. II* (1973), 2157

20 Crampton, M.R.; Gold, V., *J. Chem. Soc. B* (1966), 893

21 Gibson, B., PhD Thesis, 1984

Chapter 5
Infrared Studies on Substituted Phenols

5. Infrared Studies on Substituted Phenols

The reaction of some substituted nitroanisoles with halogen anions in DMSO to yield the corresponding phenoxides (Chapter 2) was first observed when recording the Infrared spectra of those compounds in DMSO using KBr plates as windows of the IR cell (Figure 2–1). This observation originated an interest on the spectral characteristics of the substituted phenoxides formed in those reactions and consequently on the corresponding neutral phenols. The Infrared study of these latter compounds, for which intramolecular hydrogen–bonds are an important feature, is presented in this chapter. The frequencies and integrated intensities of the most relevant vibrations of 2–CN–4,6–dinitrophenol and 4–CN–2,6–dinitrophenol were determined in several solvents.. The aim here was to compare the strengths of the intramolecular hydrogen–bonds for the two isomers and to relate these to the spectral characteristics of the other groups vibration, as well as to understand the effects of different classes of solvents on these vibrations.

Some other compounds, such as the corresponding anisoles, 2,4,6–trinitrophenol and –anisole and *p*–cyanophenol, were used as auxiliary.

In the frequency range analysed (4000 – 1000cm^{-1}) the most significant bands are those due to the stretching ring and the symmetric and antisymmetric vibrations of the NO_2 groups.

The selection of solvents was restricted by the low solubility of the compounds which were found to be insoluble in carbon tetrachloride, 1,4–dioxane, cyclohexane, n–hexane and isopropanol. Chloroform dissolves 4–CN-2,6–dinitrophenol but not the 2–CN isomer. Both are slightly soluble in ethanol and fairly soluble in methanol (saturated solution *ca.* 0.05M) which was used as an example of protic solvents, able to hydrogen bond with the solute.

Dipolar aprotic solvents dissolve phenols to a large extent. ^{1}H NMR and IR results show that both DMF and DMSO promote ionization of some substituted phenols. This was demonstrated by solutions of the phenols and of the corresponding sodium or potassium phenoxides, prepared independently, which gave identical spectra. Acetonitrile was tested but excluded due to its absorption

band in one of the interesting regions of the spectrum, that of the ν(CN) band.

Benzene and dichloromethane were found to dissolve both isomers at a concentration high enough to obtain a reasonable IR spectrum and to give rise to very similar results.

5.1 Results and Discussion

The frequencies ($\bar{\nu}$) and integrated intensities (A) for each mode of vibration of the two cyanodinitrophenols in different solvents are listed in Table 5–1. Frequency and half–width results are presented with an estimated uncertainty of $\pm 1 cm^{-1}$. Only approximate values are given for the integrated intensities as, due to the low solubility of both compounds in all the used solvents except DMSO, saturated solutions were prepared and concentrations were estimated rather than accurately measured.

Each of the normal modes of vibration will be discussed separately. Most of the detailed analysis of the spectral features in low–interacting solvents will be based on the spectra of benzene solutions, although the same arguments may be used to explain the similar spectra of the substituted phenols in dichloromethane. For the discussion of the characteristics of the ν(OH) band the spectra in dichloromethane will be used because, unlike benzene, this solvent does not show any strong band above $3000 cm^{-1}$.

Whenever possible, the relevant bands of the IR spectra of the phenols are compared with those of the corresponding anisoles. The use of anisoles, which cannot form intramolecular hydrogen bonds, is an attempt to obtain information on the effects of hydrogen bonding on the spectral characteristics of the groups other than the OH group.

Table 5–1

Spectral Characteristics of the main Infrared band of
2–CN–4,6–dinitrophenol (2CNDNPH) and 4–CN–2,6–dinitrophenol (4CNDNPH)

ν(CN)	2CNDNPH			4CNDNPH		
	$\bar{\nu}$ [a]	$\Delta\bar{\nu}_{\frac{1}{2}}$	A [c]	$\bar{\nu}$ [a]	$\Delta\bar{\nu}_{\frac{1}{2}}$ [b]	A [c]
C_6H_6	2239	10	160	2238	11	180
CH_2Cl_2	2249	12	200	2240	12	180
CD_2Cl_2	2242	10	200	–	–	–
$CHCl_3$	–	–	–	2241	14.5	300
CH_3OH	2241	13	220	2238[+] / 2224	24	250
CH_3OD	–	–	–	2238[+] / 2224		
DMSO	2217	12	500	2213	12	550

[+] two bands

ν(C=C)	2CNDNPH			4CNDNPH		
	$\bar{\nu}$	$\Delta\bar{\nu}_{\frac{1}{2}}$	A [d]	$\bar{\nu}$ [a]	$\Delta\bar{\nu}_{\frac{1}{2}}$	A [d]
C_6H_6	1617	18	10700	1637	14	7000
CH_2Cl_2	1617	18	10500	1640	13	7400
CD_2Cl_2	1617	18	10500	–	–	–
$CHCl_3$	–	–	–	1639	14	8300
CH_3OH	1616	27	7200	1635	27	7900
CH_3OD	–	–	–	1634	24	8900
DMSO	1612	25	14500	1635 / 1616	33	17800

Table 5–1 cont'd

Spectral Characteristics of the main Infrared band of
2–CN–4,6–dinitrophenol (2CNDNPH) and 4–CN–2,6–dinitrophenol (4CNDNPH)

ν (NO_2)	2CNDNPH			4CNDNPH		
	a $\bar{\nu}$	b $\Delta\bar{\nu}_{\frac{1}{2}}$	d A	a $\bar{\nu}$	b $\Delta\bar{\nu}_{\frac{1}{2}}$	d A
C_6H_6	1557 1536	16	9000	1547	14	18000
CH_2Cl_2	1559 1540	15	7600	1549	14	20300
CD_2Cl_2	1559 1540	15	7500	–	–	–
$CHCl_3$	–	–	–	1550	15	19200
CH_3OH	1552 1537	27	5400	1552	21	14000
CH_3OD	–	–	–	1550	20	16600
DMSO	1546	15	7200	e	e	e

solvent	2CNDNPH			4CNDNPH		
	a $\bar{\nu}$	b $\Delta\nu_{\frac{1}{2}}$	d A	a $\bar{\nu}$	b $\Delta\bar{\nu}_{\frac{1}{2}}$	d A
C_6H_6	1344	13	24800	1354 1316	30 14	9700
CH_2Cl_2	1346	14	24000	1354 1316		9600
CD_2Cl_2	1346	14	23000	–	–	–
$CHCl_3$	–	–	–	1354 1317	25	9700
CH_3OH	1348	15	16300	1354 1315	24	8700
CH_3OD	–	–	–	1353	23	7600
DMSO	1358	e	e	1340	42	10300

a $\bar{\nu}$ in cm^{-1} ±1

b $\Delta\bar{\nu}_{\frac{1}{2}}$ in $\bar{\nu}$ in cm^{-1} ±1

c A in $1mol^{-1}cm^{-2}$ ±10

d A in $1mol^{-1}cm^{-2}$ ±100

e several unresolved bands in this region

5.1.1 The 3600–2700cm^{-1} Region

This is the region of the spectrum where the vibrational bands for the OH stretching modes are expected to be found.

Figure 5–1 shows the spectra of the two cyanodinitrophenols, together with 4–cyanophenol. The inclusion of the spectrum of this latter compound seems to demonstrate the strong effect of intermolecular H–bonding on the vibrational spectrum in this region, with a large shift of the band of the O–H stretching mode to lower frequencies whenever H–bonding is present.

4–cyanophenol shows both free OH groups, $\bar{\nu}$(OH) = 3560cm^{-1}, and intermolecularly hydrogen–bonded OH groups, $\bar{\nu}$(OH) = 3330cm^{-1}, for which there are several possibilities:

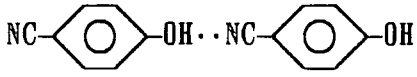

(1)

or

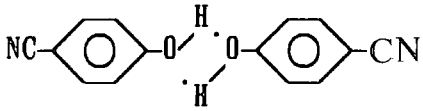

(2)

Further studies reveal that, as expected, the intensity ratio of these two ν(OH) bands changes with concentration, with the "free" ν(OH) band growing at expense of the bonded ν(OH) band upon dilution (Figure 5-2). The existence of a single narrow band corresponding to the stretching vibration of the CN bond $\bar{\nu}$(CN) = 2225cm^{-1}, $\Delta\bar{\nu}_{\frac{1}{2}}$ = 11cm^{-1}, which is essentially unaffected by changes on concentration seems to argue in favour of the H–bonding between two OH groups (2) in a cyclic dimer. A configuration like (1) would be expected to cause a shift to higher frequency of the ν(CN) band. The observed change with concentration variation is an increase of 1cm^{-1} on the bands half–width, corresponding to a small asymmetry on the high frequency side of the band, when concentration increases from 0.0125M to 0.05M. Since the experimental error on measuring half–widths is also 1cm^{-1}, this change is too small to be considered an argument for the presence of (1).

For the same compound in methanol, although the ν(OH) region becomes unavailable due to the strong absorption of the solvent, other bands related to vibration involving the hydroxyl group may be analysed. The (C–O) stretching band (1200–1100cm^{-1}) is very little shifted from CH_2Cl_2 to methanol although there are two bands in this region when the solvent is CH_2Cl_2 corresponding to bonded and free (OH) and only one in methanol (all OH is hydrogen-bonded). The hydrogen–bonding of the hydroxyl group to methanol may be represented by (3)

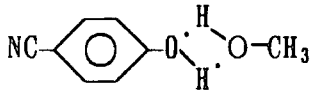

(3)

which is very similar to the cyclic dimer (2) and therefore expected to lead to the same degree of resonance interaction of the hydroxyl group with the ring. If the complex (1) was significant in CH_2Cl_2 a greater change on this resonance and on the ν(C–O) band frequency would be expected in methanol.

In spectra taken at approximately the same concentration (*ca.* 0.01M) as for 4–cyanophenol, the substituted nitrophenols show only one band each in this region that can be attributed to ν(OH) vibrations (Figure 5–1). The intensity of this band was found to be independent of concentration.

From the frequency and the shape of the ν(OH) band for the substituted nitrophenols, it is clear that in dichloromethane, as in benzene, there is a strong intramolecular hydrogen–bond between the OH group and the adjacent NO_2 substituent.[1]

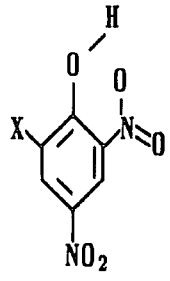

(5)

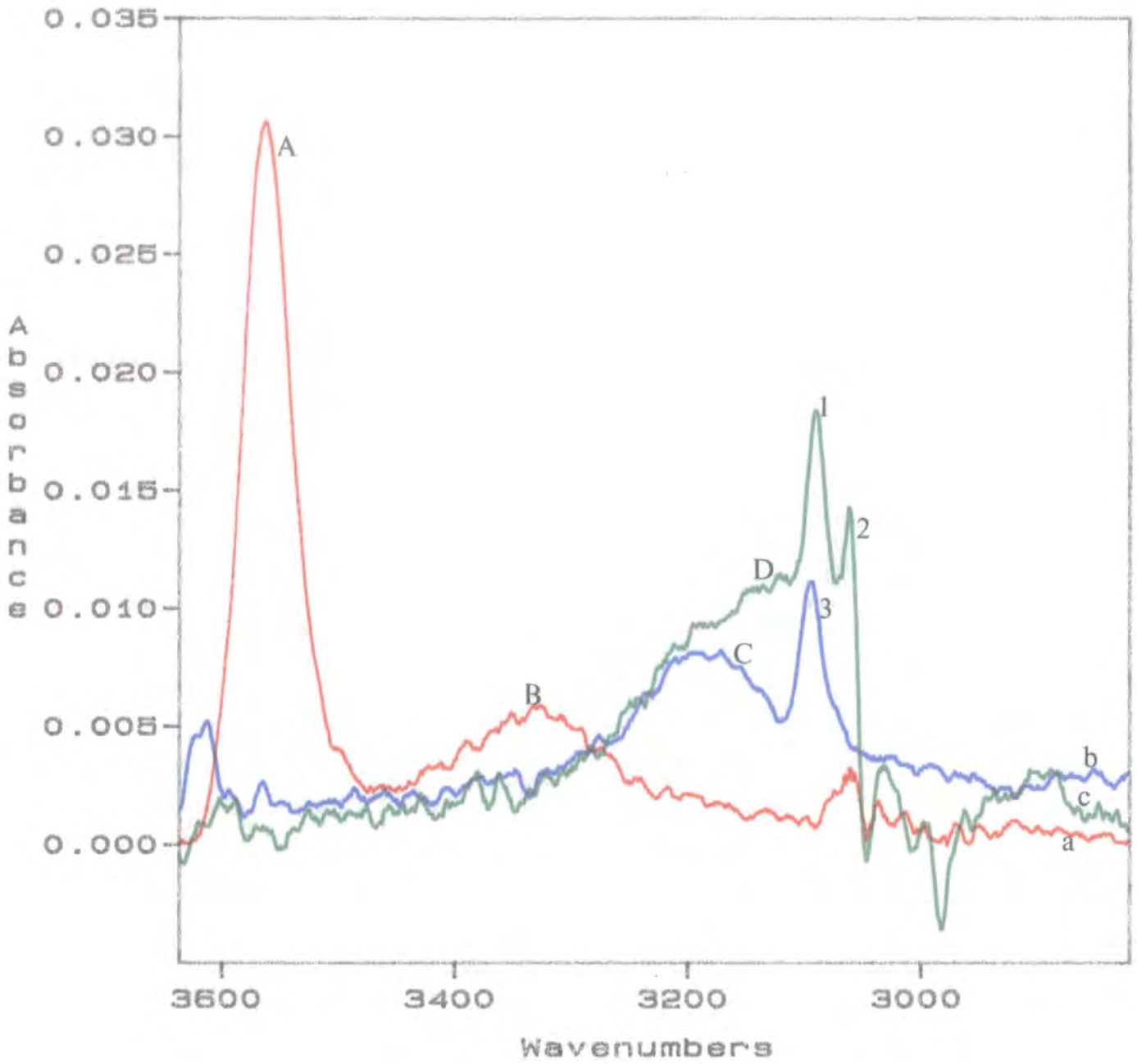

Figure 5–1 **Stretching vibrations of the OH group, in dichloromethane, of**

a) 4–cyanophenol

b) 2–CN–4,6–dinitrophenol

c) 4–CN–2,6–dinitrophenol

A: "free" OH ν(OH)=3560 cm^{-1}

B: Intermolecularly hydrogen bonded OH ν(OH)=3330 cm^{-1}

C: Intramolecularly hydrogen bonded OH ν(OH)=3174 cm^{-1}

D: Intramolecularly hydrogen bonded OH ν(OH)=3130 cm^{-1}

1,2 and 3 are bands due to ν(C–H) vibrations

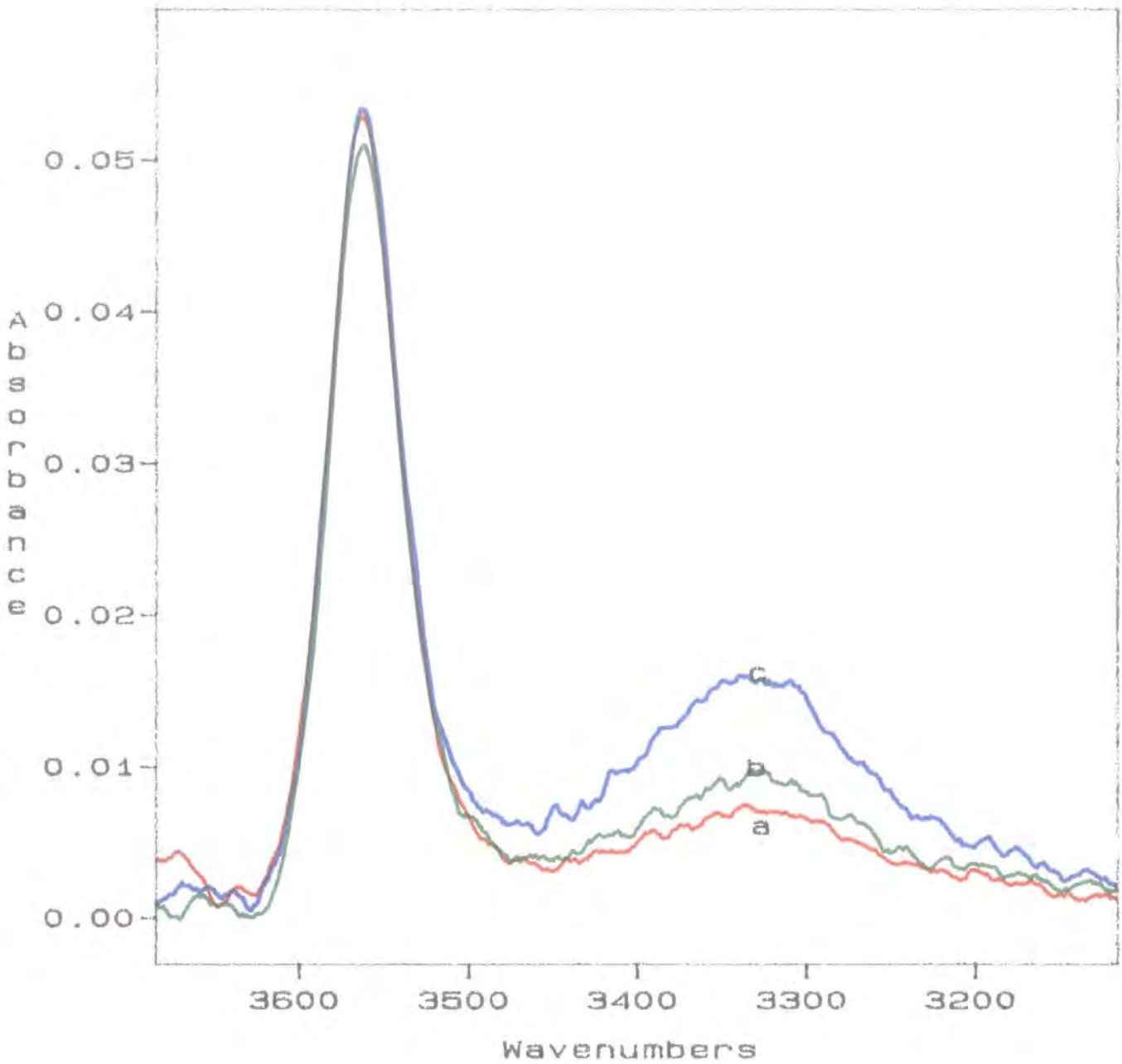

Figure 5–2 Effect of concentration on the ν(OH) bands of *p*-cyanophenol in CH_2Cl_2

a) 0.0125 M
b) 0.025 M
c) 0.5 M

A comparative analysis of the ν(OH) bands of these two isomers raises some questions. If the magnitude of the shift, $\Delta\bar{\nu}$, gives some measure of the energy of the interaction, then the H–band seems to be stronger in the compound that has two nitro groups in the *ortho*–positions. The band is also broader for this compound.

4–CN–2,6–dinitrophenol $\bar{\nu} = 3130\text{cm}^{-1}$ $\Delta\bar{\nu}_{\frac{1}{2}} = 195\text{cm}^{-1}$

2–CN–4,6–dinitrophenol $\bar{\nu} = 3175\text{cm}^{-1}$ $\Delta\bar{\nu}_{\frac{1}{2}} = 125\text{cm}^{-1}$

This shows good agreement with some of the literature results on dinitrophenols. Brown *et al* (1972)[2] reported intra– and intermolecular hydrogen bonds for a large number of substituted phenols including 2,4–dinitro– and 2,6–dinitrophenol which $\bar{\nu}$(OH) characteristics are stated to be

2,4–dinitrophenol $\bar{\nu}(\text{OH}) = 3200\text{cm}^{-1}$ $\Delta\bar{\nu}_{\frac{1}{2}} = 195\text{cm}^{-1}$ [2]

2,6–dinitrophenol $\bar{\nu}(\text{OH}) = 3168\text{cm}^{-1}$ $\Delta\bar{\nu}_{\frac{1}{2}} = 211\text{cm}^{-1}$ [2]

but not discussed comparatively. An halogen atom as a third substituent was found by these authors to decrease this difference in ν(OH) by lowering ν(OH) of the 2,4–dinitrophenol and increasing ν(OH) of the 2,6–dinitro isomer.

Aihara *et al* (1984)[3] state that the hydrogen bond strength is higher in 2,4– -dinitrophenol than in *ortho*–nitrophenol. This can be a result of the increased electron–withdrawing power by mesomeric effect of the second nitro group that withdraws electron density preferentially from the OH group rather than from the NO_2 group.

The formation of intramolecular hydrogen bonds in phenols is known to induce increased acidic character of the hydrogen atom of the hydroxyl group.[4,5] Geometry optimization[4] shows that in the bonded *ortho*–nitrophenol the total electron population of the oxygen atom is greater than that in the *para*–nitro phenol; similarly, there is an increase in the total electron population of the oxygen atoms of the nitro group and a decrease on that of the hydrogen atom. This electron distribution is attributed mainly to electron transfer within the fragment of the molecule composed of the two substituents and the two ring carbons to

which they are attached. As shown in (5), this transfer occurs from the acceptor group to the hydroxyl oxygen atom via the hydrogen–bonded proton.

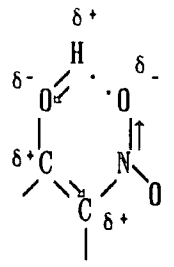

(5)

Such electron transfer induces a new π–electron distribution leading to an increase in both the π–electron donor power of the hydroxyl group and of the π–electron accepting ability of the nitro group. Another electron withdrawing substituent in *ortho* or *para* position to the OH group could reinforce this distribution by increasing the OH electron donation and, hence, stabilize the intramolecular hydrogen bond.

Determination of the acidity by U.V./visible spectroscopy gives pK_a = 0.89 for 4–CN–2,6–dinitrophenol and pK_a = 1.14 for 2–CN–4,6–dinitro–phenol which parallels the magnitude of the shift for the ν(OH) band.

As the σ and π electron accepting ability of the CN group is identical in the *ortho*– and *para*– positions,[6,7] these pK_a results suggest that a second nitro group is more effective on increasing the strength of the intramolecular H–bond when in the *ortho*– rather than the *para*– position to the OH group.

Unfortunately, theoretical calculations are available only for mono and disubstituted benzenes and no certainty exists as to whether the effect of further substituents is additive or not.[8] Steric rather than electronic factors may well contribute to the observed difference in H–bond strength of the cyanodinitro phenols as bulkiness of the 6–substituent hinders free rotation of the OH bond about its axis enhancing intramolecular bonding between OH and 2–NO_2 group.[2]

The absence of any other band at higher frequency in the spectra of the cyanodinitrophenols (Fig. 5–1) is a good indication that no intermolecularly hydrogen–bonded species, such as (6) and (7), are formed, as it has been suggested for some *para* and *meta* nitrophenols[9], over the concentration

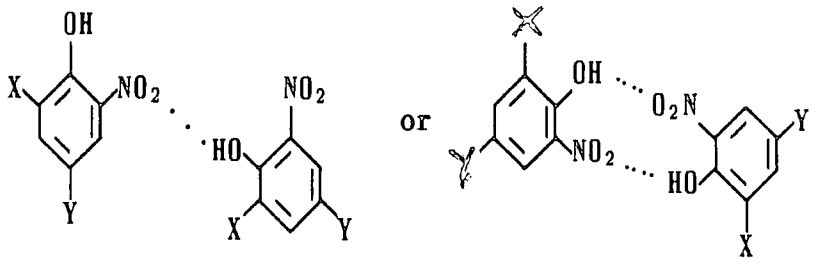

(6) (7)

range under scrutiny (0.005 – 0.02M). Also, there is no appreciable contribution of *trans* conformers, for which several possibilities could be expected.

In the planar *trans* configuration the NO_2 and the OH group retain their planarity with the ring and the presence of a second electronegtive group *ortho* to the OH will result in a competition for the hydroxyl proton.

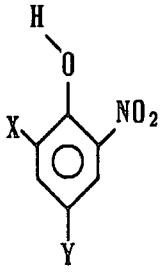

(8)

This conformer (8), though possible for the compound 2–CN–4,6–dinitrophenol, was found neither in dichloromethane nor benzene. An interaction between the hydrogen atom and the π–cloud of the C≡N group may lead only to a weak H–bond and the frequency of the OH stretching vibration would appear close to that of non–bonded phenol (or nitrophenol) around 3600cm^{-1}; no such band is observed in the spectrum. This fact accounts for a very strong H–bond between the OH group and the *ortho*–nitro group.

As for 4–CN–2,6–dinitrophenol, where X is another nitro group, the attractive interaction of the hydroxyl proton is supposed to be the same towards both *ortho*–substituents. Some authors[2,3,10] argue in favour of the formation of an hydrogen bond involving the OH group and both the nitro substituents either through a two–sided deformation of the electron cloud of the hydrogen atom[10] which would lead to a delocalisation of the hydrogen–bond[2] and a decrease of the (O–H) bond order as in (9) or due to rapid rotation of the OH group around the C–O axis with the H–bond formed alternatively with each of the o–NO_2

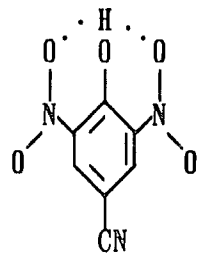

(9)

substituents as shown in Scheme 1. As this rotation would lead to an equivalent *cis*–conformer and not to a non-hydrogen bonded OH configuration, no band at

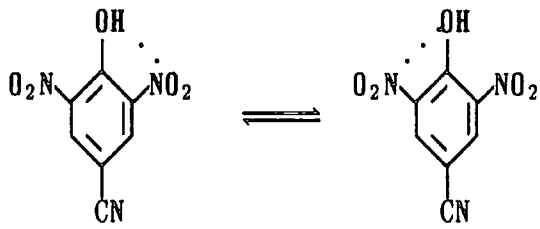

Scheme 1

higher frequency should be expected. This kind of effect could account for the large shift to low frequency and for the broader band of the ν(OH) relatively to the 2-CN– isomer as well as for the increased acidity of the hydroxyl proton and would imply equivalency of the two *ortho*–nitro groups. Granzham *et al*[11,12] strongly oppose this idea and state that the H–bond between OH and NO_2 in 2,6-dinitrophenols is as rigid as in *o*–nitrophenol and that the second nitro group is twisted away from the aromatic ring plane due to steric hindrance and therefore unable to

participate in the hydrogen–bond. The argument is based on data from the nitro groups vibrations.

The information obtained from the IR spectra of dinitrophenols in the ν(OH) region, either in the present work or the available literature, seems insufficient to draw any conclusions as to the hydrogen bond is formed with only one or the two C_6H_3–NO_2 groups. Although coplanarity with the aromatic ring is energetically favorable for each substituent due to increased conjugation, the steric strain of having all three groups in adjacent ring positions surely represents a greater (and unfavourable) factor to be taken into account.

Orthogonal configurations imply rotation of one of the groups, a situation that leads to an energetically less stable conformer. In the planar conformation of the OH group there is effective interaction of the p–type lone pair on the oxygen atom with the π^* orbitals of the ring while in the orthogonal conformer the interaction between these ring orbitals and the sp^2–type lone pair results in a poorer overlap.[6,7]

The energy difference between the two forms represents the barrier to internal rotation around the C–O bond. Substituents that increase conjugation between the OH group and the ring might be expected to increase the rotational barrier and *vice-versa*. It has been found[6] that an NO_2 group *para*- to the OH group increases the rotation barrier by 4.26 KJmol^{-1} but in the meta position the NO_2 group actually decreases the OH rotation barrier by 0.75 KJmol^{-1}. Although there are no results published for an *ortho*–nitro group the effect is expected to parallel that of the *para*–NO_2 but to be much larger since orthogonality between OH and *o*–NO_2 prevents the formation of the hydrogen bond. The bonded form effectively suppresses the repulsion effect between the lone pairs of the hydroxyl oxygen atom and those of the nitro group.[4] This may mean that when there is another nitro

group *ortho*– to OH there will be strong repulsion between the lone pairs of the oxygen atoms. In other words, if the OH group is "fixed" in its planar position by hydrogen bond, then the nitro group must rotate out of plane.

This discussion will be resumed later in this work when analysing the CN and NO_2 vibrations.

5.1.2 The ν(CN) Vibration

The frequency of the ν(CN) band seems to be remarkably little affected by the change of substituent from OH to OCH_3 despite the difference in ability for hydrogen bonding of these two groups (Figure 5–3). The relative position of the CN group with respect to the electron donor substituent does not cause noticeable changes in the spectral characteristics of the ν(CN) band, as shown in Table 5–2. The number of substituents, however, leads to a significant change in the frequency of the CN band, which decreases with the number of groups attached to the ring. The shift is accompanied by a large decrease in intensity, which is fifteen times greater in 4–cyanophenol than in 4–CN–2,6–dinitrophenol.

Table 5–2

ν(CN) frequencies for several phenols and anisoles in benzene

Compound	ν(CN) (cm^{-1})
2–CN–4,6–dinitrophenol	2239
2–CN–4,6–dinitroanisole	2240
4–CN–2,6–dinitrophenol	2238
4–CN–2,6–dinitroanisole	2240
2–CN–4 –nitrophenol	2233
2–CN–4 –nitroanisole	2234
4–CN–phenol	2225

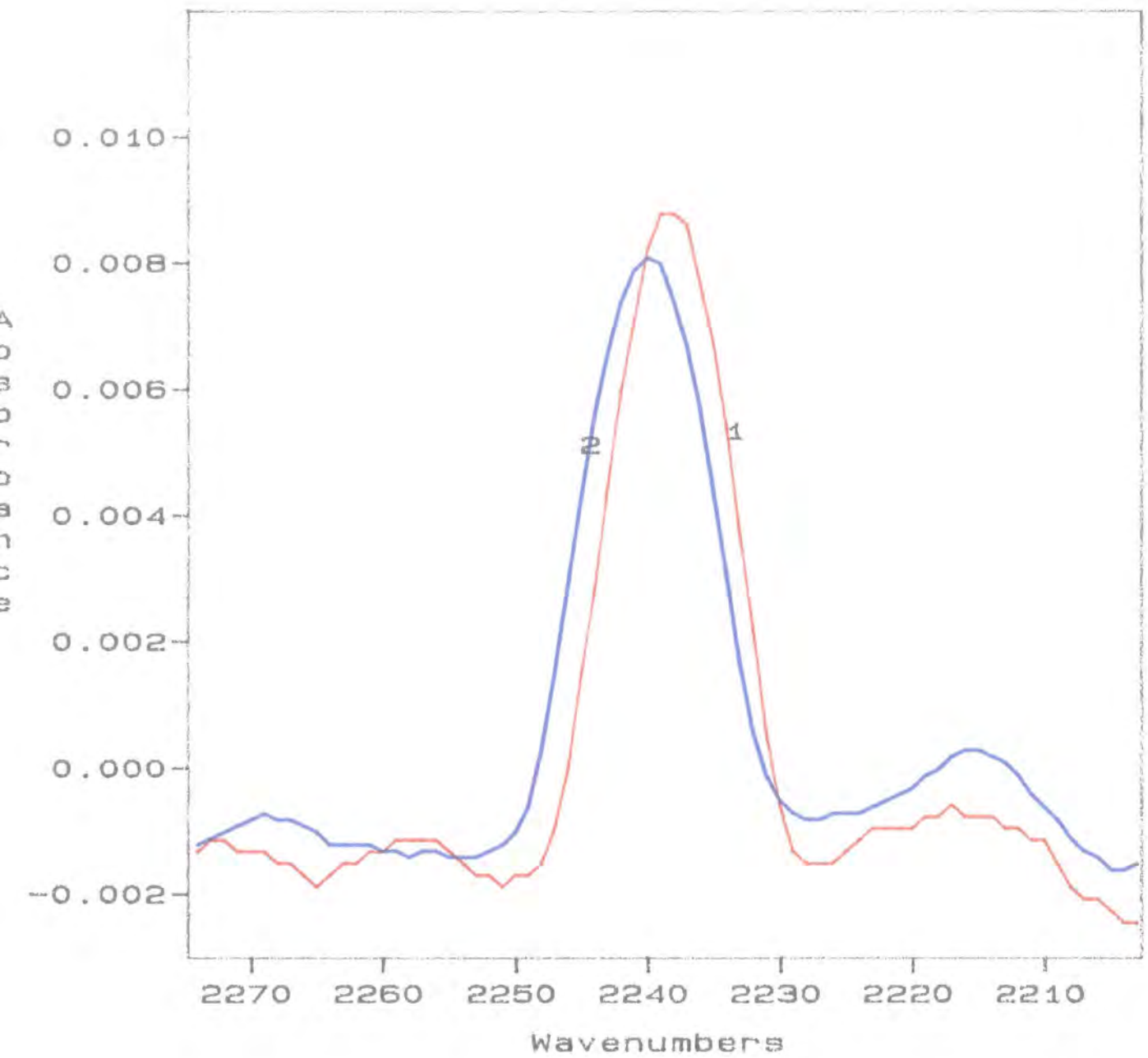

Figure 5–3 ν(CN) bands, in benzene, of

1) 4–CN–2,6–dinitrophenol, ν(CN)=2238 cm^{-1}
2) 4–CN–2,6–dinitroanisole, ν(CN)=2239 cm^{-1}

The degree of conjugation of the CN group with the ring and the electron donor group seems to be the important factor here. π–donors, such as OH or OCH_3, interact most favourably with cyanobenzenes at the *ortho*– and *para*– positions where π effects are dominant (cyanobenzenes have induced positive charge, π–population <1, at all ring positions[6]). The interaction with σ and π acceptors such as NO_2 in meta position leads to a reduction in both σ and π charge transfer from the ring to the CN group. An electron acceptor substituent lowers the energy of the ring orbitals (deshielding process[6]) making their interaction with the high–lying vacant π^* orbital of another acceptor less favourable.

In resonance terms, the effect may be represented by

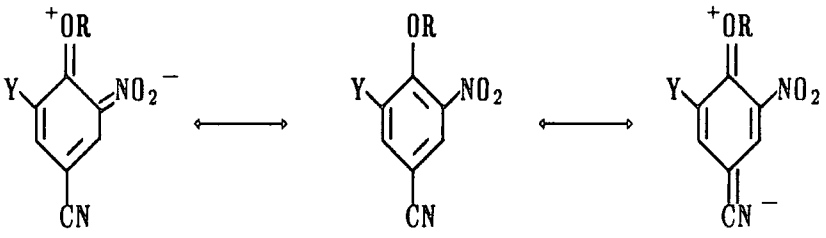

(11) (10) (12)

whereby the NO_2 and CN substituents compete with each other for conjugation with the ring. The contribution of (12) would by minimal when Y is another NO_2 but important for 4–cyanophenol where there is no competition between electron acceptor groups.

If the importance of the inductive effect is assumed to be greater than resonance,[14-19] the representation will be

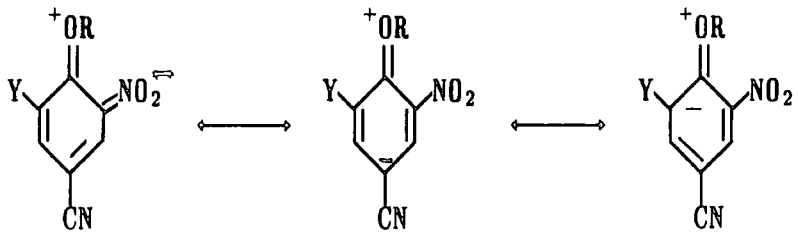

(11a) (12a) (13)

leading to identical conclusions.

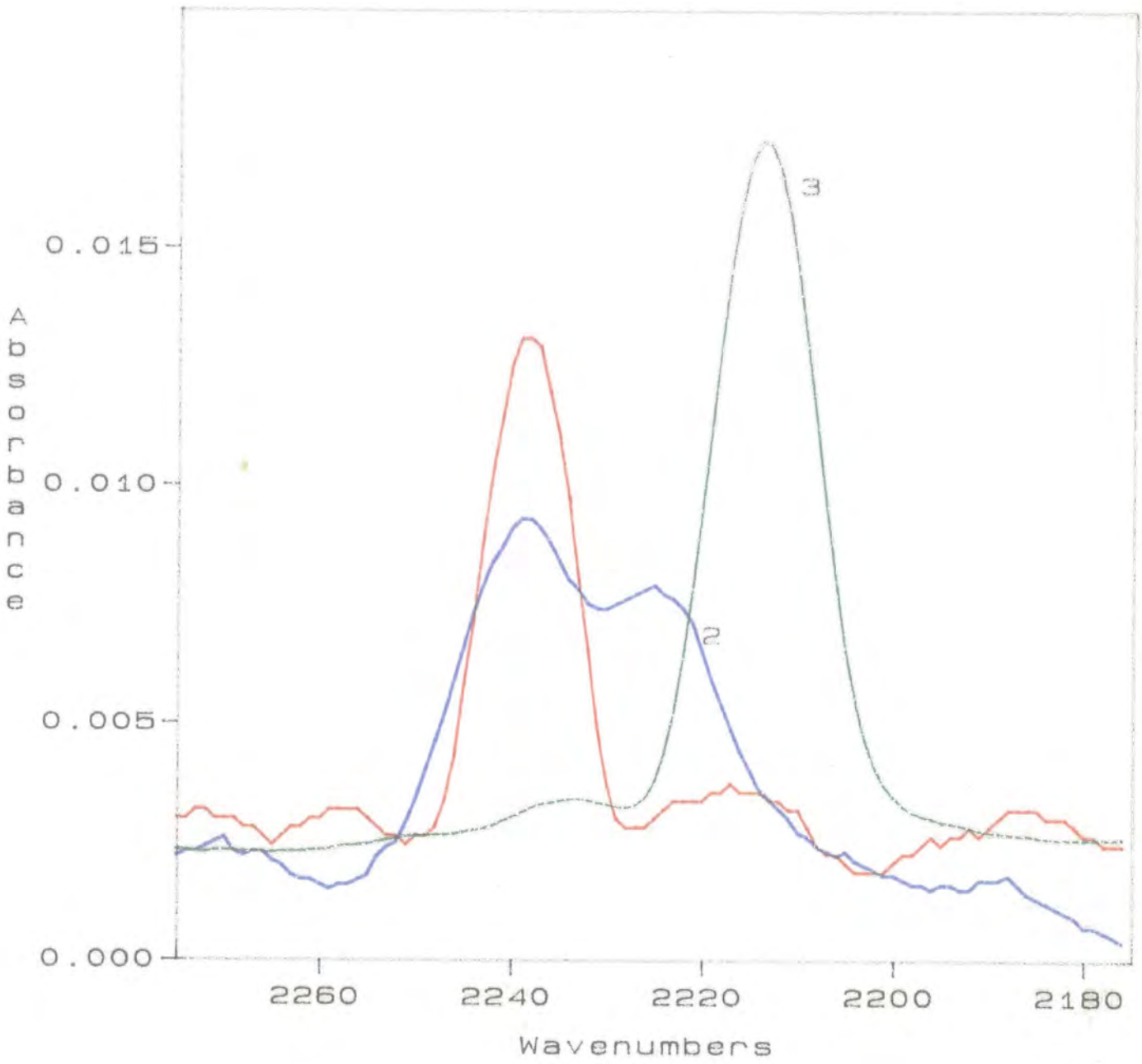

Figure 5–4 **The ν(CN) bands of 4–CN–2,6–dinitrophenol in several solvents**

1. Benzene 2. Methanol 3. DMSO

The actual scale of absorbance for 3 is 4 times larger than shown

In methanol, 4-CN-2,6-dinitrophenol shows two bands in the region of the ν(CN) vibration (Figure 5–4), one at 2238cm^{-1}, close to the frequency of the vibration in benzene, and the second one at 2224cm^{-1}. Although this band appears at the same frequency as the only ν(CN) band observed for the corresponding phenoxide, the hypothesis of ionisation of the phenol in methanol is eliminated by the inspection of the other regions of the infrared spectrum which shows very different bands for phenol and phenoxide. The isomer 2-CN-4,6-dinitrophenol also shows two bands but the band at the higher frequency 2241cm^{-1}, is much stronger than the one at 2227cm^{-1} (Figure 5–5).

In a protic solvent, such as methanol, it is expected that an interaction solute–solvent, via a hydrogen bond process as shown in (14), is reflected in the frequency and the intensity of the ν(CN) band. Due to the strongly directional

$$R–C{\equiv}N...HOCH_3 \qquad (14)$$

character of the lone-pair electrons of the sp hybridised nitrogen atom, nitriles are usually good hydrogen–bonding bases.[20] Spectroscopic studies on aliphatic nitriles have proved that intermolecular hydrogen-bonding, as alkali metal complexation, occurs via the nitrogen lone–pair and not via the π-electrons of the triple bond. The result of these interactions in the infrared spectrum is an increase of the frequency of the ν(CN) band. This increase has been attributed[21] to a change in the electronic structure of the nitrile bond as donation of lone–pair electron density on the nitrogen leads to a less polar C≡N bond which results on decrease in the electron-withdrawing power of the N atom. Since electron density withdrawn by nitrogen must come from the bonding orbitals, the triple bond becomes stronger when complexation occurs. For example, it is known[22] that for the system acetonitrile/methanol in CCl_4, even in proportions as low as 1/1000, two bands are detected for the C≡N stretching vibration, corresponding to 'free' CN, $\bar{\nu}$ 2257cm^{-1} and hydrogen-bonded CN, $\bar{\nu}$ 2262cm^{-1}.

Thus solvation of the functional group CN cannot be the factor responsible for the appearance of a second band in the 2300–2150cm^{-1} region in the spectrum of 4–CN–2,6–dinitrophenol in methanol. Indeed, this frequency is very close to that

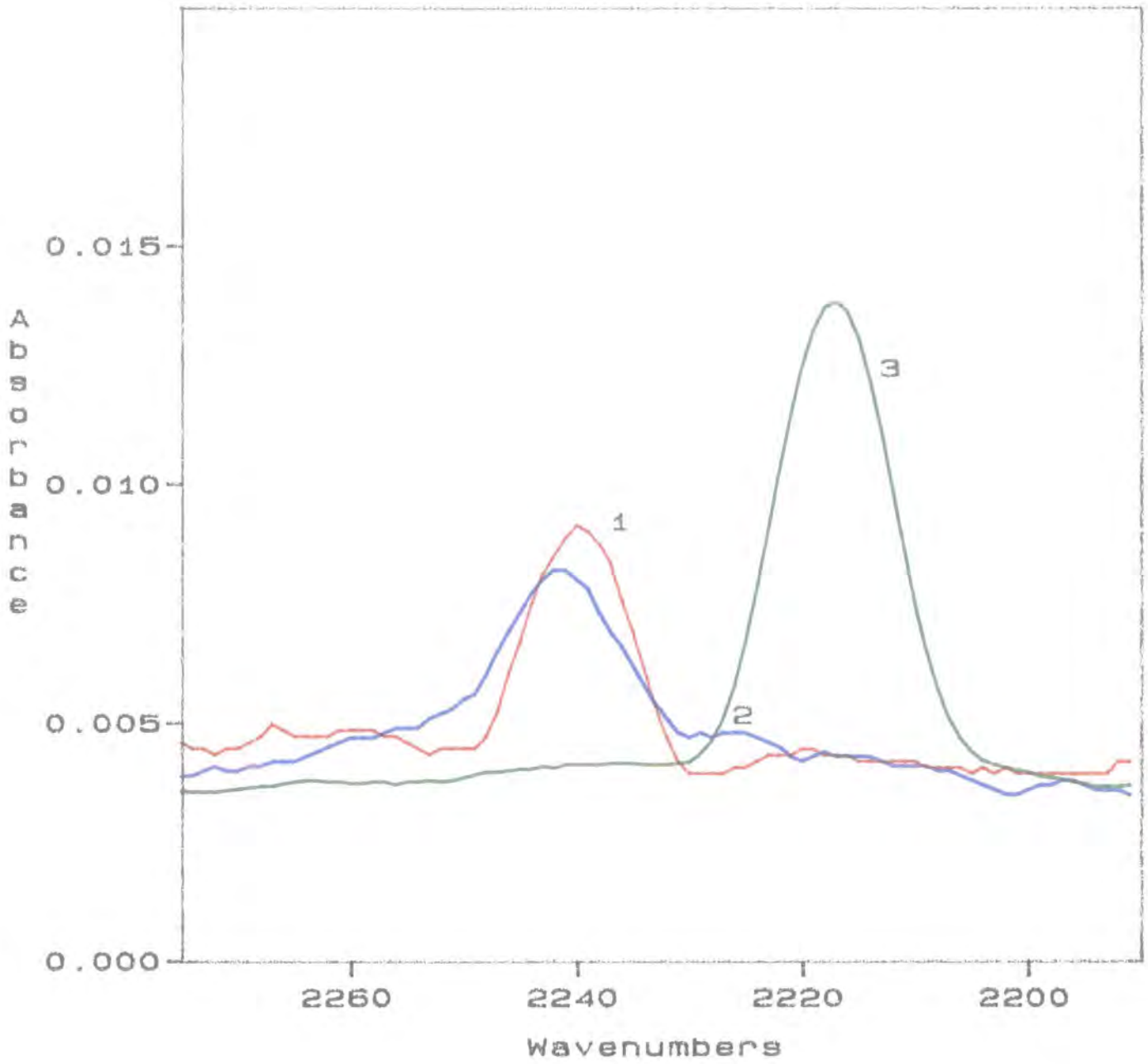

Figure 5–5 **The ν(CN) bands of 2–CN–4,6–dinitrophenol in several solvents**

1. Benzene 2. Methanol 3. DMSO

The actual scale of absorbance for 3 is 4 times larger than shown

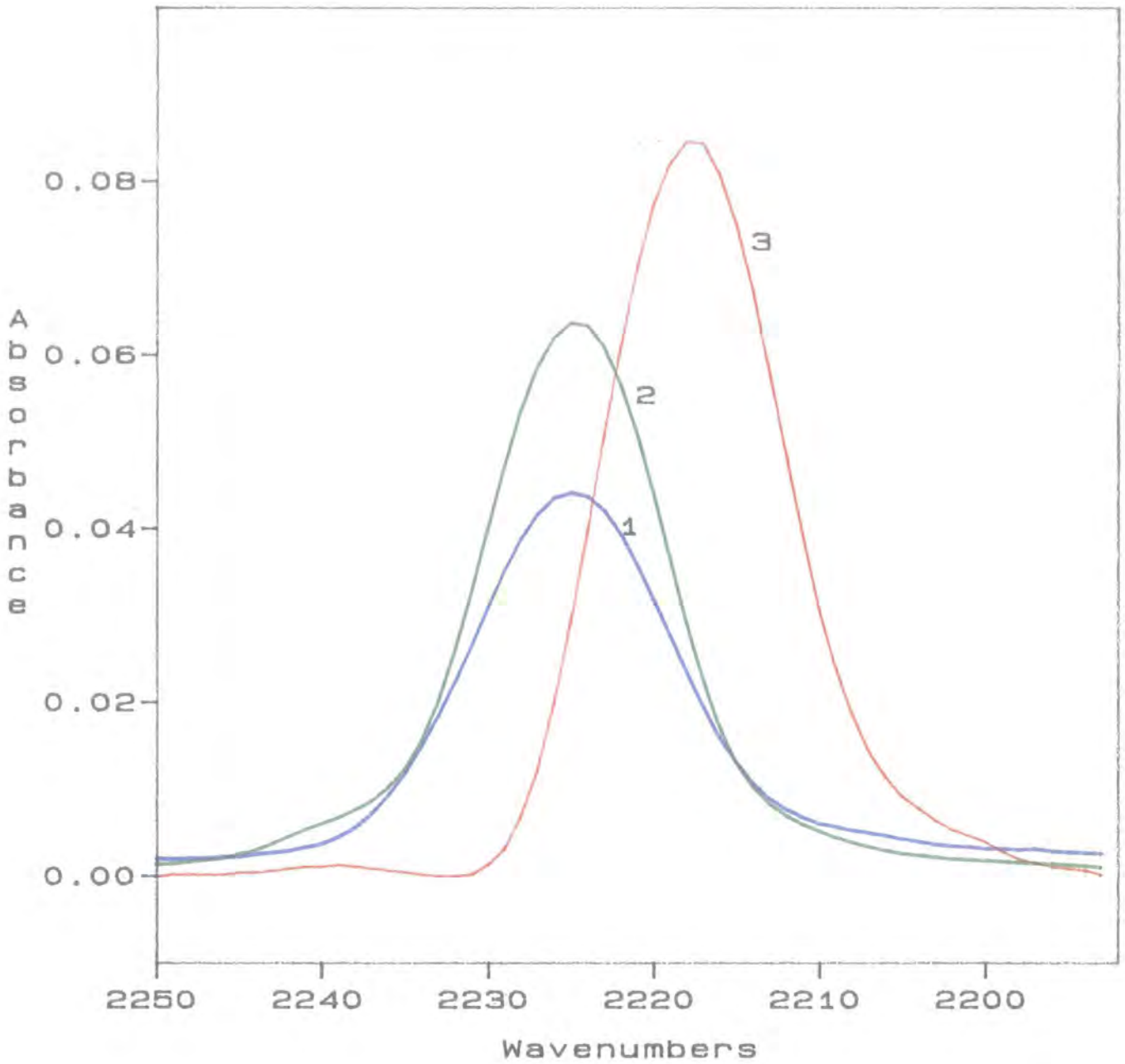

Figure 5–6 The ν(CN) bands of *p*–cyanophenol in several solvents

1. Dichloromethane 2. Methanol 3. DMSO

The actual scale of absorbance for 3 is 4 times larger than shown

of the only ν(CN) bands of *p*–cyanophenol in dichloromethane and methanol, although the band is clearly shifted to lower frequency in DMSO. Inspection of other regions of the infrared spectra of *p*–cyanophenol shows that the breathing modes of the aromatic ring are also similar in CH_2Cl_2 and methanol, with bands at 1610, 1589 and 1512cm^{-1}, variations not exceeding ±2cm^{-1}, indicating that the electronic distribution of the ring π–system is not significantly disturbed with change of solvent. Also, the (C–O) stretching bands suggest that the resonance of the hydroxyl group with the ring is not greatly modified by the change of solvent, as discussed in the previous section.

Benzonitrile itself shows a ν(CN) at 2228cm^{-1} in a range of non-hydrogen-bonding solvents.[23]

Infrared studies on solvent mixtures benzene/methanol of 4–CN–2,6-dinitrophenol (Section 5.2) undoubtedly relate the low frequency ν(CN) band to the opening of the intramolecular hydrogen–bond between the nitro and the hydroxyl groups.

It seems that in aromatic nitriles the electronic rearrangements caused by the hydrogen bond are somehow compensated by adjustments of the degree of resonance of the CN group with the ring, providing that there are no major modifications in other groups that can interfere with that resonance. In other words, intramolecular effects are much more important than intermolecular ones. So, in 4–CN–2,6–dinitrophenol it is possible that, by breaking the intramolecular hydrogen bond and forming intermolecular hydrogen–bonds with the OH and with the nitro groups, methanol forces both the *ortho*–nitro substituents out of the ring plane, thus reducing their π–accepting character and leaving the CN group as the only effective π–acceptor in a situation similar to 4–CN–phenol in methanol. This effect can be described by the classical view of through resonance in terms of an increase of the contribution of the canonical structure (15) shown on the following page to the overall description of the molecule.

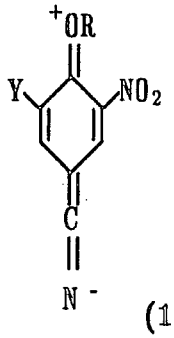

(15)

In the case of 2–CN–4,6–dinitrophenol, the NO_2 group *para* to OH is not subjected to the same kind of steric congestion thus retaining its coplanarity with the ring and competing with the CN group in accepting π–charge.

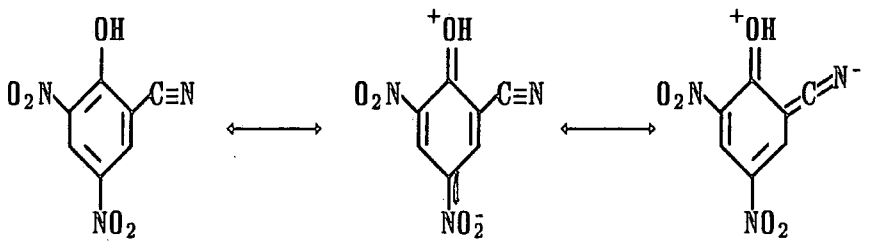

(16) (17) (18)

The contribution of (18) is certainly less important than that of (17) as the nitro group is a stronger electron withdrawing substituent than the nitrile group. Because of the high bond moments of the cyano group, the nitriles interact strongly with the other molecules having polar groups by dipole–dipole forces. Ritchie *et al*[24] studied the areas of the infrared C≡N stretching bands for benzonitriles with increasing amounts of polar molecules such as DMSO, DMF and acetone in CCl_4. The data were interpreted in terms of complex formation since the formation constants were found to be independent of the substituent on the benzene ring for various benzonitrile/DMSO systems which eliminates interactions involving the π–electrons of the aromatic ring or dipolar effects involving the entire molecule. This complex formation was ascribed to specific interactions between the dipoles of the cyano and the sulphoxide groups. A geometry with

antiparallel alignment of the C≡N and the S=O dipoles has been suggested.[25]

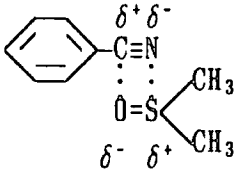

(19)

This interaction which involves the π–electrons of the multiple bonds, has been found[20,26] to cause the ν(CN) band to shift to lower frequency with a sharp increase of intensity. Both shift and integrated intensity show very good correlation with substituent constants.[27]

All the substituted benzonitriles studied in the present work show the ν(CN) band in DMSO at a lower frequency relatively to other solvents (Figs. 5–4 to 5–6).

For *p*–cyanophenol, other regions of the spectrum, namely the ring breathing modes region, show bands at similar frequencies as in methanol and dichloromethane in good agreement with the hypothesis of complex formation; in the ν(OH) region, the 'free' ν(OH) band is absent and the bonded ν(OH) band is very much enhanced.

5.1.3 The NO_2 groups stretching vibration

The $\nu(NO_2)$ stretching vibrational bands of trisubstituted anisoles are very stable in frequency despite variations in position relative to the methoxy group and in number of nitro groups. Table 5–3 shows data for some anisoles studied in the present work in benzene solution, plus two results from the literature[12] where the solvent was CCl_4. A_{as}/A_s represents the ratio of integrated intensities of the band of the antisymmetric vibration (ν_{as}) an that of the symmetric vibration (ν_s).

A reduction in the number of electron–withdrawing substituents causes a shift to lower frequency on the $\nu_{as}(NO_2)$ band, consistent with an increase of conjugation with the ring. The frequency of the symmetric vibration band remains essentially unaltered except for *ortho*–nitroanisole where it is shifted to higher frequency.

Table 5–3

Frequencies, half–widths and intensity ratio of the symmetric and antisymmetric stretching vibrations bands of some substituted anisoles in benzene

	$\nu_{as}(NO_2)$		$\nu_s(NO_2)$		
Anisole	$\bar{\nu}(cm^{-1})$	$\Delta\bar{\nu}_{\frac{1}{2}}(cm^{-1})$	$\bar{\nu}(cm^{-1})$	$\Delta\bar{\nu}_{\frac{1}{2}}(cm^{-1})$	A_{as}/A_s
2,4,6–trinitro	1546	19	1344	14	1.1
2–CN–4,6–dinitro	1546	19	1345	13	0.7
4–CN–2,6–dinitro	1548	16	1347	20	3.0
2–CN–4–nitro	1535	17	1347	13	1.03
2–nitro[12]	1532	12	1354	19	2.08
2,4–dinitro[12]	1538	21	1345	9	1.17

Of the spectral characteristics listed in Table 5–3, what is most remarkable is the variation in halfwidth and ratio of intensities of *o*-nitroanisole and 4-CN-2,6-dinitroanisole; these are the compounds that do not have a nitro group *para*– to the methoxy substituents. This fact may or may not be a coincidence. While for the other anisoles the intensities of the ν_s and $\nu_{as}(NO_2)$ bands are of the same order of magnitude, for these particular compounds the antisymmetric band is much more intense than the band for the symmetric vibration as a result of both an increase of the intensity of the ν_{as} band and decrease the ν_s band intensity. The ν_s band is, however, broader than that of the ν_{as} band, in contrast with what is found for the other anisoles. Crystallographic studies on 1-alkoxy-2,6-dinitrobenzenes[30,31] indicate that, in the solid–state, there is no coplanarity between the *ortho*–nitro groups and the aromatic ring, both groups being twisted by angles of 30°–60°. Of course, this does not have to be true in solution, especially in a low–interfering solvent as benzene or dichloromethane, where some rotation around the C–N bond may be expected. That rotation may be responsible for the relatively large halfwidth, *ca.* $30cm^{-1}$, of the *ortho*–nitroanisoles. When there

is a nitro group in *para* position, always planar with the ring, the observed intensity of the $\nu_{as}(NO_2)$ band is mainly due to this group, so the measured halfwidth relates only to it, although it is possible to detect the shoulder due to the broad, less intense, $\nu_{as}(o\text{–}NO_2)$ band whenever such a group is present in the molecule (see Figures 5–7b and 5–9b). Although for some of the listed anisoles, namely the first two and the last one in Table 5–3, the nitro substituents are not equivalent, only one band for each mode of vibration was found in the spectra.

In the corresponding trisubstituted phenols, intramolecular hydrogen bond is one of the factors responsible for the changes seen in these bands. The increased electron donor ability of the OH group compared to that of the OCH_3 group must also be considered since it leads to greater electron density charge on the *ortho*– and *para*– ring positions. Nitro groups at those positions will have their electron withdrawing power reinforced either by resonance or by the inductive effect.

Table 5–4 summarises, in a schematic way, what has been found in the (scarce and old) literature about changes on NO_2 band characteristics due to several factors.

Table 5–4

	$\nu_{as}(NO_2)$		$\nu_{s}(NO_2)$	
type of effects	**freq**	**int**	**freq**	**int**
steric[a]	$\uparrow^{28,32}$	$\uparrow^{12}$	$\uparrow^{12}$	
conjugation	$\downarrow^{28}$	–	$\downarrow^{6}$	$\uparrow^{6}$
hydrogen–bonding	$\uparrow^{12}$	$\uparrow^{12}$	$\downarrow^{12}$	$\uparrow^{12}$

a) NO_2 rotates out of the ring plane[12,28]

It has been stated[12,28,32,33] that the $\nu_s(NO_2)$ band is more sensitive to both steric effects and intramolecular hydrogen bond formation than the $\nu_{as}(CN)$ and that when the NO_2 group is involved in intra hydrogen-bonding $\nu_s(NO_2)$ is shifted

to lower frequencies and $\nu_{as}(NO_2)$ to higher frequencies.[12] However, because the symmetric mode $\nu_s(NO_2)$ is partially coupled with the (C–N) vibration[28,29,34] and with ring modes, the direction and extent of its shifts may be more difficult to interpret than those of the uncoupled $\nu_{as}(NO_2)$,[28] particularly when more than one type of effect has to be taken in account.

The experimental data for the NO_2 stretching vibrations of the compounds analysed in the present work in benzene solutions, presented in Table 5–5, show very good agreement with the results published by Grantzan *et al* (1968)[12] for some substituted nitrophenols in CCl_4 or DCE which are also listed in the same table for comparison.

Table 5–5 **Frequencies, halfwidths and intensity ratios for some substituted nitrophenols**

	ν (NO_2)		ν (NO_2)		A_s/A_{as}
Phenol	$\tilde{\nu}$(cm^{-1})	$\Delta\nu_{\frac{1}{2}}$	$\tilde{\nu}$(cm^{-1})	$\Delta\nu_{\frac{1}{2}}$	
a,d					
2–CN–4,6–dinitro	1557 1536	13	1344 1323	13	0.36
b,d					
4–CN–2,6–dinitro	1547	14	1354 1316	30 14	1.86
2,4,6–trinitro c,d	1560 1550 1537sh	24	1356sh 1344 1318	14	0.48
2,4,6–trinitro[12] (DCE)	1557 1550 1538sh	25	1346 1320	11 –	
2,4–dinitro[12] (CCl_4)	1553 1537	11 12	1345 1329	9 7	
2,6–dinitro[12] (CCL_4)	1544	21	1354 1312	28 14	

sh shoulder

* asymmetric band

a spectrum presented in Figure 5–7

b spectrum presented in Figure 5–8

c spectrum presented in Figure 5–9

d solvent: benzene

The position of the band maxima for the substituted phenols appears to be less sensitive to the number of substituents than for the anisoles. From the data in Figures 5–7 to 5–9 and Table 5–5 it is possible to conclude that, for all the phenols analysed in this work, there is non–equivalence of the nitro groups.

For 2–CN–4,6–dinitrophenol both symmetric and antisymmetric vibrations are split into doublets: the ν_s band of the *para*–NO_2 group remains identical to the corresponding anisole and a second, less intense, band appears at lower frequency and is associated with the *ortho*–NO_2 substituent involved in intramolecular hydrogen bonding. The two new $\nu_{as}(NO_2)$ bands appear one at each side of the vibrational band of the anisole. The band at higher frequency is assigned to the H-bonded NO_2 group and the one at low frequency to the *para*–NO_2 group. There is also an increase of the intensity ratio $A(\nu_s)/A(\nu_{as})$ in the phenol relatively to the anisole. Frequency shifts to lower values and the increase of intensity are usually indicators of an increase degree of resonance but if the conjugation of the *para*–NO_2 group is augmented (which is not impossible as intramolecular hydrogen bond formation increases the electron donor ability of the OH group) it should be expected to find its ν_s band at a lower frequency than in the anisole as it is known that this band is much more sensitive to conjugation effects than $\nu_{as}(NO_2)$.[35,36]

In the case of 4–CN–2,6–dinitrophenol, the antisymmetric vibration shows a band which is similar to that of the anisole in frequency, intensity and bandwidth. A new weak band can be found in both benzene and dichloromethane at *ca.* 1580cm^{-1}. Although it could be expected to find a band at higher frequency than that of the anisole due to the hydrogen bonding of one *ortho*–nitro group, this frequency 1580cm^{-1} seems too high to be assigned to a nitro group vibration (for example, in 2,6–dinitrophenol the $\nu_{as}(NO_2)$ band has a maximum at 1544cm^{-1} with a shoulder at higher frequency, less than 10cm^{-1} apart[12]) and is probably associated with the ring breathing modes. The symmetric $\nu_s(NO_2)$ vibration of 4–CN–2,6–dinitrophenol in benzene gives rise to two bands. The same split can also be found in dichloromethane and chloroform but not in methanol or ethanol.

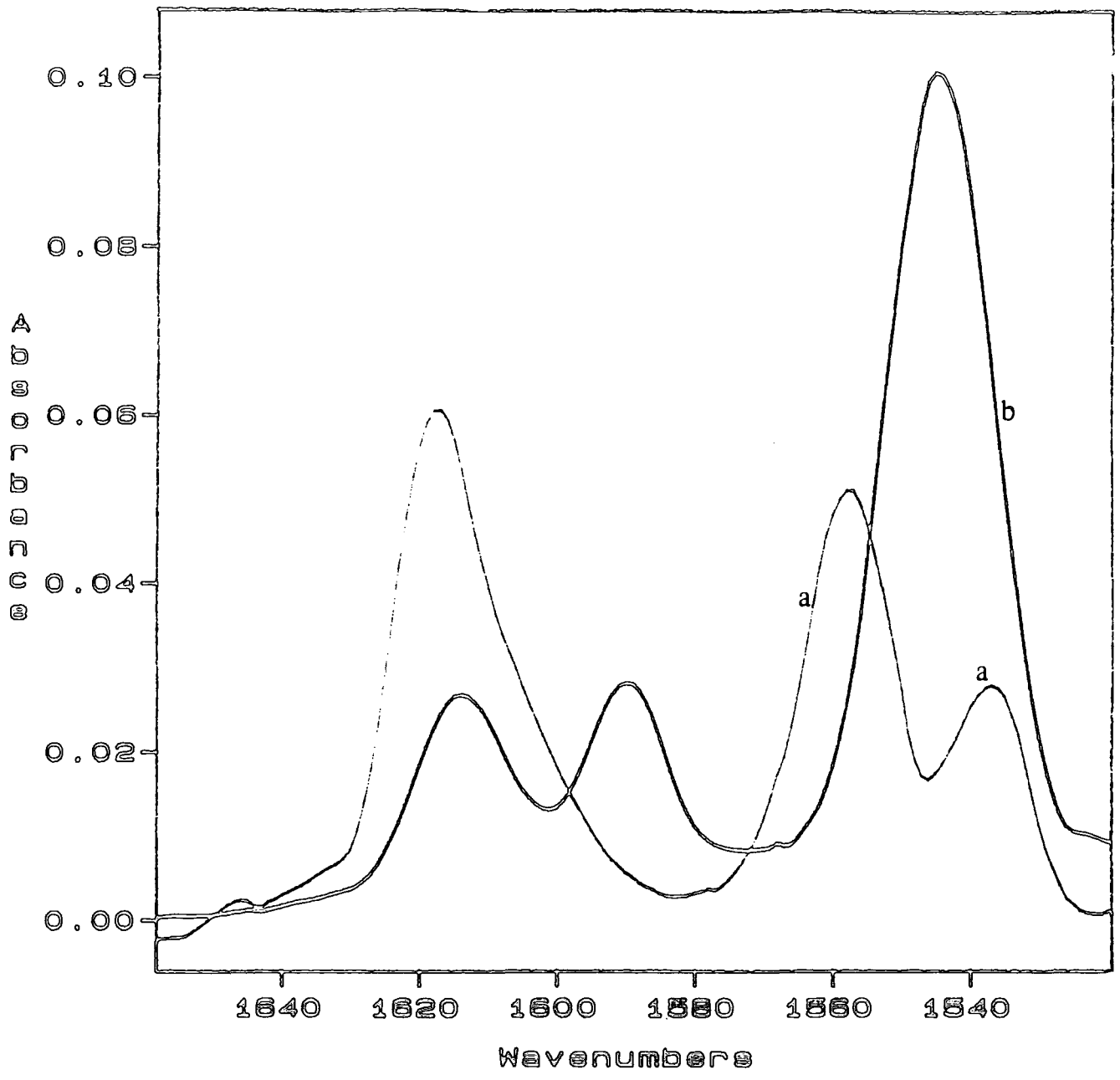

Figure 5–7a Absorption spectra in the $\nu_{as}(NO_2)$ region of 2-CN-4,6-dinitrophenol (a, ——) and 2–CN–4,6–dinitroanisole (b, ═══) in benzene

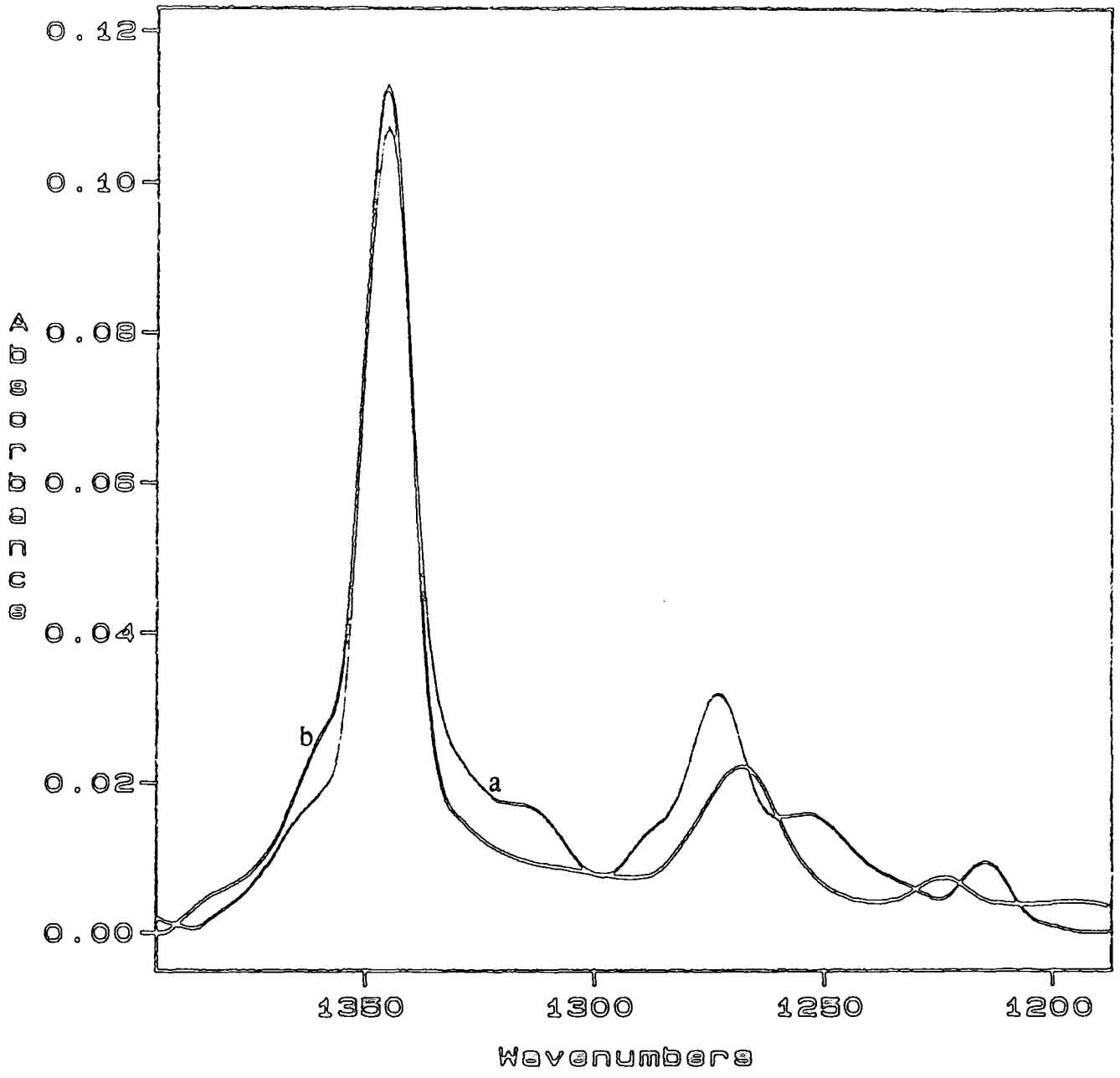

Figure 5–7b Absorption spectra in the $\nu_s(NO_2)$ region of 2-CN-4,6-dinitrophenol (a, ——) and 2–CN–4,6–dinitroanisole (b, ——) in benzene

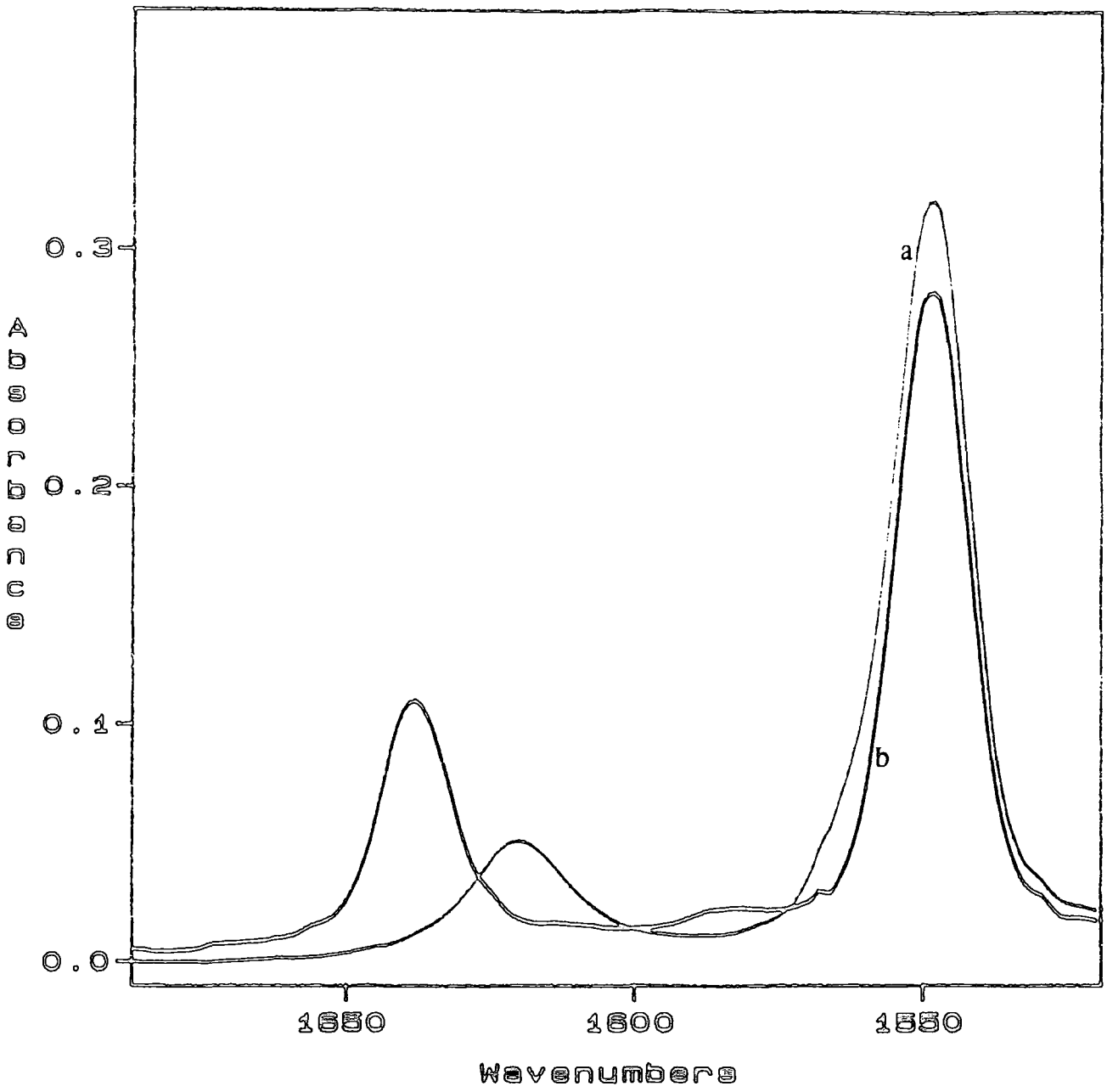

Figure 5–8a Absorption spectra in the $\nu_{as}(NO_2)$ region of 4-CN-2,6-dinitrophenol (a,——) and 4–CN–2,6–dinitroanisole (b,═══) in benzene

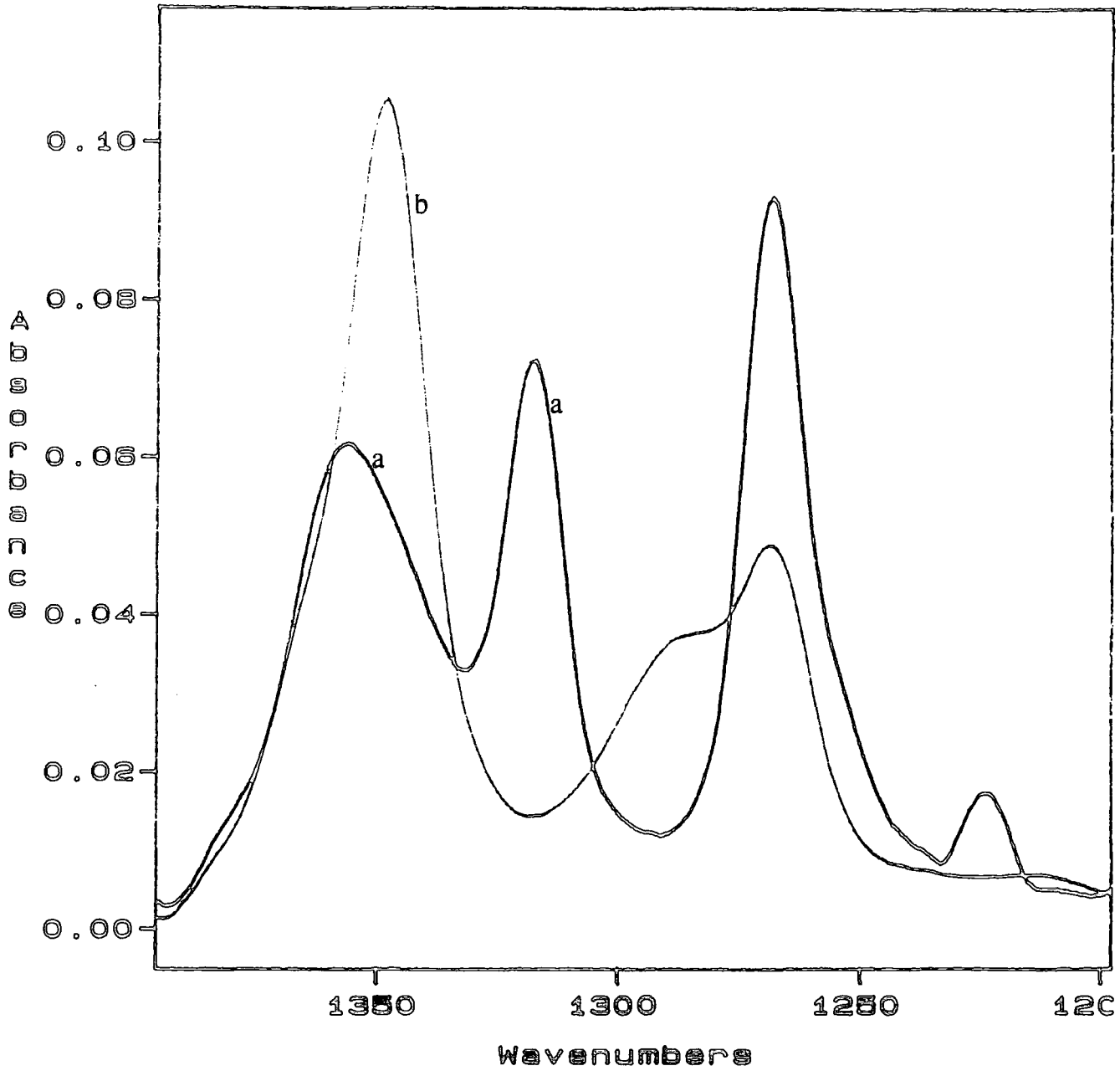

Figure 5–8b Absorption spectra in the $\nu_s(NO_2)$ region of 4-CN-2,6-dinitrophenol (a, ——) and 4–CN–2,6–dinitroanisole (b, ——) in benzene

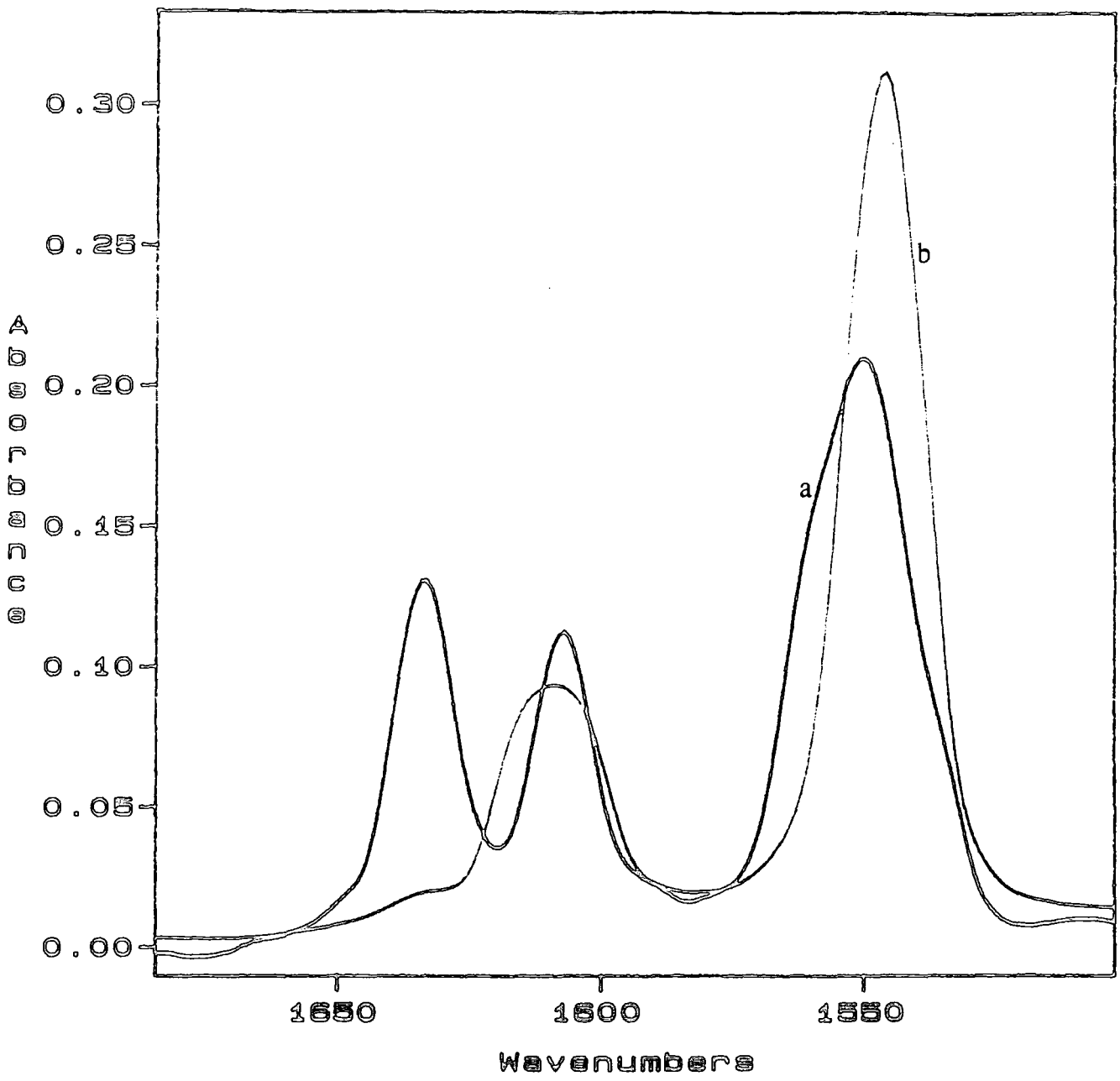

Figure 5–9a Absorption spectra in the $\nu_{as}(NO_2)$ region of 2,4,6-trinitrophenol (a,——) and 2,4,6-trinitroanisole (b, ——) in benzene

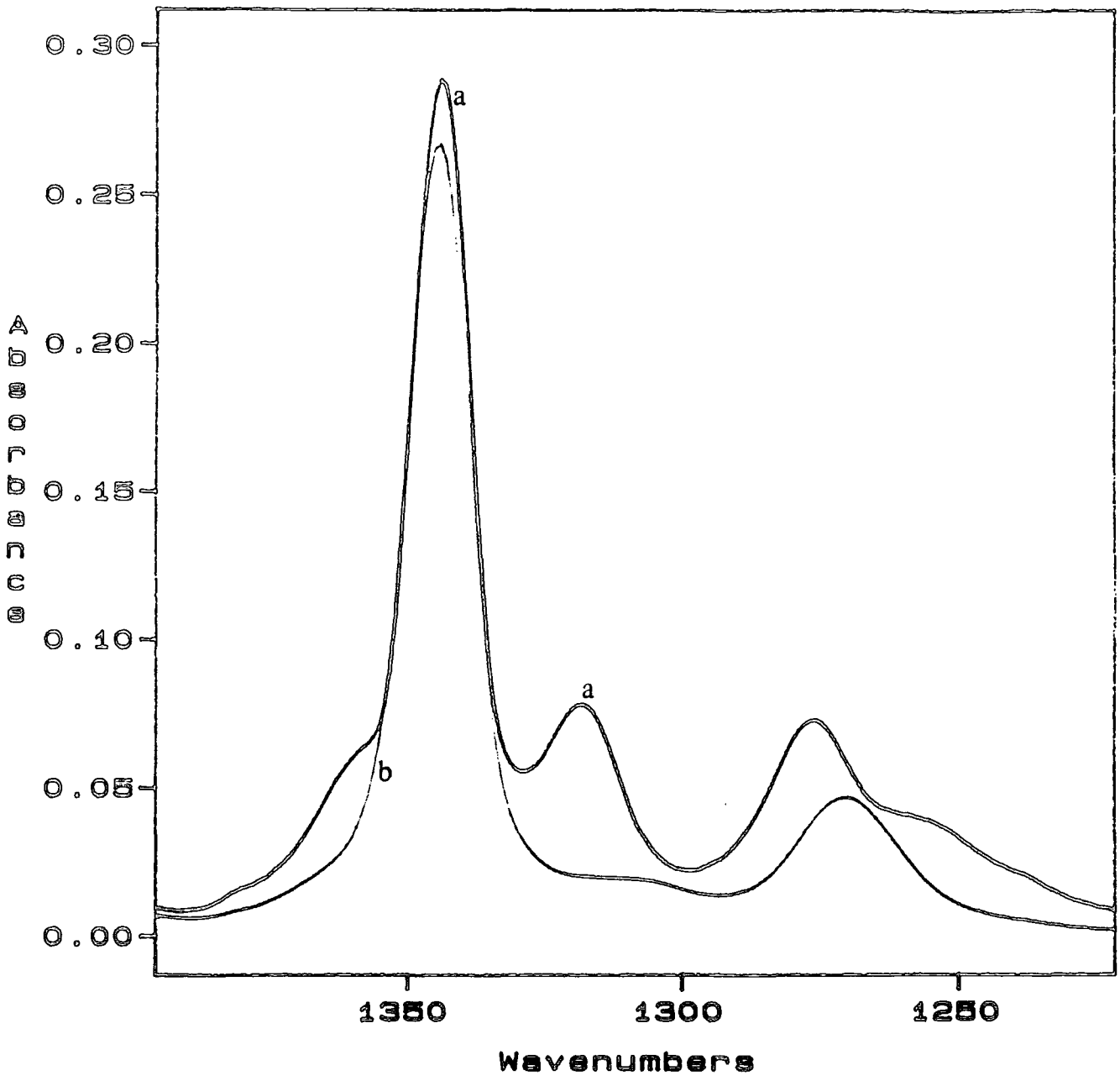

Figure 5–9b Absorption spectra in the $\nu_s(NO_2)$ region of 2,4,6-trinitrophenol (a, ——) and 2,4,6-trinitroanisole (b, ——) in benzene

The band at lower frequency, associated with the hydrogen bonded nitro group , is shifted 30cm^{-1} relatively to the only $\nu_s(NO_2)$ of corresponding anisole and two factors may contribute to this shift, both related to the hydrogen–bond: one is the electronic redistribution within the 6–membered chelate ring previously shown in (5), and the other is the planarity towards the aromatic ring achieved by the NO_2 when hydrogen bonded which favours its resonance. The other band is shifted 7cm^{-1} to higher frequency compared to the anisole, which is consistent with the view that the 'free' NO_2 group is forced to assume a twisted position relatively to the ring due to repulsion between the electronic clouds of the oxygen atoms of the nitro and hydroxyl groups and, therefore, its electron accepting ability is diminished.

For picric acid (2,4,6–trinitrophenol) both the antisymmetric and the symmetric bands are split into 'triplets', with all the nitro groups being non–equivalent: one *ortho*–NO_2 group is involved in the hydrogen bond (higher ν_{as}, low ν_s), the other non–bonded *ortho*–NO_2 group rotates out of the ring plane due to steric hindrance (ν_s shifted to higher frequency) and the *para*–NO_2 group is planar with the ring and non–bonded (low ν_s).

A change in solvent from benzene to methanol leads to several modifications on the NO_2 stretching vibrational bands of the 2–CN–4,6–dinitro– and 4–CN–2,6-dinitrophenols. The antisymmetric band of the 4–CN isomer is little affected by the change of solvent but the pair of band for $\nu_{as}(NO_2)$ of the 2-CN-4,6-dinitrophenol is less separated in methanol, retaining to a certain extent its ratio of intensities. The band previously assigned to the hydrogen bonded NO_2 moves to lower frequency while the one due to *para*–NO_2 is not shifted. For both isomers there is a decrease on the total intensity of the $\nu_{as}(NO_2)$ band(s).

In the spectrum of 2–CN–4,6–dinitrophenol, the stronger $\nu_s(NO_2)$ band, corresponding to the *para*–NO_2 group, is shifted to higher frequency in methanol and its intensity is decreased (Figure 5–11a). It is possible to detect the presence of a much weaker band between 1330–1320cm^{-1} that could be attributable to ν_s(o–NO_2).

The 4–CN– compound shows only one band for $\nu_s(NO_2)$ with maximum at approximately the same frequency as in benzene and with a similar shape. The band at 1316cm^{-1} in benzene assigned to the bonded NO_2 is absent from the spectrum in methanol (Figure 5–11b).

2–CN–4,6–Dinitrophenol

Benzene	Methanol
ν_{as} { 1557(*ortho*) / 1536(*para*) } ν_s { 1344(*para*) / 1323(*ortho*) sh }	ν_{as} { 1552(*ortho*) / 1537(*para*) } ν_s: 1349(*para*) shoulder at lower $\tilde{\nu}$

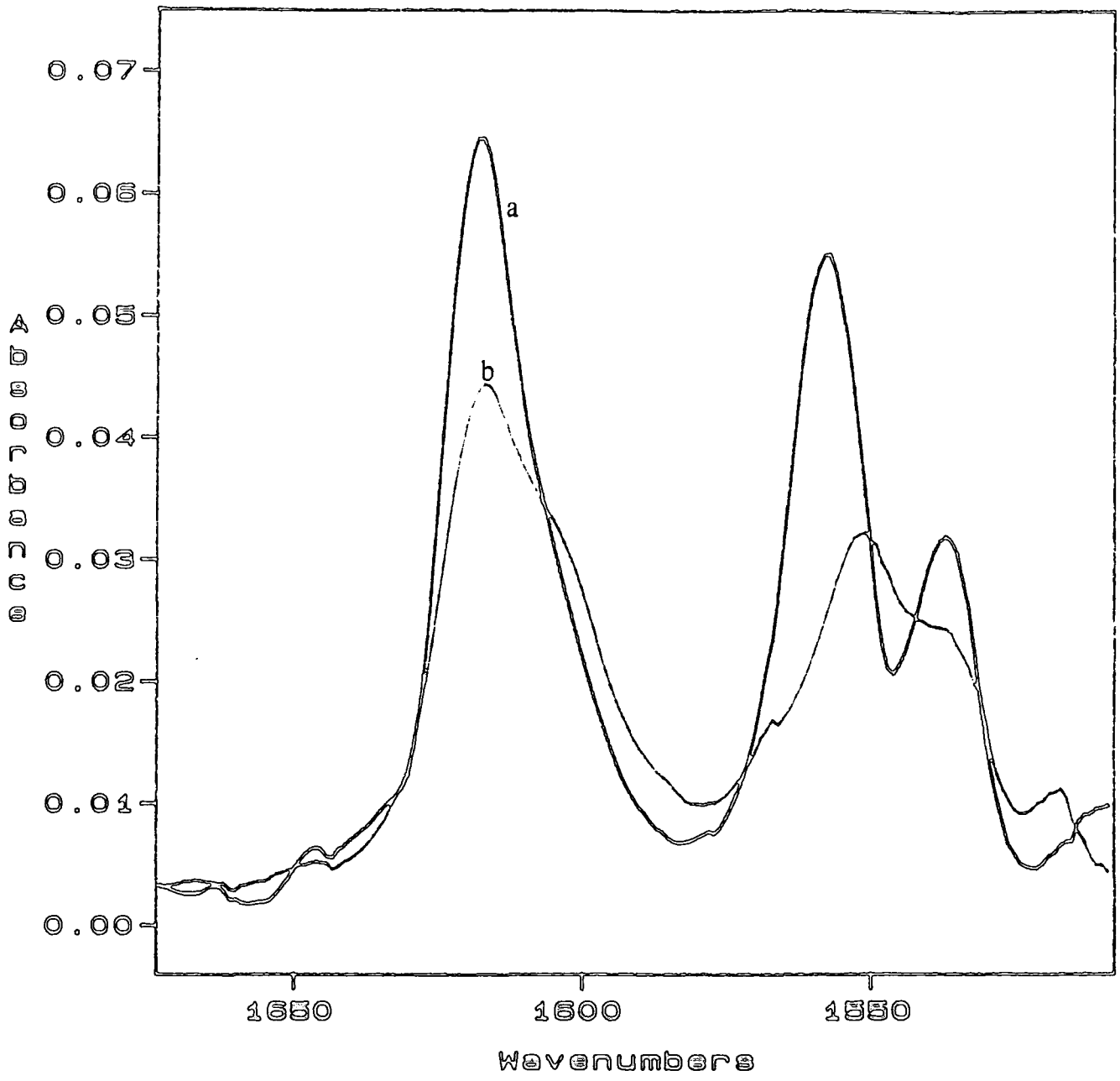

Figure 5–10a Absorption spectra of 2–CN–4,6-dinitrophenol in benzene (a, ——) and methanol (b, ——). Ring breathing modes and $\nu_{as}(NO_2)$ bands.

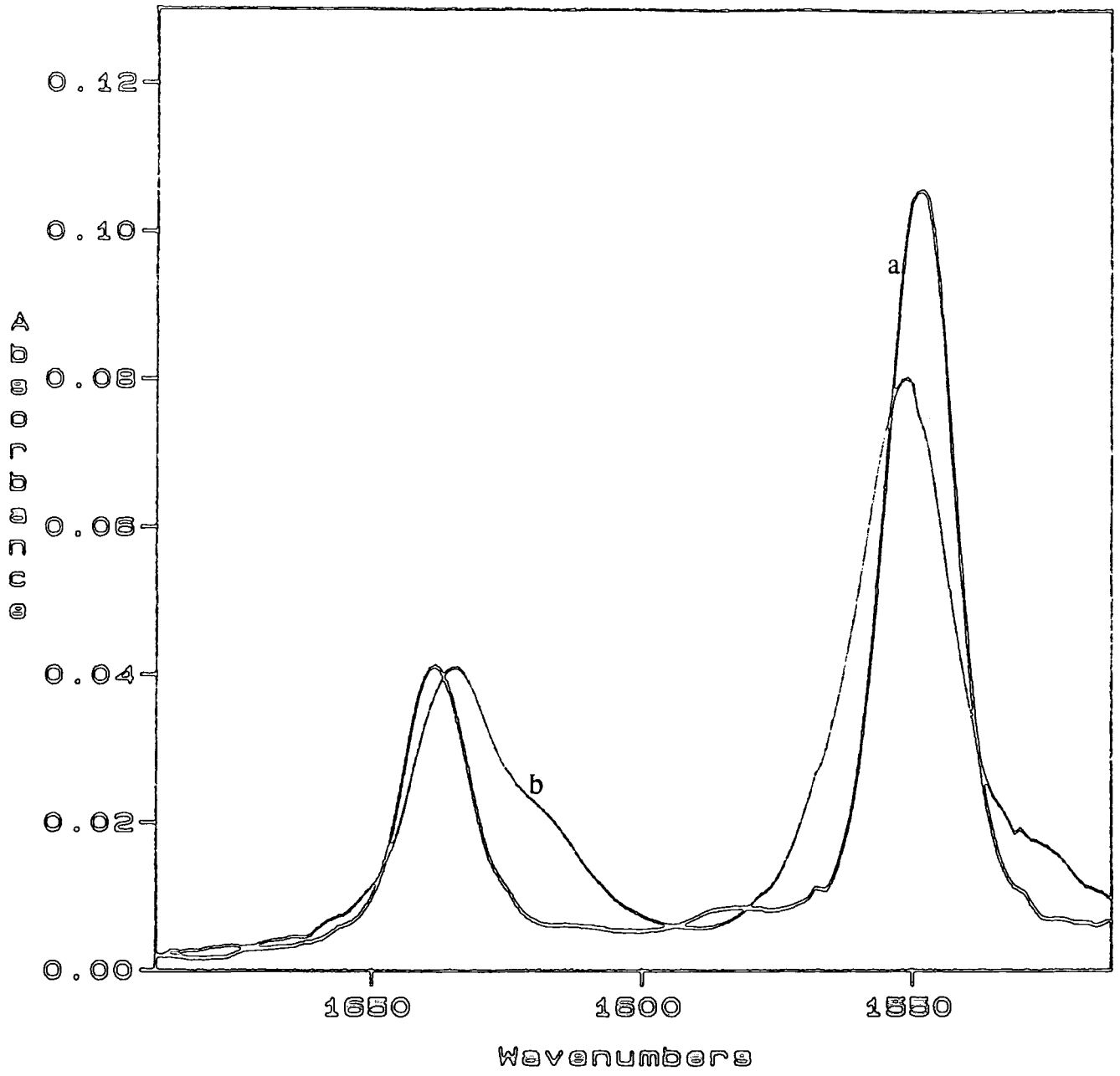

Figure 5–10b Absorption spectra of 4–CN–2,6-dinitrophenol in benzene (a, ——) and methanol (b, ——). Ring breathing modes and $\nu_{as}(NO_2)$ bands.

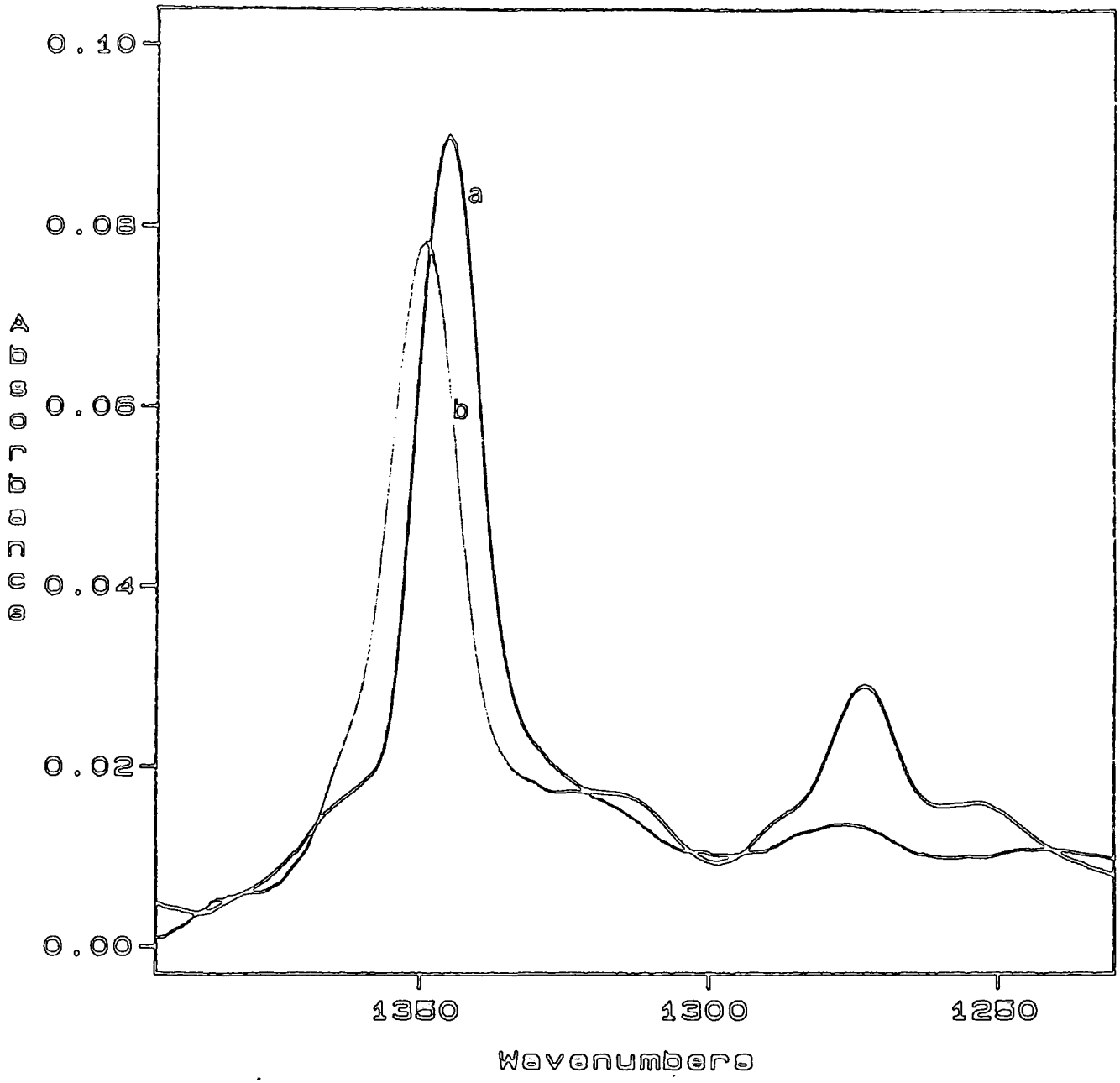

Figure 5–11a Absorption spectra of 2–CN–4,6-dinitrophenol in benzene (a, ——) and methanol (b, ——). $\nu_s(NO_2)$ and $\nu(CO)$ bands.

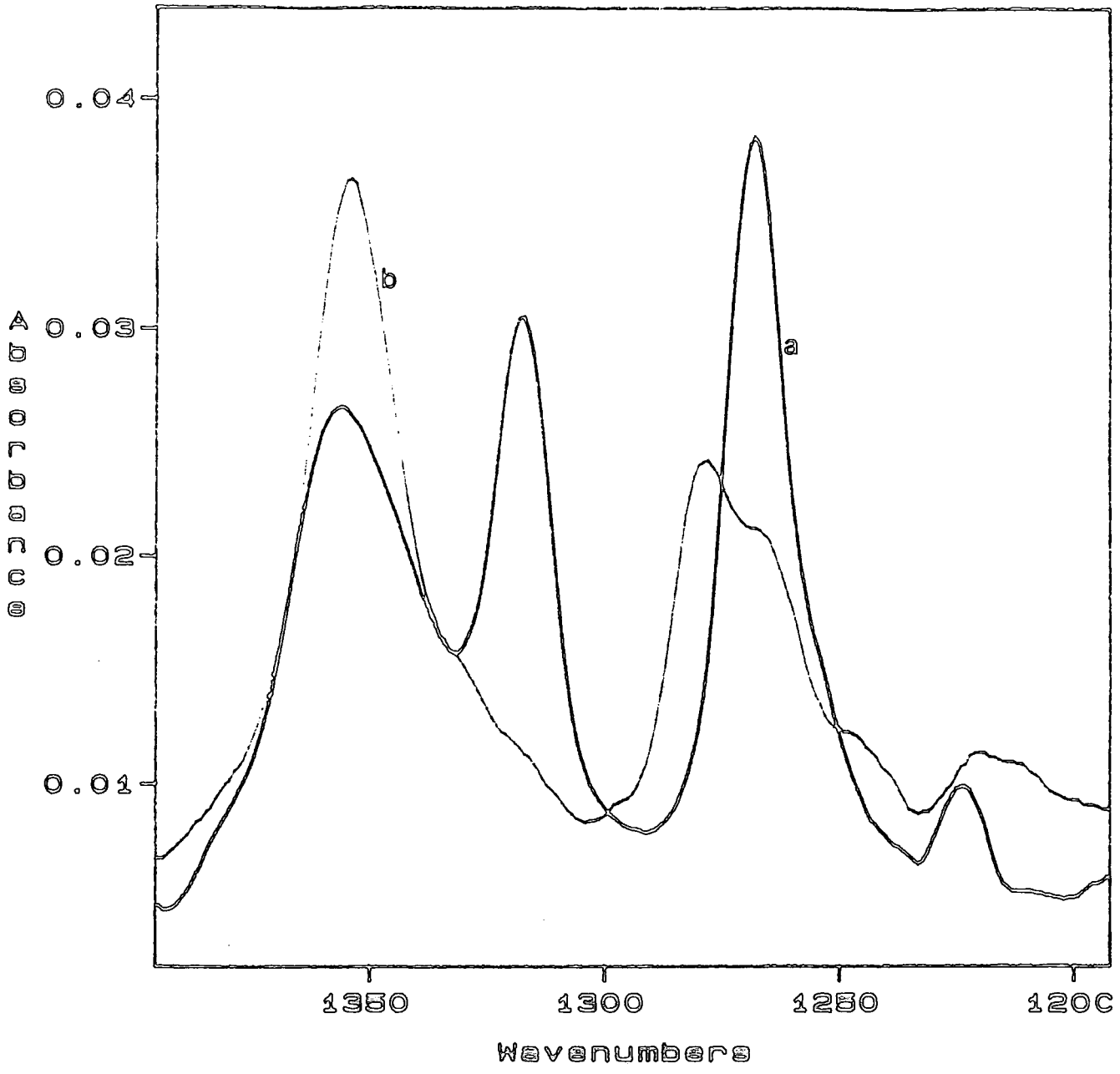

Figure 5–11b Absorption spectra of 4–CN–2,6-dinitrophenol in benzene (a,——) and methanol (b, ——). $\nu_s(NO_2)$ and $\nu(CO)$ bands.

5.2 Infrared Measurements on 4-CN-2,6-dinitrophenol in mixtures Benzene/Methanol

In order to study the influence of the breaking of the intramolecular hydrogen–bond on the several functional groups of the molecule, spectra of 4-CN-2,6-dinitrophenol were recorded in solutions with variable molar fraction of methanol in benzene. Each spectrum presented corresponds to that of the solution 4CNDNPH / MeOH / C_6H_6 from which the spectrum of the corresponding MeOH / C_6H_6 has been subtracted. It is not possible to obtain much information about the interaction methanol – 4CNDNPH from the ν(OH) region. The most important information from this part of the spectrum is that methanol does not cause the ionisation of the the phenol but forms intermolecular hydrogen bonds with it, as shown in figure 5–12 where the spectrum of 4-CN-2,6-dinitrophenol in deuterated methanol is compared with that of the same compound in benzene. The spectra of methanol in benzene show the formation of methanol dimer and higher order chains even at very low concentration (Figure 5-13). The presence of the substituted phenol in such MeOH/Benzene mixtures modifies these chains and a "negative absorption" is obtained from the subtraction of spectra.

The most promising regions for this study are the ν(CN) and the $\nu_s(NO_2)$ regions which are shown in Figures 5–14 and 5–15, respectively, for five of the fourteen solvent mixtures analysed.

In a crude empirical analysis, it is possible to detect a correspondence between the increase of the molar fraction of methanol in the mixture and the ratio of height of the two nitro bands, corresponding to the symmetric stretching vibrations of the "free" nitro group ($\bar{\nu}_1$= 1355cm^{-1}) and hydrogen–bonded nitro group ($\bar{\nu}_2$ = 1316cm^{-1}), which is shown in Figure 5–16, where R = Height(ν_1) / Height(ν_2). Heights rather than integrated intensities were used here since there is some degree of overlap of the two bands which makes intensities very difficult to determine. The gradual disappearance of ν_2, assigned to the hydrogen-bonded nitro group, and therefore the increase of R, must be due to the breaking of

the intramolecular $OH\cdots O_2N$ bond of the substituted phenol with formation of new hydrogen bonds to the solvent which do not lead to any shift of the $\nu_s(NO_2)$ band relatively to the position of the "free" NO_2 group band, ν_1.

In the benzene/methanol mixtures up to $x \simeq 0.5$, the breaking of the intramolecular hydrogen-bond reflected by the decrease of ν_2 intensity is linearly proportional to the molar fraction of methanol in the mixture. In other words, the substituted-phenol molecule is surrounded mainly by benzene molecules with methanol gradually penetrating this sphere of solvation. At higher methanol concentration, the rate of intramolecular hydrogen-bond breaking is faster as shown by the increase in slope of R *vs.* x_{MeOH} in a relation that is still close to linearity. In this situation it is expected to find phenol molecules solvated entirely by methanol, by benzene or by molecules of both solvents. Curiously, within the range of methanol molar fractions where the ratio of heights, R, versus x_{MeOH} is approximately linear, up to $x \simeq 0.5$ the observed effect on the ν(CN) band is only a slight broadening although the effect of the presence of methanol is noticed on the nitro group bands from very low alcohol concentrations. The second band in the CN region (Figure 5-15) starts to be noticeable when R starts to increase more rapidly with x_{MeOH}.

This seems to indicate that the appearance of a band at lower frequency in the ν(CN) region is somehow connected to what is happening on the rest of the molecule, particularly with the solvation of the nitro groups.

The observed spectral changes in methanol / benzene mixtures are intermediate situations of those found when comparing the spectra in pure solvents. It was suggested then that the ν(CN) band at lower frequency ($2224cm^{-1}$) which appears in methanol and cannot be related to direct solvation (by hydrogen-bonding) of the CN group since that would lead to a shift in the opposite direction, was due to an increase of resonance of the CN group with the ring π-system when the nitro groups are solvated and twisted out of the molecular plane, with breaking of the intramolecular hydrogen bond to the hydroxyl group. If this twisting and thus drastic reduction of the π-accepting power of the nitro

group occurs only when there is a large number of protic solvent molecules near it, then the small effect on the ν(CN) band at "low" (x<0.5) methanol concentration may be explained as a result of a situation like (20) where the intramolecular hydrogen bond is replaced by intermolecular interaction with methanol maintaining a coplanar NO_2 group.

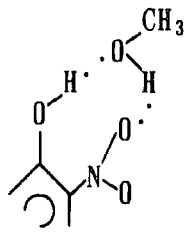

(20)

When the protic solvent molecules are predominant in the sphere of solvation of the substituted phenol (21), certainly more than one will be attached to the NO_2 group as well as the *ortho*- OH group, with bulkiness forcing rotation. This is a situation that leaves the CN group as the more effective π-acceptor in the molecule and may therefore lead to the appearance of another ν(CN) in the spectrum.

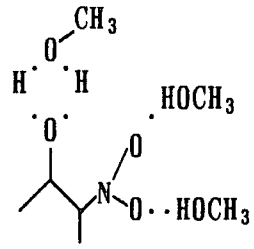

(21)

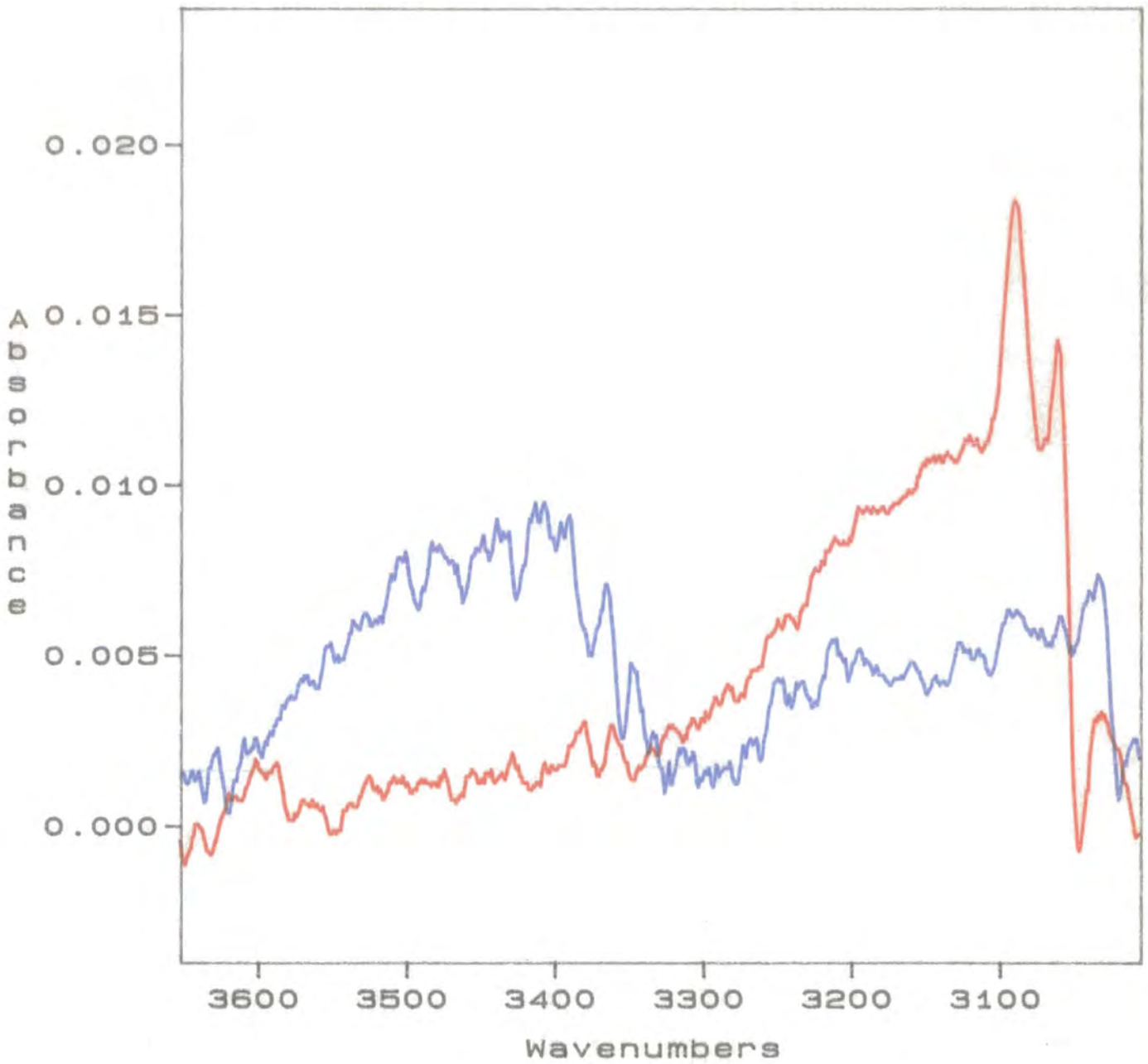

Figure 5–12 ν(OH) bands of 4–CN–2,6–dinitrophenol in benzene (———) and deuterated methanol (———).

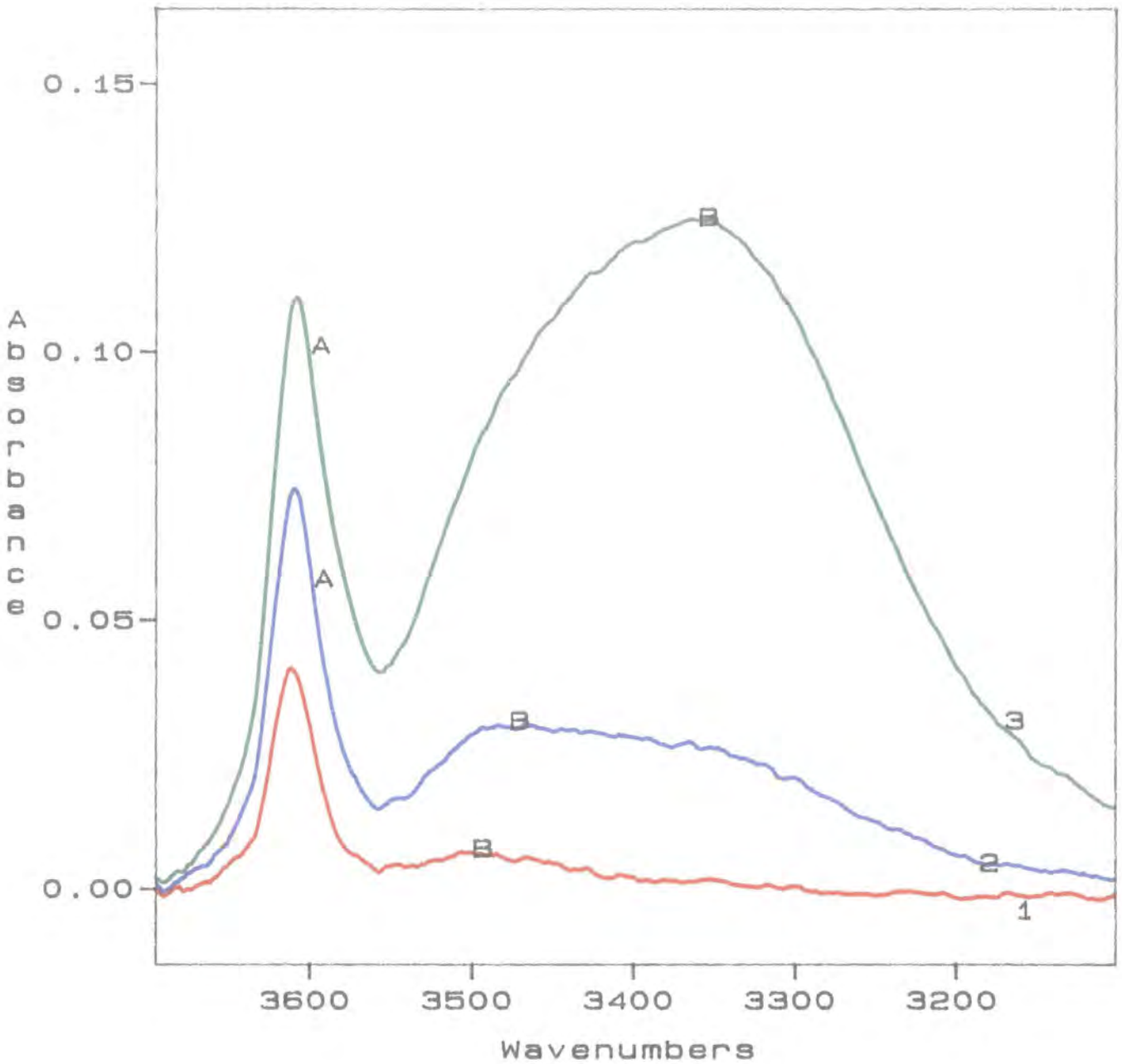

Figure 5–13 **Infrared spectra of binary mixtures methanol / benzene in the ν(OH) region.**

A: monomer B:polymer

1) x_{MeOH}=0.017 2) x_{MeOH}=0.043 3) x_{MeOH}=0.085

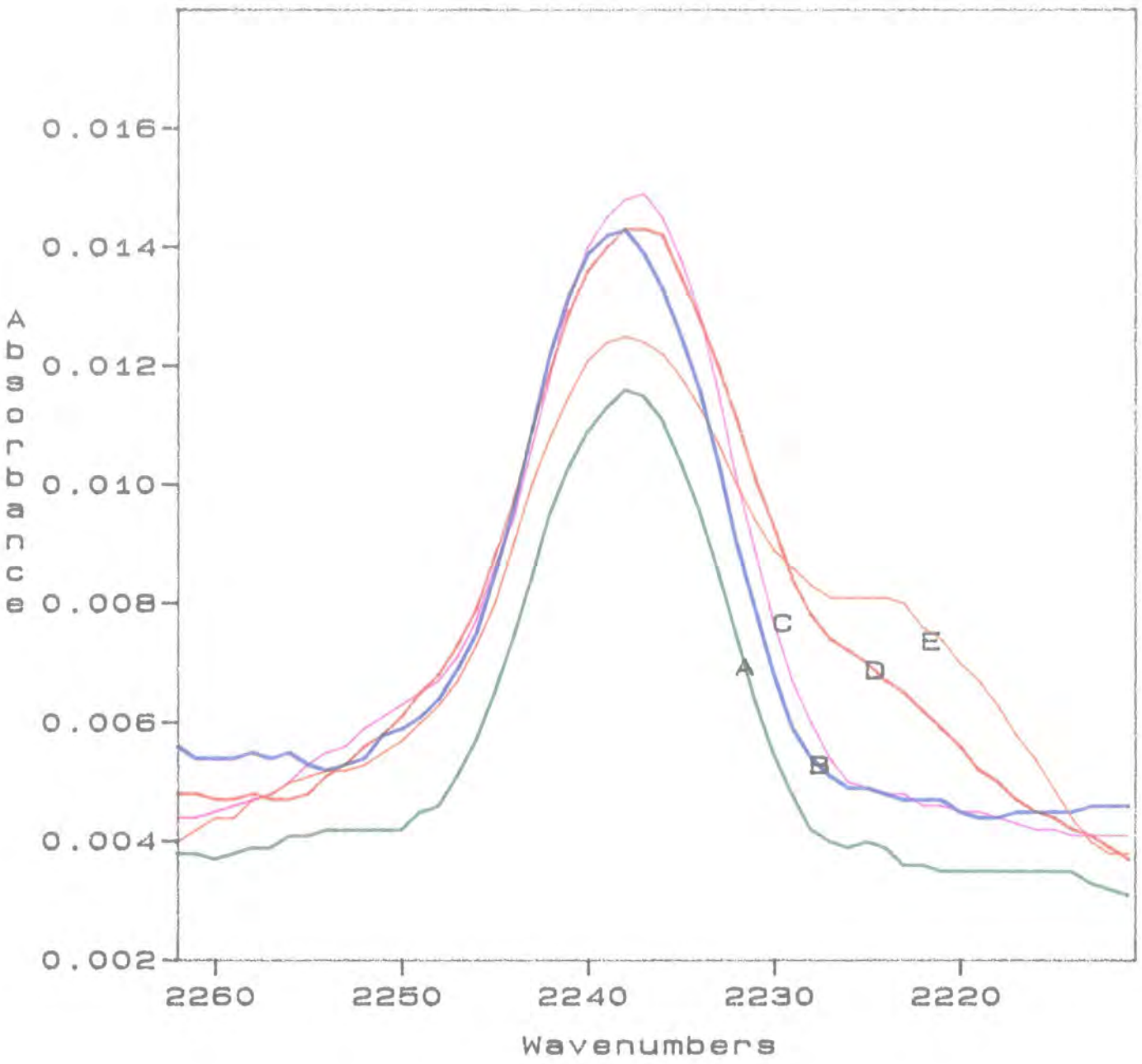

Figure 5–14 ν(CN) band of 4–CN–2,6–dinitroanisole in solvent mixtures methanol / benzene, with varying methanol molar fraction, f(MeOH):

A: 0.043, B: 0.085, C: 0.160, D: 0.495, E: 0.688

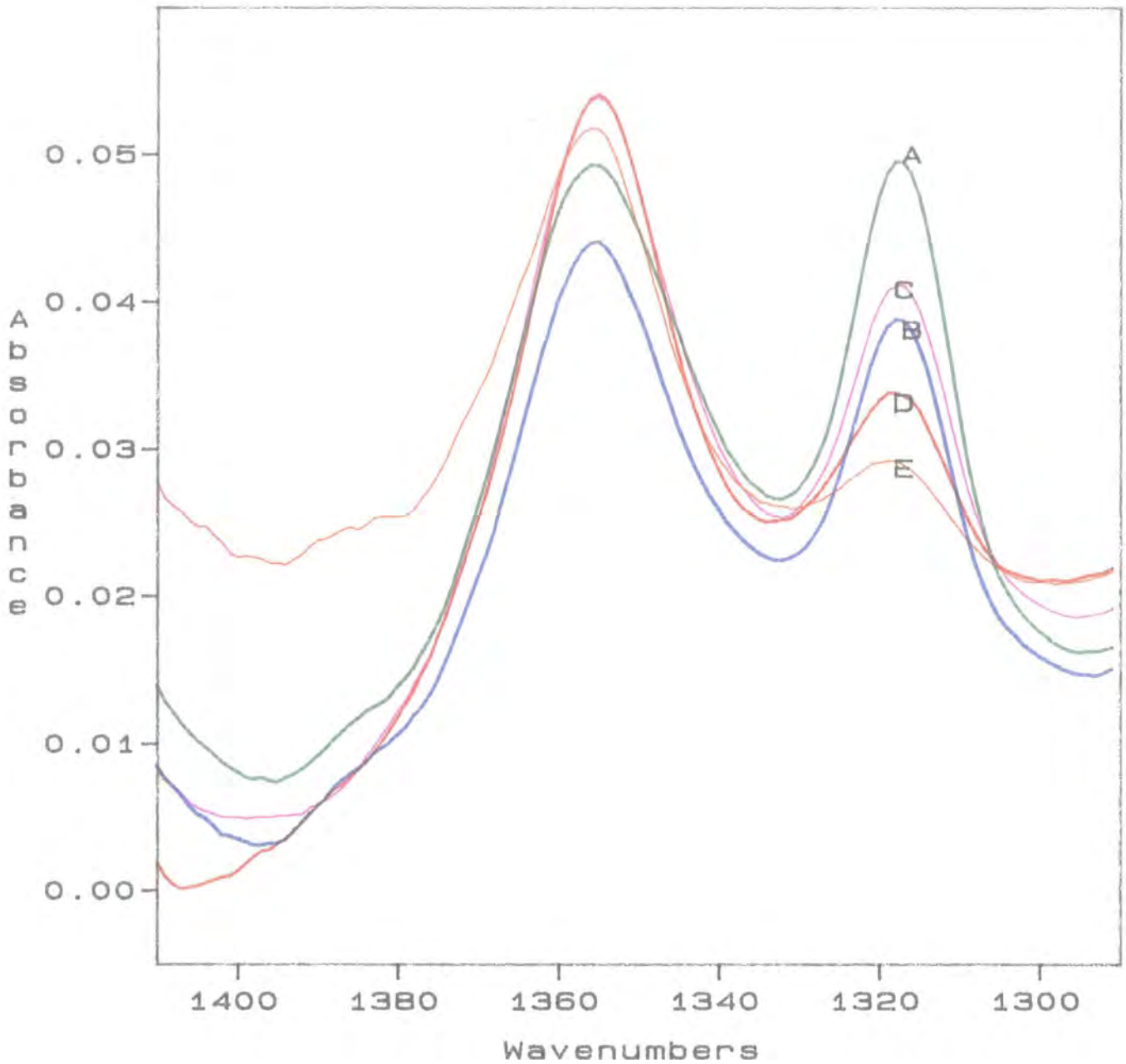

Figure 5–15 $\nu_s(NO_2)$ bands of 4–CN–2,6–dinitroanisole in solvent mixtures methanol / benzene, with varying methanol molar fraction, f(MeOH):

$\bar{\nu}_1(NO_2)$=1355 cm^{-1} $\bar{\nu}_2(NO_2)$=1316 cm^{-1}

Figure 5-16

4-CN-2,6-dinitrophenol in benzene/methanol mixtures.
Ratio of the $\nu_s(NO_2)$ band heights (R) vs
methanol molar fraction f_{MeOH} in benzene

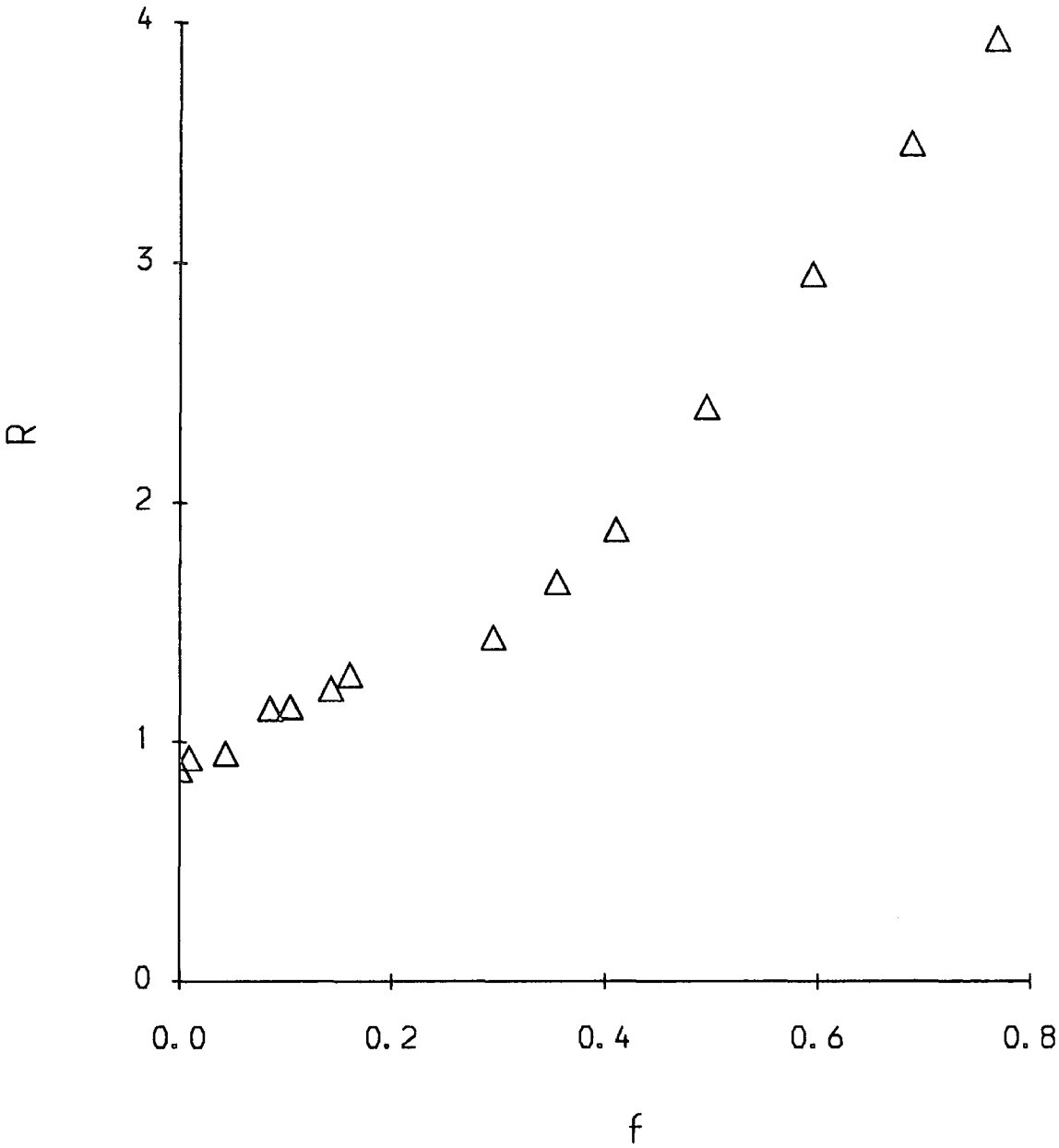

5.3 Effects of Dipolar Aprotic Solvents in Substituted Phenols

5.3.1 Infrared and ^{1}H NMR Data for the Interaction of Phenols with DMSO

It has been discussed in a previous chapter how the interaction of DMSO with substituted anisoles and phenetoles is strong enough to lead to the decomposition of the molecules, leading to the formation of phenoxides.

The results of the interaction of DMSO with phenols has been found to depend on the number and type of substituents in the aromatic ring since they determine the acidity of the phenol.

For mono– and disubstituted phenols, good correlation has been found[37] between pKa values, measured in water, and the ^{1}H NMR downfield shift of the hydroxyl proton in DMSO. In a solution with DMSO as a solvent, strong intermolecular hydrogen–bonds are formed between the compound and solvent. The hydroxyl proton is held in a relatively fixed position. In *ortho*–nitrophenol the chemical shift in DMSO and CCl_4 are very similar, suggesting that the electronic deshielding of the hydroxyl proton results in this case mainly from the strong intramolecular hydrogen–bond.

Infrared and ^{1}H NMR data for the substituted phenols analysed in this work in DMSO solution show that their interaction with the solvent depends on the acidity of the phenol.

p–Cyanophenol, which has a pK of *ca.* 8.0[37] in water, has been found to dimerize in non-hydrogen-bonding solvents. In Figure 5–2 it was shown how the ν(OH) infrared band of "bonded" OH group varies with concentration and Figure 5–17 presents the ^{1}H NMR spectra of the same compound in deuterated chloroform at two different concentrations showing how the peak of the hydroxyl proton is shifted downfield with the increase of concentration.

For *p*-cyanophenol in DMSO, only one ν(OH) band was found in the infrared spectrum centred at *ca.* 3400cm^{-1} and the ν(CN) band is shifted to lower frequency as shown in Figure 5–6 and discussed in Section 5.1.2. In the ^{1}H NMR spectrum, the peak of the hydroxyl proton is found at δ10.68 which corresponds to a shift at 3.95 ppm relatively to the saturated solution in chloroform and the

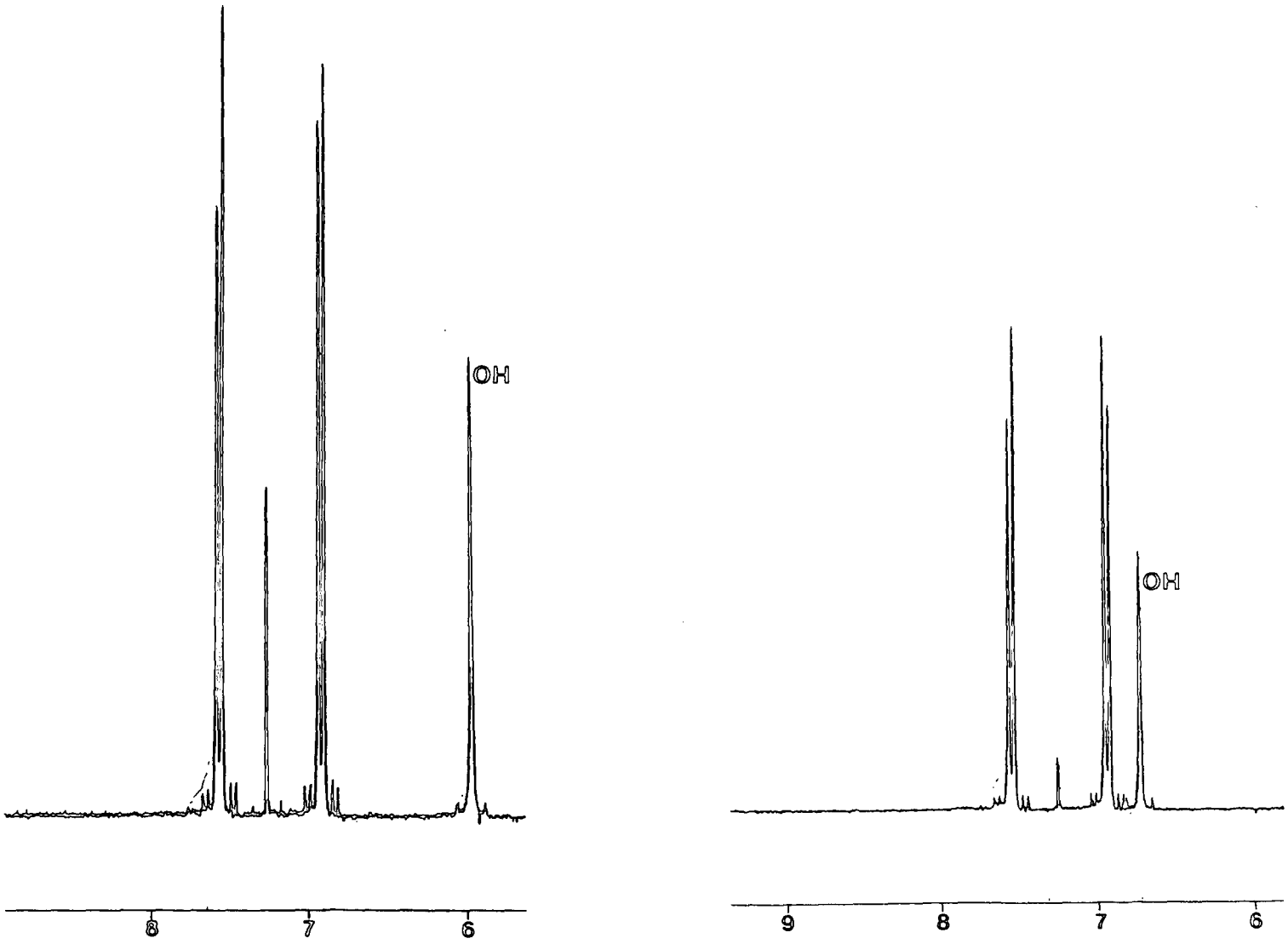

Figure 5–17 ^{1}H NMR spectra of *p*-cyanophenol in $CDCl_3$

a) Dilute solution. b) saturated solution.

doublet due to the ring protons *ortho*- to the CN group suffers a shift of 0.1 ppm in the same direction. This result suggests that the intermolecular hydrogen–bonds between two phenol molecules leading to the formation of the dimer is replaced in DMSO by a strong hydrogen-bond, phenol–DMSO. It is interesting to note that the infrared results do not indicate alterations in the electronic distribution in the ring but NMR shows that the ring protons suffer a small deshielding effect, possibly due to the direct dipolar interaction with the solvent of the vicinal CN group.

Data for 2–CN–4,6–dinitrophenol have some similarity with those found for *p*–cyanophenol in the sense that a new intermolecular hydrogen–bond is formed between the solute and the solvent as proved by the single ν(OH) band at 3360cm^{-1} shown in Figure 5–18 and confirmed by the ^{1}H NMR results in Figure 5–19. Here, the intramolecular hydrogen bond which exists in benzene and is shown by the broad peak at δ10.67 is broken to be replaced by the hydrogen–bond with the solvent resulting in the peak at δ11.88. The signals due to the ring protons can provide some interesting information. These protons are, of course, non–equivalent thus the presence of two doublets in the ^{1}H NMR spectrum.

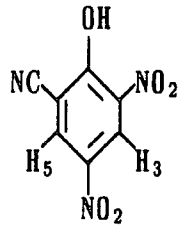

(22)

In benzene, the chemical shifts for these doublets are centred at δ8.06 for H_3 and at δ7.53 for H_5 with a separation of 0.53ppm, while in DMSO the shifts become H_3 δ8.65 and H_5 δ8.42 separated by only 0.23ppm. This indicates that the

deshielding effect of DMSO on H_5 is stronger than on H_3. The complexation of the CN group by DMSO may explain this effect, as it causes a drastic change in the magnetic environment of H_5 by putting an Sx group in its vicinity instead of a nitrile group.

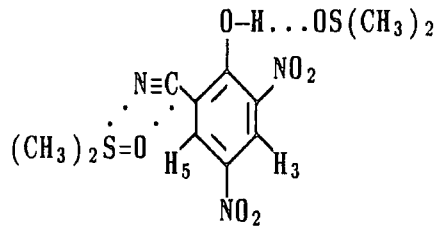

(23)

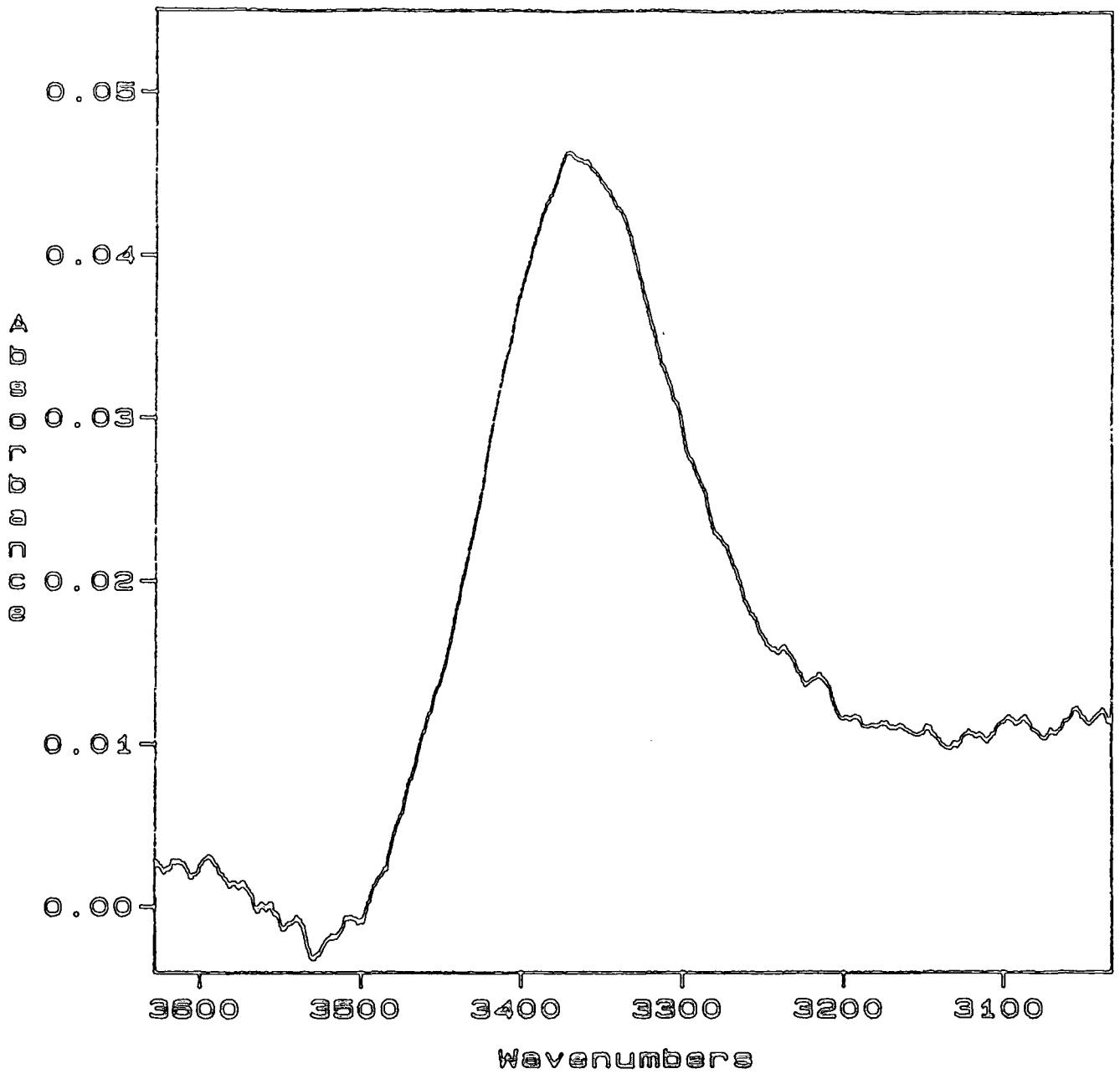

Figure 5–18 ν(OH) stretching vibration of 2–CN–4,6–dinitrophenol in DMSO

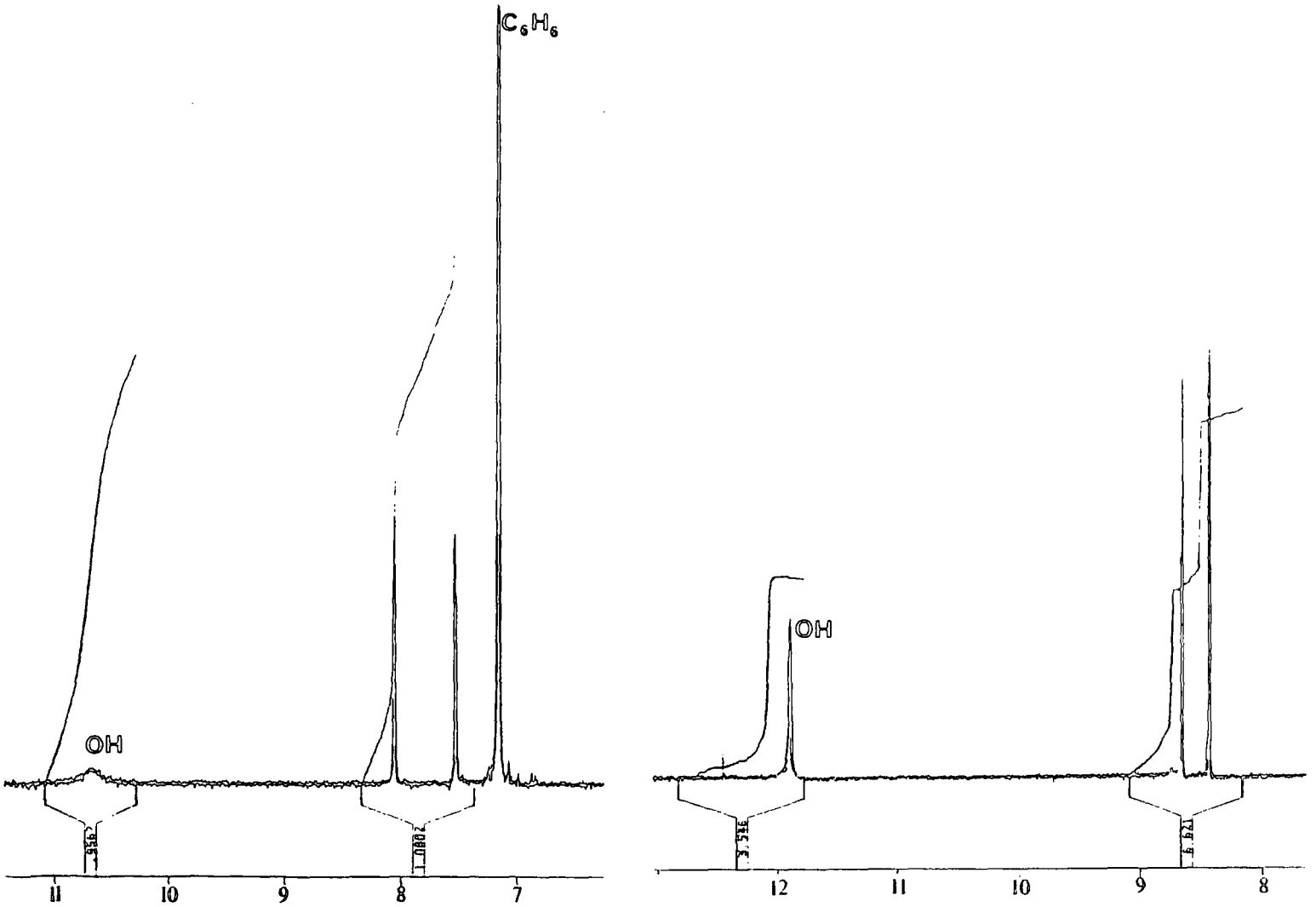

Figure 5–19 ^{1}H NMR spectra of 2–CN–4,6–dinitrophenol

a) in C_6D_6 b)in DMSO.d_6

With 4–CN–2,6–dinitrophenol, interaction with DMSO leads to quite different results. The inspection of the ν(OH) region in the infrared spectrum of this compound in DMSO does not give any useful information since the results are not reproducible. The shape and intensity of the broad band sometimes recorded at *ca.* 3550cm^{-1} varies at random with concentration and the band is sometimes absent which suggests that there is an OH group in the molecule, *i.e.* ionisation occurs in DMSO. The band may be due to contamination by atmospheric water adsorbed by DMSO while the solution was being prepared, as its frequency is too high to consider the possibility of intermolecular hydrogen-bond OH-DMSO.

The ^{1}H NMR spectroscopic study gives more positive information. In deuterated benzene, the hydroxyl proton is shown as a broad band at δ10.79 and the two ring protons as a singlet at δ7.01. In DMSO.d_6 the spectrum consists of one singlet at δ8.26 with a broad band, whose shape changes with concentration, at *ca.* δ7.00 (Figure 5–20). These results indicate that the molecule is ionised in DMSO since it is not possible to find any peak in the region δ10–15. Also, it is known[38] that protonated DMSO gives a singlet at δ6.83 and that multiple association like (24) is possible.

$$[Me_2SO...H...OSMe_2]^+ \qquad (24)$$

The formation of these species may account for the band at *ca.* δ7.00.

This hypothesis of ionisation is indeed in good agreement with the infrared data as the spectra obtained for 4–CN–2,6–dinitrophenol in DMSO and for 4–CN–2,6–dinitro-sodium phenoxide in DMSO which are essentially identical.

5.3.2 4–CN–2,6–dinitrophenol in Benzene/DMSO Mixtures

Infrared spectra were recorded on solutions of 4CNDNPH in five mixtures of Benzene/DMSO with different DMSO composition. The ν(CN) region and the NO_2 groups stretching vibrational bands were analysed and the results are shown

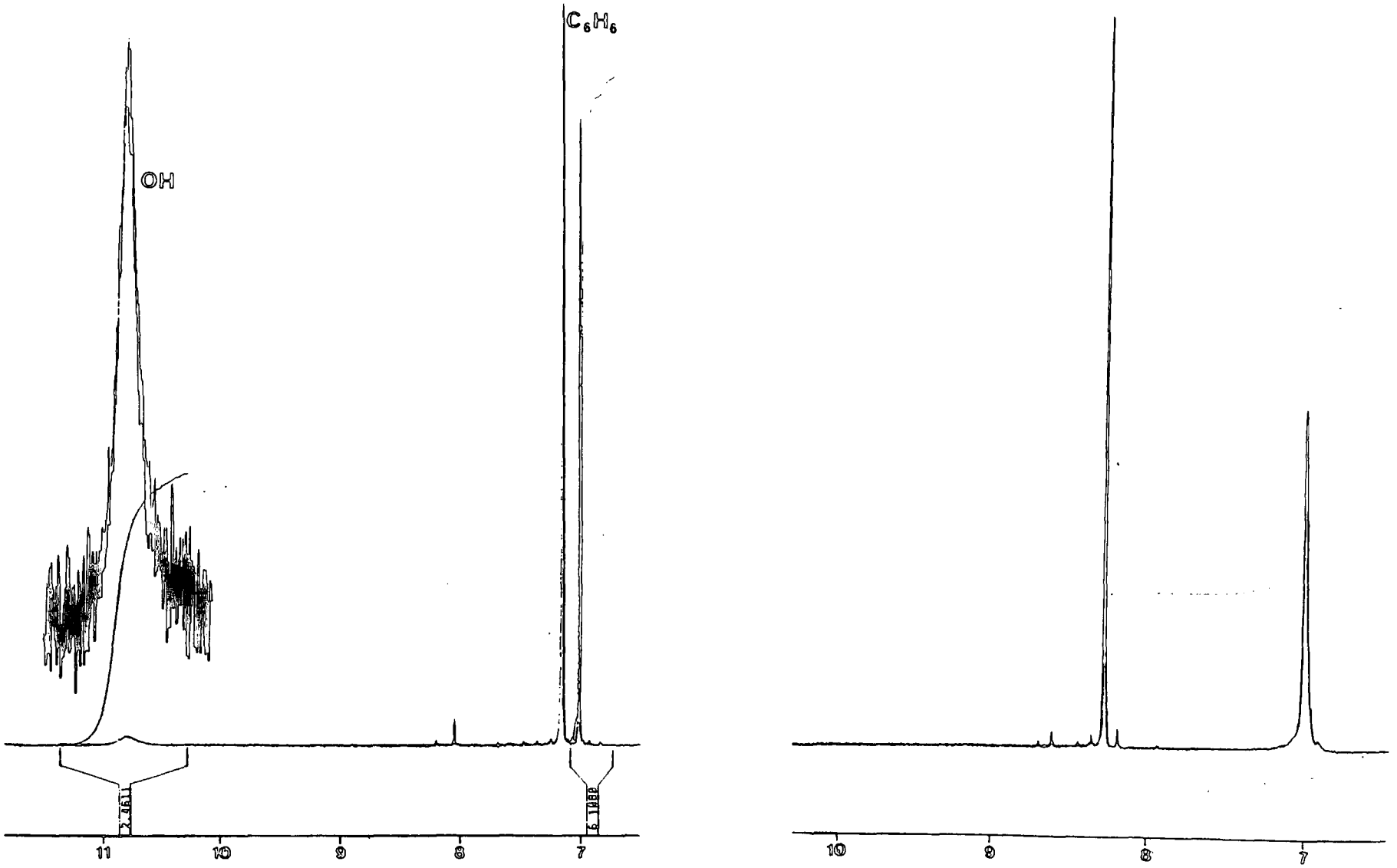

Figure 5–20 ^{1}H NMR spectra of 4–CN–2,6–dinitrophenol

a) in C_6D_6 b)in DMSO.d_6

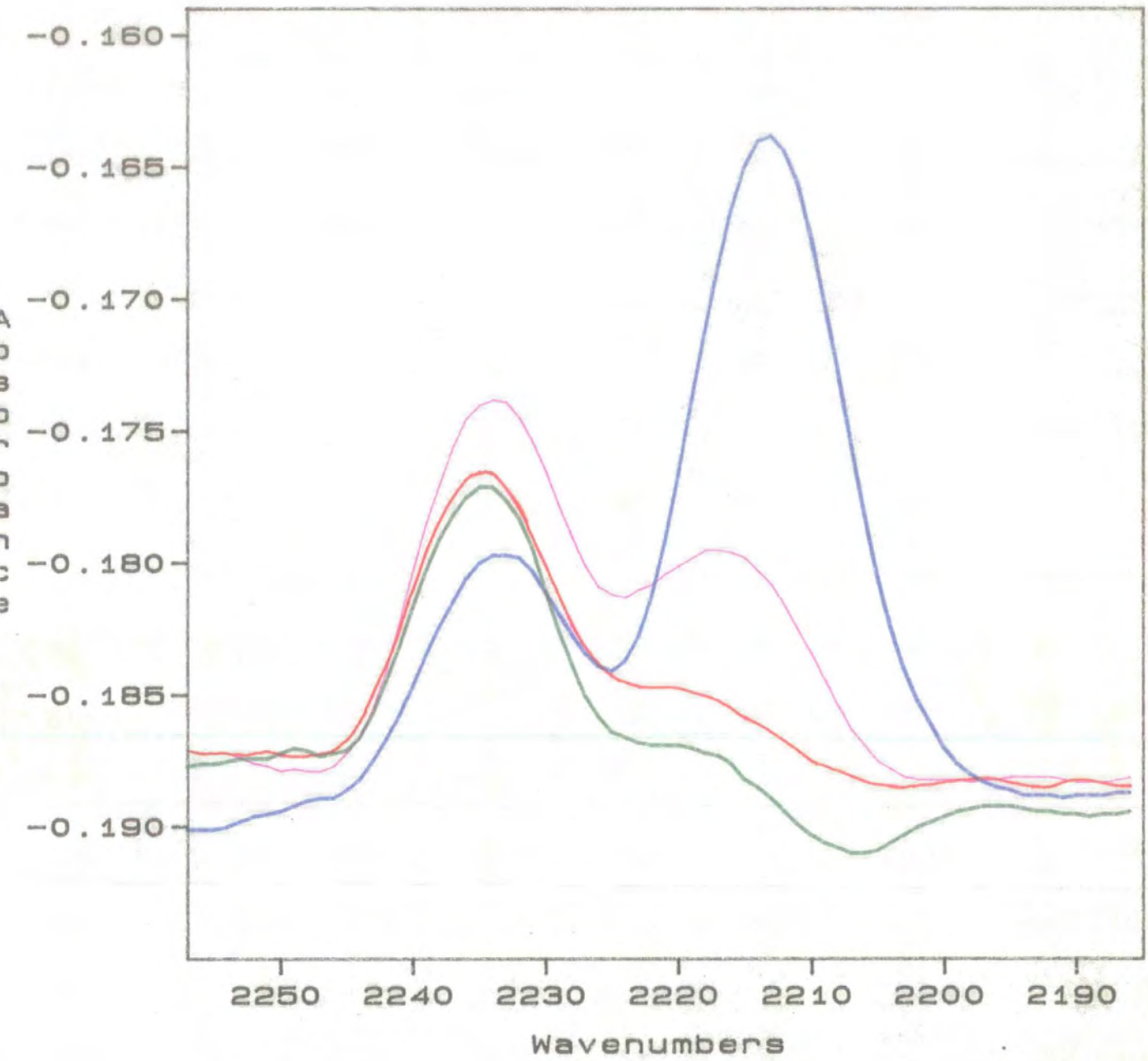

Figure 5–21 The infrared ν(CN) bands of 4–CN–2,6–dinitrophenol in solvent mixtures benzene / DMSO of different composition.

in Figure 5–21 and listed in Table 5–7 where MO represents the solution of 4CNDNPH in pure benzene and M6 the solution in pure DMSO. The composition of the mixtures is on Table 5–6, where x_A indicates the molar fraction of the component A.

Table 5–6 Composition of mixtures 4CNDNPH/DMSO/Benzene

Designation of Mixture	x_{DMSO}	$x_{4CNDNPH}$
M1	0.011	0.0034
M2	0.057	0.0043
M3	0.108	0.0063
M4	0.221	0.0058
M5	0.431	0.0065

The absorption spectra shown in Figure 5–21 were obtained by subtracting the spectrum of the mixture of solvents benzene / DMSO from that of the corresponding solution.

In Table 5–7 and in Figure 5–21 it is observed that in these mixtures of solvents there are two bands in the ν(CN) region even at very low DMSO molar fraction: band A shifting from 2239cm^{-1} in pure benzene to 2232cm^{-1} in mixture M5, its intensity decreasing with increasing amounts of DMSO, and band B which has its maximum at 2219cm^{-1} in solution M1 where the DMSO concentration is very small and shifts gradually to reach 2213cm^{-1} in pure DMSO, with increasing intensity.

It has been seen (Table 5–1) that in different solvents band A always appears at the same frequency of 2239±2cm^{-1}, independently of the polarity of the solvent and it has been discussed (Sections 5.1.2 and 5.2) that its sensitivity to hydrogen–bonding is low.

Table 5–7 Infrared bands of 4–CNDNPH in solvent mixtures Benzene/DMSO

Mixture	ν(CN) A	a B	ν(ring)	$\nu_{as}(NO_2)$	b $\nu_{s1}(NO_2)$	c $\nu_{s2}(NO_2)$	ν(CO)
M0	2239	–	1637	1547.0	1354.5	1316.0	1267.1
M1	2234.3	2219.0	1630	1547.3	1354.7	1306.8[1]	1268.7
M2	2234.3	2219.0	1630	1547.3	1354.7	1315.2	1267.0
M3	2233.4	2216.8	1631	1547.0	1354.7	1311.8	1262.9
M4	2233.4	2214.0	1633	1547.0	1354.7	1313.2	1258.7
M5	2232.8	2212.8	1636/1618	1547.5	1354.4[2]		1256.7
M6	2233.0	2213.0	1635/1615		1340		1257.0

a spectra shown in Figure 5–21

b $\nu_{s1}(NO_2)$: symmetric stretching vibration of the "free" O–NO_2 group

c $\nu_{s2}(NO_2)$: symmetric stretching of the hydrogen–bonded O–NO_2 group

[1] with a shoulder at higher frequency

[2] with a shoulder at lower frequency

In the presence of DMSO, the two bands A and B certainly correspond to two different species and the increase on DMSO concentration causes the shift of both bands to lower frequency, separating them, since B shifts faster than A. This shift to lower frequency may correspond to two processes occurring simultaneously. DMSO can interact with the CN group of the neutral molecule (Band A) as shown in (19), lowering slightly its frequency. At the same time DMSO is able to deprotonate the phenol, forming the corresponding phenoxide and giving rise to band B which frequency is again decreased by complexation of the CN group by DMSO.

Conclusions

The changes observed in the various regions of the infrared spectra of the two trisubstituted phenols are consistent with the hypothesis that, in protic solvents, the intramolecular hydrogen bond between the hydroxyl group and one *ortho* nitro group is broken and there is formation of a new, intermolecular, hydrogen bond to the solvent.

In the ν(OH) region, shown in Figure 5–12 for 4–CN–2,6–dinitrophenol, it is possible to observe the band due to the intramolecularly hydrogen bonded OH group in benzene, centred at *ca* 3150cm^{-1} being shifted to a much higher frequency in methanol where the band is centred at *ca.* 3450cm^{-1}.† However, some residual absorbance in the range 3250–3050cm^{-1} may be an indication that although the

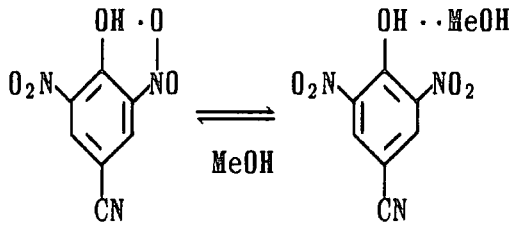

equilibrium is driven to the right, some molecules remain intramolecularly hydrogen bonded.

Comparing the nitro group vibrations of the substituted phenols with the corresponding anisoles in benzene, it was seen that the $\nu_{as}(NO_2)$ band is shifted to higher frequency by hydrogen–bonding. This shift, though smaller, is still present in methanol. If the extent of the shift reflects the strength of the H–bond then the intermolecular bond NO_2...solvent is less strong than the internal OH...O_2N bond. There is no contradiction between this difference in strength and the fact that the solvent actually breaks the stronger intramolecular bond because, by doing so, it allows for the formation of more than one type of solvent–solute hydrogen bond, *i.e.* OH···solvent as well as NO_2···solvent.

---

†Deuterated methanol was used to study this region of the spectrum.

The $\nu_s(NO_2)$ band of the *para*–NO_2 group of the 2–CN isomer is shifted to higher frequency in methanol (Figure 5–11a) as the intramolecular hydrogen bond, which promotes π–donation by the OH group into the ring/substituents π–system, is eliminated. The breaking of this bond not only removes this extra π–donation effect but, allowing the formation of new solvent–OH hydrogen–bonds involving the lone pair of the oxygen atom, it actually decreases the electron releasing power of OH towards the ring. The *para*–NO_2 group resonance with the ring is, therefore, reduced in methanol. The solvation of this substituent by methanol, N–O...$HOCH_3$, causes an increase of electron density at the oxygen atom and shifts the $\nu_s(NO_2)$ band in opposite direction, thus the overall effect resulting in a small ($5cm^{-1}$) shift to higher frequency.

The $\nu_{as}(NO_2)$ band of the 4–CN isomer appears at the same frequency as in the 2–CN–4,6–dinitrophenol (Figure 5–10), which is consistent with the formation of hydrogen bonds to the solvent. The variation of the $\nu_s(NO_2)$, which consists of growing in intensity of the high frequency band at the expense of that at lower frequency, again indicates breaking of the intramolecular H–bond (Figure 5–11b). The band for the non–bonded NO_2 group appears at the same frequency in both methanol and benzene is maybe due to cancellation of the two opposite effects, decrease of conjugation and solvation of the nitro group.

The difference in ^1H NMR chemical shift for the hydroxyl proton between the two cyanodinitrophenols examined in benzene is in a very good agreement with the results obtained from the ν(OH) region of the infrared spectrum in dichloro–methane and with the measured pKa values, indicating a stronger intramolecular hydrogen-bond in the isomer 4-CN-2,6-dinitrophenol.

Although the differences may seem small, they are significant enough to allow for the 4–CN–2,6–dinitrophenol to be ionised by DMSO while the isomer 2–CN–4,6–dinitrophenol remains essentially in the neutral form in that solvent.

References

1 Schreiber, V.M., *J. Mol. Struct.* (1989), 197, 73

2 Brown, D.; Clifford, D..R.; Watkins, D.A.M., *Pestic. Sci.* (1972), 3, 551

3 Fukushige, T; Aihara, A., *Denki Tsushin Daigaku Gakuho* (1984),35(1), 53

4 Seguin, J.P.; Guilhaume, F.; Uzan, R.; Doucet, J.P., *J. Chem. Soc. Perkin Trans. II* (1986), 773

5 Lutskii, A.E.; Korunova, A. F.; Dollzhenko, Yu. I., *Zh. Obshchei. Khim.* (1980) 50(10), 2339

6 Pross, A.; Radom, L., *Prog. Phys. Org. Chem.* (1981), 13, 1

7 Radom, L.; Hehre, W.J.; Pople J.A.; Carlson, G.L.; Fateley, W.G., *Chem. Commun.* (1972), 308

8 Topsom, R.D., *Prog. Phys. Org. Chem.* (1987), 16, 85

9 Shevchenko, L.L.; Pilipenko, A.T.; Dubina, L.F., *Ukr. Khim. Zh.* (1973), 39(a), 930

10 Shigorin, D.N.; Dokunikhin, N.S., *Zh. Fiz.* (1955), 29, 1958

11 Granzhan, V.A.; Semenenko, S.V.; Zaitsev, P.M., *Zh. Prikl. Spektr.* (1970), 12(5), 922

12 Granzhan, V.A.; Semenenko, S.V.; Zaitsev, P.M., *Zh. Prikl. Spektr.* (1968), 9(3), 407

13 Bureiko, S.O.; Golubev, N.S.; Mattinen, J.; Pihlaja, K., *J. Mol. Liq.* (1990), 45, 139

14 Lipkowitz, L.B., *J. Am. Chem. Soc.* (1982), 104, 2647

15 Vorpagel, E.R.; Streitwieser, A.; Alexandratos, S.D., *J. Am. Chem. Soc.* (1981), 103, 3777

16 Hiberty, P.C.; Ohasessian, G., *J. Am. Chem. Soc.* (1984), 106, 6963

17 Krygowski, T.M.; Anvlewicz, R., *J. Acta. Cryst.* (1983), B39, 732

18 Krygowski, T.M., *Prog. Phys. Org. Chem.* (1990), 17, 239

19 Exner, O.; Folli, V.; Marcaccioli, S.; Vivarelli, P., *J. Chem. Soc. Perkins Trans 2* (1983), 757

20 Grundnes, J.; Klaboe, P., "*Basicity, Hydrogen-bonding and Complex Formation*" in: The Chemistry of the Cyano Group, Ed. Z. Rappoport, Wiley, N.Y., 1970

21 Yarwood, J., "*Spectroscopy and Structure of Molecular Complexes*", Plenum Press, London, N.Y., 1973

22 Strehle, F.; Besnard, M.; Yarwood, J., unpublished results

23 Bayliss, N.S.; Cole, A.R.H.; Little, L.H., *Spectrochim. Acta.* (1959), 15, 12

24 Ritchie, C.D.; Bierl, B.A.; Honour, R.J., *J. Am. Chem. Soc.* (1962), 84, 4687

25 Ritchie, C.D.; Bierl, B.A.; Honour, R.J., *J. Am. Chem. Soc.* (1962), 84, 1571

26 Yuchnovski, I.N.; Binev, I.G., "*Infrared Spectra of Cyano and Isocyano Groups*" in : The Chemistry of Functional Groups, Suppl. C., Ed. S. Patai and Z. Rappoport, Wiley, N.Y., 1982

27 Binev, I.G.; Kuzmanova, R.; Kaneti, Kh.; Yukhnovsky, I.N., *Izv. Khim.* (1981) 14(4), 470

28 Bellamy, L.J., "*The Infrared Spectra of Complex Molecules*", vol. 1 and 2, 2nd Ed., Chapman and Hall, London, N.Y., 1980

29 Kross, R.D.; Fassel, V.A.; Ritchie, C.D.; Bierl, B.A.; Honour, R.J., *J. Am. Chem. Soc.* (1956), 78, 4225

30 Cody, V.; Hazel, J.; Lehmann, P.A., *Acta. Cryst.* (1978), B34, 3449

31 Grimaccioli, C.M.; Destro, R.; Simonetta, M., a) *Chem. Commun.* (1967), 331; b) *Acta. Cryst.* (1968), B24, 1369

32 Borek, , *Naturweiss* (1963), 50, 471

33 Popov , *Optics and Spectroscopy* (1963), 15, 174

34 Katritzky, A.R.; Simmons, P., *Rec. Trav. Chim. Pays Bas* (1960), 79, 361

35 Kaminskaya, E.G.; Gitis, S.S.; Kaminskii, A. Ya., *Doklady Akad. Nauk. SSSR* (1975), 221(3), 617

36 Iogansen, A.V.; Litovchenko, G.D., *Zh. Prikl.* (1965), 2(3), 243; *ibid*, 3(6), 38

37 Socrates, G., *Trans. Faraday Soc.* (1970), 66, 1052

38 Olah, G.A.; Ku, A.T.; Olah, J.A., *J. Org. Chem.* (1970), 35, 3904

39 Detoni, S.; Hadzi, D,; Smerkolj, R,; Hawranek, J.; Sobczyk, L., *J. Chem. Soc.* (1970), 2851

Chapter 6
Infrared Studies on Anionic Derivatives of Alkyl Aryl Ethers

6.1 Introduction

In previous chapters, the way in which alkyl aryl ethers with electron-withdrawing substituents react with nucleophiles by either aromatic or aliphatic substitutions has been discussed. The former process leads to the formation of intermediates of Meisenheimer-complex type; the latter results in dealkylation of the ether and formation of the corresponding phenoxide. The present chapter will deal with the infrared study of the products of these reactions.

The formation of phenoxides from alkyl aryl ethers was first achieved, in the present work, by attack of metal halides in DMSO (Chapter 2). Not only this is a very slow process but DMSO is also the best solvent for the phenoxides rendering the isolation of the final product quite difficult. Thus the substituted phenoxides studied here were obtained by ionization of the respective phenols, the procedure being described in Chapter 7. The materials obtained this way were sodium-*p*-cyanophenoxide, sodium 4-CN-2,6-dinitrophenoxide and lithium, sodium and potassium 2-CN-4,6-dinitrophenoxide.The Meisenheimer adducts studied were the sodium and potassium 1,1-dimethoxy adducts of 2,4,6-trinitroanisole, 2-CN-4,6-dinitroanisole and 4-CN-2,6-dinitroanisole. Their preparation is also described in Chapter 7.

For both types of reaction, the products are anionic species for which some degree of association with alkali metal cations is expected. This interaction has already been discussed in Chapters 3 and 4 which deal with the kinetic and equilibrium studies using U.V./Visible techniques. The aim of this infrared study is to relate the variations in spectral characteristics (between the parent compounds and the products of reaction), to changes on charge distribution and extent of delocalisation effects. An attempt was also made to analyse the effect of ion association on the spectral properties of some vibrational bands but results were poor and often inconsistent.

6.2 The Infrared Spectra of some Substituted Phenoxides

In the nitro substituted neutral compounds analysed in Chapter 5, the band due to the (C-O) stretching vibration, which appears around 1270cm^{-1} for both phenols and corresponding anisoles is quite a strong band in benzene (for example, A=1.3x10^{4}dm^{3}mol^{-1}cm^{-2} for 2-CN-4,6-dinitrophenol and 1.5x10^{4}dm^{3}mol^{-1}cm^{-2} 4-CN-2,6-dinitrophenol), but sometimes shows a sharp decrease in intensity when the solvent is methanol although the frequency shift to higher values is rather small. This was presented in Figure 5-11a. It seems the polarity of the bond is much reduced when the OH group is hydrogen-bonded to the solvent compared to when it is internally hydrogen-bonded to a nitro group. This is not an unexpected observation since, in the intramolecular hydrogen-bonding situation, the oxygen atom of the hydroxyl group has two unshared, occupied orbitals while in methanol at least one hydrogen-bond is formed to the hydroxyl group of the solvent molecule in a closed cycle involving those occupied orbitals. This can be roughly represented by (1) and (2).

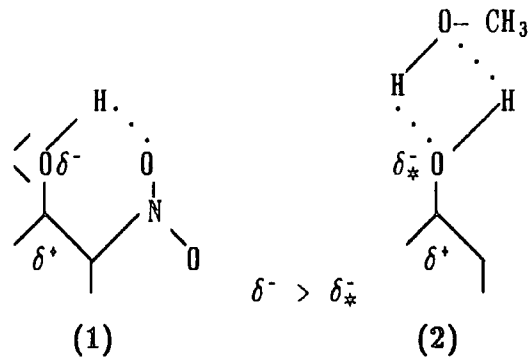

(1) (2)

The corresponding trisubstituted phenoxides in methanol show an intense band in the same region of the infrared spectrum (1270-1280cm^{-1}). If this band is assigned to the (C-O) stretching vibration, and actually there is no obvious alternative, then it seems that the polarity of the bond is restored, and indeed increased. However, the bond order is essentially the same as in the respective phenol, i.e., it can be represented by (3) with negative charge formally in the oxygen atom.

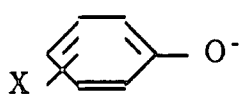

(3)

Theoretical calculations[1] for *p*–nitrophenoxide predict a change in the π–character of the C–O bond from 0.05e to 0.24e on ionization. In *p*–cyanophenol the predicted change is from 0.044e to 0.233e.

The present infrared results for *p*–cyanophenol are in good agreement with these calculations. Figure 6–1 shows the region of the infrared spectrum where the ν(CO) bands for *p*–cyanophenol and *p*–cyanophenoxide are observed in methanol. The shift to higher frequency of the ν(CO) band ($\Delta\bar{\nu} = 18cm^{-1}$) supports the predicted increase in the π–character of the (CO) bond and consequent increase of the bond order. The increase on bandwidth from $14cm^{-1}$ in the phenol to $31cm^{-1}$ in the phenoxide may be an indication of the difference in hydrogen–bonding to the solvent of the two species. While the hydrogen–bonding process between phenol and methanol can lead to rigid closed cycles involving both hydroxyl groups as in (2), it will be more disordered in the phenoxide. The degree of double–bond character of the (C–O) bond, responsible for the frequency shift, may be expected to be quite sensitive to changes on environment at the negatively charged oxygen atom which has three lone pairs of electrons available for hydrogen–bonding and is therefore capable of a variety of hydrogen–bonds to the solvent with different strengths.

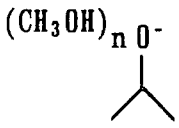

For the pair of isomers of cyanodinitrophenoxide under study, there are three electron-withdrawing substituents in the ring so a greater π-donation from O^- and consequently greater double-bond character of (C-O) is expected. However, it seems that the frequency of this vibration does not change much from substituted phenol in benzene or methanol to substitute phenoxide in methanol. In 4-CN-2,6-dinitrophenoxide this ν(CO) band is well isolated while in the corresponding phenol it is part of a pair of bands (Figure 6–2). For the 2-CN-4,6-dinitrophenol

the band is very weak and in the corresponding phenoxide it is overlapped with other bands making a clear identification, and thus discussion of spectral feature variations (Figure 6-3), quite difficult.

Ionization causes modifications in other regions of the infrared spectrum which are compatible with a certain degree of delocalisation of negative charge throughout the ring and electron-attracting substituents (Figures 6-1 to 6-9) so the first interpretations from the ν(CO) region must be regarded with caution.

p-Cyanophenoxide has its ν(CN) bond shifted to lower frequency relatively to *p*-cyanophenol with greatly increased bandwidth as shown in Table 6-2 and in Figure 6-4. As previously discussed (see Chapter 5) this shift may be related to a greater degree of resonance of the CN group with the ring. Figure 6-7 shows that there is a marked alteration of the relative intensity of the pair of bands near 1600cm^{-1} and a shift to lower frequency, accompanied by intensity and bandwidth increase of the ring mode band at *ca.* 1500cm^{-1}. This is the mode associated with the (C-C) stretching vibration parallel to the axis of the molecule that contains the two substituents.[2]

The 4-CN-2,6-dinitrophenol shows two bands in the ν(CN) region in methanol, as already discussed and again shown in Figure 6-5. The corresponding phenoxide has only one band at the lower frequency with a much greater intensity. The opposite happens for the ring breathing modes at *ca.* 1600cm^{-1} and the $\nu_{as}(NO_2)$ bands. The phenol shows only one band but there are two in the spectrum of the corresponding phenoxide. The second appears at a lower frequency for both cases (Figure 6-8). There is also a small shift of $\nu_s(NO_2)$ to lower wavenumbers (Figure 6-2) in the 4-CN-2,6-dinitrophenoxide. These are the sort of band shifts expected for an increase of delocalisation of charge through the ring and electron-withdrawing substituents, generally observed in aromatic anions. The lowering of frequency of both the symmetric and antisymmetric bands of nitro groups is usually associated with increase of conjugation. However, for both substituted phenol and phenoxide in methanol, resonance of the nitro groups with the ring is expected to have a minor contribution since the coplanarity, essential for

conjugation, is unlikely due to the steric effect of the hydrogen bonded O^- group (or OH), situated between the two nitro substituents. Nevertheless, even when out of the ring plane the nitro group is able to withdraw charge by inductive effect,[1] leading to identical results, as previously discussed (Chapter 1).

Table 6-1 shows the spectral characteristics for both 4-CN-2,6-dinitrophenol and phenoxide in methanol and DMSO.

Table 6-1

Frequencies and intensities of the main bands of 4-CN-2,6-dinitrophenol and corresponding sodium phenoxide in methanol and DMSO

	4CNDNPh			4CNDNPh$^-$Na$^+$		
	$\bar{\nu}$(c□$^{-1}$)	$\bar{\nu}_{\frac{1}{2}}$(c□$^{-1}$)	A§	$\bar{\nu}$(c□$^{-1}$)	$\bar{\nu}_{\frac{1}{2}}$(c□$^{-1}$)	A
ν(CN)						
CH_3OH	2238 (2224) sh	24	250	2224	14	600
DMSO	2213	12	550	2213	12	600
ν(Ring)						
CH_3OH	1635	27	7900	(1637) 1619	33	9100
DMSO	1635 (1615) sh	33	17800	1634 (1613)	32	21000
$\nu_{as}(NO_2)$						
CH_3OH	1554	21	19200	1556 (1530)	28	9800
DMSO	(4 unresolved bands)			1567	22	5000
$\nu_s(NO_2)$						
CH_3OH	1354	24	8700	1346	31	10000
DMSO	1340	42	10300	1337	44	12000
ν(CO)						
CH_3OH	1278 / 1266	24	1500	1265	19	12000
DMSO	1257	23	22000	1256	24	20200

sh = shoulder

§ = $dm^3mol^{-1}cm^{-2}$

The results in Table 6-1 show the impossibility of obtaining a spectrum of the neutral substituted phenol in DMSO since this solvent causes the deprotonation of the compound. The different types of interaction with protic and aprotic solvent are noticeable in some of the infrared bands of the phenoxide. The bands that usually shift to lower frequency with the increase of conjugation, such as ν(CN), $\nu_s(NO_2)$ and ν(CO) do appear at lower values in DMSO. The two $\nu_{as}(NO_2)$ bands in methanol, (resulting perhaps from differences in the twisting angle of the two solvated, hydrogen-bonded to methanol, nitro groups) become a single band at higher frequency ($\Delta\tilde{\nu} = 11cm^{-1}$) in DMSO where no hydrogen-bonding is possible.

The pair of bands associated with ring breathing modes appear at quite similar frequencies in the two solvents, although with very different intensities (higher in DMSO). The intensities of these particular bands have been found[4,5] to derive mainly from C-C stretching modes and to correlate well with the σ_R^0 value of the substituent. This parameter represents the disturbance of the π-electron system in a monosubstituted benzene along is axis and is variable with temperature and solvent. Indeed, differences in the solvent interaction at the π-donor (O^-) and π-acceptor (CN) groups in para-position are certainly responsible for the increased intensity of the ring-mode bands in DMSO. Contribution from DMSO interaction at the NO_2 groups to these ring-mode changes is likely to be small since the two nitro substituents are symmetrically placed relative to the axis containing the O^- and CN groups. The solvent effects may be interpreted as if the dipole moment of the molecule is decreased by hydrogen-bonding to the protic solvent at the more sensitive substituents since it can decrease the electron donor ability of the O^- and the electron-accepting power of the CN group, as discussed before.

The $10cm^{-1}$ shift to lower frequency of the ν(CN) band from methanol to DMSO may be simply the result of direct solvent interaction. While the CN group is involved in bonding in methanol, an effect that generally tends to raise the ν(CN) band, in DMSO there is an antiparallel dipole-dipole interaction involving the π-electron system of the triple bond, which lowers the frequency.[3]

The frequency shifts in *p*-cyanophenol/*p*-cyanophenoxide in the same solvents may be used for comparison and are shown in Table 6-2.

The effect of depronation upon the frequency of the ν(CN) band in methanol is reflected by the shift of $14cm^{-1}$ to lower values when the molecule contains two nitro groups (Table 6-1) and $15cm^{-1}$ in the absence of those nitro groups. It seems that solvation is important only at the donor group (O^-) and the CN groups and the shift $\Delta\bar{\nu}_1$ is governed by the extent of resonance between the ring and the CN group. This assumes that the amount of negative charge withdrawn by the twisted NO_2 groups is the same for both phenol and phenoxide.

The effect of different solvent interaction with the phenoxides results in ν(CN) frequency shifts, $\Delta\nu_2$, of $11cm^{-1}$ in the nitrosubstituted compounds and $22cm^{-1}$ in the absence of nitro groups.

Table 6-2
Frequency maxima and shifts (cm^{-1}) for the ν(CN) band of *p*-cyanophenol and *p*-cyanophenoxide

	DMSO	MeOH	$\Delta\nu_2$
p–cyanophenol	2217	2225	8
p–cyanophenoxide	2188[6]	2210	22
$\Delta\bar{\nu}_1$	29	15	

$$\Delta\bar{\nu}_2 = \bar{\nu}(CN)_{MeOH} - \bar{\nu}(CN)_{DMSO}$$

$$\Delta\bar{\nu}_1 = \bar{\nu}(CN)_{phenol} - \bar{\nu}(CN)_{phenoxide}$$

The origin of this difference in ν(CN) band position maybe connected with interaction of DMSO with the nitro substituents. Such dipolar coupling may result in increase of their electron withdrawing power, thus decreasing the amount of charge transfer to the CN group. This sort of interaction may also account for the frequency shifts found for the symmetric and antisymmetric bands of the NO_2 groups.

The effects of deprotonation on the ν(CN) and ring-mode bands of 2-CN-4,6-dinitrophenol (Table 6-3) are very similar to those in the 4-CN-2,6-dinitrophenol and are consistent with a large extent of delocalisation of the negative charge throughout the anionic species. The pair of bands related to the $\nu_{as}(NO_2)$ vibration (Figure 6-9) shows a small shift to high frequency and although the total intensity of the pair is approximately the same upon ionisation the relative heights of the two maxima are inverted.

The $\nu_s(NO_2)$ vibrational features of 2-CN-4,6-dinitrophenol do not differ substantially from those of the corresponding anisole apart from a shoulder near 1330cm^{-1} present in the phenol spectrum only (Figure 6-10). In benzene, a similar shoulder at a slightly lower frequency has been attributed to an intramolecular hydrogen-bonded NO_2 group (Chapter 5). In methanol, such assignment is questionable since the internal hydrogen-bond is expected to be broken by the protic solvent and the NO_2 group frequencies are known to be quite insensitive to intermolecular hydrogen-bonding.[2]

The band at 1349cm^{-1} for both phenol and anisole dominates the spectrum in this region. In the respective phenoxide the dominant band appears at 1320cm^{-1} and may therefore be assigned to the *para*-nitro group since the negative charge in the aromatic species is delocalised through the extended π-system composed by the ring and substituents with suitably oriented π-orbitals. The coplanar *p*-NO_2 group falls in this category. This "through conjugation" effect or internal charge transfer has been questioned in the case of nitrophenols but its importance is well recognised in the negatively charged compounds.[3] One of the bands at *ca.* 1350cm^{-1} may be attributed to the symmetric stretching vibration of the *ortho*-nitro group although the presence of several overlapped bands in the region makes the correct assignment difficult.

Table 6-3

Spectral Characteristics of the Main Bands of 2-CN-4,6-dinitrophenol and corresponding Sodium Phenoxide in methanol and DMSO

	2CNDNPH			2CNDNPH⁻Na⁺		
	$\bar{\nu}$(c□$^{-1}$)	$\Delta\bar{\nu}_{\frac{1}{2}}$(c□$^{-1}$)	A§	$\bar{\nu}$(c□$^{-1}$)	$\Delta\bar{\nu}_{\frac{1}{2}}$(c□$^{-1}$)	A§
ν(CN)						
MeOH	2241	13	220	2227	15	550
DMSO	2217	12	500	2214	13	1200
ν(Ring)						
MeOH	1616	27	7200	1608	25	7500
DMSO	1612	25	14500	1610	25	20000
$\nu_{as}(NO_2)$						
MeOH	1552/ 1537	27	5400	1563/ 1548	26	5300
DMSO	1546	15	7200	1560	23	5000
$\nu_{s}(NO_2)$						
MeOH	1348	15	16300	1358/sh 1347 1320	a	a
DMSO	1358	a	a	1359,1315	a	a
ν(CO)						
MeOH	1270	b	b	1280	a	a
DMSO	1273	a	a	1287	a	a

sh = shoulder

a = several unresolved bands in the region

b = very weak band

§ = $dm^3mol^{-1}cm^{-2}$

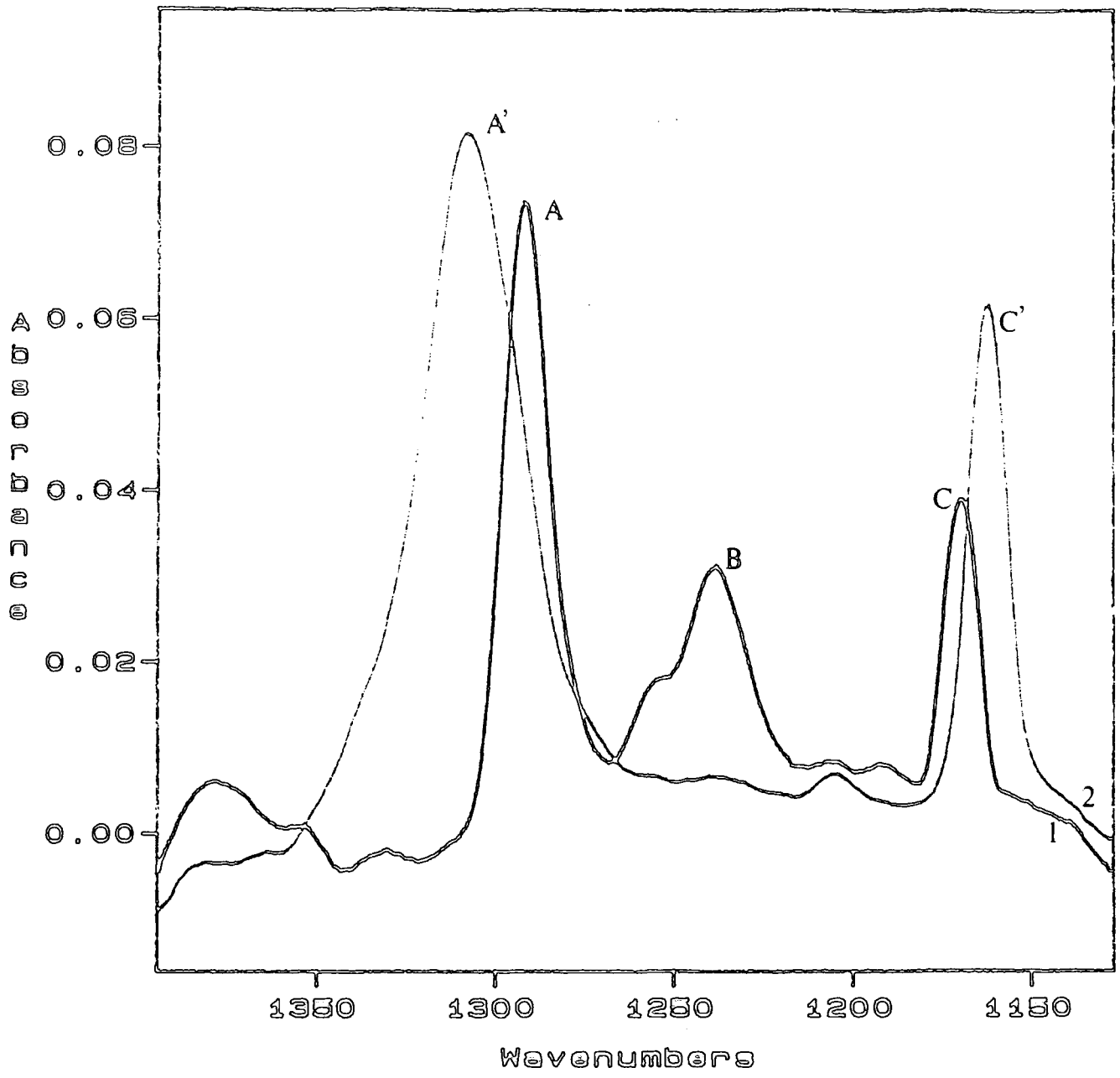

Figure 6–1 **Infrared bands of *p*–cyanophenol (1) and *p*-cyanophenoxide (2) in methanol.**

ν(CO)	A: 1292 cm^{-1}, A': 1308 cm^{-1}
δ(OH)[8]	B: 1238 cm^{-1}
δ(CH) in plane[8]	C: 1169 cm^{-1}, C': 1162 cm^{-1}

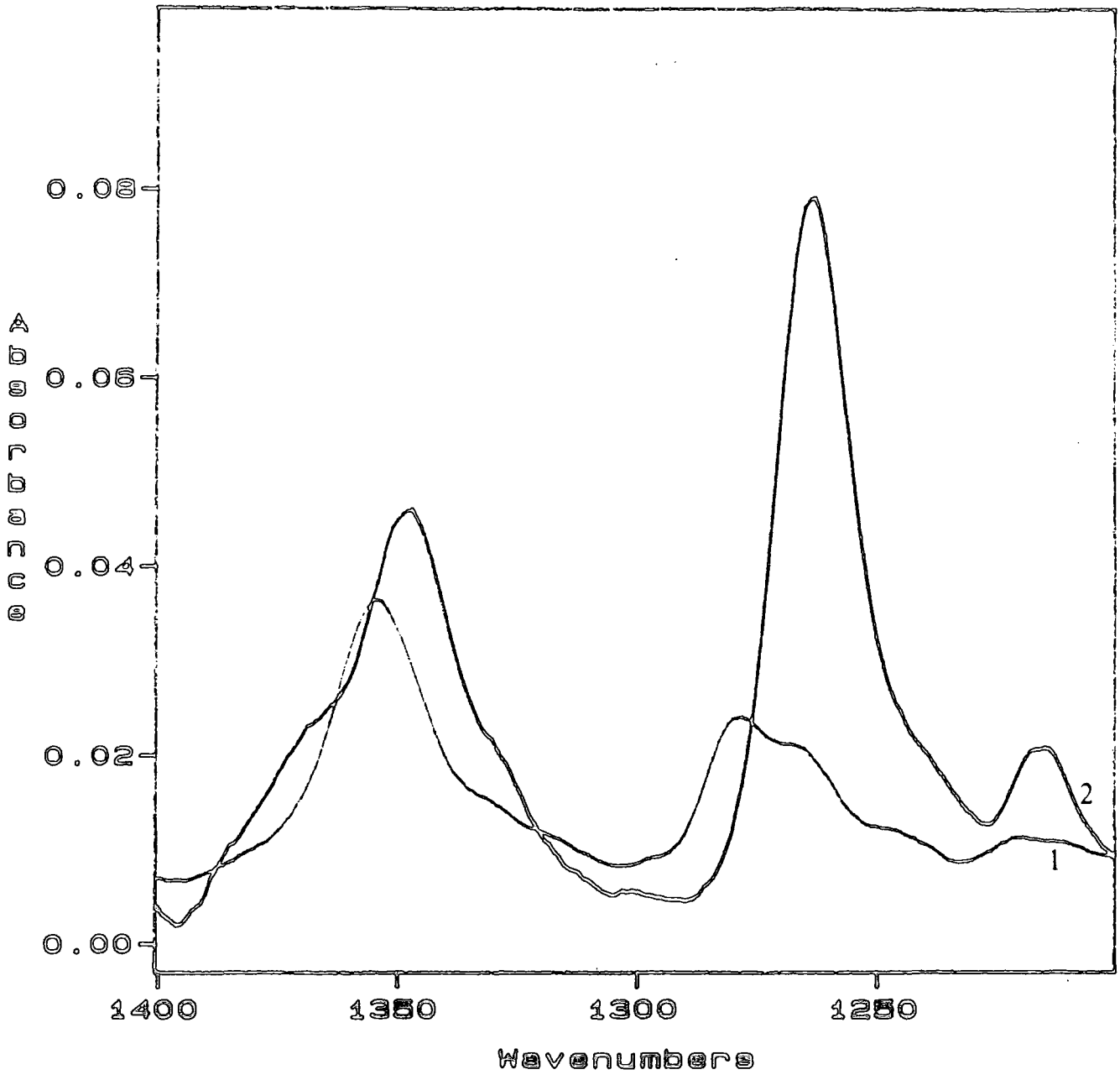

Figure 6–2 $\nu_s(NO_2)$ and $\nu(CO)$ bands of 4-CN-2,6-dinitrophenol (1) and 4-CN-2,6-dinitrophenoxide (2) in methanol.

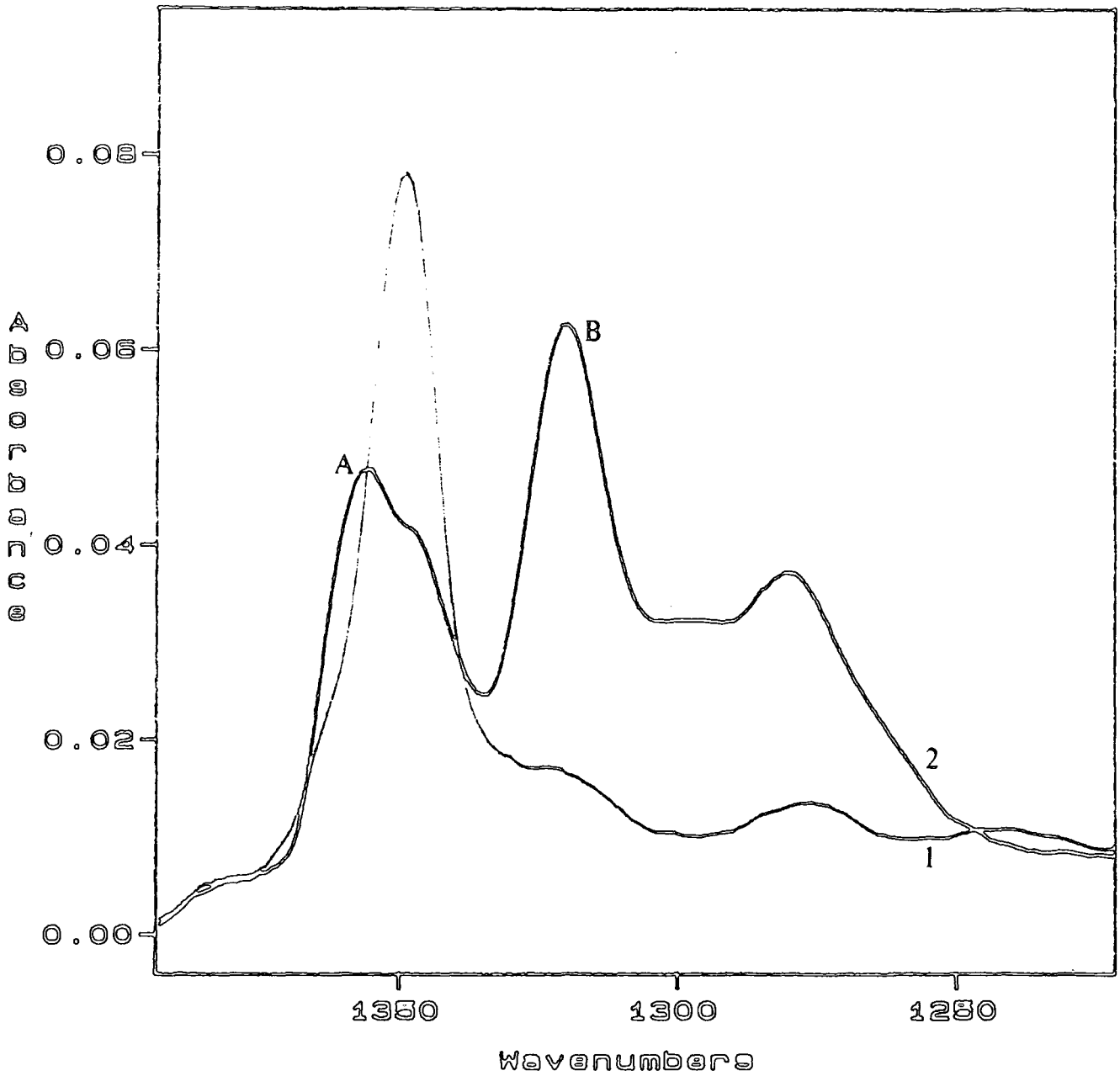

Figure 6–3 $\nu_s(NO_2)$ and $\nu(CO)$ bands of 2-CN-4,6-dinitrophenol (1) and 2-CN-4,6-dinitrophenoxide (2) in methanol.

A: $\nu_s(o\text{–}NO_2) = 1357\ cm^{-1}$
B: $\nu_s(p\text{–}NO_2) = 1320\ cm^{-1}$

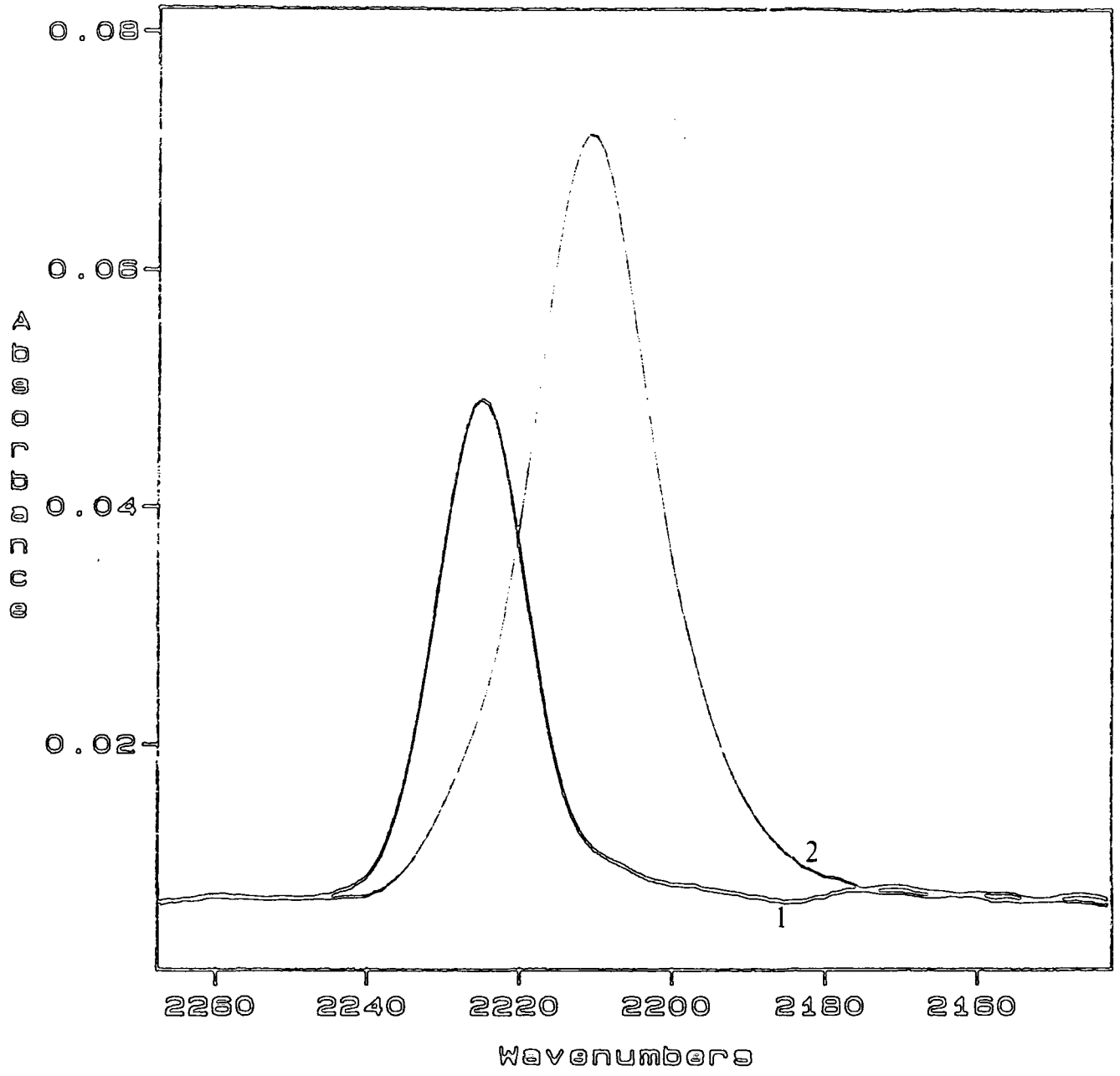

Figure 6–4 ν(CN) bands of *p*–cyanophenol (1) and *p*–cyanophenoxide (2) in methanol.

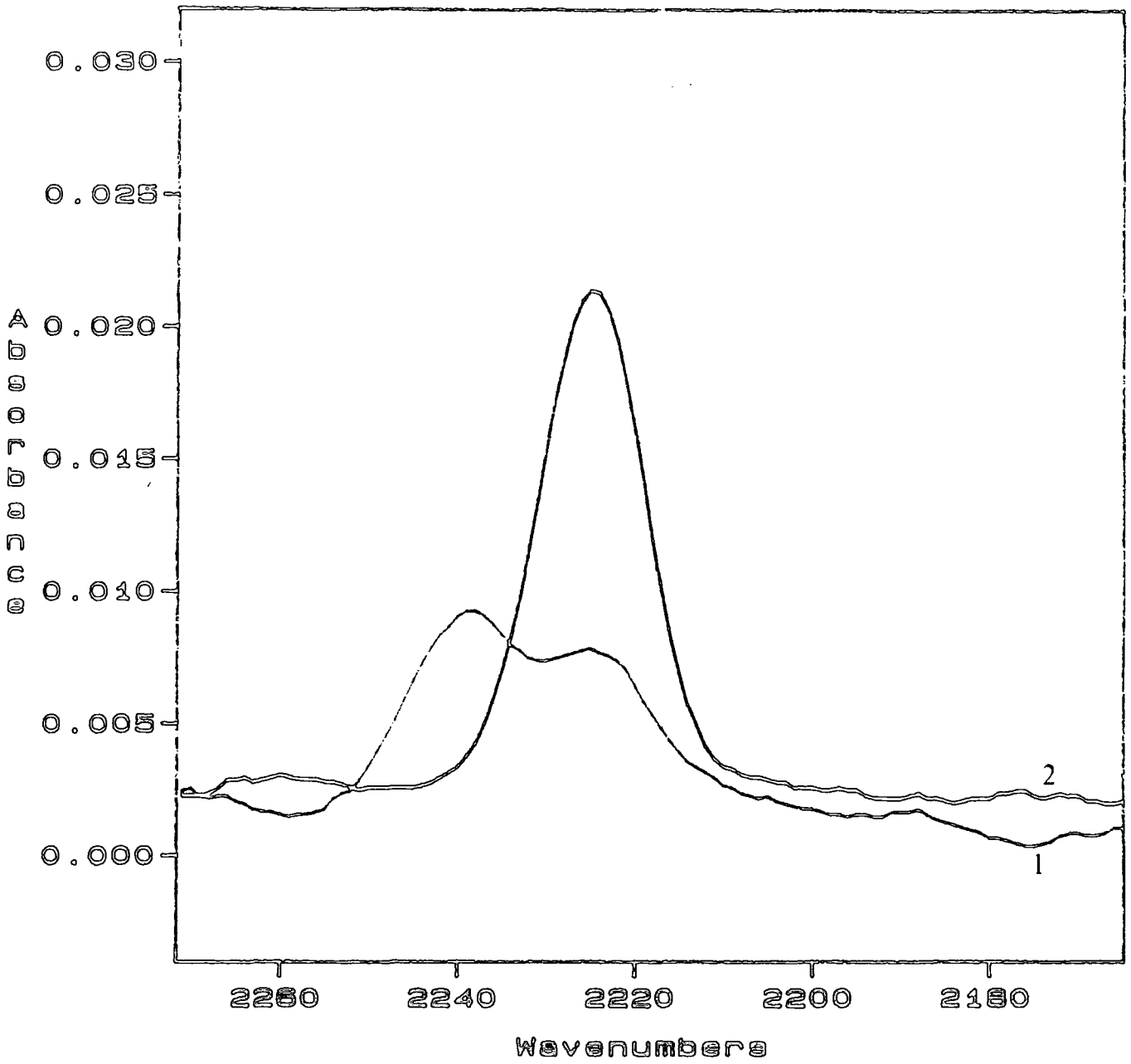

Figure 6–5 ν(CN) bands of 4-CN-2,6-dinitrophenol (1) and 4-CN-2,6-dinitrophenoxide (2).

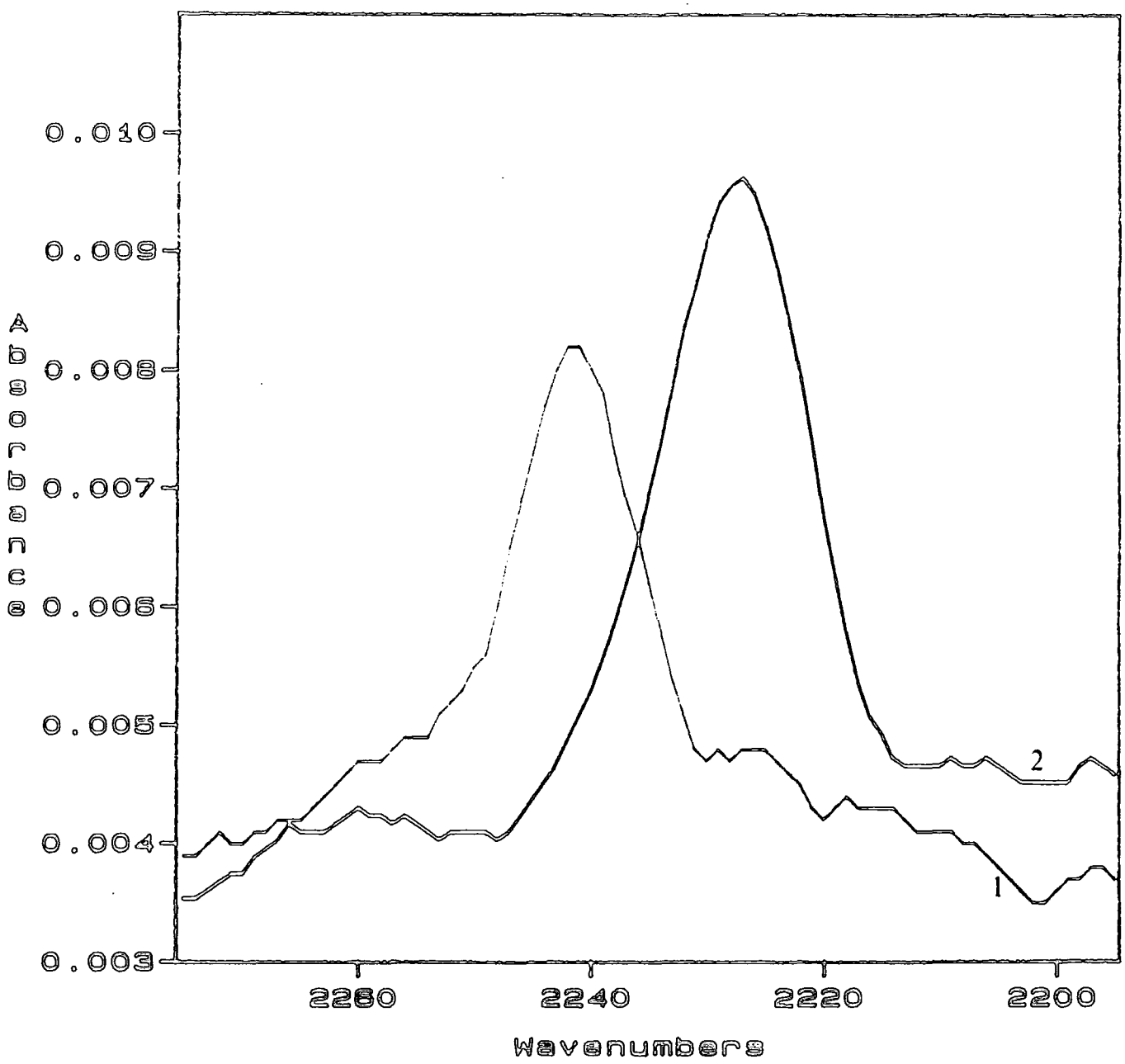

Figure 6–6 ν(CN) bands of 2-CN-4,6-dinitrophenol (1) and 2-CN-4,6-dinitrophenoxide (2).

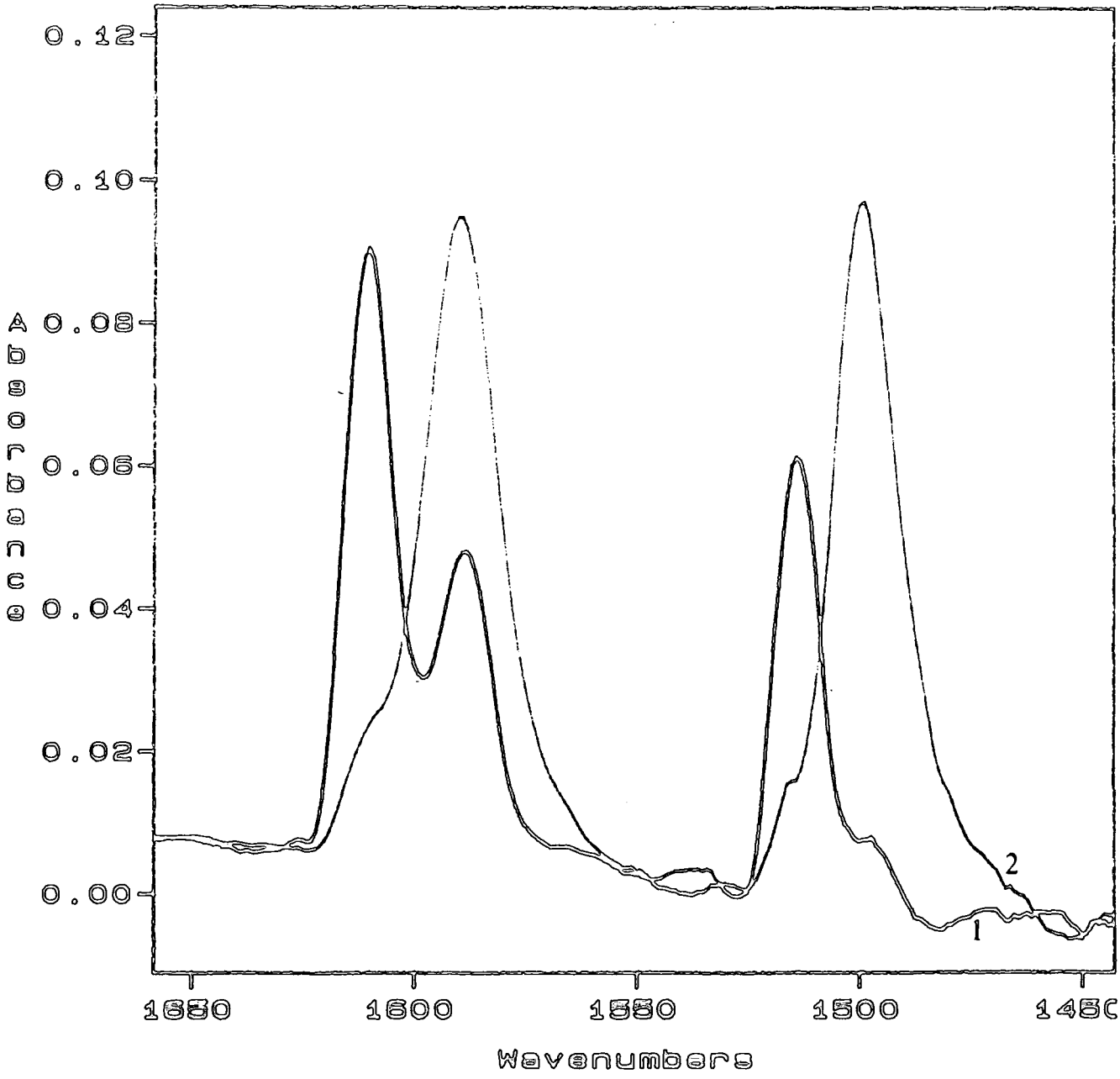

Figure 6–7 Ring stretching bands of *p*–cyanophenol (1) and *p*–cyanophenoxide (2)

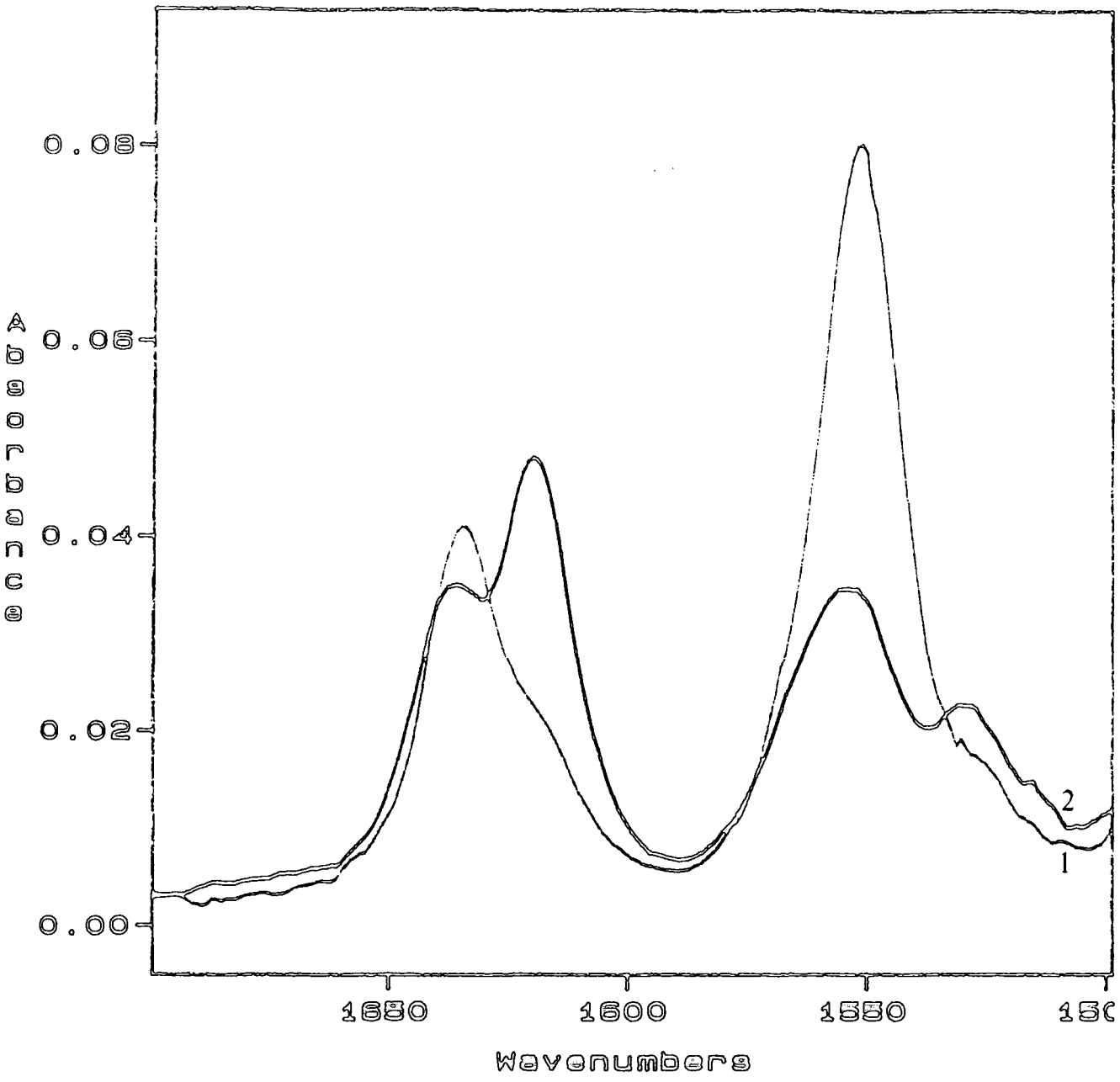

Figure 6–8 Ring stretching and $\nu_s(NO_2)$ bands of 4-CN-2,6-dinitrophenol (1) and 4-CN-2,6-dinitrophenoxide (2)

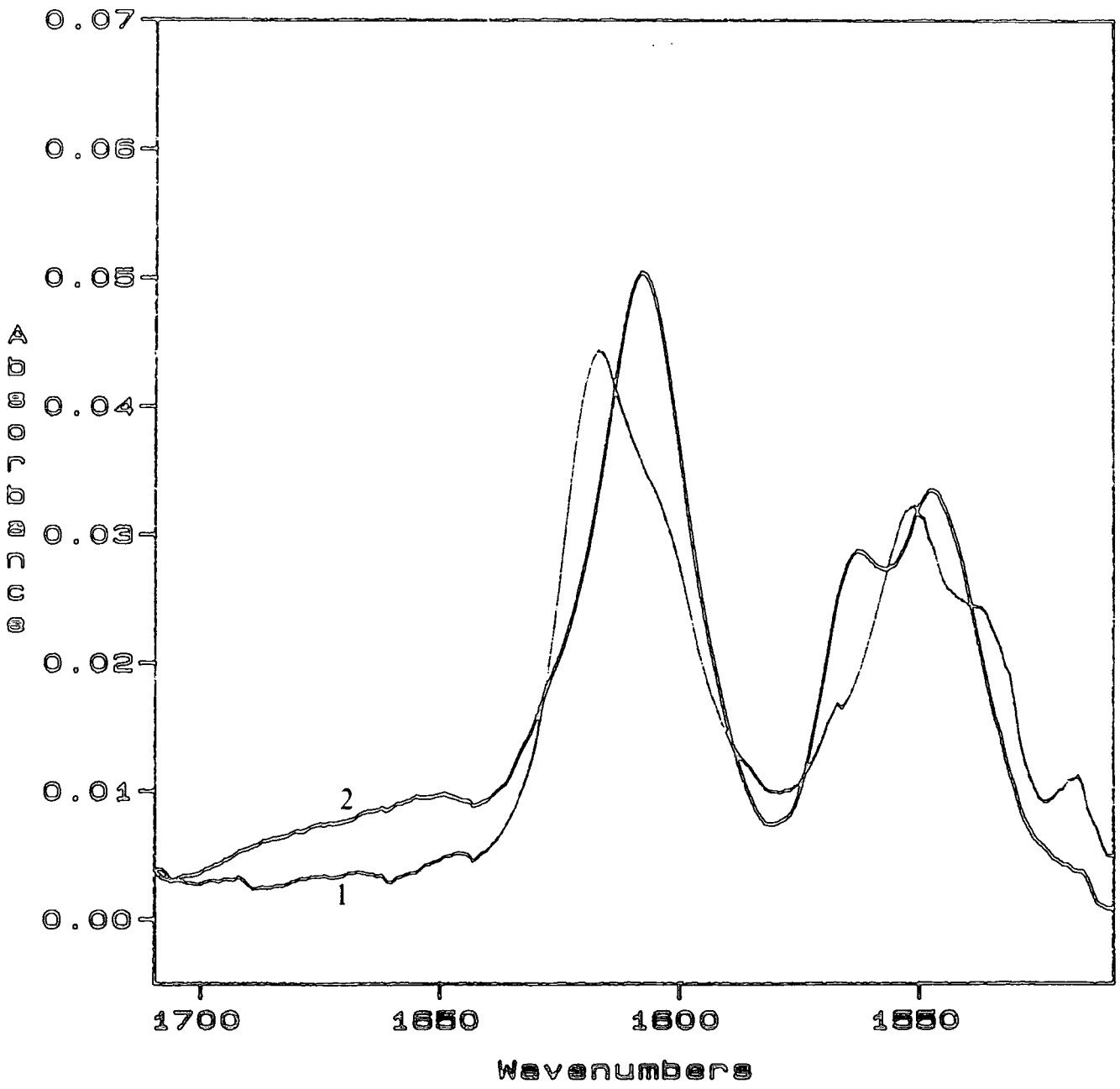

Figure 6–9 Ring stretching and $\nu_s(NO_2)$ bands of 2-CN-4,6-dinitrophenol (1) and 2-CN-4,6-dinitrophenoxide (2)

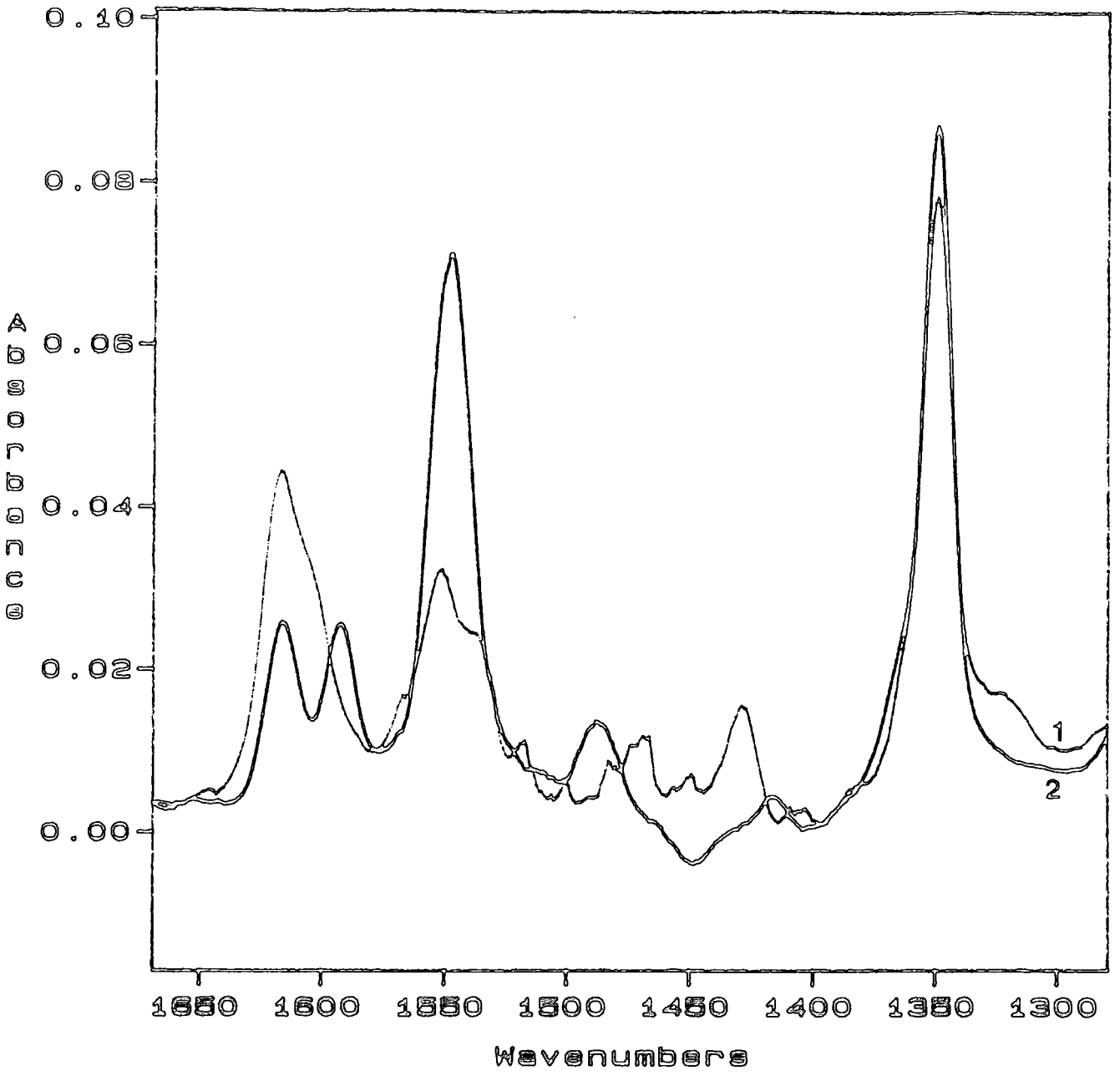

Figure 6–10 Infrared spectra of 2-CN-4,6-dinitrophenol (1) and 2-CN-4,6-dinitroanisole (2), in methanol.

6.3 Infrared Spectra of Meisenheimer Complexes

As mentioned in Chapter 1, most IR studies on Meisenheimer adducts have been performed in the solid state, due mainly to the great difficulty in finding good solvents for these compounds that are suitable for infrared spectroscopy.

In the present study, some work has been done on the solid state for 1,1-dimethoxy adducts of trinitro and cyanodinitroanisoles.

IR spectra in KBr disks were recorded for adducts and respective anisoles and are shown in Figures 6-11 to 6-15. Whenever possible, the spectra for both sodium and potassium complexes are presented, although the spectrum of the pure sodium adducts are usually more difficult to obtain since the material is less stable and some reaction with potassium bromide is possible (Chapter 2). In some cases, it was possible to detect bands that are due to the presence of some phenoxide resulting from the slow decomposition of the Meisenheimer complex. Spectra of lithium adducts are of very poor quality and are therefore not represented here. The assignments of the most prominent bands in the infrared spectra of anisoles and their 1,1-dimethoxy adducts were made using results published in the literature and are presented in Tables 6-3 to 6-5.

Due to the complexity of the spectra in the solid state, it was impossible to attribute each band to a specific vibration; special attention was paid to the bands that appear also in solution.

Solvents of high polarity were needed to obtain reasonable infrared spectra of the σ-adducts. Their stability and the stability of some of them are low in methanol. The Meisenheimer complexes studied here are very soluble and stable in acetonitrile and DMSO. However, comparative analysis of infrared bands of those adducts and their "parent" compounds (anisoles) was not without problems. Acetonitrile was a very good solvent for 2,4,6-trintroanisole (TNA) and its 1,1-dimethoxy adducts, for which results are shown in Figures 6-16 and 6-17, but not so good for the two cyanonitroanisoles and their adducts since acetonitrile has an absorption band for the (CN) stretching vibration at the same frequency as those anisoles and deuterated acetonitrile has its ν(CN) band at the same frequency of

the corresponding σ-adducts. DMSO does not pose these problems of interference, at least not with the more interesting bands but it was found to react with all the anisoles with formation of phenoxide (Chapter 2 and Section 6-1).

Table 6–4

Infrared Spectra of 2,4,6–trinitroanisole (TNA) and its Sodium and Potassium 1,1–dimethoxy adducts, in the solid state

TNA	TNA.MeO$^-$Na$^+$	TNA.MeO$^-$K$^+$	Assignment
3124	3080	3085	$\nu_{as}(C-H)_{ring}$
3102	3010	3003	$\nu_{s}(C-H)_{ring}$
2962	2938	2938	$\nu_{as}(CH_3)$
2872	2830	2835	$\nu_{s}(CH_3)$
1602/1610	1611	1607	$\nu(C-C)_{ring}$
1545			$\nu_{as}(NO_2)$
	1509	1510	$\nu_{as}(NO_2)$
	1492	1481	$\nu_{as}(p-(NO_2)$
1429	1445	1444	$\delta_{as}(CH_3)$
1412	1417	1404 1385	$\delta_{s}(p-NO_2)$
1346			$\nu_{s}(NO_2)$
1305	1301	1297	
1265		1266	$\nu(C-O-C)$
	1244	1244	$\nu_{s}(O-NO_2)$
	1228	1222	$\nu_{s}(p-NO_2)$
	1200		$\nu_{as}(C-O-C)$
1183	1163	1163	$\delta(CH)$ [a]
1084	1127	1123	$\nu_{s}(C-O-C)$
	1091	1063	$\nu_{s}(C-O-C-O-C)$

a = out–of–phase, in plane

Table 6–5

Infrared Spectra of 4–CN–2,6–dinitroanisole (4CNDNA) and its Sodium and Potassium 1,1–dimethoxyadducts, in the solid state

4CNDNA	4CNDNA.MeO⁻Na⁺	4CNDNA.MeO⁻K⁺	Assignment
3101/3083	3110/3083	3105	$\nu_{as}(C-H)_{ring}$
3022	3008	3005	$\nu_{s}(C-H)_{ring}$
2952	2934	2932	$\nu_{as}(CH_3)$
2879	2831	2819	$\nu_{s}(CH_3)$
2244	2211/2195^{sh}	2210	$\nu(CN)$
1626	1609	1606	$\nu(C-C)_{ring}$
1536			$\nu_{as}(NO_2)$
	1488/1464	1437/1459	$\nu_{as}(NO_2)$
1494			ring vibration
1429/1412	1414	1407	$\delta(CH_3)$
1358			$\nu_{s}(NO_2)$
	1324	1331/1316	
1295/1274		1210	$\nu_{as}(C-O-C)$
	1176	1173	$\nu(NO_2)$
1119			$\nu_{as}(C-O-C)$
	1054/1044	1063	$\delta(C-H)$ ^{a}

sh = shoulder

a = in–phase, in–plane

Table 6–6

Infrared Spectra of 2–CN–4,6–dinitroanisole (2CNDNA) and its 1,1–dimethoxy adducts, in the solid state

2CNDNA	2CNDNA.MeO⁻Na⁺	2CNDNA.MeO⁻K⁺	Assignment
2237	2207	2209	ν(CN)
1612/1588	1605	1605	ν(C–C)$_{ring}$
1534	1523/1505	1523/1503	$\nu_{as}(NO_2)$
1485			ring vibration
1352			$\nu_{s}(NO_2)$
	1218/1179	1228/1181	$\nu_{s}(NO_2)$
1318	1307	1305	
1267	1159	1155	ν_{as}(C–O–C)
	1055	1055	δ(C–H)

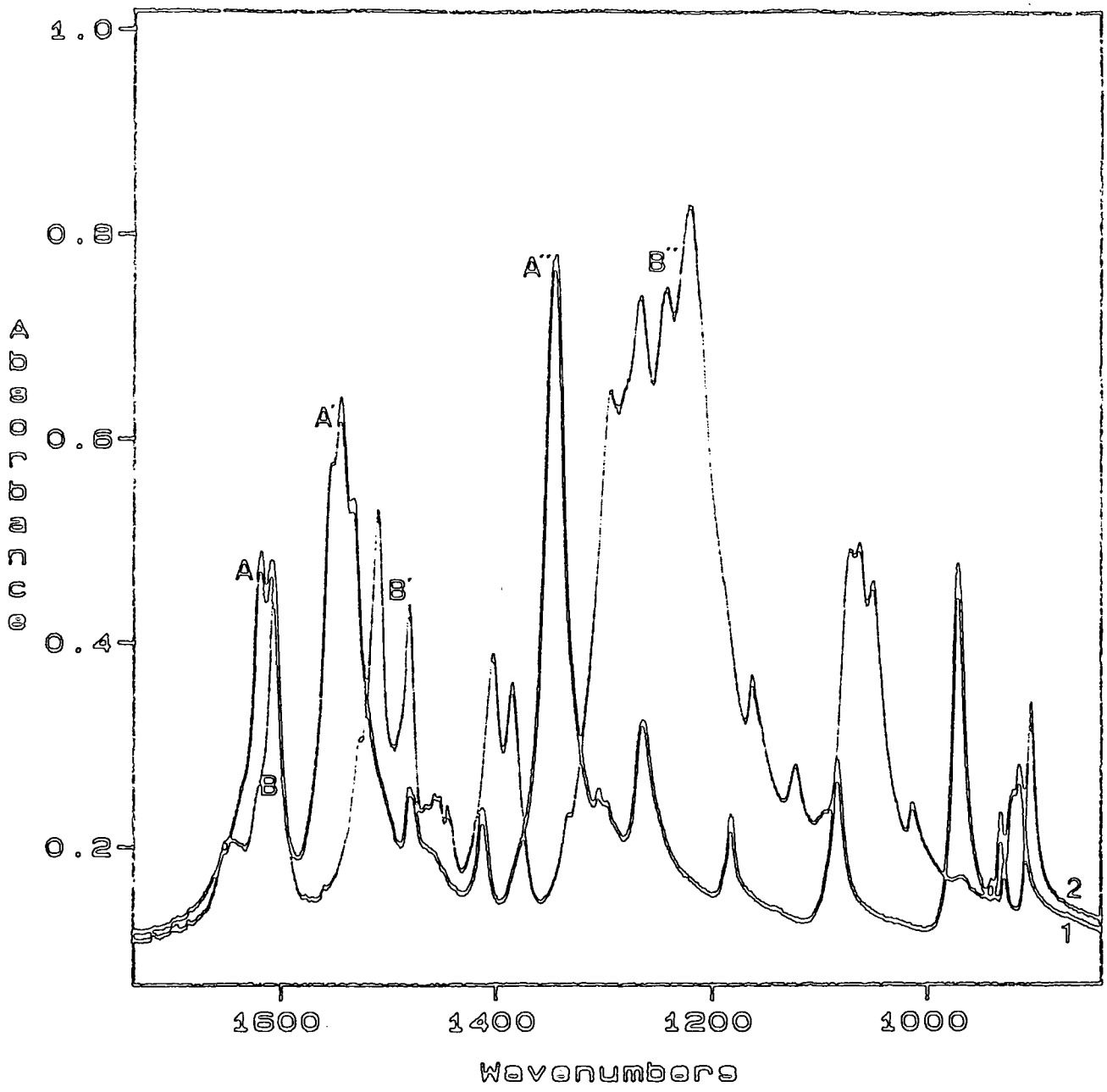

Figure 6–11 **Infrared spectra, in the solid state, of TNA (1) and its potassium 1,1-dimethoxy complex TNA·MeO⁻K⁺ (2)**

A,A' and A'' are the ν(C–C), $\nu_{as}(NO_2)$ and $\nu_s(NO_2)$ respectively for TNA

B,B' and B'' are the ν(C–C), $\nu_{as}(NO_2)$ and $\nu_s(NO_2)$ of the complex.

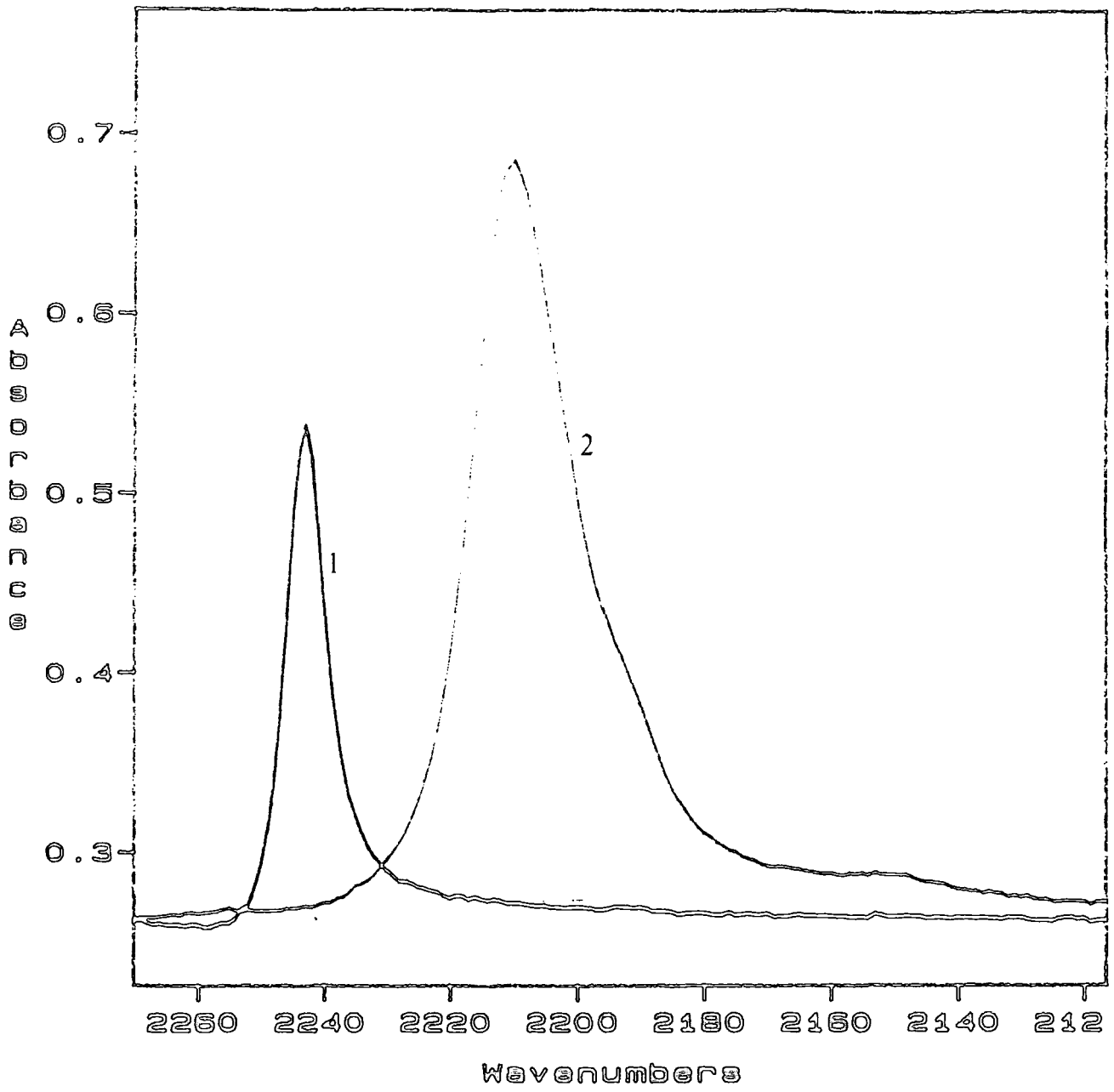

Figure 6–12 The ν(CN) bands of 4CNDNA (1) and of its sodium 1,1-dimethoxy adduct 4CNDNA · MeO^-Na^+ (2), in the solid state.

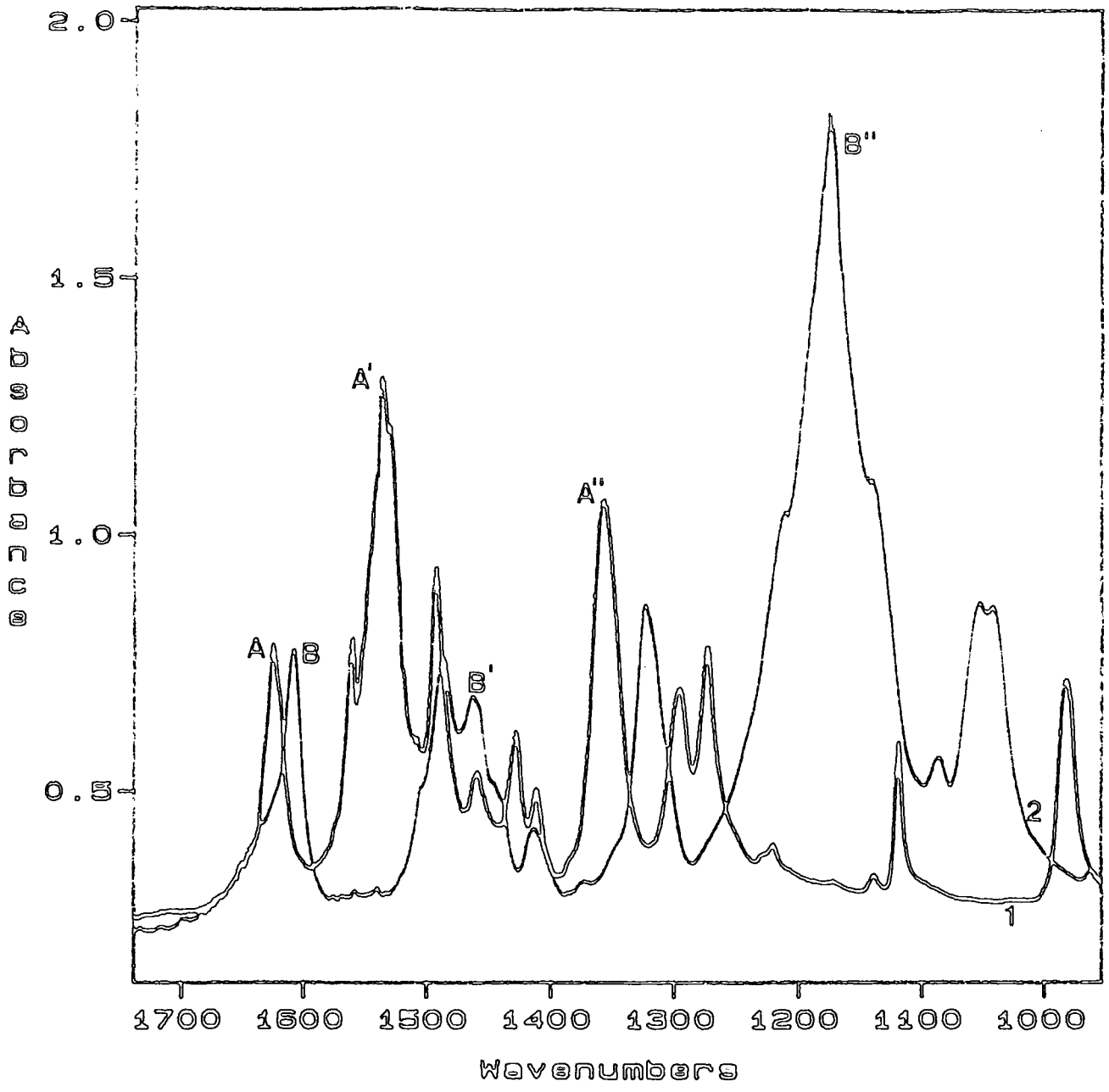

Figure 6–13 Infrared spectra of 4CNDNA (1) and 4CNDNA·MeO^-Na^+ (2) in the solid state.
ν(C–C), $\nu_{as}(NO_2)$ and $\nu_s(NO_2)$ are marked A,A',A'' and B,B',B'' respectively for (1) and (2).

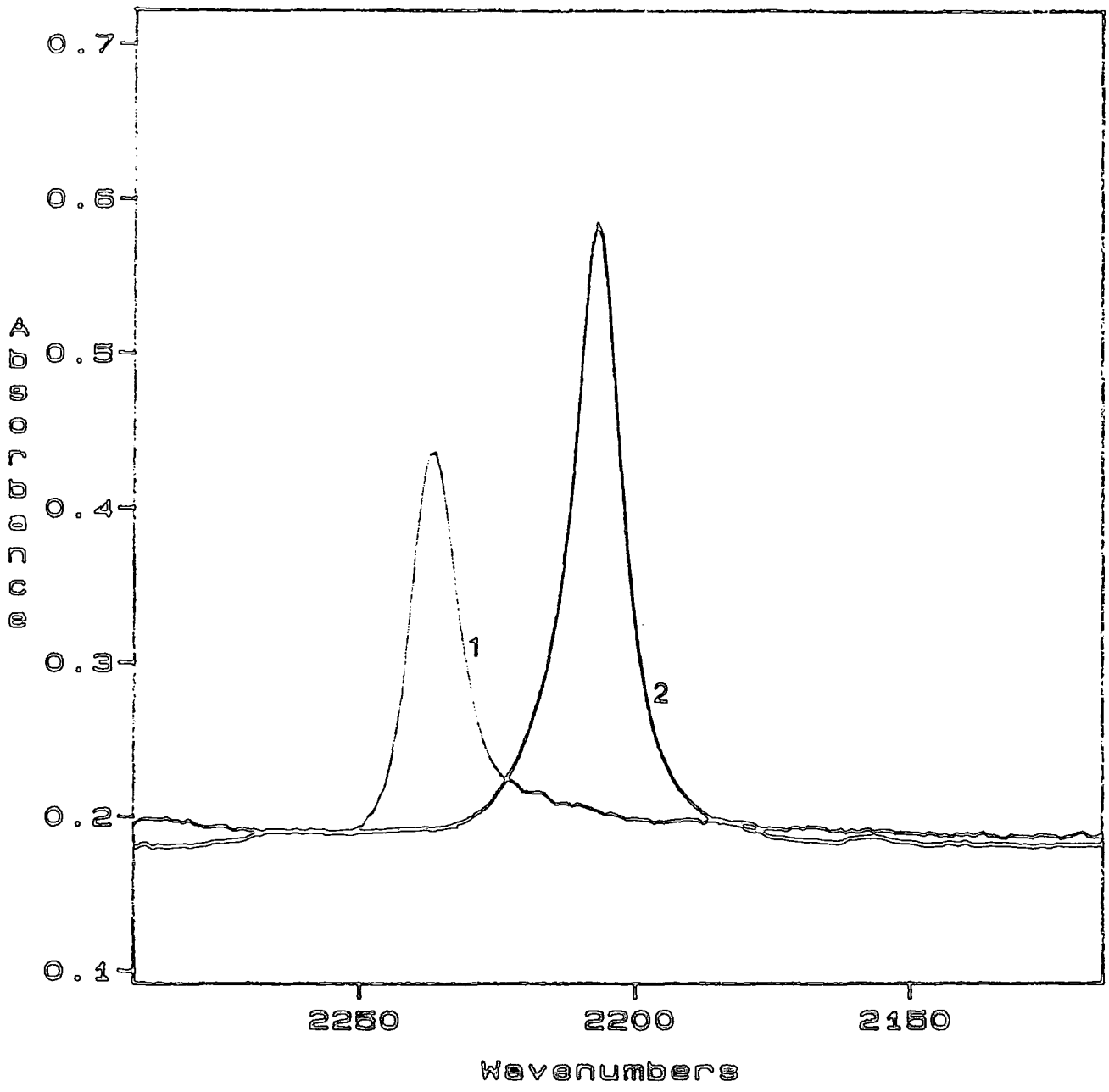

Figure 6–14 The ν(CN) bands of 2CNDNA (1) and of 2CNDNA·MeO^-Na^+ (2), in the solid state.

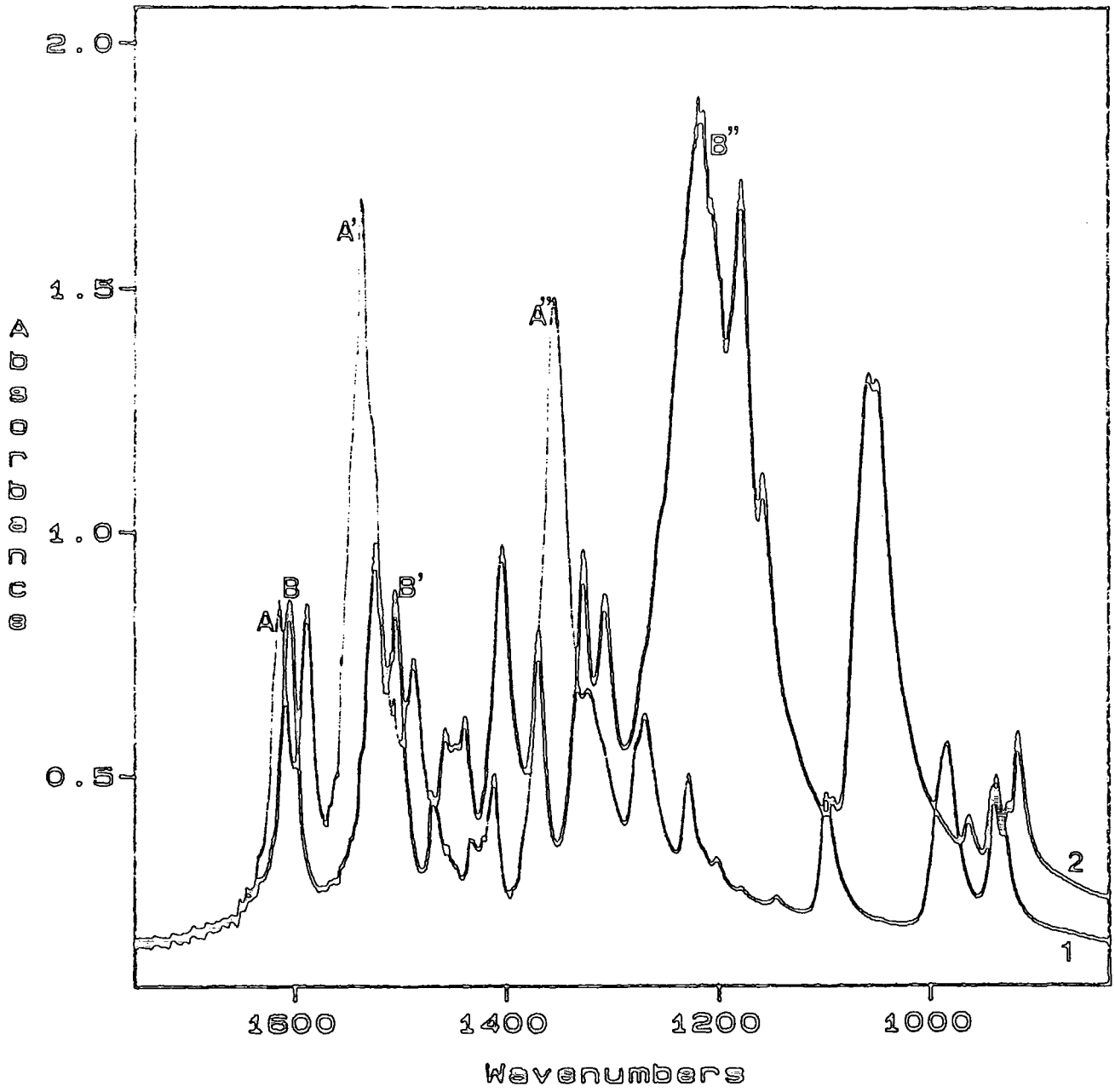

Figure 6–15 Infrared spectra of 2CNDNA (1) and 2CNDNA·MeO^-Na^+ (2), in the solid state.
ν(C–C), $\nu_{as}(NO_2)$ and $\nu_s(NO_2)$ are marked A,A',A'' and B,B',B'' for (1) and (2), respectively.

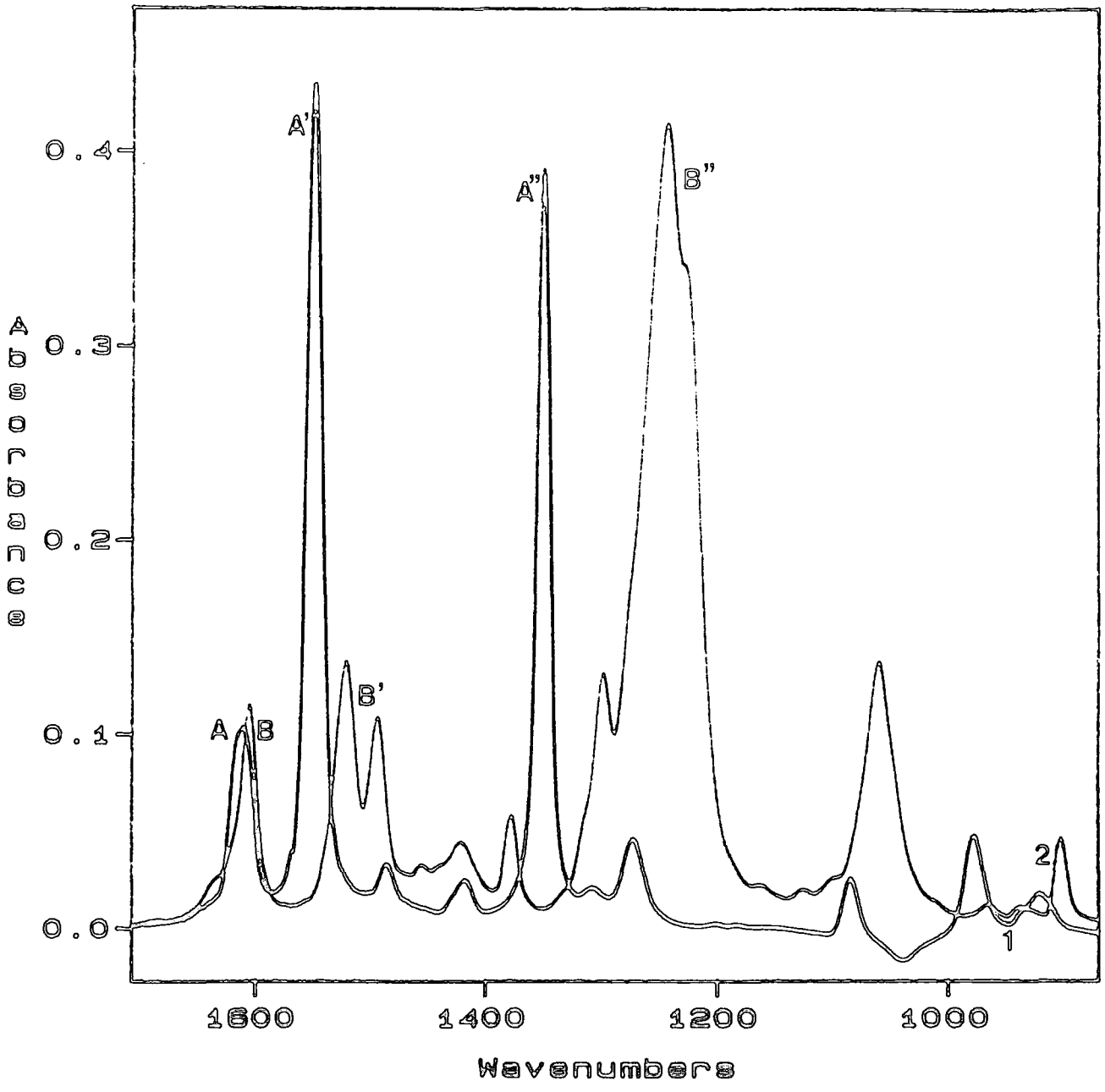

Figure 6–16 Infrared spectra of TNA (1) and TNA·MeO^-Na^+ (2) in CD_3CN ν(C–C), $\nu_{as}(NO_2)$ and $\nu_s(NO_2)$ are marked A,A',A'' and B,B',B'' for (1) and (2), respectively.

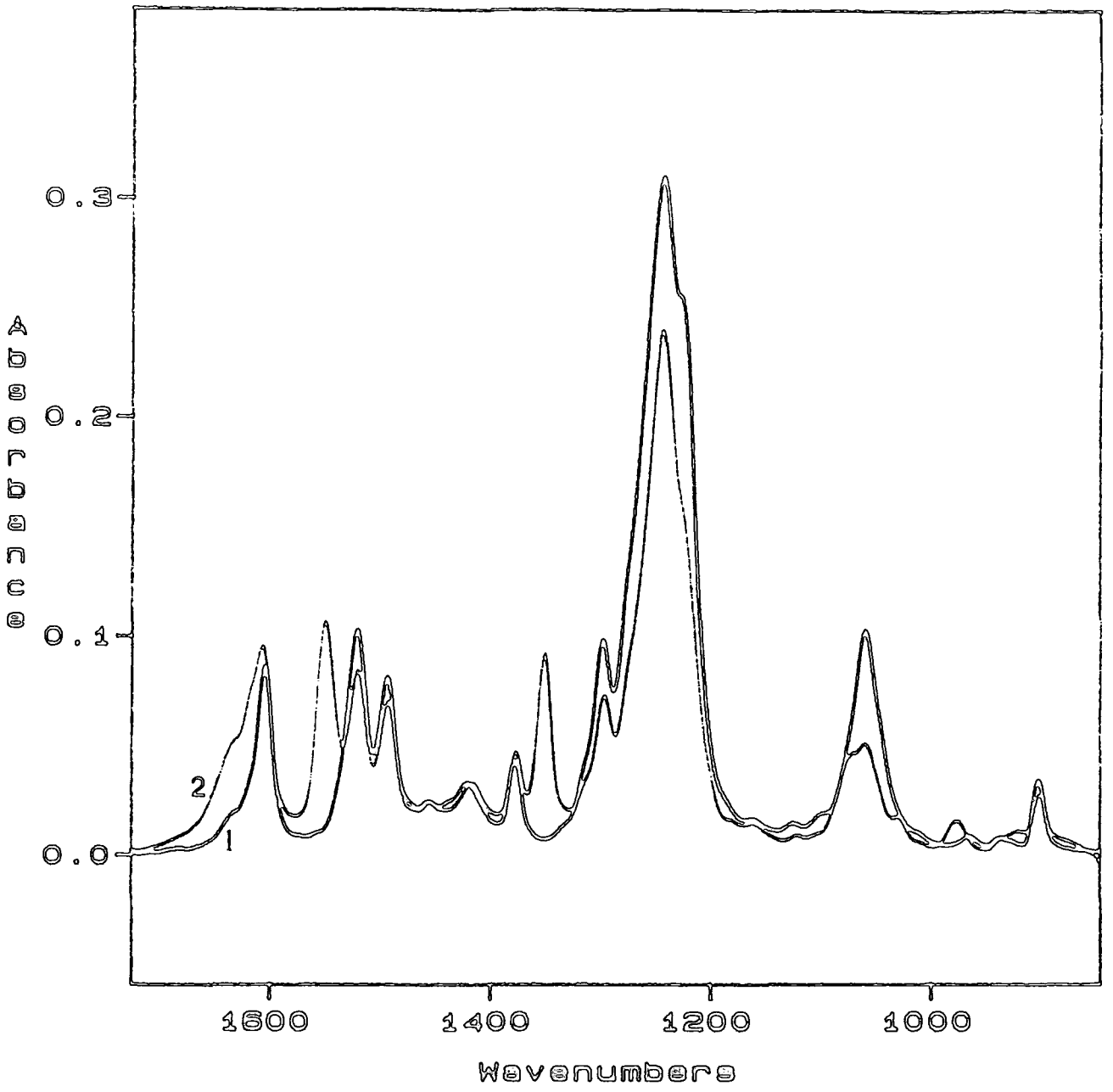

Figure 6–17 Infrared spectra of sodium (1) and potassium (2) 1,1-dimethoxy adducts of TNA in CD_3CN

When the infrared spectrum of a nitro-substituted σ-adduct is compared to that of its parent anisole, the most remarkable difference is that observed for the $\nu_s(NO_2)$ band, which shows shifts to lower frequency that can reach 180cm^{-1} and a very large increase in intensity (Figure 6-13). As discussed in Chapter 5 and in the previous section (6-2), this band is quite sensitive to intramolecular effects that may modify the extent of conjugation with the ring of the nitro groups. However, variations in the band position, either in neutral nitro-aromatic molecules or even in anions such as nitrophenoxides do not exceed ±10cm^{-1} relatively to the "normal" value of 1350cm^{-1} for the $\nu_s(NO_2)$ of nitrobenzene. Intramolecular hydrogen-bonding, such as that found in *ortho*-nitrophenols, can cause a shift frequency of 35cm^{-1}. The very large shift of the $\nu_s(NO_2)$ in σ-adducts is understood in terms of the delocalisation of negative charge in the nitro substituents, mainly in the nitro group in *para*-position to the tetrahedric carbon.[10] Formation of a 1,1-dimethoxy adduct relieves the steric interaction of the methoxy group with nitro groups in *ortho*-position existent in the alkyl aryl ether, since in the adduct the geminal methoxy groups are perpendicular to the ring and the nitro substituents are allowed to achieve coplanarity with it.

The antisymmetric $\nu_{as}(NO_2)$ band also shifts to lower frequency with the formation of 1,1-dimethoxy adduct but the shifts are smaller.

From the results in solution, where the spectra are simpler, it can be seen that whenever the species has nitro groups in non-equivalent position (one *para*- to the methoxy group(s) and at least one *ortho*-nitro substituent) there are two bands for each symmetric and antisymmetric vibration of the NO_2 group (Figures 6-16 and 6-18). For the σ-adduct of 4-CN-2,6-dinitroanisole, both nitro groups are in the *ortho*-position being therefore equivalent and only one band is found for each NO_2 vibration (Figure 6-19). The shoulder in the $\nu_{as}(NO_2)$ in solution, as well as those found in ν_s and $\nu_{as}(NO_2)$ in the solid state are probably due to ring vibrations.[9]

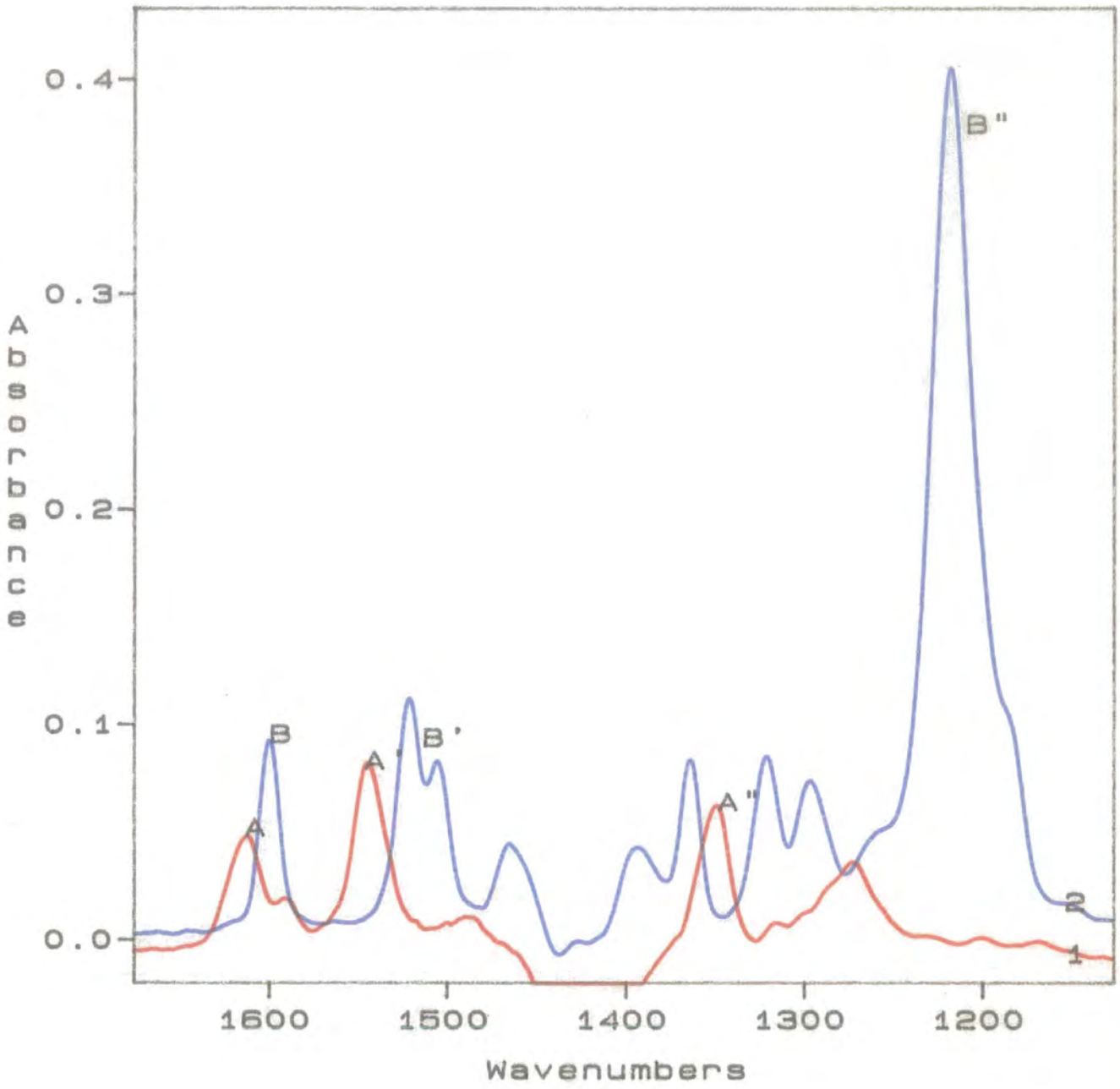

Figure 6–18 Infrared spectra of 2CNDNA (1) and 2CNDNA·MeO^-Na^+ (2) in DMSO. ν(C–C), $\nu_{as}(NO_2)$ and $\nu_s(NO_2)$ are marked A,A',A'' and B,B',B'' for (1) and (2), respectively.

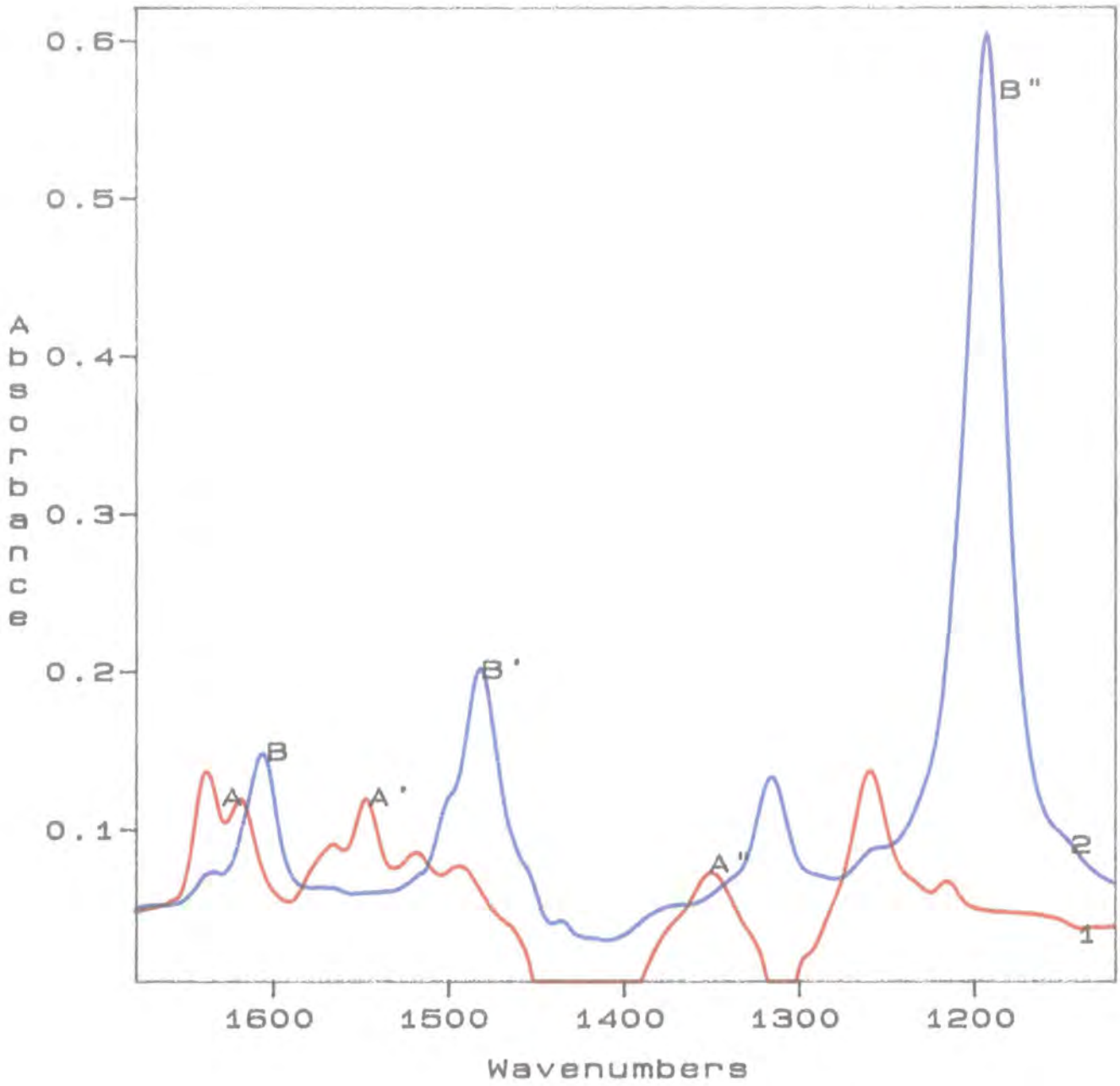

Figure 6–19 Infrared spectra of 4CNDNA (1) and 4CNDNA·MeO^-Na^+ (2) in DMSO. ν(C–C), $\nu_{as}(NO_2)$ and $\nu_s(NO_2)$ are marked A,A',A'' and B,B',B'' for (1) and (2), respectively.

Table 6–7

Frequency shifts (cm^{-1}) of the symmetric and antisymmetric stretching NO_2 bands from anisoles to σ–complexes

Shift	TNA/complex		4CNDNA/complex		2CNDNA/complex	
	solid	solution[a]	solid	solution[b]	solid	solution[b]
$\Delta\bar{\nu}_{as}$	53,26	58,29	48	71	29,11	39,23
$\Delta\bar{\nu}_{s}$	118,102	120,105	182	153	173,134	165,131

a) solvent: Acetonitrile

b) solvent: DMSO

The extent of resonance of the nitro groups can be analysed by comparing the band shifts of trinitro- and cyanodinitro- σ-adducts relatively to their parent compounds. These shifts are presented in Table 6-7, in solid state and solution (acetonitrile for the TNA/complex system, DMSO for the other two) for both the symmetric and antisymmetric bands.

$$\Delta\bar{\nu}_{as} = \bar{\nu}_{as}(NO_2)_{parent} - \bar{\nu}_{as}(NO_2)_{complex}$$

$$\Delta\bar{\nu}_{s} = \bar{\nu}_{s}(NO_2)_{parent} - \bar{\nu}_{s}(NO_2)_{complex}$$

The larger shifts of the $\bar{\nu}_s(NO_2)$ band, or pair of bands, in the cyanonitro-complexes are compatible with the idea of a less delocalised system, relatively to the trinitro complexes. In other words, since the CN group is a less strong electron-withdrawing group, more charge density reaches the nitro substituents.

The differences in the shifts between solid state and solution may have their origin in several effects and are therefore difficult to interpret. For example, while the $\nu_{as}(NO_2)$ band of TNA shifts $5cm^{-1}$ to higher frequency from solid state to solution in acetonitrile, the band of 4CNDNA shifts $17cm^{-1}$ in the same conditions.

Another factor that forces these changes to be regarded with caution is the decomposition of the cyanodinitroanisoles by DMSO. It is known (Chapter 2) that the solutions under analysis have some substituted phenoxide present, to which the

band in the ν(CN) region at *ca.* 2215cm^{-1}can be assigned (Figure 6-20). The bands observed for NO_2 vibrations in these solutions may be the overlap of bands for the anisole and the phenoxide or even mainly due to phenoxide.

The shift of the $\nu_s(NO_2)$ band in the 4CNDNA/complex system shows a large decrease when the compounds are dissolved in DMSO which can be seen as a decrease of the NO_2 groups resonance. This may be a result of the complexation of the CN group by DMSO[3] with an increase on its electron-withdrawing power. In other words, the CN group, in DMSO, competes with the two nitro groups for electron density withdrawal in a larger scale than in the solid state, extending the delocalised π-system to all substituents in a more even way. The effectiveness of this type of complexation of the CN group by DMSO may be prevented in the 2CNDNA complexes by steric hindrance of the methoxy groups *ortho-* to the CN substituents. In the anisoles themselves it can be seen that the ν(CN) band of 4CNDNA shifts 5cm^{-1} to lower frequency from solid state to DMSO solution while for 2CNDNA the band is unchanged.

	$\Delta\tilde{\nu}_{CN}$(4CNDNA/complex)	$\Delta\tilde{\nu}_{CN}$(4CNDNA/complex)
solid	33 (Figure 6–12)	30 (Figure 6–14)
solution	42 (Figure 6–20)	34 (Figure 6–21)

The differences in the position of bands for sodium and potassium salts are generally small and, in most cases difficult to interpret.

The spectra for sodium and potassium salts of the 1,1-dimethoxy adduct of trinitroanisole have been published by Osawa and Takeda (1980)[9] and are totally consistent with the results obtained here, between 1650 and 1000cm^{-1}, as far as the differences between the salts are concerned. These are the shifts to lower frequency in the potassium complex relative to the sodium complex of the three bands, viz: the ring breathing band, $\Delta\tilde{\nu}$ = 4cm^{-1}, the two bands of antisymmetric stretching vibrations of the nitrogroups, $\Delta\tilde{\nu}$ = 10cm^{-1}, and the CH_3 symmetric

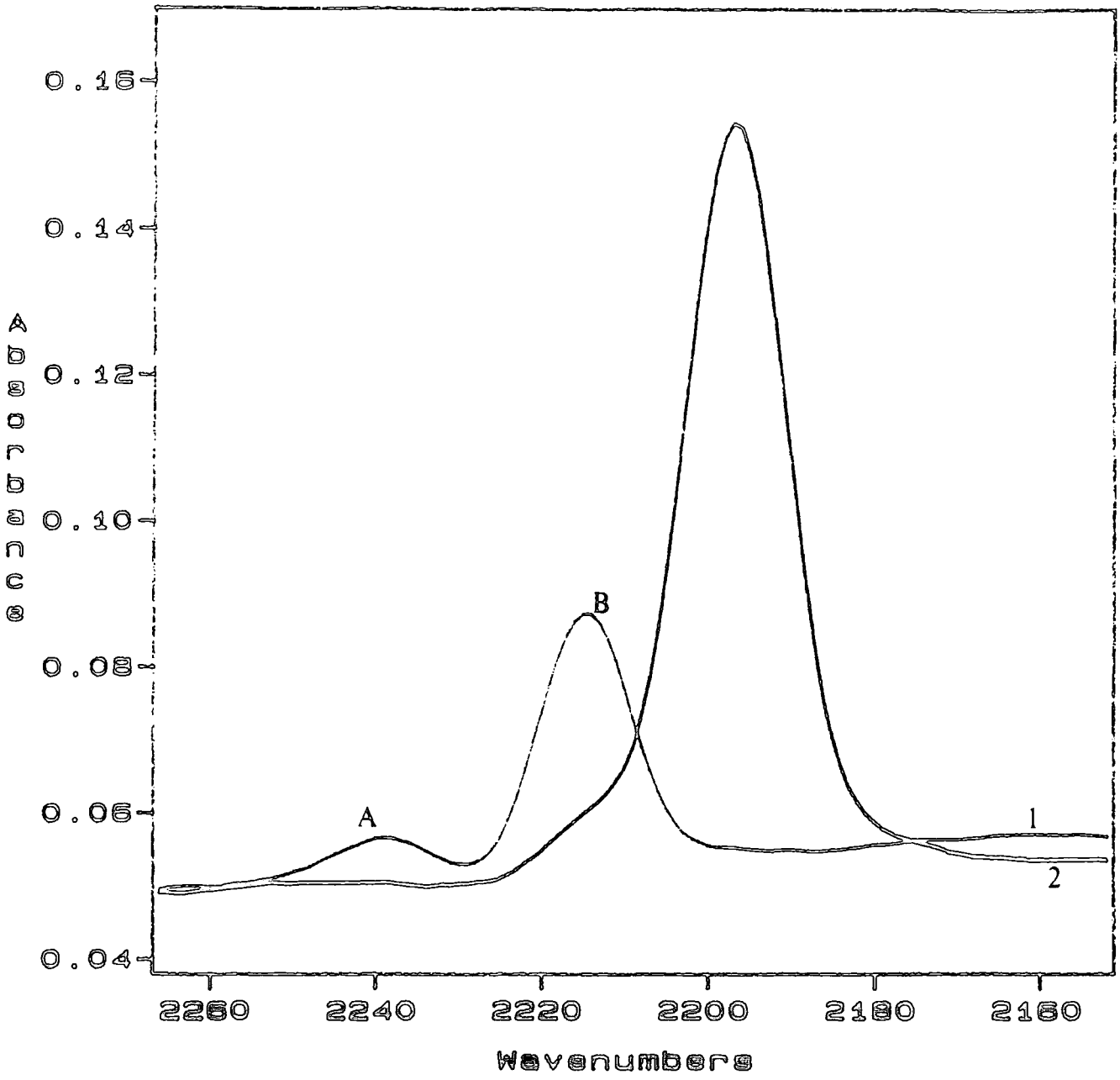

Figure 6–20 ν(CN) bands of 4CNDNA (1) and 4CNDNA·MeO^-Na^+ (2) in DMSO.The large extent of conversion of 4CNDNA to the corresponding phenoxide by interaction with DMSO is revealed by the existence of the two bands A (anisole) and B (phenoxide) in (1)

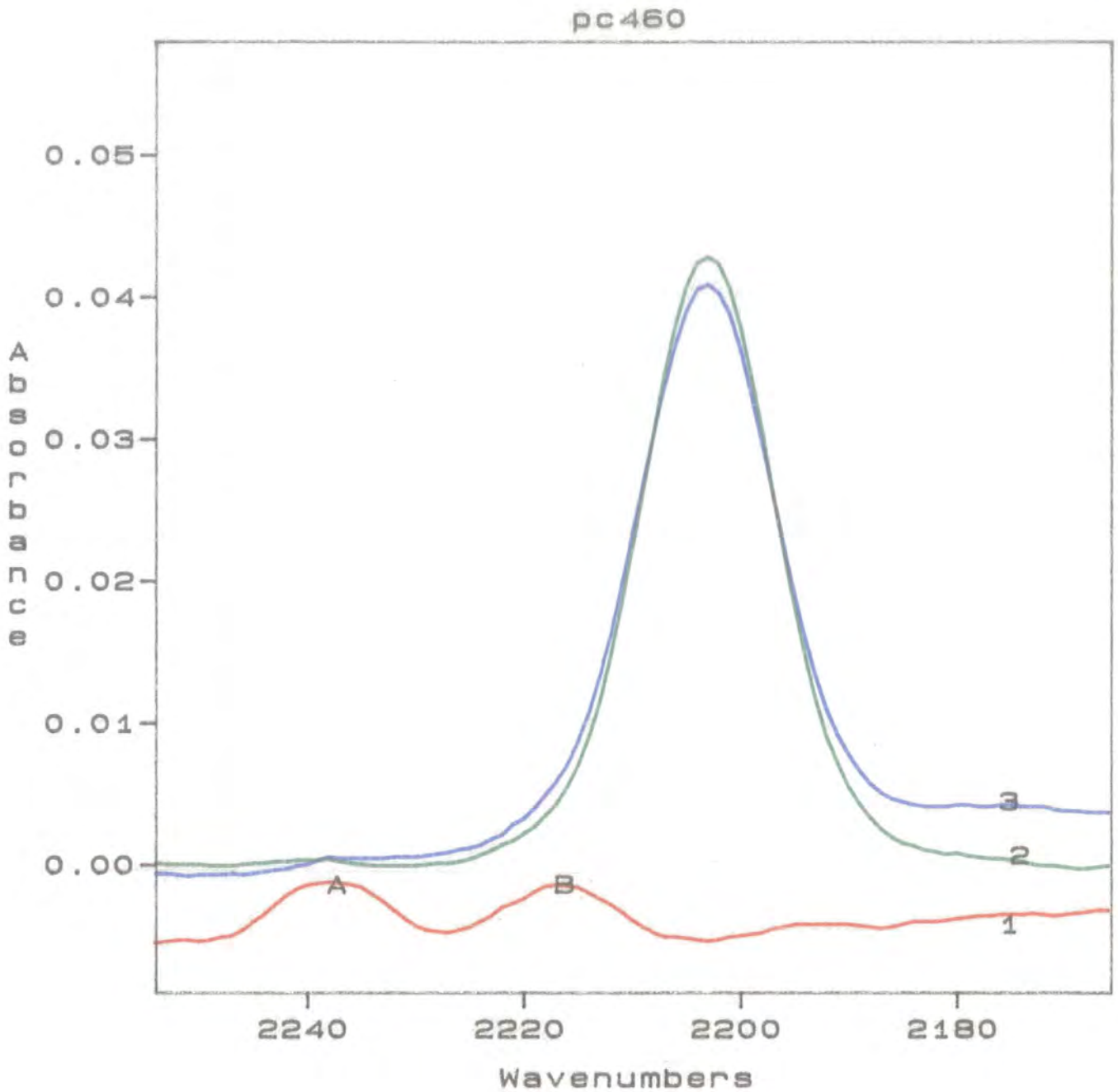

Figure 6–21 ν(CN) bands of 2CNDNA (1), 2CNDNA·MeO^-Na^+ (2) and 2CNDNA·MeO^-K^+ (3).
Bands A and B in (1) are due to anisole and phenoxide, respectively.

deformation band, $\Delta\bar{\nu} = 13cm^{-1}$. The band at *ca.* $1300cm^{-1}$ which some authors' assign to a (C⋯⋯N) stretching mode also shows a $5cm^{-1}$ shift in the same direction.

The sodium complex, whose spectrum is, unfortunately, not shown in figure 6-11, has a band at $1200cm^{-1}$ which is not present in the K_4 complex nor in the parent compound, TNA. There is a larger difference in frequency between the $\nu_{as}(NO_2)$ and the $\nu_s(NO_2)$ pairs of bands in the K^+ complex spectrum and there are two bands at *ca.* $1050cm^{-1}$ compared to only one in the sodium adduct.

The spectra of the sodium and potassium adducts of 2-CN-4,6-dinitroanisole show good coincidence for all the bands (Figure 6-22) except the ν(CN) band (Figure 6-23). The large width difference on the ν(CN) band (Figure 6-23) between sodium and potassium 1,1-dimethoxy complexes represents a problem for which no answer was found. Analysis of the corresponding complexes of 4-CN-2,6-dinitroanisole was not helpful since the spectrum for the potassium salt was quite poor. So, it is not known if the same cation effect is present for these complexes.

It has been reported that for 1,1-dimethoxy adducts of TNA, the oxygen atoms of both methoxy groups as well as the oxygen atoms of the o-NO_2 groups are involved in ion-pairing. 1,1-dimethoxy adducts of 2-CNDNA can be visualised in the same way, with one *o*-NO_2 group replaced by the CN group. Thus, it is possible that this substituent is also involved in cation coordination, providing the size of that cation is appropriate.

Although it is not intended here to fully explain the difference in ν(CN) bandwidth, maybe it can be related to the different sizes of the sodium and potassium cations.

In solution, the differences between sodium and potassium complexes tend to disappear for the σ-adducts of TNA. The bands coincide within $\pm 3cm^{-1}$, as shown in Figure 6-17, apart from two bands at $1585cm^{-1}$ and $1385cm^{-1}$ which are present only in the K^+ complex spectrum. Spectra in DMSO and acetonitrile show all the bands in essentially the same position while in methanol there is a general shift to

higher frequency of 3-10cm^{-1}, depending on the particular mode, but the general features of the bands are not modified.

For the sodium and potassium complexes of 2CNDNA, the only band, ν(CN), that was different in the solid state appears at the same position, with identical intensity and shape, when the compound is dissolved in DMSO.

This seems to prove that as DMSO is capable of complexing alkali metal cations, as well as of solvating delocalised anions, no ion-pairing of σ-adduct-cation is present in solution.

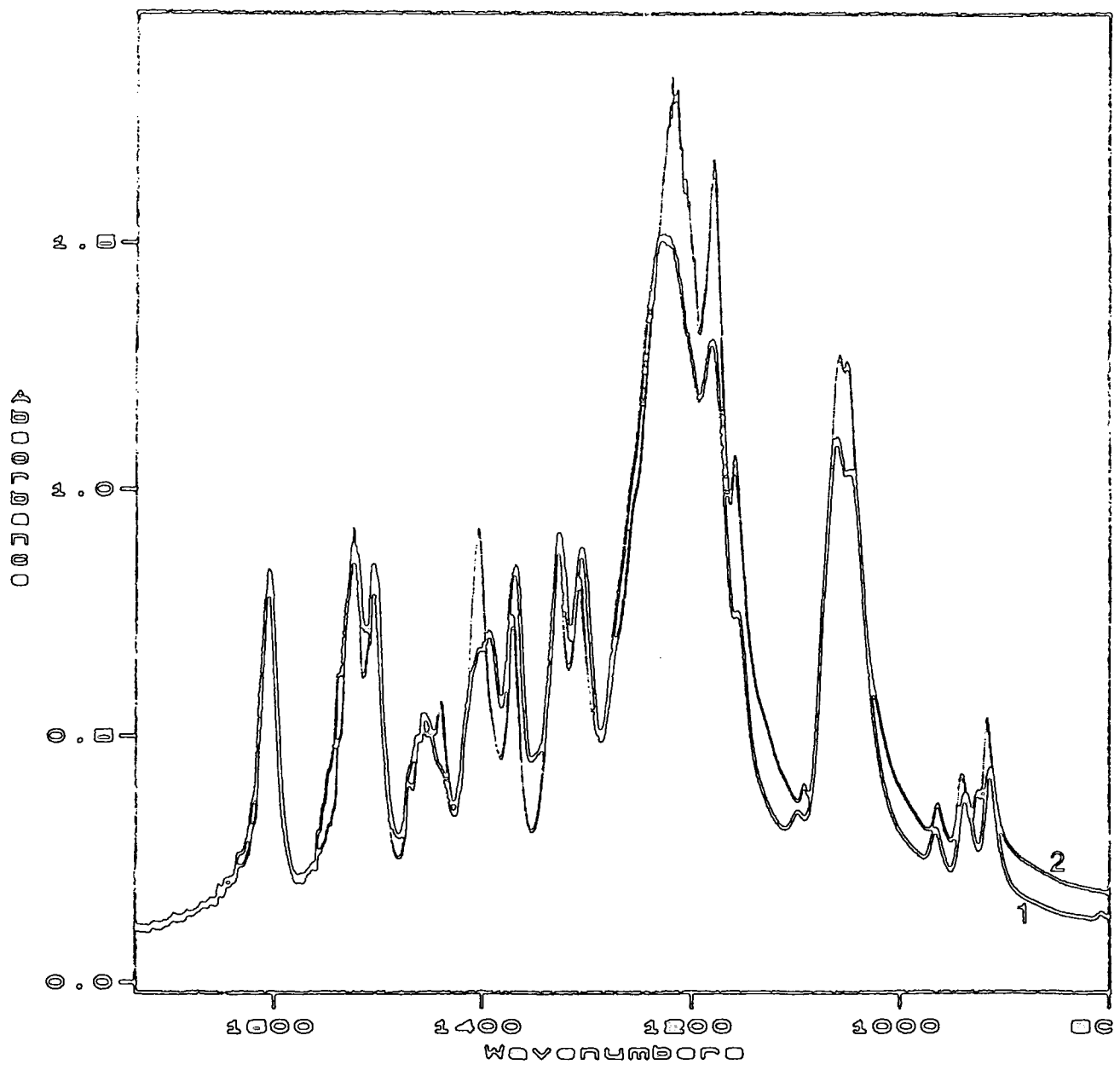

Figure 6–22 Infrared spectra of 2CNDNA·MeO^-K^+ (1) and 2CNDNA·MeO^-Na^+ (2) in the solid state.

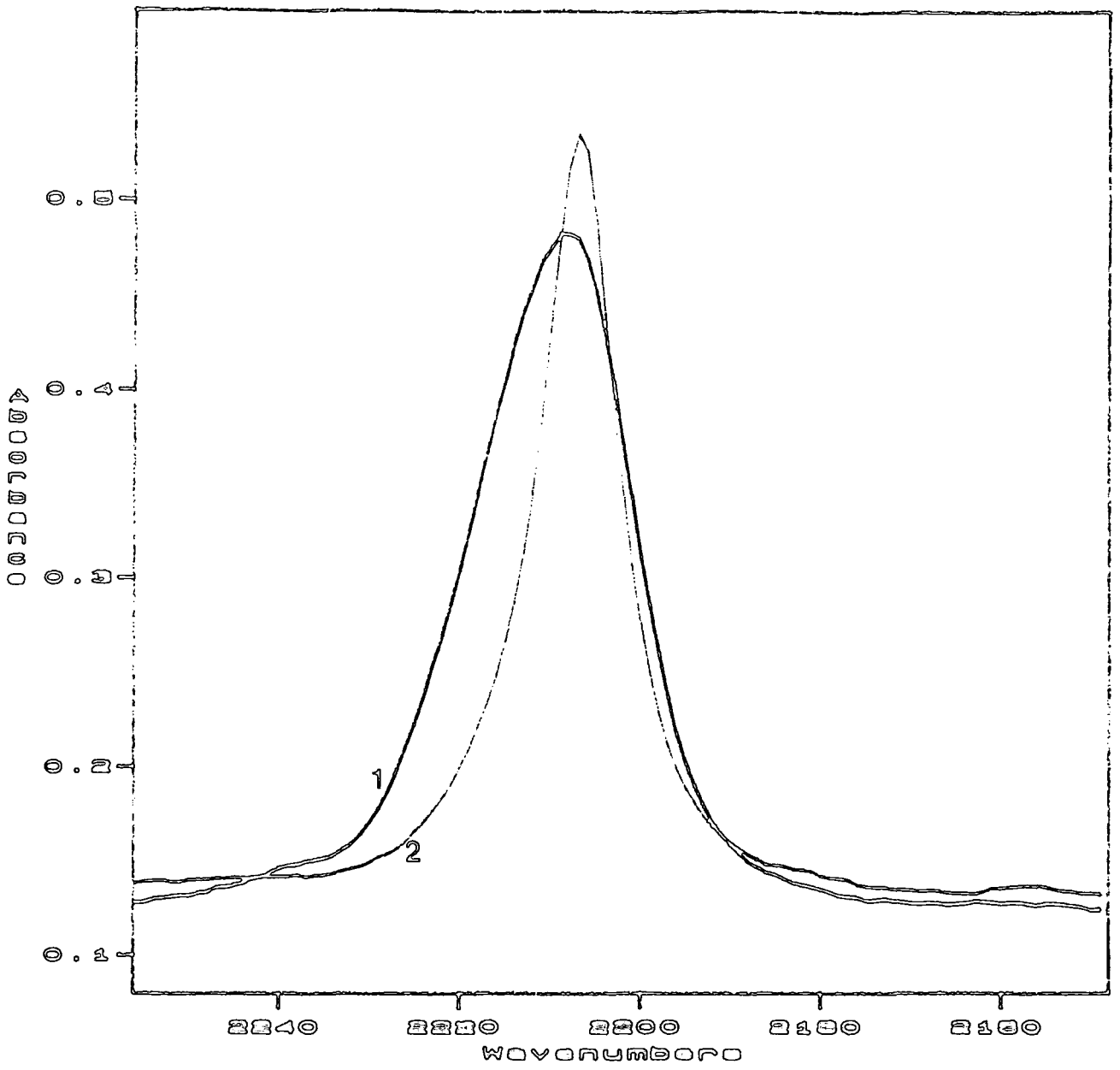

Figure 6–23 ν(CN) band 2CNDNA·MeO$^-$K$^+$ (1) and 2CNDNA·MeO$^-$Na$^+$ (2)
$\Delta\bar{\nu}_{\frac{1}{2}}(K^+)=21\ cm^{-1}$; $\Delta\bar{\nu}_{\frac{1}{2}}(Na^+)=11\ cm^{-1}$

References

1 Pross, A.; Radom, L., *Prog. Phys. Org. Chem.*, (1981) 13, 1

2 Bellamy, L.J., "*The Infrared Spectra of Complex Halides*", vols. I and II, 2nd. ed., Chapman and Hall, London, N.Y., 1980

3 Yuchnovsky, I.N.; Binev., I.G., "*Infrared Spectra of Cyano and Isocyano Groups*", The Chemistry of Functional Groups, Suppl. C., Ed. S. Patai and Z. Rappoport, Wiley, N.Y., 1982

4 Katritzky, A.R.; Topsom, R.D., *Angew. Chem. Internat. Edit.*, (1970), 9(2), 87

5 Katritzky, A.R.; Topsom, R.D., *Chem. Rev.* (1977) 77(5), 639

6 Binev, I.G.; Kuzmanova, R.; Kanet. K.;Yukhnovsky, N., *Izv. Khim.*, (1981) 14(4), 470

7 Topsom, R.D., *Prog. Phys. Org. Chem.*, (1987), 16, 85

8 Slavinskaya, R.A.; Mulgadaliev, K.K.; Kovaleva, T.A., *Izv. Akad. Nauk. Kaz. SSR, Ser. Khim.*, (1990), 1, 23

9 Osawa, S.; Takeda, M., *Ibaraki Daigaku Kogakubu Kenkyu Shuho* (1980), 28, 101

10 Buncel, E.; Crampton, M.R.; Strauss, M.I.; Terrier, F., "*Electron Deficient Aromatic and Heteraromatic-Base Interactions. The Chemistry of Anionic Sigma Complexes*" Elsevier, Amsterdam, Oxford, N.Y., Tokyo, 1984

Chapter 7
Experimental

7.1. Materials

7.1.1 Solvents

Methanol:	AnalaR spectrophotometric grade, used without further treatment.
DMSO:	Spectrophotometric grade, dried with calcium hydride and fractionated under reduced pressure.
Benzene:	Spectrophotometric grade, stored over molecular sieve type 4A.
Chloroform:	Spectrophotometric grade, used without further treatment.
Dichloromethane:	AnalaR grade, used without further treatment.
Acetonitrile:	Spectrophotometric grade, rubber sealed used without further treatment.
Deuterated forms of the mentioned solvents:	Commercial samples used as supplied.

7.1.2 Nucleophiles

Lithium methoxide:	Prepared by dissolving clean lithium metal in AnalaR methanol under nitrogen and titrated with standard acid.
Sodium methoxide:	Prepared in the same way as lithium methoxide, using clean sodium metal.
Potassium methoxide:	Prepared the same way as lithium methoxide , using clean potassium metal.
Tetramethylammonium: methoxide	Prepared by dilution of 25% aqueous tetramethyl-ammonium hydroxide in methanol and titrated with standard acid.

7.1.3 Substrates

2,4,6–trinitroanisole TNA:	Prepared from picryl chloride and sodium methoxide and recrystallised from methanol. Yellow plates, m.p.66–68°C (lit[1] 68°C).
2,4,6–trinitrophenol:	Prepared from picryl chloride with sodium hydroxide and recrystallised from methanol. Yellow plates, m.p.121°C (lit[1] 122.5°C)
2,4,6–trinitrophenoxide:	Prepared from 2,4,6-trinitrophenol and sodium methoxide, recrystallised from methanol. Deep yellow crystals.
p–cyanoanisole:	Commercial sample, recrystallised from methanol. Colourless crystals, m.p.57–59°C.
o–cyanoanisole:	Prepared from 2–cyanochlorobenzene and sodium methoxide, recrystallised from methanol, m.p. 25°C (lit[8] 24.5°C).
4–cyano–2,6–dinitroanisole:	Prepared from *p*–cyanoanisole and fuming nitric acid. Recrystallised from methanol. Pale cream needles, m.p.113°C (lit[2] 114°C).
4–hydroxybenzonitrile (p–cyanophenol):	Commercial sample, recrystallised from methanol. Colourless crystals m.p.119°C (lit[8] 119°C).
4–cyano–2,6–: dinitrophenol	Prepared from *p*–cyanophenol with fuming nitric acid at room temperature for 24 hours. On dilution with iced water, yellow crystals appeared which were dissolved in methanol, traces of water removed with magnesium sulphate and twice re-crystallised. Pale cream crystals, m.p.134–136°C.

2–cyano–4,6–dinitroanisole:	Prepared in three–stages from 2–cyano–chlorobenzene; nitration yielded 2–cyano–4.nitrochlorobenzene, methoxy–dechlorination produced the anisole which was then nitrated by fuming nitric acid at 70°C. Recrystallised from methanol. Fine pale cream needles, m.p.73°C (lit[3] 72°C[4]).
2–cyano–4,6–: dinitrophenol	Prepared in three–stages from 2–cyano–chlorobenzene with fuming nitric acid to yield 2–cyano–4.nitro–benzene which reacts with concentrated sodium hydroxide to form 2–cyano–4.nitro–phenol; further nitration gave the wanted compound, which was recrystallised from methanol. Pale cream plates, m.p.180°C.
2,4,6-trinitrophenetole (TNP):	Prepared from picryl chloride and sodium ethoxide, recrystallised from methanol. Yellow brown needles, m.p. 80°C (lit[9] 78.5°C).
1-isopropoxy-2,4,6-trinitrobenzene:	Prepared[5] from picryl chloride and sodium isopropoxide. Fine pale brown crystals, m.p. 94–95°C (lit[6] 95°C).
N,N–dimethylpicramide	Prepared by addition of excess aqueous dimethylamine to a solution of picryl chloride in methanol and recrystallised from glacial acetic acid. Deep yellow needles, m.p. 139°C (lit[1] 138°C).

7.1.4 Salts

All salts used throughout the work were AnalaR grade and were oven–dried at 100°C for at least 24 hours.

Potassium Fluoride	Potassium Chloride
Potassium Bromide	Potassium Iodide
Sodium Chloride	Sodium Bromide
Sodium Azide	Sodium Thiocyanide
Calcium Chloride	Barium Chloride
Trimethylsulphoxonium Bromide	Trimethylsulphoxonium Iodide

7.2 Measurement techniques

7.2.1 UV/visible measurements

All U.V./visible spectra were recorded using fresh solutions in 1cm quartz cells on either a Perkin–Elmer Lambda 3 or Philips PU8725 instrument. These same instruments were also used for kinetic and equilibrium measurements (made at 25°C), except in the case of fast reactions, in which case the stopped–flow spectrophotometer was used (see later).

All kinetic measurements were made under first–order conditions, and observed rate coefficients were determined by following the change in absorbance at an appropriate wavelength. Measured absorbance values were entered into a suitable program running on an Apple IIe microcomputer, which calculated the observed rate coefficient based on the following derivation.

For a decrease in absorbance:

$$-\frac{d[A]}{dt} = k_{obs}[A] \qquad [A] = \text{absorbance}$$

$$\int_{[A]_0}^{[A]_t} \frac{d[A]}{[A]} = -k_{obs}\int_0^t dt \qquad \begin{array}{l}\text{where} \\ [A]_0 = \text{initial absorbance} \\ [A]_t = \text{absorbance at time t}\end{array}$$

$$\ln\left[\frac{[A]_t}{[A]_0}\right] = -k_{obs}t$$

Assuming absorbance does not fade to zero:

$[A]_0$ becomes $[A]_0-[A]_\infty$ and $[A]_t$ becomes $[A]_t-[A]_\infty$ where $[A]_\infty$ is the absorbance at 'infinite' time

Therefore $$\ln\left[\frac{[A]_t-[A]_\infty}{[A]_0-[A]_\infty}\right] = -k_{obs}t$$

$$[A]_0-[A]_\infty = \text{constant}$$

Thus a plot of $\ln([A]_t-[A]_\infty)$ *vs.* time has a gradient of $-k_{obs}$. If following an increase in absorbance a plot of $\ln([A]_\infty-[A]_t)$ *vs.* time has a gradient of $-k_{obs}$.

For measurement of rate coefficients of reactions too fast for the conventional machines a Hi–Tech Scientific SF–3L stopped flow spectrophotometer was used. This is shown schematically in Figure 7–1.

The two solutions A and B, which undergo reaction are stored in glass reservoirs, and from there enter identical syringes. A single piston drives both syringes, so that equal volumes of each solution are mixed at point M (halving the concentration of each solution), before passing into a thermostatted 2mm quartz cell at point O. When the plunger of the third syringe hits the stop the flow of reactants stops and the trigger causes monitoring of the reaction at O to begin. This is done by passing a beam of monochromatic light of the appropriate wavelength through the cell. The reaction within the cell causes an increase or decrease in the transmitted light which is fed through a photomultiplier and displayed on an oscilloscope screen, from where voltage changes can be read off. Although the output of the photomultiplier is not linear, for a small percentage change the voltage can be assumed to be proportional to the absorbance of the reaction mixture, and therefore a plot of log $|V_t-V_\infty|$ *vs.* time gives k_{obs} from |gradient|.

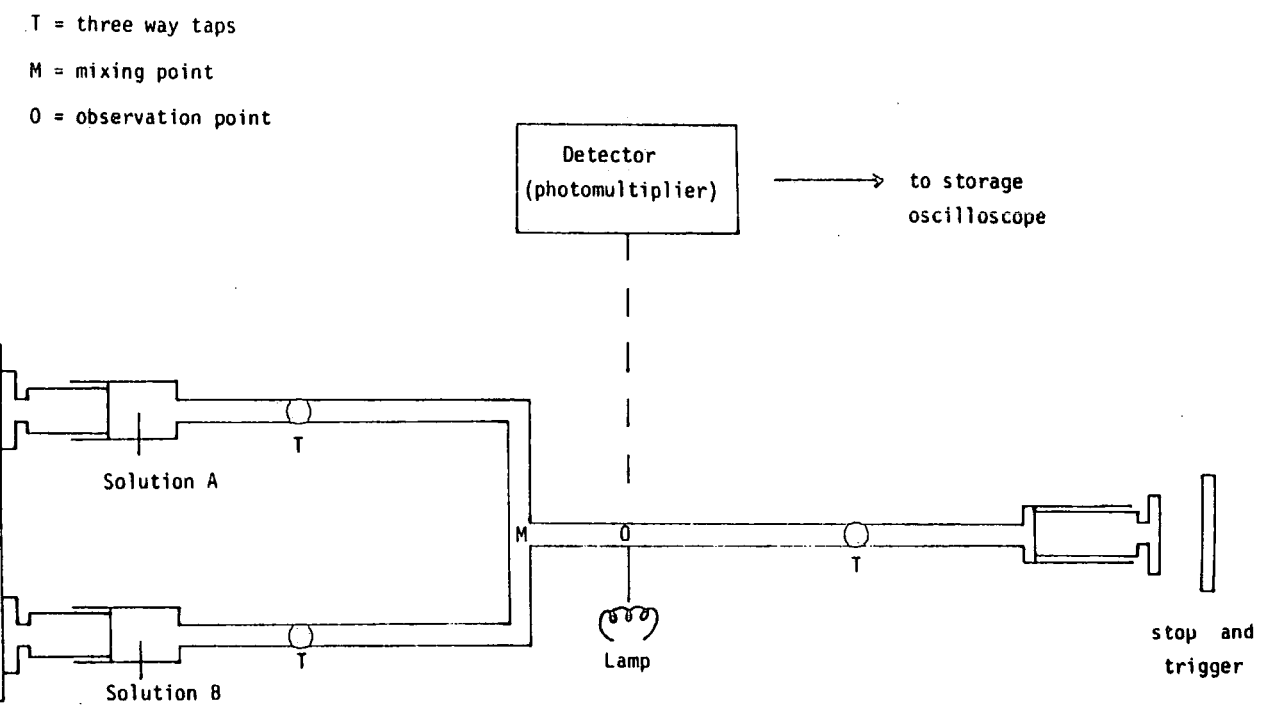

Figure 7–1 Schematic representation of stopped-flow UV/visible spectrophotometer.

7.2.2 Mass spectrometry

Mass spectrometric measurements were made using 7070E instrument supplied by V.G. Analytical Ltd. Both Electron Impact and Chemical Ionisation methods were employed, the most suitable for any particular compound being determined empirically.

7.2.3 NMR spectrometry

All NMR spectra were recorded on a Bruker AC250 (250MHz) instrument. Shift measurements are quoted as "δ" values relative to tetramethylsilane (TMS).

7.2.4 Infrared measurements

The IR spectra were recorded using freshly prepared solution in cells of previously determined thickness with calcium fluoride plates. For each case, the same cell was first used to record the spectrum of the respective solvent or mixture of solvents, in identical conditions.

All measurements were performed with a Perkin–Elmer 580B instrument, a double beam ratio recording IR spectrophotometer. The operation of such instruments relies on beam division with one beam traversing the sample and the other acting as a reference signal as shown in the schematic diagram in Figure 7.2.

Broad band i.r. radiation emitted from a source S (usually a glowbar) is split into two beams by a chopper, C_1. The sample beam is reflected by the chopper while the reference is allowed to pass through the sector. Having traversed the sample the transmitted radiation passes through a second chopper, C_2 in synchronization with C_1 and on to the monochromator, (the reference is reflected off the chopper). In such a way alternate and independent pulses of sample and reference beams impinge on the entrance slit of the monochromator. The diffraction grating, which is usually synchronized with the scan motor, disperses the beam through an exit slit, the width of which determining the signal to noise and resolution of the spectrophotometer. Before emerging through a filter which subtracts unwanted stray frequencies.

The alternating signals from the detector are amplified into sample and reference signals. These are ratioed and filtered by the signal processing electronics giving a voltage siganl which drives the recorder.

Another important feature of the PE580B is the dual chopper assembly which operates at 12.5Hz and compensates for re–radiation originating from the sample area. The combination of the two choppers cycle. Figure 7–3 shows these regions which fall on the monochromator successively from left to right.

The signal processing electronics is able to distinguish between these signals and thus compensates for re–radiation.

The PE508 incorporates a minicomputer which is able to control the spectrometer and also perform additional manipulations and data anaylsis.. Such functions include repeated scans of low intensity spectra, solvent subtraction, data smoothing, *etc.* some of which have been used in the present work.

Another very important feature of the PE580B is the dual chopper assembly which operates at 12.5Hz and compensates for re-radiation originating from the sample area. The combination of the two choppers gives rise to a total of four regions in a single chopper cycle. Figure 7–3 shows these regions which fall onto the monochromator successively from left to right. The signal processing electronics is able to distinguish between these signals and thus compensates for re-radiation.

The PE580 incorporates a minicomputer which is able to control the spectrometer and also perform additional manipulations and data analysis. Such functions include repeated scans of low intensity spectra, solvent subtraction, data smoothing *etc.*, some of which have been used in the present work

The selected experimental conditions used throughout this work were:

maximum resolution	$2.3cm^{-1}$
relative noise	0.3
slit width	$3.1cm^{-1}$

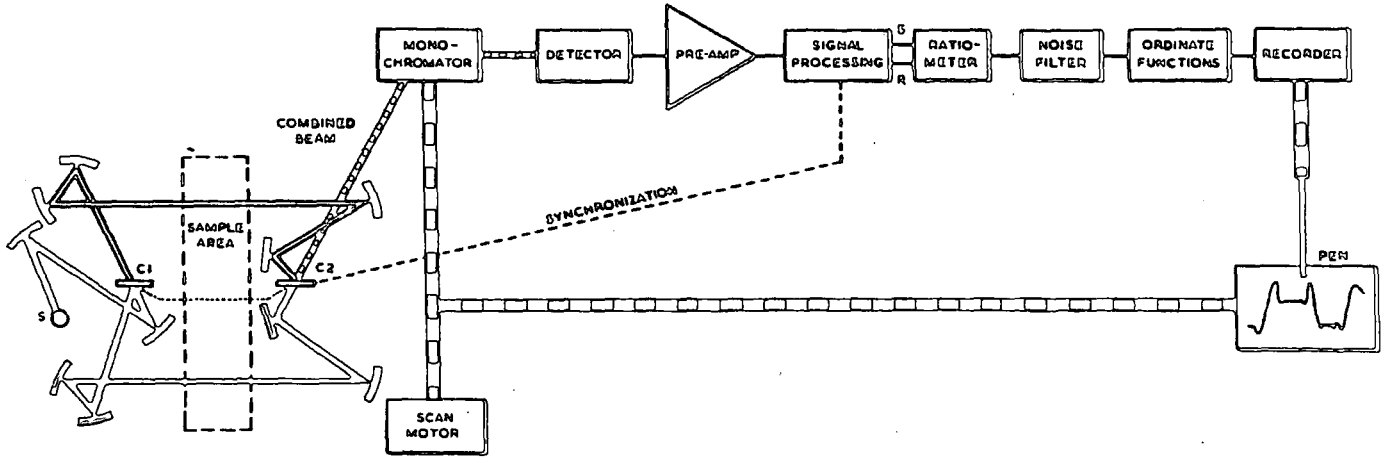

Figure 7–2 Schematic diagram of a Ratio Recording Double Beam Spectrophotometer (reproduced from reference[7])

FIGURE

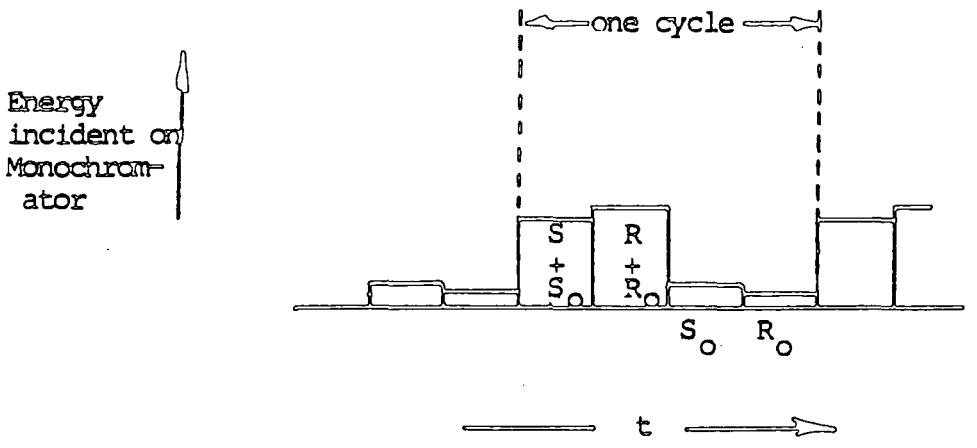

where $S + S_O$ = total sample beam energy

$R + R_O$ = total reference beam energy

R_O = re-radiation from reference area

S_O = re-radiation from sample area.

References

1 "Dictionary of Organic Compounds" 4th Ed., Eyre and Spottiswoode, London, 1965

2 Dickeson, J.E.; Dyall, L.K.; Pickles, V.A., *Aust. J. Chem.* (1968), 21, 1267

3 Fendler, J.H.; Fendler, E.J.; Griffin, C.E., *J. Org. Chem.* (1969), 34, 689

4 Blanksma, J.J., *Rev. Trav. Chim.* (1901), 20, 411

5 Crampton, M.R.; Gibson, B.; Gilmore, F.W., *J. Chem. Soc. Perkin Trans II* (1979), 91

6 Holleman, A.F., *Rec. Trav. Chim.* (1930), 49, 112

7 Perkin Elmer 580B Operators Manual, Beaconsfield, 1979

8 "Handbook of Chemistry and Physics" 63rd Ed., CRC Press, Florida, 1982–3

9 Hantzsch, A.; Gorke, H., *Ber.*, (1906), 39, 1097

Appendix

The Board of Studies in Chemistry requires that each postgraduate research thesis contain an appendix listing:

a) all research collquia, research seminars and lectures by external speakers arranged by the Department of Chemistry since October 1987 (* signifies those attended)

b) All research conferences attended and papers read out by the writer of the thesis during the period when the research was carried out.

a) Colloquia, Lectures and Seminars given by Invited Speakers

1st August 1987 to 31st July 1990

BIRCHALL, Prof. D. (I.C.I. Advanced Materials)
Environmental Chemistry of Aluminium — 25th April 1988

BORDER, Dr. K. (University of Durham Industrial Research Laboratories)
The Brighton Bomb – A Forensic Science View — 18th February 1988

BOSSONS, L, (Durham Chemistry Teachers' Centre)
GCSE Practical Assessment — 16th March 1988

BUTLER*, Dr. A.R. (University of St. Andrews)
Chinese Alchemy — 5th November 1987

CAIRNS-SMITH*, Dr. A. (Glasgow University)
Clay Minerals and the Origin of Life — 28th January 1988

DAVIDSON, Dr. J. (Herriot-Watt University)
Metal Promoted Oligomerisation Reactions of Alkynes — November 1987

GRADUATE CHEMISTS (Northeast Polytechnics and Universities)
R.S.C. Graduate Symposium — 19th April 1988

GRAHAM, Prof. W.A.G. (University of Alberta, Canada)
Rhodium and Iridium Complexes in the Activation of
Carbon-Hydrogen Bonds — 3rd March 1988

GRAY, Prof. M.P. (University of Hull)
Liquid Crystals and their Applications — 22nd October 1987

HARTSHORN*, Prof. M.P. (University of Canterbury, New Zealand)
Aspects of Ipso-Nitration — 7th April 1988

HOWARD, Dr. J. (I.C.I. Wilton)
Chemistry of Non-Equilibrium Processes — 3rd December 1987

JONES, Dr. M.E. (Durham Chemistry Teachers' Centre)
GCSE Chemistry Post-Mortem — 29th June 1988

JONES, Dr. M.E. (Durham Chemistry Teachers' Centre)
GCSE Chemistry A Level Post-Mortem — 6th July 1988

KOCH*, Prof. H.F. (Ithaca College, U.S.A.)
Does the E2 Mechanism Occur in Solution? — 7th March 1988

LACEY, Mr. (Durham Chemistry Teachers' Centre)
Double Award Science — 9th February 1988

LUDMAN*, Dr. C.J. (Durham University)
Explosives — 10th December 1987

McDonald, Dr. W.A. (I.C.I. Wilton)
Liquid Crystal Polymers — 11th May 1988

Majoral, Prof. J.-P. (Université Paul Sabatier)
Stabilisation by Complexation of Short-Lived
Phosphorus Species — 8th June 1988

MAPLETOFT, Mrs. M. (Durham Chemistry Teachers' Centre)
Salters' Chemistry — 4th November 1987

NIETO DE CASTRO*, Prof. C.A. (University of Lisbon and Imperial College)
Transport Properties of Non-Polar Fluids — 18th April 1988

OLAH, Prof. G.A. (University of Southern California)
New Aspects of Hydrocarbon Chemistry — 29th June 1988

PALMER*, Dr. F. (University of Durham)
Luminescence (Demonstration Lecture) — 21st January 1988

PINES*, Prof. A. (University of California, Berkley, U.S.A.)
Some Magnetic Moments — 28th April 1988

RICHARDSON*, Dr. R. (University of Bristol)
X-Ray Diffraction from Spread Monolayers — 27th April 1988

ROBERTS, Mrs. E. (SATRO Officer for Sunderland)
Talk – Durham Chemistry Teachers' Centre – "Links
Between Industry and Schools" — 13th April 1988

ROBINSON, Dr. J.A. (University of Southampton)
Aspects of Antibiotic Biosynthesis — 27th April 1988

ROSE van Mrs. S. (Geological Museum)
Chemistry of Volcanoes — 29th October 1987

SAMMES, Prof. P.G. (Smith, Kline and French)
Chemical Aspects of Drug Development — 19th December 1987

SEEBACH, Prof. D. (E.T.H. Zurich)
From Synthetic Methods to Mechanistic Insight — 12th November 1987

SODEAU, Dr. J. (University of East Anglia)
Durham Chemistry Teachers' Centre Lecture:
"Spray Cans, Smog and Chemistry" — 11th May 1988

SWART, Mr. R.M. (I.C.I.)
The Interaction of Chemicals with Lipid
Bilayers — 31st December 1987

TURNER, Prof. J.J. (University of Nottingham)
Catching Organometallic Intermediates — 11th February 1988

UNDERHILL*, Prof. A. (University of Bangor)
Molecular Electronics — 25th February 1988

WILLIAMS, Dr. D.H. (University of Cambridge)
Molecular Recognition — 26th November 1987

WINTER, Dr. M.J. (University of Sheffield)
Pyrotechnics (Demonstration Lecture) — 15th October 1987

ASHMAN, Mr. A. (Durham Chemistry Teachers' Centre)
The Chemical Aspects of the National Curriculum — 3rd May 1989

AVEYARD, Dr. R. (University of Hull)
Surfactants at your Surface — 15th March 1989

AYELETT, Prof. B.J. (Queen Mary College, London)
Silicon-Based Chips:- The Chemist's Contribution — 16th February 1989

BALDWIN, Prof. J.E. (Oxford University)
Recent Advances in the Bioorganic Chemistry of
Penicillin Biosynthesis — 9th February 1989

BALDWIN & WALKER*, Drs. R.R. & R.W. (Hull University)
Combustion: Some Burning Problems — 24th November 1988

BOLLEN, Mr. F. (Durham Chemistry Teachers' Centre)
Lecture about the use of SATIS in the classroom — 18th October 1988

BUTLER, Dr. A.R. (St. Andrews University)
Cancer in Lin Xian: The Chemical Dimension — 15th February 1989

CADOGAN, Prof. J.I.G. (British Petroleum)
From Pure Science to Profit — 10th November 1988

CASEY, Dr. M. (University of Salford)
Sulphoxides in Stereoselective Synthesis — 20th April 1989

CRESSEY & WATERS, Mr. D. & T. (Durham Chemistry Teachers' Centre)
GCSE Chemistry 1988: "A Coroner's Report" — 1st February 1989

CRICH, Dr. D. (University College, London)
Some Novel Uses of Free Radicals in Organic Sythesis — 27th April 1989

DINGWELL, Dr. J. (Ciba-Geigy)
Phosphorus-containing Amino-Acids: Biologically Active Natural
and Unnatural Products — 18th October 1988

ERRINGTON, Dr. R.J. (University of Newcastle-Upon-Tyne)
Polymetalate Assembly in Organic Solvents — 1st March 1989

FREY, Dr. J. (Southampton University)
Spectroscopy of the Reaction Path: Photodissociation Raman spectra
of NOIC — 11th May 1989

GRADUATE CHEMISTS*, (Polytechs and Universities in North East England)
R.S.C. Symposium for presentation of papers by
postgraduate students — 12th April 1989

HALL*, Prof. L.D. (Addenbrookes Hospital, Cambridge)
NMR – A Window to the Human Body — 2nd February 1989

HARDGROVE, Dr. G. (St. Olaf College, USA)
Polymers in the Physical Chemistry Laboratory — December 1988

HARWOOD Dr. L. (Oxford University)
Synthetic Approaches to Phorbols Via Intramolecular Furan Diels–Alder Reactions: Chemistry Under Pressure — 25th January 1989

JÄGER, Dr. C. (Freidrich–Schiller University GDR)
NMR Investigations of Fast Ion Conductors of the NASCON Type. — 9th December 1988

JENNINGS, Prof. R.R. (Warwick University)
Chemistry of the Masses — 26th January 1989

JOHNSON, Dr. B.F.G. (Cambridge University)
The Binary Carbonyls — 23rd February 1989

JONES, Dr. M.E. (Durham Chemistry Teachers' Centre)
Discussion Session on the National Curriculum — 14th June 1989

JONES, Dr. M.E. (Durham Chemistry Teachers' Centre)
GCSE and A–level Chemistry 1989 — 28th June 1989

LUDMAN*, Dr. C.J. (Durham University)
The Energetics of Explosives — 18th October 1988

MacDOUGALL*, Dr. G. (Edinburgh University)
Vibrational Spectroscopy of Model Catalytic Systems — 22nd February 1989

MARKO, Dr. I. (Sheffield University)
Catalytic Asymmetric Osmylation of Olefins — 9th March 1989

McLAUCHLAN, Dr. K.A. (University of Oxford)
The Effect of Magnetic Fields on Chemical Reactions — 16th November 1988

MOODY, Dr. C.J. (Imperial College)
Reactive Intermediates in Heterocyclic Synthesis — 17th May 1989

MORTIMER, Dr. C. (Durham Chemistry Teachers' Centre)
The Hindenburg Disaster – an Excuse for Some Experiments — 14th December 1988

NICHOLLS, Dr. D. (Durham Chemistry Teachers' Centre)
Demonstration "Liquid Air" — 11th July 1989

PAETZOLD, Prof. P. (Aachen)
Iminoboranes XB≡NR: Inorganic Acetylenes ? — 23 May 1989

PAGE, Dr. P.C.B. (University of Liverpool)
Stereocontrol of Organic Reactions using 1,3–dithiane–1–oxides — 3rd May 1989

POLA, Prof. J. (Czechoslovak Academy of Sciences)
Carbon Dioxide Laser Induced Chemical Reactions – New Pathways in Gas–Phase Chemistry — 15th June 1989

REES, Prof. C.W. (Imperial College London)
Some Very Heterocyclic Compounds — 27th October 1988

REVELL, Mr. P. (Durham Chemistry Teachers' Centre)
Implementing Broad and Balanced Science 11–16 — 14th March 1989

SCHMUTZLER, Prof. R. (Technische Universitat Braunschweig)
Fluorophosphines Revisited – New Contributions
to an Old Theme 6th October 1988

SCHROCK, Prof. R.R. (M.I.T.)
Recent Advances in Living Metathesis 13th February 1989

SINGH, Dr. G. (Teeside Polytechnic)
Towards Third Generation Anti–Leukaemics 9th November 1988

SNAITH*, Dr. R. (Cambridge University)
Egyptian Mummies: What, Where, Why and How ? 1st December 1988

STIBR, Dr. R. (Czechoslovak Academy of Sciences)
Recent Developments in the Chemistry of Intermediate–Sited
Carboranes 16th May 1989

VON RAGUE SCHLEYER, Prof. P. (Universitat Erlangen Nurnberg)
The Fruitful Interplay Between Calculational and Experimental
Chemistry 21st October 1988

WELLS, Prof. P.B. (Hull University)
Catalyst Characterisation and Activity 10th May 1989

UNIVERSITY OF DURHAM
Board of Studies in Chemistry

ASHMAN, Mr. A. (Durham Chemistry Teachers' Centre)
The National Curriculum – an update — 11th October 1989

BADYAL, Dr. J.P.S. (Durham University)
Breakthroughs in Heterogeneous Catalysis — 1st November 1989

BECHER, Dr. J. (Odense University)
Synthesis of New Macrocyclic Systems using Heterocyclic Building Blocks — 13th November 1989

BERCAW, Prof. J.E. (California Institute of Technology)
Synthetic and Mechanistic Approaches to Zeigler-natta Polymerization of Olefins — 10th November 1989

BLEASDALE, Dr. C. (Newcastle University)
The Mode of Action of some Anti-tumour Agents — 21st February 1990

BOLLEN, Mr. F. (Formerly Science Advisor, Newcastle LEA)
What's New in Satis, 16-19 — 27th March 1990

BOWMAN*, Prof. J.M. (Emory Univeristy)
Fitting Experiment with Theory in Ar-OH — 23rd March 1990

BUTLER*, Dr. A. (St. Andrew's University)
The Discovery of Penicillin: Facts and Fancies — 7th December 1989

CAMPBELL, Mr.. W.A. (Durham Chemistry Teachers' Centre)
Industrial Catalysis – some ideas for the National Curriculum — 12th September 1989

CHADWICK, Dr. P. (Dept. of Physics, Durham University)
Recent Theories of the Universe (with Reference to National Curriculum Attainment Target 16) — 24th January 1990

CHEETHAM*, Dr. A.K. (Oxford University)
Chemsitry of Zeolite Cages — 8th March 1990

CLARK, Prof. D.T. (I.C.I. Wilton)
Spatially Resolved Chemistry (using Natures' Paradigm in the Advanced Materials Arena) — 22 February 1990

COLE-HAMILTON, Prof. D.J. (St. Andrews University)
New Polymers from Homogeneous Catalysis — 29th November 1989

CROMBIE, Prof. L. (Nottingham University)
The Chemistry of Cannabis and Khat — 15th February 1990

DYER, Dr. U. (Glaxo)
Synthesis and Comformation of C-Glycosides — 31st January 1990

FLORIANI*, Prof. C. (University of Lausanne, Switzerland)
Molecular Aggregates – A Bridge between Homogeneous and Heterogeneous Systems — 25th October 1989

GERMAN, Prof. L.S. (USSR Academy of Sciences – Moscow)
New Synthesis in Fluoroaliphatic Chemistry: Recent Advances in the Chemistry of Fluorinated Oxiranes — 9th July 1990

GRAHAM, Dr. D. (B.P. Research Centre)
How Proteins Absorb to Interfaces — 4th December 1989

GREENWOOD*, Prof. N.N. (University of Leeds)
Novel Cluster Geometries in Metalloborane Chemistry — 9th November 1989

HOLLOWAY, Prof. J.H. (University of Leicester)
Nobel Gas Chemistry — 1st February 1990

HUGHES, Dr. M.N. (King's College, London)
A Bug's eye View of the Periodic Table — 30th November 1989

HUISGEN, Prof. R. (Universität München)
Recent Mechanistic Studies of [2+2] Additions — 15th December 1989

IDDON, Dr. B. (University of Salford)
Schools' Christmas Lecture – The Magic of Chemistry — 15th December 1989

JONES, Dr. M.E. (Durham Chemistry Teachers' Centre)
The Chemistry A Level 1990 — 3rd July 1990

JONES, Dr. M.E. (Durham Chemistry Teachers' Centre)
GCSE and Dual Award Science as a starting point for A Level Chemistry – how suitable are they? — 21st November 1989

JOHNSON, Dr. G.A.L. (Durham Chemistry Teachers' Centre)
Some aspects of local Geology in the National Science Curriculum (attainment target 9) — 8th February 1990

KLINOWSKI*, Dr. J. (Cambridge University)
Solid State NMR Studies of Zeolite Catalysis — 13th December 1989

LANCASTER*, Rev. R. (Kimbolton Fireworks)
Fireworks – Principles and Practice — 8th February 1990

LUNAZZI, Prof. L. (University of Bologna)
Application of Dynamic NMR to the Study of Conformational Enantiomerism — 12th February 1990

PALMER, Dr. F. (Nottingham University)
Thunder and Lightning — 17th October 1989

PARKER*, Dr. D. (Durham University)
Macrocycles, Drugs and Rock 'n' Roll — 16th November 1989

PERUTZ, Dr. R.N. (York University)
Plotting the course of C-H Activations with Organometallics — 24th January 1990

PLATONOV, Prof. V.E. (USSR Academy of Sciences – Novosibirsk)
Polyfluoroindanes: Synthesis and Transformation — 9th July 1990

POWELL*, Dr. R.L. (I.C.I)
The Development of CFC Replacements — 6th December 1989

POWIS*, Dr. I. (Nottingham University)
Spinning off in a huff: Photodissociation of Methyl Iodide 21st March 1990

RICHARDS, Mr. C. (Health and Safety Executive, Newcastle)
Safety in School Science Laboratories and COSHH 28th February 1990

ROZHKOV, Prof. I.N. (USSR Academy of Sciences – Moscow)
Reactivity of Perfluoroalkyl Bromides 9th July 1990

STODDART, Dr. J.F. (Sheffield University)
Molecular Lego 1st March 1990

SUTTON, Prof. D. (Simon Fraser University, Vancouver B.C.)
Synthesis and Applications of Dinitrogen and Diazo Compounds of Rhenium and Iridium 14th February 1990

THOMAS, Dr. R.K. (Oxford University)
Neutron Reflectometry from Surfaces 28th February 1990

THOMPSON, Dr. D.P. (Newcastle University)
The Role of Nitrogen in Extending Silicate Crystal Chemistry 7th February 1990